BEILSTEIN JOURNAL OF ORGANIC CHEMISTRY

Photocycloadditions and photorearrangements

Edited by Axel G. Griesbeck

Imprint

Beilstein Journal of Organic Chemistry
www.bjoc.org
ISSN 1860-5397
Email: journals-support@beilstein-institut.de

The *Beilstein Journal of Organic Chemistry* is published by the Beilstein-Institut zur Förderung der Chemischen Wissenschaften.

Beilstein-Institut zur Förderung der Chemischen Wissenschaften
Trakehner Straße 7–9
60487 Frankfurt am Main
Germany
www.beilstein-institut.de

Beilstein Journal of Organic Chemistry

Photocycloadditions and photorearrangements

Axel G. Griesbeck

Editorial

Open Access

Address:
University of Cologne, Department of Chemistry, Organic Chemistry, Greinstr. 4, D-50939 Köln, Germany; Fax: +49(221)470 5057

Email:
Axel G. Griesbeck - griesbeck@uni-koeln.de

Beilstein J. Org. Chem. **2011,** *7,* 111–112.
doi:10.3762/bjoc.7.15

Received: 15 December 2010
Accepted: 04 January 2011
Published: 26 January 2011

This article is part of the Thematic Series "Photocycloadditions and photorearrangements".

Guest Editor: A. G. Griesbeck

Organic synthesis using light as reagent and producing complex molecules from simple starting materials is realized in exemplary fashion in natural photosynthesis. Mankind still struggles for an efficient molecular system that mimics this natural process. In order to harvest light energy and to transform it into chemical energy, photochemical reactions must be studied and optimized for synthetic applications. Two major reaction paths that use electronic excitation are photocycloadditions and photochemical rearrangements. These reactions have been intensively investigated in recent decades in terms of regio-, stereo-, spin- and (electronic) configurational selectivities.

Prior to every photochemical reaction, an electronically excited state is generated either by direct light absorption or by energy transfer sensitization. This excited state has to be sufficiently well characterized in order to understand its chemical and physical behaviour. Organic molecules can react either as triplet or singlet excited states, often showing spin-specific reactivities and selectivities. Additionally, the nature of the excited state, as characterized by the state configuration, is crucial for the reactivity of the molecule, for example, nπ* states favour hydrogen abstraction and addition modes whereas ππ* states favour addition and electron transfer modes.

Photocycloaddition reactions can be performed in numerous ways using unsaturated substrates such as carbonyl compounds, Michael acceptors, monoalkenes, polyenes, or aromatic substrates leading to complex products that can be used in subsequent transformations. The carbonyl-ene photocycloaddition, for example, is an important route to oxetanes, products that have recently gained increasing attention as building blocks in organic synthesis as well as in materials science [1]. Photochemical rearrangements are impressive reactions with regard to the generation of complexity: 1,2- and 1,3-acyl shifts are known from carbonyl photochemistry, di-π-methane and oxa-di-π-methane rearrangements are processes that can occur with a remarkable increase in molecular and stereochemical complexity, as can *meta* arene photocycloadditions.

It was a great pleasure to act as the editor of this Thematic Series on photochemical reactions and I would like to thank all authors for their excellent contributions and the staff of the Beilstein-Institut for their support.

Axel G. Griesbeck

Cologne, January 2011

Reference

1. Burkhard, J. A.; Wuitschik, G.; Rogers-Evans, M.; Müller, K.; Carreira, E. M. *Angew. Chem., Int. Ed.* **2010,** *49,* 9052–9067. doi:10.1002/anie.200907155

License and Terms

Beilstein Journal of Organic Chemistry

Synthesis of 2a,8b-Dihydrocyclobuta[*a*]naphthalene-3,4-diones

Kerstin Schmidt and Paul Margaretha*

Full Research Paper

Open Access

Address:
Chemistry Department, University of Hamburg, Martin-Luther-King Platz 6, D-20146 Hamburg, Germany

Email:
Paul Margaretha* - Paul.Margaretha@chemie.uni-hamburg.de

* Corresponding author

Keywords:
cyclobutenes; photocycloaddition; quinone monoacetals

Beilstein J. Org. Chem. **2010,** *6,* No. 76. doi:10.3762/bjoc.6.76

Received: 07 May 2010
Accepted: 02 July 2010
Published: 13 July 2010

Guest Editor: A. G. Griesbeck

Abstract

On irradiation (λ = 350 nm) in neat hex-1-yne, naphthalene-1,2-dione monoacetals **1** afford mixtures of pentacyclic photodimers and up to 25% (isolated yield) of mixed photocycloadducts **2**. Careful acidic hydrolysis of the acetal function of **2** gives the title compounds **3**, the overall sequence representing a first approach to a (formal) [2 + 2] photocycloadduct of a 1,2-naphthoquinone to an alkyne.

Introduction

The behaviour of excited 1,2- and 1,4-quinones towards ground-state molecules differs greatly. Whereas the former typically react via H-abstraction by an excited carbonyl group [1], the latter smoothly undergo [2 + 2] cycloaddition to alkenes to afford cyclobutane-type products [2]. Very recently we reported the use of 1,2-dihydro-1,1-dimethoxynaphthalen-2-ones **1** as protected precursors for the synthesis of both photocyclodimers and ketene-photocycloadducts of 1,2-naphthoquinones [3,4]. Here we report the preparation of – novel – 2a,8b-dihydrocyclobuta[*a*]naphthalene-3,4-diones, i.e. (formal) 1,2-naphthoquinone + alkyne [2 + 2] cycloadducts.

Results

Irradiation of **1** in the presence of alkynes affords the – known [3] – pentacyclic dimers and variable amounts (0–33%) of enone + alkyne cycloadducts as indicated by ^{1}H NMR spectroscopy. The yields of mixed cycloadducts with many alkynes (3,3-dimethylbut-1-yne, trimethylsilylacetylene, 3-[(trimethylsilyl)oxy]prop-1-yne or hex-3-yne were invariably low (<5%). Moderately higher yields (15–25%) were obtained using hex-1-yne in either benzene or acetonitrile as solvent. Best results were obtained using hex-1-yne, both as reaction partner and as solvent. Thus, irradiation of either **1a** or **1b** in neat hex-1-yne affords a mixture of the corresponding dimeric dibenzophenylenediones (two regioisomers [3], 67–70%) and up to 30–33% of cycloadducts **2a** or **2b**, respectively. Compounds **2** can easily be isolated by chromatography (25% isolated yield) as they exhibit much higher R_f-values than the corresponding dimers. In contrast, naphthalenone **1c** under the same conditions only affords <5% of **2c**. Hydrolysis of cycloadducts **2** in a

two phase mixture (CH_2Cl_2, aq HCl) at r.t. [5] leads to quantitative deprotection of the acetal function as indicated by ^{1}H NMR spectroscopy to afford compounds **3a** or **3b**, respectively (Scheme 1). Compounds **3** are also easy to purify by chromatography (83–85% isolated yield) which is greatly assisted by the fact that they are easily detectable on account of their yellow colour.

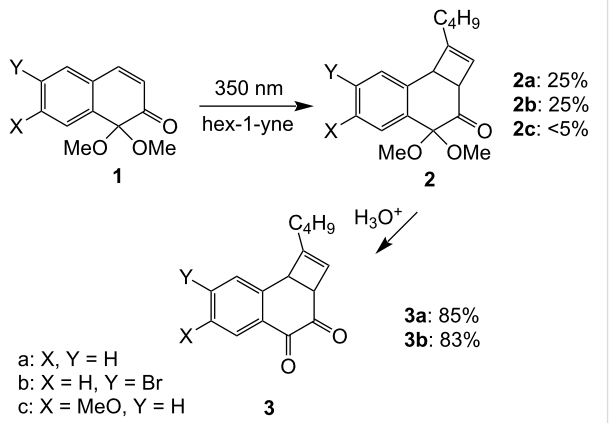

Scheme 1: Synthesis of 2a,8b-dihydrocyclobuta[*a*]naphthalene-3,4-diones.

Discussion

At first glance, the (relatively) low yield of mixed cycloadduct formation from excited **1** and alkynes seems disappointing. Nevertheless, one should bear in mind that *a*) dimer formation on irradiation of phenyl-conjugated enones, e.g., 3-phenylcyclohex-2-enone, is not suppressed even in neat alkenes as solvent [6], as these compounds tend to associate via π–π-stacking, and *b*) radical additions to alkynes usually proceed with significantly lower relative rates (30–50%) than those to the corresponding alkenes [7]. Taking these findings and the observed regioselectivity of the cycloaddition into consideration, the maximum relative yield (33%) of compounds **2a** or **2b** at total conversion of starting material is acceptable. Moreover, the fact that hydrolysis of the cycloadducts proceeds quantitatively, then the overall yields in the preparation of the – novel – 1,2-naphthoquinone + alkyne cycloadducts even becomes satisfactory. In the same experiment with **1c**, the MeO-group apparently tends to increase the efficiency in photodimerization vs mixed photocycloaddition, otherwise there is no obvious explanation for this result.

Experimental

1. General. Acetals **1** were synthesized according to [8]. Both **1b**, m.p. 60–62 °C, and **1c**, m.p. 76–78 °C, originally described as oils, solidified on standing. Hex-1-yne was commercially available. Photolyses were conducted in a *Rayonet RPR-100* photoreactor equipped with (16) 350 nm lamps. Column chromatography (CC) was carried out with silica gel 60 (Merck; 230–400 mesh). ^{1}H and ^{13}C NMR spectra (including 2D plots) were recorded with a *Bruker WM-500* instrument at 500.13 and 125.8 MHz, resp., in $CDCl_3$, δ in ppm, *J* in Hz.

2. Photolyses. Ar-Degassed solns. of **1** (1 mmol) in hex-1-yne (10 ml) were irradiated for 15 h up to total conversion (monitoring by TLC). After evaporation of the excess alkyne, the crude mixtures were analyzed by ^{1}H NMR in order to determine the crude yield. CC (SiO_2, pentane/Et_2O 6:1) gave the photocycloadducts **2**. *1-Butyl-3,4-dihydro-4,4-dimethoxy-2a*H*,8b*H*-cyclo-buta[a]naphthalen-3-one* (**2a**): 72 mg (25%), colourless oil, R_f = 0.65. ^{1}H NMR: 7.70 (d, *J* = 8.4, 1H); 7.36 (t, *J* = 8.4, 1H); 7.30 (m, 2H); 5.97 (s, 1H); 4.52 (d, *J* = 4.6, 1H); 4.00 (bs, 1H); 3.53 & 3.00 (s, 3H); 2.16 (t, *J* = 7.0, 2H); 1.52 (m, 2H); 1.38 (m, 2H); 0.92 (t, *J* = 6.9, 3H). ^{13}C NMR: 203.1 (s); 156.2 (s); 137.3 (s); 134.5 (s); 129.1 (d); 128.6 (d); 128.4 (d); 127.8 (d); 125.2 (d); 99.1 (s); 51.0 (q); 50.1 (d); 49.2 (q); 48.3 (d); 30.2 (t); 28.6 (t); 22.5 (t); 14.2 (q). Anal. Calcd for $C_{18}H_{22}O_3$: C, 75.50; H, 7.74. Found: C, 75.43; H, 7.78. *7-Bromo-1-butyl-3,4-dihydro-4,4-dimethoxy-2a*H*,8b*H*-cyclo-buta[a]naphthalen-3-one* (**2b**): 91 mg (25%), light yellow solid, m.p. 50 – 52 °C, R_f = 0.61. ^{1}H NMR: 7.55 (d, *J* = 8.4, 1H); 7.42 (s, 1H); 7.41 (d, *J* = 8.4, 1H); 5.96 (s, 1H); 4.46 (d, *J* = 4.6, 1H); 3.95 (bs, 1H); 3.52 & 2.97 (s, 3H); 2.16 (t, *J* = 7.0, 2H); 1.52 (m, 2H); 1.38 (m, 2H); 0.93 (t, *J* = 6.9, 3H). ^{13}C NMR: 203.2 (s); 156.2 (s); 135.9 (s); 135.5 (s); 133.0 (s); 131.9 (d); 129.9 (d); 129.8 (d); 125.8 (d); 99.1 (s); 51.1 (q); 50.2 (d); 49.1 (q); 48.2 (d); 30.2 (t); 28.6 (t); 22.5 (t); 14.2 (q). Anal. Calcd for $C_{18}H_{21}BrO_3$: C, 59.19; H 5.79. Found: C, 59.22; H, 5.82.

3. Hydrolyses. To a soln. of the acetal **2** (0.2 mmol) in CH_2Cl_2 (2 ml), was added 8N HCl (1.5 ml) and the mixture stirred for 5 h at room temperature. The org. phase was washed with sat. aq NaCl, dried ($MgSO_4$) and the residue (100% conversion to product from ^{1}H NMR) purified by CC (SiO_2, pentane/Et_2O 1:1) to afford the diketones **3**. *1-Butyl-2a,8b-dihydrocyclobuta[a]naphthalene-3,4-dione* (**3a**): 37 mg (85%), viscous yellow oil, R_f = 0.45. ^{1}H NMR: 8.06 (d, *J* = 8.5, 1H); 7.62 (t, *J* = 8.5, 1H); 7.42 (t, *J* = 8.5, 1H); 7.37 (d, *J* = 8.5, 1H); 5.72 (s, 1H); 4.25 (d, *J* = 3.2, 1H); 4.16 (bs, 1H); 1.97 (m, 2H); 1.40 (m, 2H); 1.26 (m, 2H); 0.83 (t, *J* = 6.9, 3H). ^{13}C NMR: 196.2 (s); 184.5 (s); 164.1 (s); 144.2 (s); 137.1 (s); 134.5 (d); 130.1 (d); 128.4 (d); 127.8 (d); 122.5 (d); 48.5 (d); 46.4 (d); 28.8 (t); 28.0 (t); 27.4 (t); 22.4 (q). Anal. Calcd for $C_{16}H_{16}O_2$: C, 79.97; H, 6.71. Found: C, 79.92; H, 6.85. *7-Bromo-1-butyl-2a,8b-dihydrocyclobuta[a]naphthalene-3,4-dione* (**3b**): 48 mg (83%), viscous yellow oil, R_f = 0.41. ^{1}H NMR: 7.94 (d, *J* = 8.5, 1H); 7.58 (d, *J* = 8.5, 1H); 7.53 (s, 1H); 5.74 (s, H); 4.19 (d, *J* = 3.1, 1H); 4.15 (bs, 1H); 1.99 (m, 2H); 1.40 (m, 2H); 1.26 (m, 2H);

0.84 (t, J = 6.9, 3H). ^{13}C NMR: 196.1 (s); 184.6 (s); 164.2 (s); 144.2 (s); 137.1 (s); 134.5 (d); 130.1 (s); 128.4 (d); 127.8 (d); 122.5 (d); 48.6 (d); 46.3 (d); 28.8 (t); 28.0 (t); 27.4 (t); 22.4 (q). Anal. Calcd for $C_{16}H_{15}BrO_2$: C, 60.21; H, 4.71. Found: C, 60.13; H, 4.77.

References

1. Oelgemoeller, M.; Mattay, J. The “Photochemical Friedel-Crafts Acylation” of Quinones: From the Beginnings of Organic Photochemistry to Modern Solar Chemical Applications. In *Handbook of Organic Photochemistry and Photobiology,* 2nd ed.; Horspool, W. M.; Lenzi, F., Eds.; CRC Press: Boca Raton, USA, 2004; 88-1.
2. Gilbert, A. 1,4-Quinone Cycloaddition Reactions with Alkenes, Alkynes, and Related Compounds. In *Handbook of Organic Photochemistry and Photobiology,* 2nd ed.; Horspool, W. M.; Lenzi, F., Eds.; CRC Press: Boca Raton, USA, 2004; 87-1.
3. Schmidt, K.; Kopf, J.; Margaretha, P. *Helv. Chim. Acta* **2007,** *90,* 1667. doi:10.1002/hlca.200790172
4. Schmidt, K.; Margaretha, P. *Helv. Chim. Acta* **2008,** *91,* 1625. doi:10.1002/hlca.200890177
5. De Kimpe, N.; Verhé, R.; De Buyck, L.; Schamp, N. *J. Org. Chem.* **1978,** *43,* 2933. doi:10.1021/jo00408a047
6. McCullough, J. J.; Ramachandran, B. R.; Snyder, F. F.; Taylor, G. N. *J. Am. Chem. Soc.* **1975,** *97,* 6767. doi:10.1021/ja00856a028
7. Santi, R.; Bergamini, F.; Citterio, A.; Sebastiano, R.; Nicolini, M. *J. Org. Chem.* **1992,** *57,* 4250. doi:10.1021/jo00041a034
8. Mal, D.; Roy, H. N.; Hazra, N. K.; Adhikari, S. *Tetrahedron* **1997,** *53,* 2177. doi:10.1016/S0040-4020(96)01119-2

License and Terms

Beilstein Journal of Organic Chemistry

Heavy atom effects in the Paternò–Büchi reaction of pyrimidine derivatives with 4,4'-disubstituted benzophenones

Feng-Feng Kong, Jian-Bo Wang and Qin-Hua Song*

Full Research Paper

Open Access

Address:
Department of Chemistry, University of Science and Technology of China, Hefei 230026, Anhui, P. R. China

Email:
Qin-Hua Song* - qhsong@ustc.edu.cn

* Corresponding author

Keywords:
benzophenone; heavy atom effect; Paternò–Büchi reaction; regioselectivity; triplet diradical

Beilstein J. Org. Chem. **2011,** *7,* 113–118.
doi:10.3762/bjoc.7.16

Received: 30 October 2010
Accepted: 08 December 2010
Published: 26 January 2011

This article is part of the Thematic Series "Photocycloadditions and photorearrangements".

Guest Editor: A. G. Griesbeck

Abstract

The regioselectivity and the photochemical efficiency were investigated in the Paternò–Büchi reaction of 1,3-dimethylthymine (DMT) and 1,3-dimethyluracil (DMU) with benzophenone (**1b**) and some 4,4'-disubstituted derivatives (dimethoxy (**1a**), difluoro (**1c**), dichloro (**1d**), dibromo (**1e**) and dicyano benzophenone (**1f**)) that gives rise to two regioisomeric oxetanes, **2** and **3**. The regioselectivity (the ratio of **2**/**3**) decreased gradually for both DMT/DMU photochemical systems from **1a** to **1f**. That is, a halogen atom as an electron-withdrawing group (EWG) has a pronounced effect on the regioselectivity. However, the photochemical efficiency of the **1e** systems did not show the expected increase, but decreased relative to systems with **1b.** Temperature effects on the regioselectivity of **1b–e** systems showed some interesting features for systems with heavy atoms (including the **1d** and **1e** systems), such as higher inversion temperatures, and an entropy-controlled regioselectively whereas the regioselectivity for two other systems (**1b** and **1c**) is enthalpy–entropy controlled. A heavy atom effect is suggested to be responsible for these unusual phenomena based on the triplet-diradical mechanism of the Paternò–Büchi reaction.

Introduction

The regio- and stereoselectivity in the Paternò–Büchi reaction, which is a photochemical [2 + 2] cycloaddition of a carbonyl compound with an olefin, has been extensively studied [1-4]. The ene–carbonyl photocycloaddition generally proceeds through attack of the excited carbonyl state (singlet or triplet or both) on a ground-state olefin. For aromatic carbonyl compounds, the reaction is a triplet cycloaddition, that is, a triplet-excited carbonyl compound adding to an olefin to yield a triplet 1,4-diradical intermediate, which undergoes intersystem crossing (ISC) to produce a singlet 1,4-diradical. Ring-close of the latter gives an oxetane. The higher selectivity observed for the triplet reaction is rationalized by the optional conformation

of the intermediate 2-oxabutane-1,4-diyl for ISC to the singlet diradical, which is preferentially controlled by spin-orbit coupling, thus leading to substantial control of regio- and stereoselectivity [5-13].

The "heavy atom effect" is a term which has been used to describe the influence of "heavy atom" substitution on a spin-forbidden transition such as various intersystem crossings. If heavy atoms are present in a Paternò–Büchi reaction, spin-transition processes would be affected, and this may lead to interesting results.

Abe et al. [14] investigated the effect of a sulfur atom on the stereoselective formation of oxetanes in Paternò–Büchi reaction of aromatic aldehydes with silyl *O*,*S*-ketene acetals to give *trans*-3-siloxyoxetanes and found that this was ca. 70/30 to 90/10. The trans-selectivity is explained by the sulfur atom effect in the silyl *O*,*S*-ketene acetal which controls the approach direction of the electrophilic oxygen of triplet n,π^* aldehyde to the nucleophilic alkene. A fast ISC process of the triplet 1-alkylthio-1-siloxy-2-oxatetramethylene 1,4-diradical in competition with the bond rotation was proposed [14]. Griesbeck et al. [15] observed substantial ^{2}H-magnetic isotope effects on the diastereoselectivity of triplet photocycloaddition reactions. Weaker isotope effects on the diastereoselectivity were detected for the reaction of α-deuterated propionaldehyde [15].

In this work, we have investigated the Paternò–Büchi reaction of 1,3-dimethylthymine (DMT) and 1,3-dimethyluracil (DMU) with benzophenone (**1b**) and its 4,4'-disubstituted derivatives **1a** and **1c**–**1f** with the formation of the regioisomeric oxetanes **2** and **3** (Scheme 1). By changing the halogen at para positions in the benzophenones, the photochemical efficiency and the regioselectivity were significantly affected, and the effects cannot be considered as a pure electronic effect (of the electron-withdrawing groups, EWGs), by comparing the observations with those of systems of **1a** (with electron-donating groups, EDGs), and **1b** and **1f** (also with EWGs). However, as a heavy atom effect, observations above can be rationalized based on the triplet mechanism of the Paternò–Büchi reaction.

Results and Discussion

Substituent effects

To investigate substituent effects of benzophenones in the Paternò–Büchi reaction, photochemical reactions of DMT/DMU with **1a**–**f** in acetonitrile-d_3 were performed in Pyrex NMR tubes. The regioselectivity (the ratio of **2**/**3**) and the yield were measured directly from the ^{1}H NMR spectra of crude product mixtures and are listed in Table 1. The substituent effect of benzophenones on the regioselectivity (**2**/**3**) is similar to our previous observations [10], a gradual decrease according to their electronic effect from **1a** to **1e**.

Table 1: Substituents (Y) of benzophenones dependence on the regioselectivity (**2**/**3**) and the efficiency in the Paternò–Büchi reactions of DMT/DMU with 4,4'-disubstituted benzophenones **1a**–**1f**[a].

	Y	DMT[b]		DMU[c]	
		Yield%	**2/3**	Yield%	**2/3**
1a	CH_3O	25	52:48	19	> 95:5[d]
1b	H	52	55:45	51	64:36
1c	F	53	56:44	64	63:37
1d	Cl	77	38:62	70	56:44
1e	Br	46	33:67	28	53:47
1f	CN	82	14:86	75	39:61

[a]Average of two parallel determinations, DMT (DMU)/benzophenones = 10 mM:10 mM, in d_3-acetonitrile, irradiation at 10 °C with 125 W high-pressure Hg lamp, values determined by ^{1}H NMR of the crude product mixture, the experimental error < 5%.
[b]Irradiation for 30 min.
[c]Irradiation for 90 min.
[d]Oxetane **3a$_2$** was not detected, see Experimental section.

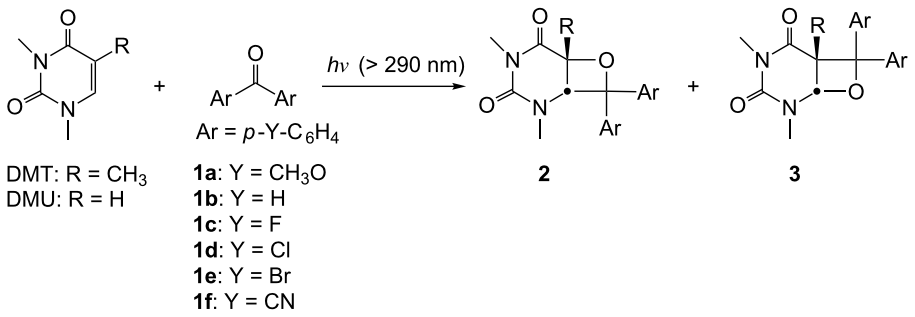

Scheme 1: The Paternò–Büchi reaction of DMT/DMU with benzophenones to generate two regioisomeric photoproducts.

In our previous papers [10,13], the photochemical [2 + 2] cycloadditions of DMT and DMU with benzophenones generate two series of regioisomeric oxetanes, **2** and **3**, via 1,4-diradical intermediates, and reveal notable substituent effects on the regioselectivity and the photochemical efficiency. The reactions initiated by triplet benzophenones with EDGs give a higher proportion of **2** and a lower photochemical efficiency, whilst benzophenones with EWGs yield a lower proportion of **2** and have a higher efficiency.

The data in Table 1 show that the regioselectivity (**2**/**3**) and the photochemical efficiency correlates clearly with electronic property of substituents. The benzophenones with EWGs give more efficient Paternò–Büchi reactions (except **1e** systems) and lower ratios of **2**/**3**, and the benzophenones with EDGs undergo less efficient Paternò–Büchi reactions and have higher ratios of **2**/**3**, in accord with our previous observations [10,13]. However, the photochemical efficiency of the **1e** systems decreased significantly. According to our understanding of these oxetanes [10], this low efficiency was considered to be due to poor stability of the photoproducts, in particular oxetanes **3**.

To verify this speculation, the yield and the regioselectivity were tracked over an irradiation time of 15 min for the DMT-**1e** (5 mM/5 mM) system (Figure 1). Figure 1 clearly shows that the yield increases with irradiation time and the ratio of **2**/**3** is slightly higher (37:63) during the initial irradiation period (1–3 min), and then becomes constant (33:67) on further irradiation (> 3 min). However, this change is within the experimental error of 5%. According to our understanding of the stability of oxetanes, **3** are less stable than **2**. The constant ratio of **2**/**3** implies that no significant decomposition of the photoproduct oxetanes occurs in the photochemical reaction. In other words, the stability of photoproducts in the systems is not responsible for the low yields. Therefore, the effect of halo-substituted benzophenones on the Paternò–Büchi reaction is not a "pure" substituent effect.

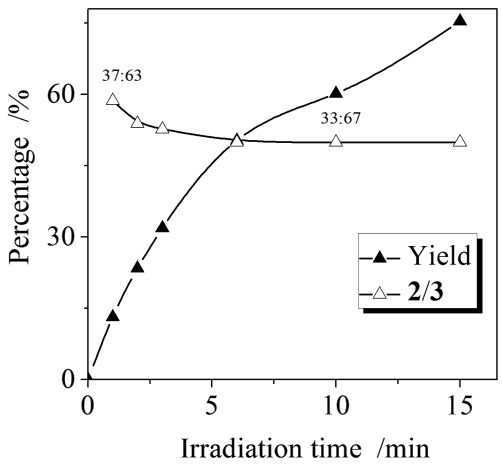

Figure 1: The yield and the ratio of **2**/**3** at different reaction times in the Paternò–Büchi reaction of DMT with **1e** (DMT:**1e** = 5 mM:5 mM, irradiation at 10 °C).

Temperature effects

In our previous papers [9,11], the photochemical [2 + 2] cycloadditions of DMT/DMU with benzophenones revealed notable temperature effects on the regioselectivity and the photochemical efficiency. We have demonstrated that the temperature-dependent regioselectivity is derived from the conformational properties of the intermediate triplet 1,4-diradicals. The observations show that the reaction temperature influences the regioselectivity by changing the populations of two regioisomeric diradicals as a result of differences in the potential energies of two stable conformers, the productive conformation of the triplet diradical and the unproductive conformation of the triplet diradical, for each regioisomeric diradical [9,11].

To investigate further the temperature effects in four systems with 4,4'-dihalo-substituted benzophenones, we carried out the Paternò–Büchi reactions of DMT with **1b–1e** over a temperature range of −30 to 70 °C: Notable temperature effects were observed. Both the photochemical efficiency and the regioselectivity (**2**/**3**) decreased with increasing temperature from the general trend (Table 2).

Table 2 shows clearly that efficiencies of the **1b** system are lower than those of the **1c** and **1d** systems except for the values at the initial three temperatures, i.e., the efficiency of **1b** system is the most sensitive to reaction temperature, and the efficiency of **1e** system is the lowest among the four systems studied. In addition, the data show that a higher reaction temperature is unfavorable for Paternò–Büchi reactions.

The regioselectivity (**2**/**3**) data in Table 2 have been plotted in Figure 2 against the inverse absolute temperature according to the Eyring formalism [16].

$$\ln\left(\frac{k_2}{k_3}\right) = \ln\left(\frac{2}{3}\right) = \frac{\Delta\Delta H^{\neq}}{RT} + \frac{\Delta\Delta S^{\neq}}{R} \qquad (1)$$

Where k_2 and k_3 are the overall rate constants of the reactions leading to the two regioisomers **2** and **3**, respectively.

The Eyring plots obtained are nonlinear across the whole temperature range. The nonlinear Eyring plot is indicative of a change of the selectivity-determining step during the change in the reaction temperature [1,17-19].

Although the Eyring plots obtained were nonlinear over whole temperature range, strict linearities (correlation coefficients R > 0.99) on both sides of inversion points were found. The temperature at the point of inversion is called the inversion temperature, T_{inv}, of the system. The temperatures increase gradually from H- to Br-substituted Paternò–Büchi systems (Table 2). In our previous paper [11], the temperature effect of the Paternò–Büchi reaction DMU with three benzophenones, **1b**, **1c** and **1f**, was investigated, and similar inversion temperatures could be obtained from the Eyring plots, 295 K for **1b**, 294 K for **1c** and 291 K for **1f**. Although CN is a strong EWG, **1f**-DMU system did not give a high inversion temperature. Hence, this result indicates that the halogen (Cl or Br) acts not as a pure EWG but as a heavy atom and induces a higher inversion temperature.

Table 2: Temperature dependence on the regioselectivity (**2**/**3**) and the yields in the Paternò–Büchi reactions of DMT with compounds **1b–e**[a].

Temp./°C	**2/3** (yield %)			
	1b	**1c**	**1d**	**1e**
−27.4	70:30 (63.9)	73:27 (62.2)	54:46 (75.6)	50:50 (37.6)
−21.4	68:32 (61.1)	70:30 (58.4)	52:48 (68.5)	46:54 (37.5)
−11.5	64:36 (62.5)	67:33 (62.3)	46:54 (69.6)	40:50 (44.4)
−0.9	61:39 (51.0)	62:38 (52.5)	42:58 (74.7)	36:64 (38.3)
9.9	56:44 (46.9)	58:42 (49.7)	39:61 (75.0)	31:69 (38.5)
20.1	52:48 (44.0)	56:44 (47.4)	34:66 (74.4)	30:70 (32.8)
30.0	48:52 (43.1)	51:49 (45.9)	30:70 (63.4)	25:75 (29.2)
40.0	41:59 (36.3)	41:59 (43.0)	26:74 (67.4)	23:77 (26.7)
49.5	37:63 (32.2)	35:65 (43.8)	21:79 (62.8)	18:82 (22.4)
60.0	31:69 (24.1)	29:71 (43.5)	17:83 (63.5)	14:86 (14.5)
69.1	27:73 (25.8)	25:75 (41.3)	14:86 (59.8)	10:90 (11.4)

[a]See Table 1.

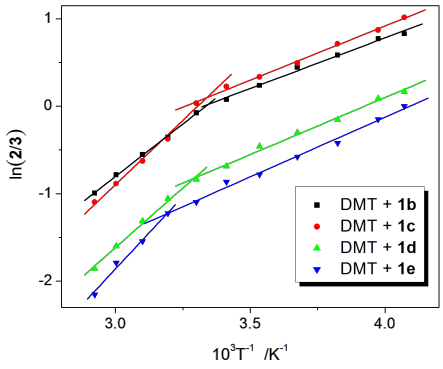

Figure 2: Eyring plots for the photoreaction of DMT with compounds **1b–e**.

According to the Eyring theory, when this relationship is plotted, the slope corresponds to the difference in the overall activation enthalpies ($\Delta\Delta H^{\neq}$) and the intercept represents the difference in the overall activation entropies ($\Delta\Delta S^{\neq}$) (Figure 2). The inversion temperature reveals two sets of activation parameters ($\Delta\Delta H_1^{\neq}$ and $\Delta\Delta S_1^{\neq}$ ($T > T_{inv}$), $\Delta\Delta H_2^{\neq}$ and $\Delta\Delta S_2^{\neq}$ ($T < T_{inv}$)), which were obtained from the slope and the intercept of the linear plot for each system. Table 3 presents the parameters of activation $\Delta\Delta H_{1,2}^{\neq}$ and $\Delta\Delta S_{1,2}^{\neq}$ values. These large parameters of activation are unprecedented, $\Delta\Delta H_1^{\neq}$ values range from −19.9 to −27.5 kJ mol^{-1} and are much higher than the published values −4.2 kJ mol^{-1} [1], 4.3 kJ mol^{-1} [8] and −4.8 kJ mol^{-1} [7]. Therefore, the regioselectivity in the Paternò–Büchi reaction is strongly temperature-dependent. Moreover, these activation parameters ($\Delta\Delta H^{\neq}$ and $\Delta\Delta S^{\neq}$) increase gradually from the F- to Br- benzophenones systems, with the exception of $\Delta\Delta H_1^{\neq}$ for **1d**.

Table 3: Inversion temperature, T_{inv} and parameters of activation, $\Delta\Delta H_1^{\neq}$, $\Delta\Delta S_1^{\neq}$ ($T > T_{inv}$), and $\Delta\Delta H_2^{\neq}$, $\Delta\Delta S_2^{\neq}$ ($T < T_{inv}$).

	$\Delta\Delta H_1^{\neq}$ $\Delta\Delta H_2^{\neq}$ /kJ mol^{-1}	$\delta\Delta\Delta H^{\neq}$ /kJ mol^{-1}	$\Delta\Delta S_1^{\neq}$ $\Delta\Delta S_2^{\neq}$ /J mol^{-1}K^{-1}	$\delta\Delta\Delta S^{\neq}$ /J mol^{-1}K^{-1}	T_{inv} /K
1b	−19.9 −9.6	10.9	−66.4 −32.0	34.4	299.0
1c	−24.4 −10.3	14.1	−80.7 −33.5	47.2	299.3
1d	−22.6 −10.8	11.8	−81.3 −42.5	38.8	303.6
1e	−27.5 −11.4	16.1	−97.9 −46.4	51.5	313.6

In addition, the values of $\Delta\Delta H^{\neq}$ are similar to $T_{inv}\Delta\Delta S^{\neq}$ for the **1b** and **1c** systems since the ratio of **2**/**3** is ~50:50. However, the values of $\Delta\Delta H^{\neq}$ are less than $T_{inv}\Delta\Delta S^{\neq}$ for two other systems (−2.1 J/mol for **1d**, −3.2 kJ/mol for **1e**). In other words, this is an entropy-determined selection for the regioselectivity over the whole temperature range investigated.

Interception of heavy atom effects

Based on the triplet mechanism of the Paternò–Büchi reaction, it is possible to have a more detailed discussion on a heavy atom effect on the Paternò–Büchi reaction based on the phenomena noted above. The formation of two regioisomers in the Paternò–Büchi reaction is detailed in Scheme 2.

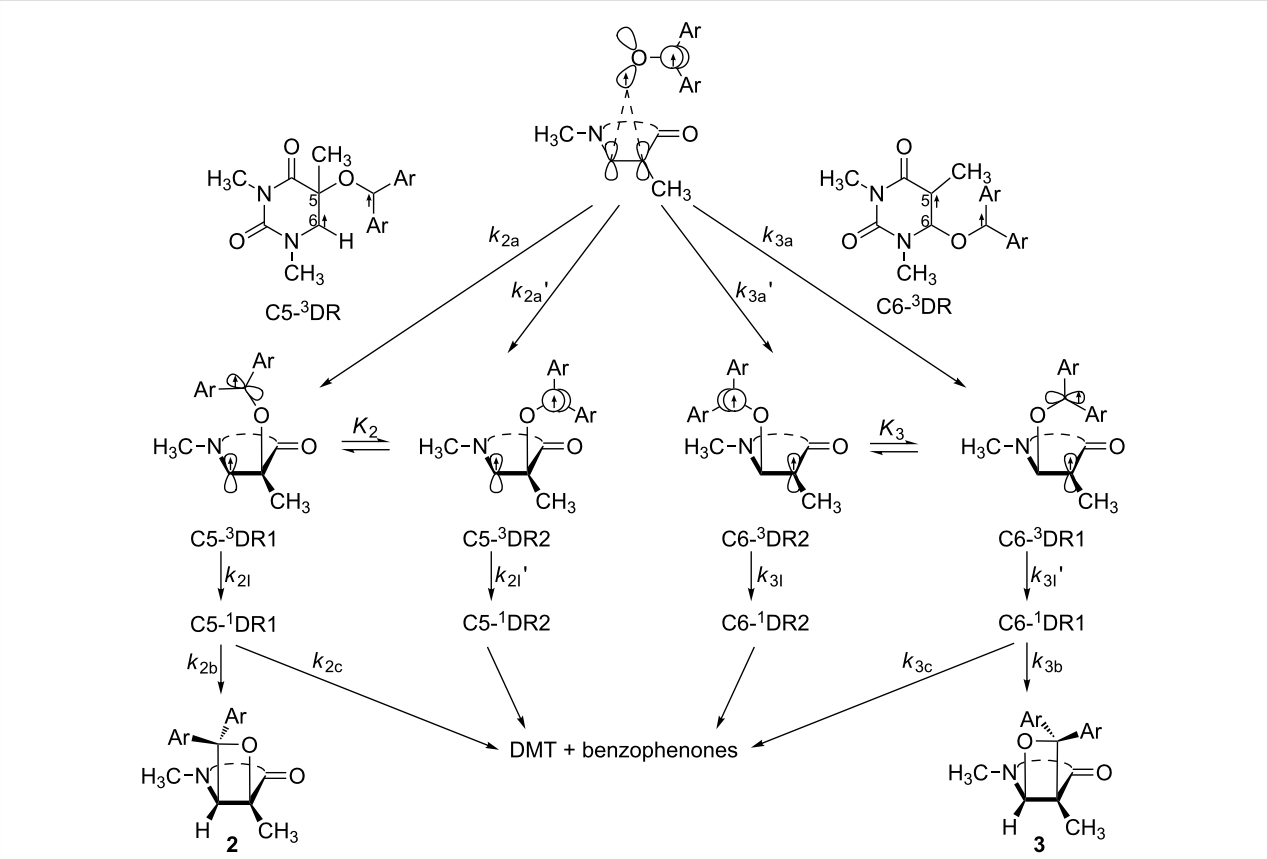

Scheme 2: The formational processes of two regioisomers in the Paternò–Büchi reaction of DMT/DMU with benzophenones [9].

Among these processes, there are four factors that determine the regioselectivity [7]. (i) Initial *O*-attacked site selection at the double bond by ^{3}benzophenones*, k_{2a}+ $k_{2a'}$ versus k_{3a}+ $k_{3a'}$, (ii) equilibrium constants, K_2 (= [C5-^{3}DR2]/[C5-^{3}DR1]) versus K_3 (= [C6-^{3}DR2]/[C6-^{3}DR1]): This factor only operates when the conformational change is faster than the ISC process, (iii) the relative rate constants of the ISC processes in the triplet 1,4-diradicals, $k_{2I}/k_{2I'}$ versus $k_{3I}/k_{3I'}$ and (iv) the relative rate constants of the bond-forming and bond-breaking step from the singlet 1,4-diradical C5-^{1}DR1 and C6-^{1}DR1, k_{2b}/k_{2c} versus k_{3b}/k_{3c}.

According to the Curtin–Hammett principle [20], the ratios of the productive conformers of singlet diradicals C5-^{1}DR1 and C6-^{1}DR1 are determined not only by the populations of C5-^{3}DR1 and C6-^{3}DR1 but also by the relative rate constants of ISC processes, the $k_{2I}/k_{2I'}$ and $k_{3I}/k_{3I'}$. The former is determined by the equilibrium constants, K_2 and K_3, whilst the latter processes (k_{2I}, $k_{2I'}$, k_{3I} and $k_{3I'}$) would be accelerated by heavy atoms. Thus, the equilibrium between the productive conformers and the unproductive conformers, of the triplet 1,4-diradicals, would be achieved at a higher temperature for the system with heavy atoms than that without heavy atoms. Due to the energy barriers between the two stable conformers [9], the equilibrium is more favorable for the formation of oxetanes **3** rather than oxetanes **2** at a higher temperature. This would lead to a higher inversion temperature and a higher ratio of **2**/**3**. In addition, the ISC process from singlet excited state to triplet excited state is very fast, 10^{11} s^{-1} for benzophenones, and not affected by heavy atoms, but the ISC process of triplet benzophenones to singlet ground state would be accelerated, reducing lifetime of triplet benzophenones. Finally, triplet benzophenones with a short lifetime would give rise to a less efficient Paternò–Büchi reaction.

Experimental

Materials

1,3-Dimethylthymine (DMT) and 1,3-dimethyluracil (DMU) were was prepared from thymine and uracil, respectively. 4,4'-Dimethoxybenzophenone, 4,4'-dichlorobenzophenone, 4,4'-dibromobenzophenone and 4,4'-dicyanobenzophenone were prepared. Benzophenone, 4,4'-difluorobenzophenone, acetonitrile-d_3 and other materials were obtained from commercial suppliers and used as received without further purification. ^{1}H and ^{13}C NMR spectra were measured with a Bruker AV 300 spectrometer operating at 300 MHz and 75 MHz, respectively.

The Paternò–Büchi reaction of DMT/DMU with benzophenones generates two regioisomers **2** and **3**. The oxetanes were numbered by using subscript "1" for DMT and "2" for DMU, e.g., oxetanes from DMT-**1a** system are denoted as $\mathbf{2a_1}$ and $\mathbf{3a_1}$. For oxetanes mentioned in this work, most were reported in our previous papers [9,10] except for the following oxetanes. $\mathbf{3a_2}$ has not been detected by ^{1}H NMR. $\mathbf{3d_1}$, $\mathbf{3d_2}$, $\mathbf{3e_1}$, $\mathbf{2e_2}$ and $\mathbf{3e_2}$ could be detected by ^{1}H NMR, but could not be isolated because of their poor stability towards acid and silica gel. $\mathbf{2e_1}$ was isolated and the characterization data of $\mathbf{2e_1}$ was as follows:

8,8-Bis-(4-bromo-phenyl)-2,4,6-trimethyl-7-oxa-2,4-diaza-bicyclo[4.2.0]octane-3,5-dione ($\mathbf{2e_1}$). ^{1}H NMR (300 MHz, $CDCl_3$) δ = 1.73 (s, 3H, CH_3), 2.91 (s, 3H, NCH_3), 3.11 (s, 3H, NCH_3), 4.50 (s, 1H, NCH), 7.13–5.54 (m, 8H, H_{Ar}) ppm; ^{13}C NMR (75 MHz, $CDCl_3$) δ = 24.1, 27.6, 35.9, 66.8, 91.0, 122.5, 122.8, 126.8, 127.4, 131.8, 132.1, 137.6, 142.8, 151.6, 169.6 ppm; IR (KBr) 3435 (*s*), 2930 (*w*), 1704 (*m*), 1673 (*s*), 1484 (*s*), 1282 (*s*), 1068 (*s*), 1008 (*m*), 818 (*m*), 746 (*m*) cm^{-1}; TOFMS (CI) *m/z* calcd for $(M+H)^+$ $C_{20}H_{18}N_2O_3Br_2$: 494.9742, found 494.9731.

Photoproduct assay

The Paternò–Büchi reactions of DMT/DMU with benzophenones were performed in acetonitrile-d_3. A solution of the reactants was placed in a Pyrex NMR tube (transmitted light > 290 nm), purged with high purity N_2 for 10 min and then irradiated with a 125 W high-pressure Hg lamp at 10 °C. The sample tubes were placed on a merry-go-round equipment moving around the Hg lamp. Photoproducts **2** and **3** have no significant absorption for light at above 290 nm. Hence, a secondary photolysis of the oxetane products (**2** or **3**) should not occur unless there is prolonged irradiation. Compositions in photoreaction mixture were quantified by ^{1}H NMR spectroscopy (300 MHz) directly on the crude product mixture, using the sum of 5-methyl (5-H) and 6-H signals as internal standards. The yields and the ratios of the two regioisomeric oxetanes were obtained from the peak areas of 5-methyl and 6-H for DMT system and those of 5-H and 6-H for DMU system in the ^{1}H NMR spectra. The experimental error was within 5%.

Acknowledgements

The authors thank the financial support by the National Natural Science Foundation of China (Grant Nos. 20972149, 30870581).

References

1. Buschmann, H.; Scharf, H.-D.; Hoffmann, N.; Esser, P. *Angew. Chem., Int. Ed. Engl.* **1991,** *30,* 477–515. doi:10.1002/anie.199104771
2. Griesbeck, A. G.; Mauder, H.; Stadtmüller, S. *Acc. Chem. Res.* **1994,** *27,* 70–75. doi:10.1021/ar00039a002
3. Griesbeck, A. G. *Synlett* **2003,** 451–472. doi:10.1055/s-2003-37505
4. Griesbeck, A. G.; Abe, M.; Bondock, S. *Acc. Chem. Res.* **2004,** *37,* 919–928. doi:10.1021/ar040081u
5. D'Auria, M.; Racioppi, R.; Romaniello, G. *Eur. J. Org. Chem.* **2000,** 3265–3272. doi:10.1002/1099-0690(200010)2000:19<3265::AID-EJOC3265>3.0.CO;2-6
6. Abe, M.; Torii, E.; Nojima, M. *J. Org. Chem.* **2000,** *65,* 3426–3431. doi:10.1021/jo991877n
7. Abe, M.; Kawakami, T.; Ohata, S.; Nozaki, K.; Nojima, M. *J. Am. Chem. Soc.* **2004,** *126,* 2838–2846. doi:10.1021/ja039491o
8. Adam, W.; Stegmann, V. R. *J. Am. Chem. Soc.* **2002,** *124,* 3600–3607. doi:10.1021/ja017017h
9. Hei, X.-M.; Song, Q.-H.; Li, X.-B.; Tang, W.-J.; Wang, H.-B.; Guo, Q.-X. *J. Org. Chem.* **2005,** *70,* 2522–2527. doi:10.1021/jo048006k
10. Song, Q.-H.; Zhai, B.-C.; Hei, X.-M.; Guo, Q.-X. *Eur. J. Org. Chem.* **2006,** 1790–1800. doi:10.1002/ejoc.200500862
11. Song, Q.-H.; Wang, H.-B.; Li, X.-B.; Hei, X.-M.; Guo, Q.-X.; Yu, S.-Q. *J. Photochem. Photobiol., A: Chem.* **2006,** *183,* 198–204. doi:10.1016/j.jphotochem.2006.03.018
12. Zhai, B.-C.; Luo, S.-W.; Kong, F.-F.; Song, Q.-H. *J. Photochem. Photobiol., A: Chem.* **2007,** *187,* 406–409. doi:10.1016/j.jphotochem.2006.10.028
13. Kong, F.-F.; Zhai, B.-C.; Song, Q.-H. *Photochem. Photobiol. Sci.* **2008,** *7,* 1332–1336. doi:10.1039/b810640a
14. Abe, M.; Fujimoto, K.; Nojima, M. *J. Am. Chem. Soc.* **2000,** *122,* 4005–4010. doi:10.1021/ja993997i
15. Griesbeck, A. G.; Bondock, S.; Cygon, P. *J. Am. Chem. Soc.* **2003,** *125,* 9016–9017. doi:10.1021/ja0356232
16. Glasstone, S.; Laidler, K. J.; Eyring, H. *The Theory of Rate Processes;* McGraw-Hill: New York, 1941; pp 153 ff.
17. Göbel, T.; Sharpless, K. B. *Angew. Chem., Int. Ed. Engl.* **1993,** *32,* 1329–1331. doi:10.1002/anie.199313291
18. Hale, K. J.; Ridd, J. H. *J. Chem. Soc., Chem. Commun.* **1995,** 357–358. doi:10.1039/C39950000357
19. Gypser, A.; Norrby, P.-O. *J. Chem. Soc., Perkin Trans. 2* **1997,** 939–944. doi:10.1039/a606888j
20. Seeman, J. I. *Chem. Rev.* **1983,** *83,* 83–134. doi:10.1021/cr00054a001

License and Terms

Beilstein Journal of Organic Chemistry

Synthesis of cationic dibenzosemibullvalene-based phase-transfer catalysts by di-π-methane rearrangements of pyrrolinium-annelated dibenzobarrelene derivatives

Heiko Ihmels* and Jia Luo

Full Research Paper

Open Access

Address:
Organic Chemistry II, University of Siegen, Adolf-Reichwein-Str. 2, D-57068 Siegen, Germany

Email:
Heiko Ihmels* - ihmels@chemie.uni-siegen.de

* Corresponding author

Keywords:
di-π-methane rearrangement; dibenzobarrelenes; dibenzosemibullvalenes; phase-transfer catalysis; photochemistry; polycylic compounds

Beilstein J. Org. Chem. **2011,** *7,* 119–126.
doi:10.3762/bjoc.7.17

Received: 29 October 2010
Accepted: 09 December 2010
Published: 26 January 2011

This article is part of the Thematic Series "Photocycloadditions and photorearrangements".

Guest Editor: A. G. Griesbeck

Abstract

Dibenzobarrelene derivatives, that are annelated with a pyrrolinium unit [*N*,*N*-dialkyl-3,4-(9',10'-dihydro-9',10'-anthraceno-3-pyrrolinium) derivatives], undergo a photo-induced di-π-methane rearrangement upon triplet sensitization to give the corresponding cationic dibenzosemibullvalene derivatives [*N*,*N*-dialkyl-3,4-{8c,8e-(4b,8b-dihydrodibenzo[*a*,*f*]cyclopropa[*cd*]pentaleno)}-pyrrolidinium derivatives]. Whereas the covalent attachment of a benzophenone functionality to the pyrrolinium nitrogen atom did not result in an internal triplet sensitization, the introduction of a benzophenone unit as part of the counter ion enables the di-π-methane rearrangement of the dibenzobarrelene derivative in the solid-state. Preliminary experiments indicate that a cationic pyrrolidinium-annelated dibenzosemibullvalene may act as phase-transfer catalyst in alkylation reactions.

Introduction

The di-π-methane (DPM) rearrangement is among the most thoroughly investigated organic photoreactions [1,2]. Since the discovery of the DPM rearrangement of dibenzobarrelene [3], extensive studies have been carried out to assess the mechanistic aspects of this reaction and to explore their application in synthetic organic chemistry [1-5]. Along these lines, the DPM rearrangement of dibenzobarrelene (**DBB**), also termed dibenzobicyclo[2.2.2]octatriene, and its derivatives has been investigated in detail and has provided significant insights into the mechanism of the DPM rearrangement [6,7]. The DPM rearrangement of **DBB** proceeds according to the mechanism shown in Scheme 1 through biradical intermediates **BR1** and

BR2 and leads to the formation of the corresponding dibenzosemibullvalene (**DBS**) [6,7]. Notably, the photoreactivity of the dibenzobarrelene system is multiplicity-dependent: Upon photoinduced triplet sensitization in the presence of an appropriate sensitizer, such as acetone or benzophenone, dibenzobarrelene (**DBB**) rearranges to dibenzosemibullvalene (**DBS**), whereas the direct excitation leads to dibenzocyclooctene (**DBC**) through the singlet excited-state (Scheme 1) [4,5,7]. The DPM photorearrangement of dibenzobarrelene and its derivatives is a synthetically useful reaction, because it allows the preparation of polycyclic structures which are relatively difficult to obtain by ground-state transformations [8].

During our attempts to develop novel ammonium-based phase-transfer catalysts [9-11] that are embedded within a rigid structure, we noticed that the complex dibenzosemibullvalene structure may constitute a reasonable starting point. We proposed that the general structure **pyDBS** (Figure 1), as established by the annelation of a pyrrolidinium unit to the dibenzosemibullvalene structure [12], represents an amphiphilic tetraalkylammonium derivative that exhibits three different benzene-containing concave sites to which an organic substrate may associate by attractive van der Waals interactions or π-stacking. Moreover, additional functionalities, e.g., hydroxy or amino groups, may be attached to the benzene rings of the semibullvalene structure to enable additional hydrogen bonding with the substrate. Also, the benzene rings may be further annelated with additional aromatic units to increase the potential π-stacking area [13]. Most notably, dibenzosemibullvalenes are chiral compounds, so that the propensity of an enantiopure **pyDBS** derivative to act as phase-transfer catalyst in stereoselective reactions may be considered in long-term studies. Herein we demonstrate that the pyrrolidinium-annelated dibenzosemibullvalene structure is indeed available via the DPM rearrangement of appropriately substituted dibenzobarrelene derivatives and that such a compound may act as phase-transfer catalyst in alkylation reactions.

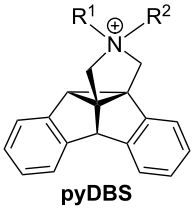

Figure 1: General structure of pyrrolidinium-annelated dibenzosemibullvalenes (**pyDBS**).

Note that according to the IUPAC rules the compounds presented in the following should be classified as pyrrolidinium or pyrrolinium derivatives because of the higher priority of the cationic heterocycles; however, for clarity and to keep the focus on the photochemical reaction we chose to name these compounds dibenzobarrelene and dibenzosemibullvalene derivatives throughout the text.

Results and Discussion

The cationic dibenzobarrelene derivatives **2a**–**g** were synthesized by the base-catalyzed reaction between the dibromomethyl-substituted dibenzobarrelene derivative **1** [14] with selected secondary amines (Scheme 2). The reaction was initially performed with a slight excess of the amine and DBU as a base in dichloromethane at room temperature, but under these conditions the products could not be completely separated from the remaining amine or the DBU catalyst, even by column chromatography. Nevertheless, the products were available in reasonable yields (47–85%) when the reaction was performed with polymer-bound DBU as catalyst (**2a**–**f**: 0.1 equiv; **2g**: 0.5 equiv) or when the quaternary ammonium derivatives were precipitated from aqueous solutions by the addition of perchloric acid to the reaction mixture and, if necessary, subsequent column chromatography. All products were identified and fully characterized by NMR spectroscopy, mass spec-

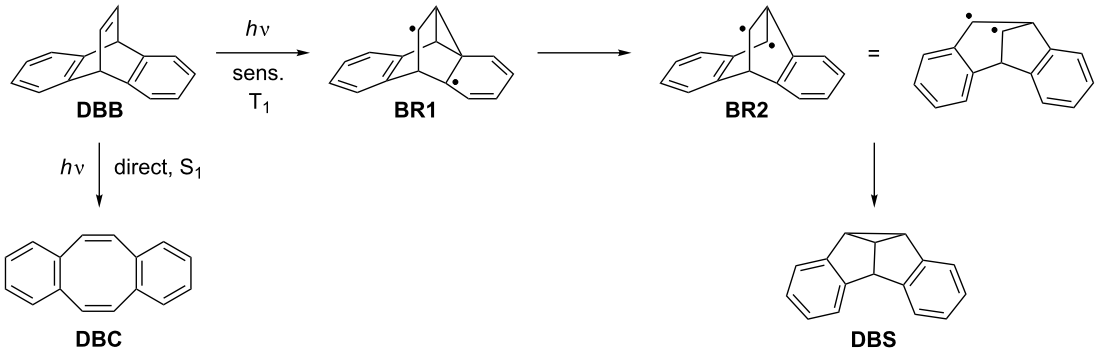

Scheme 1: Photorearrangements of dibenzobarrelene (**DBB**).

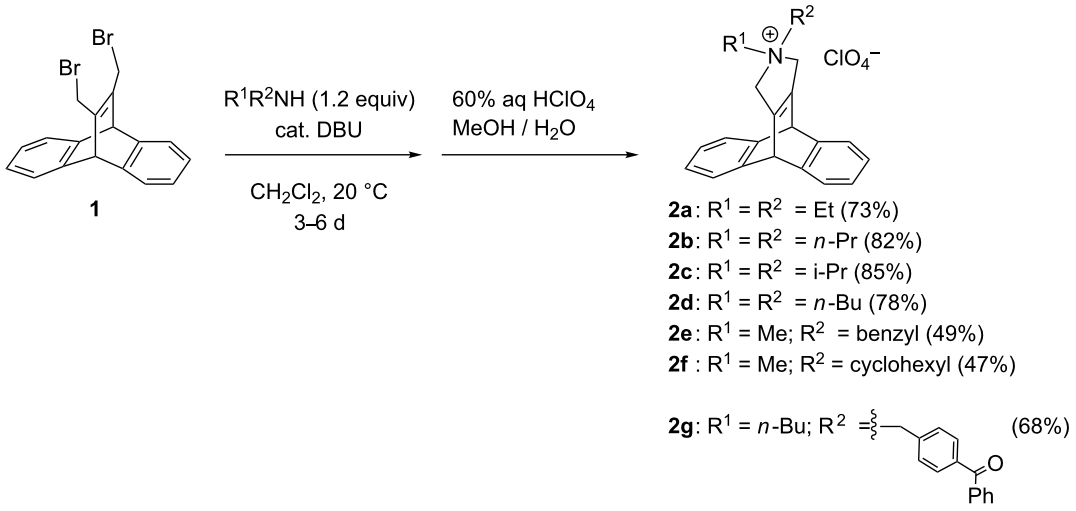

Scheme 2: Synthesis of dibenzobarrelene derivatives **2a**–**g**.

trometry and elemental analyses. In general, the perchlorate salts of **2a**–**g** have good solubility in aprotic polar solvents, especially in acetone and acetonitrile. To confer water-solubility on the cationic dibenzobarrelene derivatives **2b** and **2d**, the perchlorate salts were converted quantitatively to chlorides by ion exchange with chloride ions on an ion exchange resin.

The photolysis of the cationic dibenzobarrelene derivatives **2a**–**d**, which bear two identical *N*-alkyl substituents, was carried out in acetone solutions (λ > 310 nm), and the conversion of the dibenzobarrelene was monitored by ^{1}H NMR spectroscopy. The dibenzosemibullvalene derivatives **3a**–**d** were isolated by crystallization directly from the photolysate in 67–85% yield. The photoproducts were identified and characterized by ^{1}H NMR and ^{13}C NMR spectroscopy, mass spectrometry, and elemental analyses. The dibenzosemibullvalene structure of the photoproducts **3a**–**d** was confirmed by ^{1}H NMR spectroscopy, specifically by the characteristic singlets of the protons at the dibenzylic position at C4b (ca. 4.9 ppm) and of the cyclopropyl protons at C8b (ca. 4.0 ppm) (Scheme 3). Direct irradiation (quartz filter, λ > 254 nm) of the dibenzobarrelene derivatives **2a**–**d** resulted in complex reaction mixtures in which the characteristic ^{1}H NMR signals of dibenzosemibullvalene or dibenzocyclooctene products were not detected. Presumably, the photo-induced cleavage of the C–N bonds, i.e., a well-known photo-fragmentation of quaternary ammonium salts to give highly reactive radical intermediates [15,16], is a significant side-reaction during the direct photolysis of compounds **2a**–**d**, leading to the formation of complex reaction mixtures. The triplet-sensitized photoreaction of the dibenzobarrelene derivatives **2e**,**f**, which carry two different alkyl substituents at the quaternary pyrrolidinium, gave two isomeric dibenzosemibullvalene products **3e$^{\mathbf{I}}$**,**3f$^{\mathbf{I}}$** and **3e$^{\mathbf{II}}$**,**3f$^{\mathbf{II}}$** , in a ratio of approximately 60:40 as determined by ^{1}H NMR spectroscopic analysis of the reaction mixture (Scheme 3). The comparison was based on the two characteristic singlets of the protons at C4b and C8b

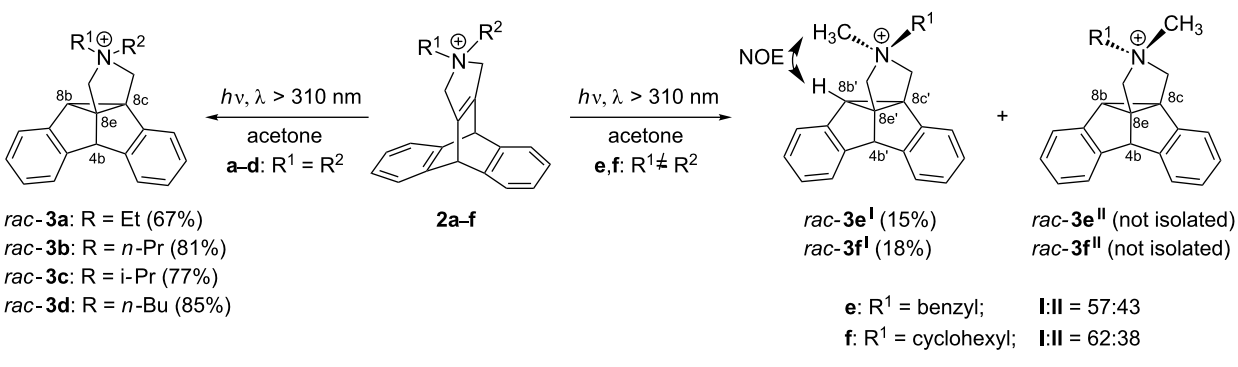

Scheme 3: Di-π-methane rearrangements of dibenzobarrelene derivatives **2a**–**f** (counter ions omitted for clarity).

of the dibenzosemibullvalene ring (**3e^{I}**: 4.30, 4.75; **3e^{II}**: 4.17, 4.91; **3f^{I}**: 4.31, 5.05 ppm; **3f^{II}**: 4.20, 5.02, in $CDCl_3$). After column chromatography and subsequent recrystallization, the major photoproducts **3e^{I}** and **3f^{I}** were isolated in low yields (15% and 18%). The relative configuration of the ammonium functionality was deduced from NOE experiments. Specifically, the close proximity between the methyl group and the methine proton (8b'-H) of the cyclopropane ring gave rise to an NOE in **3e^{I}** and **3f^{I}** (Scheme 3). The structure of the minor products **3e^{II}** and **3f^{II}**, although not isolated, were determined by ^{1}H NMR spectroscopic analyses of the photolysates. In these cases, the dibenzosemibullvalene structure was indicated by the characteristic ^{1}H NMR spectroscopic shifts of the 4b-H and 8b-H protons.

It has been demonstrated with several examples that solid-state photoreactions are an excellent tool to induce highly selective di-π-methane rearrangements of dibenzobarrelene derivatives [17], because the constrained medium within the crystal lattice allows only limited molecular movement, so that the reaction pathway with the least required molecular motion is preferred. Accordingly, the solid-state photoreactivity of the dibenzobarrelene derivatives **2a**–**f** was investigated; but unfortunately, all tested derivatives, either as chloride or as perchlorate salts, were photoinert in the crystalline state. Since one of the possible reasons for this photoinertness may be the lack of proper sensitization, the dibenzobarrelene derivative **2g** was prepared with a triplet-sensitizing functionality attached, namely the benzophenone unit. Although in acetone the dibenzobarrelene **2g** underwent a DPM rearrangement with full conversion (Scheme 4), the irradiation of **2g** in water or acetonitrile solution in the absence of an external sensitizer only induced a relatively low conversion of **2g**. Thus, irradiation of **2g** in acetonitrile for 12 h led to ca. 10% conversion with ca. 60% dibenzosemibullvalenes formed. At the same time, several unidentified byproducts were formed in significant amounts. The analysis of the photolysate by ^{1}H NMR spectroscopy revealed that independent of the solvent, the two semibullvalenes **3g^{I}** and **3g^{II}** were formed in a 45:55 ratio; however, attempts to separate the two regioisomers by chromatography were unsuccessful (Scheme 4). Derivative **2g** was also photoinert in the solid-state.

The lack of internal photosensitization of derivative **2g** resembles the behavior of the hydrochloride salt of a cationic ammoniummethyl-substituted dibenzobarrelene derivative [18] which is also photoinert in the presence of benzophenone and even acetone. It may be assumed that attachment of the benzophenone unit to the cationic dibenzobarrelene structure has an influence on the intersystem-crossing (ISC) rate or the triplet energy of the carbonyl functionality leading to insufficient sensitization. In addition, competing deactivation pathways of the excited ketone may be considered, such as rotation about the C_{ar}–CH_2 group or reaction with the chloride counter ion. However, further attempts to clarify this aspect or to optimize the conditions for sensitization were not made, because the photoreaction of **2g** upon external sensitization by acetone showed that the products of the DPM rearrangement of **2g** are formed only slowly in relatively low yield and cannot be separated.

Since the covalent attachment of a sensitizer unit to the dibenzobarrelene chromophore did not induce the desired triplet sensitization, the ionic auxiliary strategy [19] was applied to achieve triplet-sensitization in the solid-state, i.e., the sensitizer was introduced as counter anion. For this purpose, an anionic derivative of benzophenone was prepared and associated with the ammonium functionality of the dibenzobarrelene **2b** by anion metathesis (Scheme 5). The known sulfonic acid **4** [20] was transformed to the corresponding silver salt **Ag-4** by reaction with Ag_2O, and subsequent ion metathesis upon treatment with **2b-Cl** in acetonitrile gave the salt **2b-4** in 73% yield.

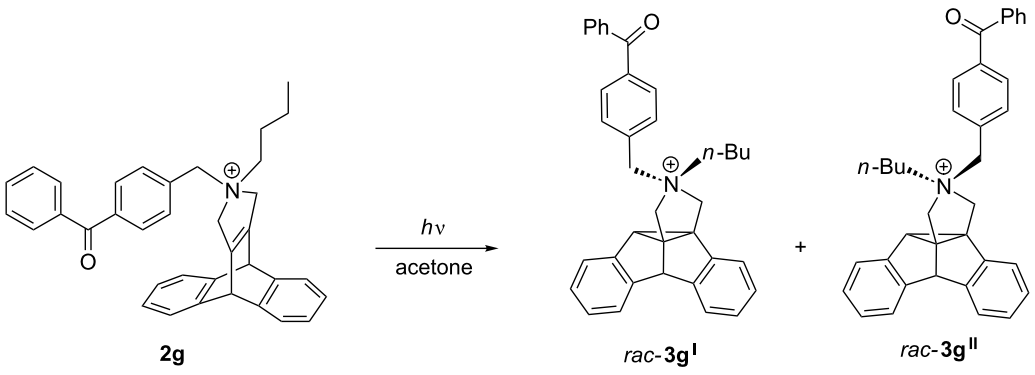

Scheme 4: Di-π-methane rearrangement of dibenzobarrelene derivative **2g**.

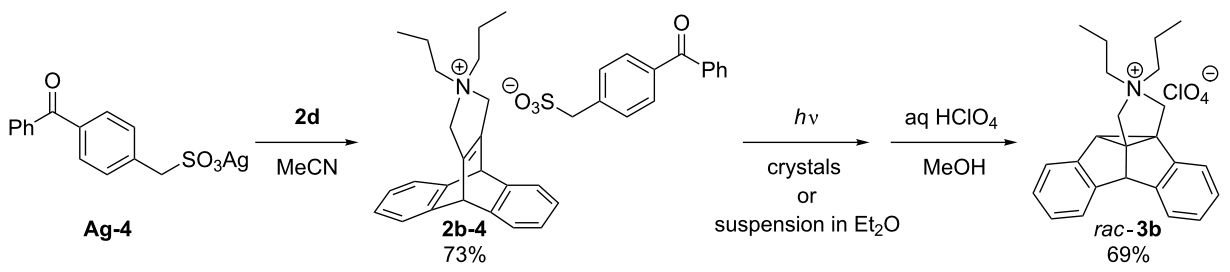

Scheme 5: Synthesis and solid-state photoreactivity of the sulfonate salt **2b-4**.

Irradiation of ground crystals of the salt **2b-4** for 2 h induced a DPM rearrangement to the dibenzosemibullvalene derivative **3b** with full conversion and without any detectable byproducts as determined by ^{1}H NMR spectroscopy. A solid-state photoreaction was also performed by the irradiation of a suspension of crystalline **2b-4** in diethyl ether. The solid products were dissolved and precipitated as perchlorate salts. Although the dibenzosemibullvalene **3b** was formed (68%), ^{1}H NMR spectroscopic analysis of the photolysate indicated the additional formation of significant amounts of byproducts (ca. 15%). These results indicate that, in principle, the internal sensitization of the DPM rearrangement of the cationic dibenzobarrelene derivatives may be achieved in a solid-state reaction with a sensitizing counter ion; however, the sensitization by acetone solvent appears to be more practical as it allows the handling of larger scales.

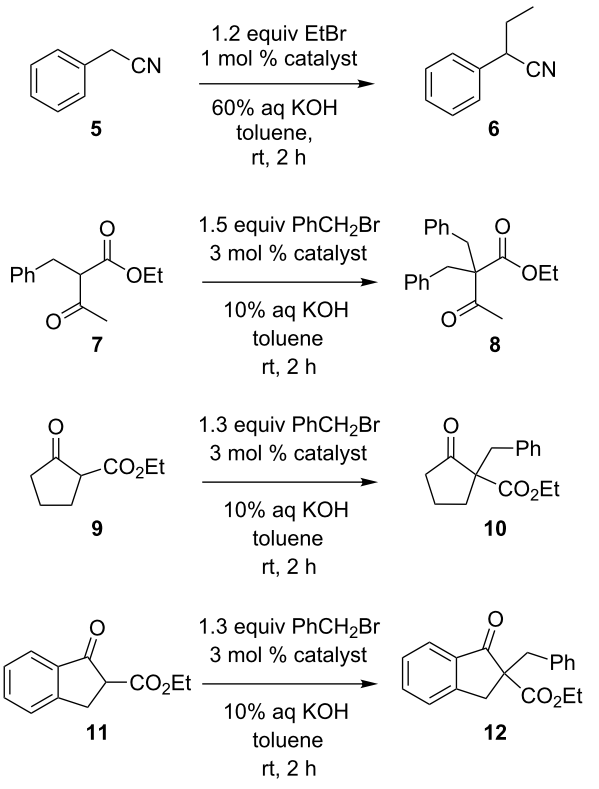

Scheme 6: Phase-transfer catalyzed alkylation reactions (see Table 1 for details).

The general catalytic ability of the dibenzosemibullvalene salt **3d** in phase-transfer catalyzed nucleophilic substitution reactions was investigated. Compounds **5** [21], **7**, **9**, and **11** were chosen as substrates in alkylation reactions under phase-transfer conditions, and the catalytic activity of **3d** was compared with a tetrabutylammonium salt (Scheme 6, Table 1; TBAB = tetrabutylammonium bromide; TBAC = tetrabutylammonium chloride.). All four reactions under investigation were significantly accelerated in the presence of substoichiometric amounts of the quaternary ammonium catalysts. Notably, under identical conditions the dibenzosemibullvalene salt **3d** induced higher conversions in the phase-transfer reactions than the tetrabutylammonium salts, except for the alkylation of compound **5**, in which

Table 1: Phase-transfer catalyzed alkylation reactions according to Scheme 6.

Substrate	Catalyst[a]	Conv.[b] / %
5	–	5[c]
5	TBAB	92[c]
5	**3d**	32[c]
7	–	2
7	TBAC	36
7	**3d**	82
9	–	5
9	TBAC	81
9	**3d**	95
11	–	4
11	TBAC	49
11	**3d**	>97

[a]TBAB = tetrabutylammonium bromide; TBAC = tetrabutylammonium chloride. [b]Conversion determined by ^{1}H NMR spectroscopic analysis of the reaction mixture, relative to 2,7-dimethyl naphthalene as internal standard; estimated error: ±3% of the given value. [c]Determined by GC analysis, relative to ethyl acetate as internal standard.

92% conversion was achieved using TBAB, whereas under identical conditions a conversion of only 32% was obtained with dibenzosemibullvalene **3d** as the catalyst. In contrast, the alkylation of the β-oxoester **7** in the presence of **3d** gave the product in 82% conversion after 2 h at room temperature, whereas with TBAC as catalyst the conversion was only 36% under identical conditions. The dibenzosemibullvalene salt **3d** was also found to be more efficient in the alkylation of cyclic β-oxoesters **9** and **11**, as compared with the TBAC catalyst (Table 1). Interestingly, the alkylation of the indanone derivative **11** is less efficient in the presence of TBAC as compared with the non-aromatic cyclopentanone derivative **9**, whereas in the presence of dibenzosemibullvalene **3d** both substrates are alkylated with comparable efficiency.

Conclusion

In summary, it was shown that cationic pyrrolinium-annelated dibenzosemibullvalene derivatives are accessable by the photoinduced di-π-methane rearrangement of appropriately substituted dibenzobarrelene substrates. With one representative example, it was demonstrated that these compounds may act as phase-transfer catalysts in alkylation reactions with comparable or even better performance than the commonly employed tetrabutylammonium salts. It is therefore concluded that this class of chiral compounds may be used as a promising platform for the development of versatile phase-transfer catalysts.

Experimental

General remarks: NMR spectra were recorded on a Bruker Avance 400 (^{1}H NMR: 400 MHz; ^{13}C NMR: 100 MHz) and a Varian NMR system 600 (^{1}H NMR: 600 MHz; ^{13}C NMR: 150 MHz). ^{1}H NMR chemical shifts are given relative to δ_{TMS} = 0.00 ppm, and ^{13}C NMR chemical shifts refer to either the TMS signal (δ_{TMS} = 0.00 ppm) or the solvent signals [$CDCl_3$: 77.0 ppm; CD_3OD: 49.0 ppm; $(CD_3)_2CO$: 29.8 ppm, CD_3CN: 118.2 ppm, $(CD_3)_2SO$: 39.5 ppm]. Melting points were determined with a Büchi 510K and are uncorrected. Mass spectra were recorded on a Hewlett-Packard HP 5968 (EI) and a Finnigan LCQ Deca instrument (ESI). Elemental analyses were performed on a KEKA-tech EuroEA combustion analyzer by Mr. H. Bodenstedt, Organic Chemistry I, University of Siegen. TLC analyses were performed on silica-gel sheets (Macherey-Nagel Polygram Sil G/UV$_{254}$). Unless otherwise noted, commercially available chemicals were reagent grade and used without further purification. Polymer-bound DBU (polystyrene cross-linked with 1% divinylbenzene; loading: 1.15 mmol/g) was obtained from Aldrich. Anhydrous THF and diethyl ether were obtained by distillation from sodium wire, and anhydrous CH_2Cl_2 was distilled from calcium hydride. Distilled water was used for all the synthetic reactions performed. Preparative column chromatography was performed on MN Silica Gel 60 M (particle size 0.04–0.063 mm, 230–440 mesh).

Synthesis of dibenzobarrelene derivatives

General procedure for the preparation of *N*,*N*-dialkyl-3,4-(9',10'-dihydro-9',10'-anthraceno-3-pyrrolinium derivatives (GP-1): A mixture of 11,12-bis(bromomethyl)-9,10-dihydro-9,10-ethenoanthracene (**1**, 1.0–5.0 mmol), the corresponding secondary amine (1.2 equiv) and catalytic amount of DBU (0.1 equiv or otherwise explicitly specified) in dichloromethane (10 ml/mmol of **1**) was stirred at room temperature for 3–6 days until TLC analysis indicated the full conversion of **1**. The solvent was removed in vacuo and the residue re-dissolved in methanol (10–25 ml depending on the scale and solubility); if necessary, gentle heating was applied to dissolve the residue. Aqueous perchloric acid (60%, 1–3 ml) was added to the mixture. The perchlorate salt of the ammonium-dibenzobarrelene derivative precipitated spontaneously, or upon subsequent addition of a few drops of water. The solid was collected by filtration, washed with cold methanol and recrystallized from acetone. In those cases when no solid product precipitated from the methanol solution, water was added and the mixture extracted with dichloromethane. The organic layer was concentrated and the product purified by column chromatography (SiO_2; 3–5% MeOH in dichloromethane).

The corresponding chloride salts were prepared by dissolving the perchlorate salt in MeCN and passing the solution through an ion-exchange column (DOWEX 1 x 8, Cl^- form). After removal of the solvent in vacuo, the residue was crystallized from Et_2O/MeOH.

***N*,*N*-Di-*n*-butyl-3,4-(9',10'-dihydro-9',10'-anthraceno)-3-pyrrolinium perchlorate (2d)**: Prepared from dibenzobarrelene **1** (1.60 g, 4.08 mmol) according to **GP-1**, yield 1.46 g (3.18 mmol, 78%), colorless prisms, mp 173–174 °C. ^{1}H NMR [400 MHz, $(CD_3)_2CO$]: δ = 0.75 (t, *J* = 7 Hz, 6H, CH_3), 1.20–1.26 (m, 4H, C*H*$_2$CH$_3$), 1.42–1.46 (m, 4H, C*H*$_2$CH$_2$CH$_3$), 3.52–3.56 (m, 4H, NC*H*$_2$CH$_2$), 4.72 (s, 4H, C=CC*H*$_2$N), 5.39 (s, 2H, C*H*), 6.99, 7.39 (AA'BB'-system, 8H, CH_{ar}). ^{13}C NMR [100 MHz, $(CD_3)_2CO$]: δ = 14.1 (CH_3), 20.7 (CH_2), 26.5 (CH_2), 49.8 (CH_2), 65.6 (CH_2), 69.0 (CH), 124.8 (CH_{ar}), 126.1 (CH_{ar}), 144.6 (C_q), 146.9 (C_q). UV (CH_2Cl_2): λ_{max} (log ε) = 273 (4.00), 280 (4.17). MS (ESI$^+$): *m/z* (%) = 358 (100). Anal. Calcd for $C_{26}H_{32}ClNO_4$ (458.0): C, 68.18; H, 7.04; N, 3.06. Found: C, 68.22; H, 7.12; N, 3.05.

***N*,*N*-Di-*n*-butyl-3,4-(9',10'-dihydro-9',10'-anthraceno-3-pyrrolinium chloride (2d-Cl)**: Obtained quantitatively (1.37 g, 3.47 mmol) as a white powder by ion exchange of the perchlorate **2d** (1.59 g, 3.47 mmol; eluent: acetonitrile; DOWEX resin).

mp 194–195 °C. ^{1}H NMR (400 MHz, CD_3CN): δ = 0.78 (t, *J* = 7 Hz, 6H, CH_3), 1.16–1.34 (m, 8H, $CH_2CH_2CH_3$), 3.28–3.30 (m, 4H, NCH_2CH_2, overlapped with the solvent signal), 4.48 (s, 4H, C=CCH_2N), 5.12 (s, 2H, C**H**), 6.99, 7.35 (AA'BB'-system, 8H, CH_{ar}). ^{13}C NMR (100 MHz, CD_3CN): δ = 13.9 (CH_3), 20.8 (CH_2), 26.5 (CH_2), 50.0 (CH_2), 65.7 (CH_2), 68.7 (CH), 126.2 (CH_{ar}), 126.7 (CH_{ar}), 144.6 (C_q), 147.0 (C_q).

Synthesis of dibenzosemibullvalene derivatives

General procedure for the photolysis in solution **(GP-2)**: Solutions of the substrates (10^{-2} to 10^{-3} mol/l) were placed in a 200 ml Duran flask (acetone) or a quartz test tube (other solvents), and argon gas was bubbled through the solution for at least 20 min. The solution was stirred and irradiated for 4–15 h until the starting material was fully converted, as determined by TLC or ^{1}H NMR spectroscopic analysis. After evaporation of the solvent in vacuo, the photolysate was analyzed by ^{1}H NMR spectroscopy, or, in preparative experiments, isolated by recrystallization or column chromatography to obtain the photoproduct.

***rac*-*N*,*N*-Di-*n*-butyl-4b',8b',8c',8e'-dibenzo[*a*,*f*]cyclopropa[*cd*]pentaleno-pyrrolidinium perchlorate (3d)**: Prepared from **2d** (50.0 mg, 0.11 mmol) according to **GP-2** in acetone solution as colorless prisms (42.0 mg, 0.09 mmol, 85%), mp 176–178 °C. ^{1}H NMR (400 MHz, CD_3CN): δ 0.61 (t, *J* = 7 Hz, 3H, CH_3), 0.74 (t, *J* = 7 Hz, 3H, CH_3), 0.85–0.94 (m, 1H, CH_2), 0.99–1.07 (m, 1H, CH_2), 1.16–1.33 (m, 4H, CH_2), 1.33–1.39 (m, 2H, CH_2), 2.74–2.82 (m, 1H, CH_2), 2.88–2.95 (m, 2H, CH_2), 3.48 (d, *J* = 13 Hz, 1H, NC*H*HC), 3.73 (d, *J* = 13 Hz, 1H, NC*H*HC), 4.04 (s, 1 H, CH), 4.24 (d, *J* = 13 Hz, 1H, NCH*H*C), 4.57 (d, *J* = 13 Hz, 1H, NCH*H*C), 4.91 (s, 1H, CH), 6.97–7.01 (m, 2H, CH_{ar}), 7.09–7.17 (m, 4H, CH_{ar}), 7.34–7.37 (m, 1H, CH_{ar}), 7.39–7.41 (m, 1 H, CH_{ar}), 7.38–7.40 (m, 1H, CH_{ar}). ^{13}C NMR (100 MHz, CD_3CN): δ 13.0 (CH_3), 13.6 (CH_3), 20.1 (CH_2), 20.3 (CH_2), 24.8 (CH_2), 25.8 (CH_2), 55.5 (CH_2), 55.7 (CH_2), 59.8 (CH_2), 60.0 (CH_2), 61.9 (C_q), 67.3 (CH), 69.4 (C_q), 70.1 (CH), 122.5 (CH_{ar}), 123.3 (CH_{ar}), 125.8 (CH_{ar}), 125.9 (CH_{ar}), 127.7 (CH_{ar}), 128.3 (CH_{ar}), 128.4 (CH_{ar}), 128.9 (CH_{ar}), 137.0 (C_q), 137.1 (C_q), 152.0 (C_q), 154.5 (C_q). MS (ESI$^+$): *m/z* (%) = 358 (100). Anal. Calcd for $C_{26}H_{32}ClNO_4$ (458.0): C, 68.18; H, 7.04; N, 3.06. Found: C, 68.22; H, 7.14; N, 3.06.

Phase-transfer catalyzed (PTC) alkylation reactions

a) Analysis with gas chromatography: A biphasic mixture of the quaternary ammonium catalyst **3d** or TBAC (0.05 mmol), phenylacetonitrile (**5**, 506 mg, 4.32 mmol) and bromoethane (808 mg, 4.75 mmol) in toluene (0.85 ml) and aqueous KOH solution (4 ml, 60%) was stirred for 2 h at 20 °C. Water (10 ml) and toluene (10 ml) were added and the mixture was thoroughly shaken. After phase separation, the organic layer was analyzed by gas chromatography.

Stationary Phase: HP-5 PhMe-Silica, crosslinked 5%, 25 m; *Mobile Phase*: Argon gas; *Flow Pressure*: 30 kPa; *Temperature*: Oven 220 °C, Injector 250 °C, Detector 250 °C; *Retention* time: $PhCH_2CN$ 9.6 min; $PhCH(CH_2CH_3)CN$ 10.6 min.

Three PTC reactions were performed in parallel with a) no catalyst, b) TBAB as the catalyst, or c) **3d** as the catalyst.

NMR-spectroscopically monitored PTC reactions: A biphasic mixture of the quaternary ammonium catalyst (0.03 mmol), the substrate (0.10 mmol), benzylchloride (1.25–1.50 equiv) and 2,7-dimethylnaphthalene (as internal standard, 0.025 mmol) in toluene (5 ml) and aqueous KOH solution (5 ml, 10%) was stirred for 2 h at 20 °C. At the end of reaction, water (10 ml) and toluene (10 ml) were added and the mixture was thoroughly shaken. The separated organic phase was analyzed by ^{1}H NMR spectroscopy, and the conversion calculated by comparison with the signal of the methyl protons of 2,7-dimethylnaphthalene (δ = 2.49 ppm, in $CDCl_3$).

Three reactions were run in parallel with a) no catalyst, b) TBAC as the catalyst or c) **3d** as the catalyst.

Supporting Information

Supporting Information File 1

Experimental procedures, characterization data and copies of ^{1}H NMR and ^{13}C NMR spectra of compounds **2a**–**g** and **3a**–**f**.
[http://www.beilstein-journals.org/bjoc/content/supplementary/1860-5397-7-17-S1.pdf]

Acknowledgements

We thank the Deutsche Akademische Austauschdienst for a fellowship to J. L. (DAAD-Abschluss-Stipendium) and Mr. Maoqun Tian, University of Siegen, for assistance during the preparation of this manuscript.

References

1. Zimmerman, H. E.; Armesto, D. *Chem. Rev.* **1996,** *96,* 3065–3112. doi:10.1021/cr910109c
2. Armesto, D.; Ortiz, M. J.; Agarrabeitia, A. R. Di-π-Methane Rearrangement In Synthetic Organic Photochemistry. In *Molecular and Supramolecular Photochemistry;* Griebeck, A.; Mattay, J., Eds.; Marcel Dekker: New York, 2005; Vol. 12, pp 161–181.

3. Ciganek, E. *J. Am. Chem. Soc.* **1966,** *88,* 2882–2883. doi:10.1021/ja00964a068
4. Armesto, D. The Aza-di-π-methane Rearrangement. In *CRC Handbook of Organic Photochemistry and Photobiology,* 1st ed.; Horspool, W. M.; Song, P.-S., Eds.; CRC Press: New York, 1995; pp 915–930. For aza-DPM rearrangements.
5. Singh, V. Photochemical Rearrangements in β,γ-Unsaturated Enones, The Oxa-di-π-methane Rearrangement. In *CRC Handbook of Organic Photochemistry and Photobiology,* 2nd ed.; Horspool, W. M.; Lenci, F., Eds.; CRC Press: New York, 2004; 78.1–78.34. For oxa-DPM rearrangements.
6. Zimmerman, H. E.; Sulzbach, H. M.; Tollefson, M. B. *J. Am. Chem. Soc.* **1993,** *115,* 6548–6556. doi:10.1021/ja00068a011
7. Scheffer, J. R.; Yang, J. The Photochemistry of Dibenzobarrelene (9,10-Ethenoanthracene) and Its Derivatives. In *CRC Handbook of Organic Photochemistry and Photobiology,* 1st ed.; Horspool, W. M.; Song, P.-S., Eds.; CRC Press: New York, 1995; pp 204–221.
8. Ramaiah, D.; Sajimon, M. C.; Joseph, J.; George, M. V. *Chem. Soc. Rev.* **2005,** *34,* 48–57. doi:10.1039/b300843f
9. Halpern, M. E. *Phase Transfer Catalysis, Mechanisms and Synthesis;* American Chemistry Society: Washington DC, 1997. For relevant aspects on phase-transfer catalysis.
10. Starks, C. M.; Liotta, C. L.; Halper, M. *Phase-transfer catalysis: fundamentals, applications, and industrial perspectives,* 1st ed.; Springer: New York, 1994.
11. Dehmlow, E. V.; Dehmlow, S. S. *Phase transfer catalysis,* 1st ed.; VCH: Weinheim, 1980.
12. Ciganek, E. *J. Org. Chem.* **1980,** *45,* 1505–1512. doi:10.1021/jo01296a032
13. Luo, J.; Ihmels, H.; Deiseroth, H.-J.; Schlosser, M. *Can. J. Chem.* **2009,** *87,* 619–626. doi:10.1139/V09-035
14. Anantanarayan, A.; Hart, H. *J. Org. Chem.* **1991,** *56,* 991–996. doi:10.1021/jo00003a019
15. Appleton, D. C.; Bull, D. C.; Givens, R. S.; Lillis, V.; McKenna, J. M.; Thackeray, S.; Walley, A. R. *J. Chem. Soc., Perkin Trans. 2* **1980,** 77–82. doi:10.1039/p29800000077
16. Breslin, D. T.; Saeva, F. D. *J. Org. Chem.* **1988,** *53,* 713–715. doi:10.1021/jo00239a001
17. Chen, J.; Scheffer, J. R.; Trotter, J. *Tetrahedron* **1992,** *48,* 3251–3274. doi:10.1016/0040-4020(92)85002-V
18. Scheffer, J. R.; Ihmels, H. *Liebigs Ann./Recl.* **1997,** 1925–1929. doi:10.1002/jlac.199719970919
19. Gamlin, J. N.; Jones, R.; Leibovitch, M.; Patrick, B.; Scheffer, J. R.; Trotter, J. *Acc. Chem. Res.* **1996,** *29,* 203–209. doi:10.1021/ar950165q
20. Barker, P.; Bottom, R. A.; Guthrie, J. T.; Godfrey, A. A.; Green, P. N.; Young, J. R. A. *Res. Discl.* **1981,** *93,* No. 20221.
21. Barbasiewicz, M.; Marciniak, K.; Fedoryński, M. *Tetrahedron Lett.* **2006,** *47,* 3871–3874. doi:10.1016/j.tetlet.2006.03.176

License and Terms

Beilstein Journal of Organic Chemistry

Photocycloaddition of aromatic and aliphatic aldehydes to isoxazoles: Cycloaddition reactivity and stability studies

Axel G. Griesbeck*, Marco Franke, Jörg Neudörfl and Hidehiro Kotaka

Full Research Paper

Open Access

Address:
University of Cologne, Department of Chemistry, Organic Chemistry, Greinstr. 4, D-50939 Köln, Germany; Fax: +49(221)470 5057

Email:
Axel G. Griesbeck* - griesbeck@uni-koeln.de

* Corresponding author

Keywords:
isoxazoles; oxetanes; Paternò–Büchi reaction; photochemistry

Beilstein J. Org. Chem. **2011,** *7,* 127–134.
doi:10.3762/bjoc.7.18

Received: 17 October 2010
Accepted: 17 December 2010
Published: 26 January 2011

This article is part of the Thematic Series "Photocycloadditions and photorearrangements".

Guest Editor: A. G. Griesbeck

Abstract

The first photocycloadditions of aromatic and aliphatic aldehydes to methylated isoxazoles are reported. The reactions lead solely to the *exo*-adducts with high regio- and diastereoselectivities. Ring methylation of the isoxazole substrates is crucial for high conversions and product stability. The 6-arylated bicyclic oxetanes **9a**–**9c** were characterized by X-ray structure analyses and showed the highest thermal stabilities. All oxetanes formed from isoxazoles were highly acid-sensitive and also thermally unstable. Cleavage to the original substrates is dominant and the isoxazole derived oxetanes show type T photochromism.

Introduction

Photochemical [2 + 2] cycloadditions are among the most efficient photoreactions and are used in numerous synthetic applications due to the generation of highly reactive four-membered rings. An important example is the photocycloaddition of electronically excited carbonyl compounds to alkenes (Paternò–Büchi reaction). This reaction is a superior route to oxetanes, which can be subsequently transformed into polyfunctionalized products [1]. With regards to the regio- and diastereoselectivity of the Paternò–Büchi reaction, recent experimental and computational studies have brought about a remarkable increase in our understanding of this reaction. Especially the role of intermediary triplet 1,4-biradicals – their stability, lifetimes and intersystem crossing geometries – was crucial for a more sophisticated description [2-5], which also improved the synthetic significance of this reaction [6].

Previous publications have clearly demonstrated the versatility of the Paternò–Büchi reaction in various synthetic applications which gives rise to a multiplicity of different products. The photocycloaddition of furans to carbonyl compounds affords the corresponding β-hydroxy-1,4-diketones after hydrolysis of the primary photochemical products (photo aldol reaction) [7],

whilst the reaction of oxazoles with carbonyl compounds is a convenient protocol for the stereoselective synthesis of α-amino β-hydroxy ketones [8,9] as well as highly substituted α-amino β-hydroxy acids [10,11].

The results on five-membered aromatic heterocycles published so far, however, has not included a study of isoxazoles as substrates in the Paternò–Büchi reaction. This class of heterocyclic compounds can be considered as masked β-amino ketones [12], and subsequently hydrolysed to the corresponding 1,3-diketones [13] or deaminated to yield Michael systems [14]. Thus, isoxazoles also appear to be important substrates for carbonyl–ene photocycloaddition due to possible applications in ring-opening transformations.

Results and Discussion

Synthesis of the isoxazole substrates

The substrates isoxazole (**7a**), 5-methylisoxazole (**7b**), 3,5-dimethylisoxazole (**7d**) and 3,4,5-trimethylisoxazole (**7e**) were synthesized by reaction of the corresponding carbonyl compounds with hydroxylamine, while 3-methylisoxazole (**7c**) was obtained by the [3 + 2]-cycloaddition of acrylonitrile with the trimethylsilylester of *aci*-nitroethane **1** (Scheme 1). The reaction of acetylacetaldehyde with hydroxylamine gave **7b**, exclusively.

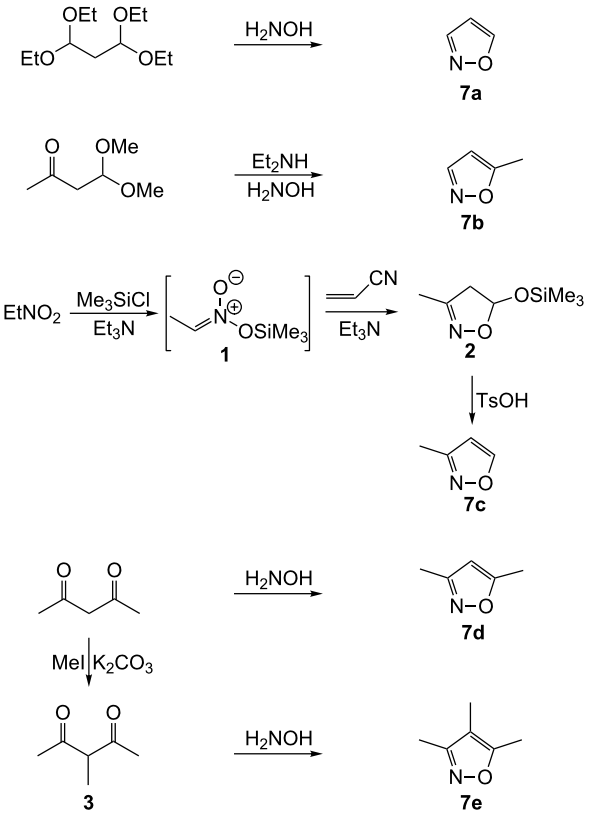

Scheme 1: Synthetic routes to isoxazoles **7a**–**7e**.

3,5-Diphenylisoxazole (**7f**) was prepared from acetophenone and methyl benzoate, followed by cyclization of the resulting diketone **4** with hydroxylamine. 5-Methoxy-3-phenylisoxazole (**7g**) and 5-(trimethylsilyloxy)-3-phenylisoxazole (**7h**) were synthesized from 3-phenylisoxazol-5-one (**5**) which was obtained by the reaction of ethyl benzoylacetate and hydroxylamine (Scheme 2). The preparation of aliphatic substituted isoxazole ethers however, could not be achieved, since the corresponding isoxazolones were unstable.

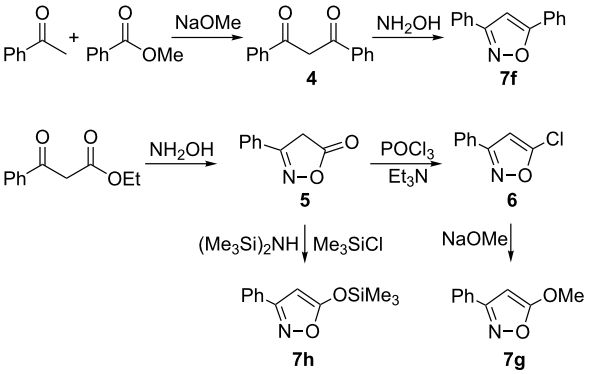

Scheme 2: Synthetic routes to isoxazoles **7f**–**7h**.

Photochemistry of the isoxazoles **7a**–**h**: test reactions

The isoxazoles **7a**–**e** were irradiated in the presence of benzaldehyde or propionaldehyde as model compounds for aromatic and aliphatic carbonyl compounds, respectively, at λ = 300 nm in perdeuterated acetonitrile. ^{1}H NMR studies showed that the expected photoadducts were formed only from isoxazoles **7d** and **7e** with benzaldehyde (Scheme 3 and Table 1). In the presence of propionaldehyde no reaction was observed.

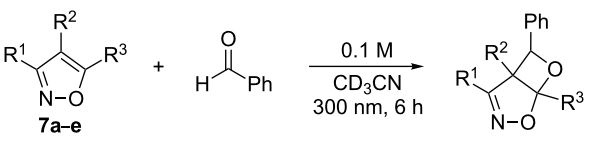

Scheme 3: Benzaldehyde photocycloaddition to **7a**–**7e**.

The use of a tenfold excess of aldehyde had no significant influence on the reaction. The use of a tenfold excess of the isoxazole, however, led to a considerable change in the reaction conversions (Table 2).

Table 1: Irradiation of isoxazoles **7a–e** with benzaldehyde.

	R^1	R^2	R^3	conversion [%][a]
7a	H	H	H	0
7b	H	H	Me	0
7c	Me	H	H	0
7d	Me	H	Me	13
7e	Me	Me	Me	41

[a]based on the formation of the photoproduct, by NMR (benzaldehyde - isoxazole ratio = 1:1, irradiation time: 6 h).

Table 2: Irradiations of **7a–e** with a tenfold excess of isoxazoles.

	R^1	R^2	R^3	conversion [%][a]
7a	H	H	H	<5
7b	H	H	Me	15
7c	Me	H	H	10
7d	Me	H	Me	40
7e	Me	Me	Me	98

[a]based on the formation of the photoproduct, by NMR (benzaldehyde - isoxazole ratio = 1:10, irradiation time: 6 h).

The conversion is highly dependent on the degree of substitution of the isoxazole used. In terms of frontier orbital interactions, the reason is the decreasing energy difference between the HOMO of the isoxazole and the SOMO of the excited aldehyde with increasing degree of substitution. Indirect proof of the increasing energy levels of the isoxazole-HOMO is provided from the corresponding ionization energies (Table 3) [15] which decrease with increasing substitution.

Table 3: Vertical ionization energies (E_{iv}) of isoxazoles **7a**, **7b** and **7d**.

	E_{iv} [eV]
7a	10.15
7b	9.61
7d	9.34

In contrast, the use of a tenfold excess of isoxazole in presence of propionaldehyde did not lead to an increased formation of the corresponding photoadducts. Only in the case of **7e** could traces of the expected photoproduct be detected (<5%). Since the LUMO energy of propionaldehyde is larger than that of benzaldehyde, it can be assumed that the energy difference between the isoxazole-HOMO and the aldehyde-LUMO is too large to promote an efficient reaction.

The isoxazoles **7f–h** were treated similarly to **7a–e**. However, in these experiments, the formation of the corresponding Paternò–Büchi products were not observed, neither in the presence of propionaldehyde nor in the presence of benzaldehyde. Instead, a reaction could be observed which also occurred both in the presence of a tenfold excess of aldehyde or without any aldehyde. This reaction was identified as the intramolecular ring contraction of **7f–h** to yield the corresponding azirines **8a–c** (Scheme 4) [16].

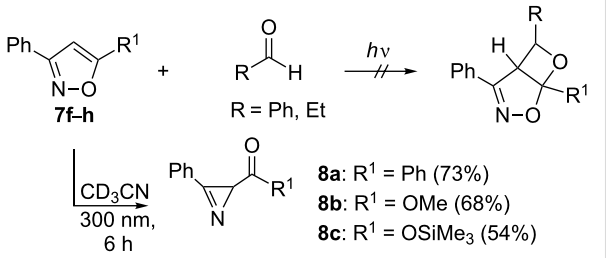

Scheme 4: Photochemical ring contraction of isoxazoles **7f–7h**.

Surprisingly, in the absence of aldehydes as the potential reaction partners, the conversions of **7f–h** were significantly lower, suggesting the possibility of an energy transfer from the excited singlet or triplet aldehyde to the isoxazole.

Since the photolysis of **7d** and **7e** in presence of benzaldehyde showed the highest conversions, further irradiations were conducted in order to examine the effect of other aryl substituted aldehydes on reaction conversions (Scheme 5, Table 4).

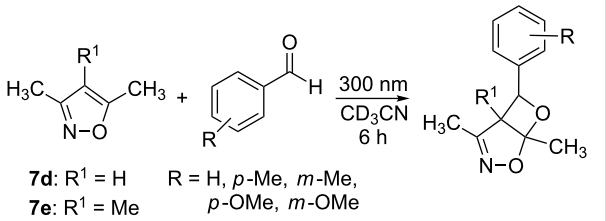

Scheme 5: Photocycloaddition of aromatic aldehydes to di- and trimethyl isoxazoles **7d** and **7e**.

The reactions of **7e** with *p*- and *m*-tolualdehyde showed no change in the reaction conversions compared with benzaldehyde, whilst the conversions of **7d** with these two aldehydes were considerably decreased. Irradiation of **7d** and **7e** with *p*- and *m*-anisaldehyde showed in all cases lower reaction conversions.

Table 4: Photocycloadditions of **7d** and **7e** with aromatic aldehydes.

	R	conversion [%][a]
7d	H	40
"	*p*-Me	18
"	*m*-Me	18
"	*p*-OMe	<5
"	*m*-OMe	0
7e	H	98
"	*p*-Me	96
"	*m*-Me	92
"	*p*-OMe	65
"	*m*-OMe	19

[a]based on the formation of the photoproduct (aldehyde - isoxazole = 1:10, irradiation time: 6 h).

Synthesis of oxetanes from **7e** and aryl substituted aldehydes

The preparative photoreactions of **7e** together with aryl substituted aldehydes were carried out in acetonitrile at −10 °C in presence of 10 mol % potassium carbonate (in order to neutralize traces of acid). In all cases, the regioisomers **9a**–**c** were formed with excellent (*exo*) diastereoselectivity (> 99:1, by ^{1}H NMR spectroscopy) in moderate yields and high purities (Scheme 6).

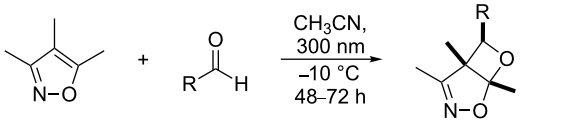

7e

9a: R = Ph 50%
9b: R = *p*-Tol 35%
9c: R = *m*-Tol 65%

Scheme 6: Preparative photocycloadditions of **7e** with aromatic aldehydes.

The chemical structures of these bicyclic oxetanes were established on the basis of the NMR- and X-ray data (Figure 1) [17].

Both regio- and diastereoselectivity are in accord with the rules previously reported for the carbonyl-furan photocycloaddition [3]: High regiocontrol due to the FMO-controlled formation of the corresponding triplet 1,4-biradical and high stereocontrol due to SOC-controlled crossing from the triplet to the singlet surface [4,5].

Reaction behavior of the photoproducts **9a–c**

All bicyclic oxetanes obtained in the analytical photochemical experiments as well as in preparative studies (i.e., **9a**–**c**) were acid labile and decomposed already in the presence of catalytic amounts of acid to give solely the starting materials. The photoproducts are also thermally labile and decompose at temperatures above approximately 100 °C, again to give solely the starting materials. Thus, isoxazole-carbonyl photocycloaddition products constitute another class of photochromic T-type systems (Scheme 7) [18].

Hydrogenation of **9a** by palladium/charcoal did not lead to the expected aminoketone **10**, but to the enamino ketone **11** and benzyl alcohol, indicating decomposition of **9a** back to the starting materials, followed by hydrogenation of these substrates (Scheme 8). Variations of reaction temperature (−10 °C), reaction time (6 h, 1 h) and solvent (ethanol, ethyl acetate) led to the same results.

Hydrogenation of **9a** by Raney-nickel led to partial decomposition without any further reaction, whilst treatment with lithium aluminium hydride (3 equiv) yielded complex mixtures with benzyl alcohol as one of the main components. By contrast, no reaction could be observed in presence of sodium borohydride or sodium cyanoborohydride. Attempted reduction with sodium triacetoxyborohydride led to decomposition, probably due to

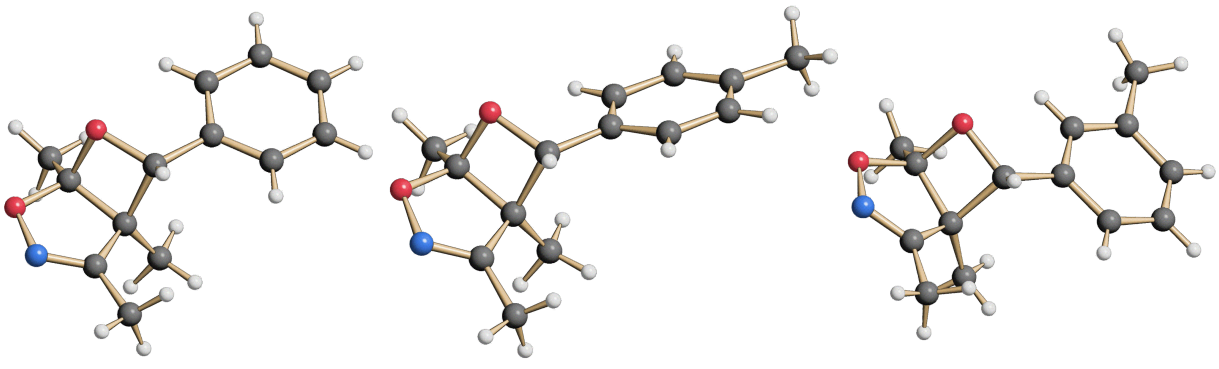

Figure 1: Structures of the photoproducts **9a**–**9c** in the crystal.

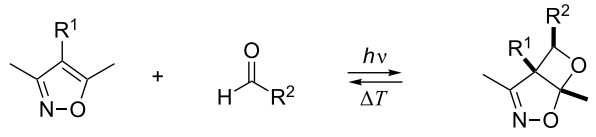

Scheme 7: T-type photochromism of isoxazole–aldehyde pairs.

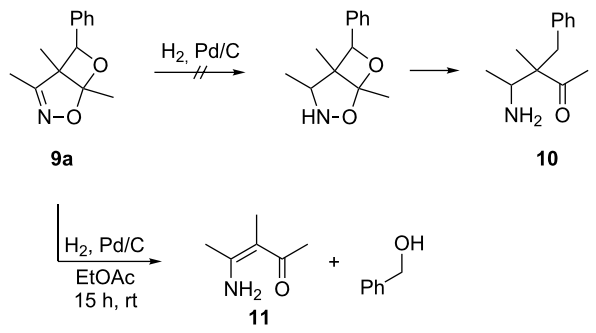

Scheme 8: Reductive cleavage of the trimethylisoxazole adduct **9a**.

traces of acetic acid contained in the hydride reagent. Reductive treatment with sodium or samarium diiodide also led to decomposition of the photoproduct. Treatment of **9a** with ethylmagnesium bromide did not lead to the alkylated photoproduct, but to partial decomposition into isoxazole **7e** and benzaldehyde, while at −78 °C, no reaction could be observed. In contrast, the use of an excess of Grignard reagent (3 equiv) at −78 °C again led to decomposition. The application of boron trifluoride at −78 °C also led to decomposition, followed by a normal nucleophilic attack of the Grignard reagent on the liberated benzaldehyde.

Conclusion

The photocycloaddition of electronically excited carbonyl compounds to isoxazoles is clearly less effective than with other five-membered aromatic or non-aromatic heterocycles (furans, thiophenes, pyrroles, oxazoles, dihydrofurans, dihydropyrroles) [1]. Only the combination of methylated isoxazoles and aromatic aldehydes is sufficient to allow photochemical addition and give adducts with sufficient thermal stability. It cannot be excluded at the current stage, that other combinations are also reactive in Paternò–Büchi chemistry resulting in thermally labile cycloadducts which thus have not yet been detected. Apparently, the bicyclic oxetanes isolated in this study are acid-labile and thermally unstable and thus constitute a new class of T-type chromophoric systems.

Experimental

General methods. All solvents were dried before use. Benzene, toluene and chloroform were distilled from CaH_2. ^{1}H NMR and ^{13}C NMR spectra were recorded on a Bruker AV 300 or a Bruker DRX 500 spectrometer. Melting points were determined with a Büchi melting apparatus (type Nr. 535) and are uncorrected. X-ray data collections were performed on a Nonius Kappa-CCD-diffractometer, using a monochromatic Mo K_α (0,71073 Å) radiation. Combustion analyses were measured using an Elemental Vario EL Instrument. All irradiations were carried out in quartz vessels. Photochemical reactors LZ-C4 (14 × 3000 Å lamps, λ = 300 ± 10 nm) and RPR-208 (8 × 3000 Å lamps, λ = 300 ± 10 nm) were used for irradiations.

Trimethylsilyl ester of *aci*-nitroethane (1) [19]**.** Chlorotrimethylsilane (43.20 g, 0.4 mol, 50.5 mL) was added to nitroethane (30.0 g, 0.4 mol, 28.7 mL) and triethylamine (40.40 g, 0.4 mol, 55.6 mL) in benzene (200 mL). The mixture was stirred vigorously for 18 h at rt, filtered and evaporated. The crude product was obtained as a yellow oil and used immediately without further purification.

3-Methyl-5-trimethylsilyloxy-2-isoxazoline (2) [19]**.** A mixture of acrylonitrile (10.61 g, 0.2 mol, 13.2 mL), triethylamine (10.12 g, 0.1 mol, 13.9 mL) and **1** (28.73 g, 0.2 mol) in toluene (90 mL) was heated at 85 °C for 1 h. The solvent was removed and the crude product fractionated (105–110 °C, 20 mbar) to give 22.50 g (65%) of **2** as a colorless oil. ^{13}C NMR (75.5 MHz, $CDCl_3$): 155.2 (1C, C_q), 97.4 (1C, CH), 47.4 (1C, CH_2), 12.9 (1C, CH_3), 0.0 (3C, 3 × CH_3). ^{1}H NMR (300 MHz, $CDCl_3$): 5.80–5.77 (dd, 1H, ^3J = 5.8 Hz, 0.9 Hz, CH), 3.04–2.96 (dq, 1H, ^3J = 5.5 Hz, 0.8 Hz, CH_2), 2.71–2.65 (dq, 1H, ^3J = 1.8 Hz, 0.8 Hz, CH_2), 2.01 (s, 3H, CH_3), 0.15 (s, 9H, 3 × CH_3).

3-Methylpentane-2,4-dione (3) [20]**.** A mixture of freshly distilled 2,4-pentanedione (28.03 g, 0.28 mol, 28.8 mL), anhydrous potassium carbonate (38.70 g, 0.28 mol) and methyl iodide (49.68 g, 0.35 mol, 21.8 mL) in acetone (200 mL) was refluxed in the dark for 20 h and then cooled to rt. The insoluble material was removed by filtration and washed thoroughly with acetone. The combined filtrate and acetone washings were then concentrated, extracted two times with chloroform, dried over magnesium sulfate and filtered. The solvent was evaporated and the residual oil distilled (170 °C) to give 23.01 g (72%) of **3** as a colorless oil. ^{13}C NMR (75.5 MHz, $CDCl_3$): 204.8 (2C, C_q), 190.1 (1C, C_q), 104.5 (1C, C_q), 61.4 (1C, CH), 28.4 (2C, CH_3), 23.0 (1C, CH_3), 20.9 (1C, CH_3), 12.2 (1C, CH_3). ^{1}H NMR (300 MHz, $CDCl_3$): 3.59 (q, 1H, ^3J = 7.2 Hz, CH), 2.06 (s, 6H, 2 × CH_3), 1.97 (s, 3H, CH_3), 1.70 (s, 1.5H, CH_3), 1.19–1.16 (d, 3H, ^3J = 6.9 Hz, CH_3).

1,3-Diphenylpropane-1,3-dione (4). A mixture of acetophenone (30.04 g, 0.25 mol, 29.2 mL), methyl benzoate (34.04 g, 0.25 mol, 31.5 mL), sodium methoxide (16.21 g, 0.3 mol) and toluene (300 mL) was refluxed for 3 h. The resulting solution was concentrated, cooled to rt, poured into hydrochloric acid (300 mL, 6 N) and stirred for 30 min. The aqueous mixture was extracted two times with toluene and the combined organic layers were neutralized with aqueous sodium hydroxide. The organic solution was then washed two times with water, dried over magnesium sulfate, filtered and evaporated. The resulting solid was recrystallized twice from ethanol to yield 6.34 g (41%) of **4** as colorless crystals. ^{13}C NMR (75.5 MHz, $CDCl_3$): 185.6 (2C, C_q), 135.4 (2C, C_q), 132.4 (2C, CH), 128.6 (4C, CH), 127.1 (4C, CH), 93.0 (1C, CH). ^{1}H NMR (300 MHz, $CDCl_3$): 8.03–7.99 (m, 4H, CH), 7.59–7.47 (m, 6H, CH), 6.87 (s, 1H, CH).

3-Phenylisoxazol-5-one (5) [21]**.** A mixture of ethyl benzoylacetate (15.38 g, 80 mmol), hydroxylamine hydrochloride (5.56 g, 80 mmol), potassium carbonate (5.53 g, 40 mmol), ethanol (40 mL) and water (40 mL) was stirred at rt for 15 h. The solid was filtered, washed with water and extracted three times with ether. The combined organic layers were dried over magnesium sulfate, filtered and the solvent was evaporated. The residue was recrystallized from ethanol to give 9.21 g (71%) of **5** as colorless crystals. ^{1}H NMR (300 MHz, $CDCl_3$): 7.69–7.67 (m, 2H, CH), 7.54–7.46 (m, 3H, CH), 3.80 (s, 2H, CH_2).

3-Phenyl-5-chloroisoxazole (6) [22]**.** A mixture of **5** (4.84 g, 30 mmol) and phosphorous oxychloride (16.3 mL, 175 mmol) was stirred at 0 °C and triethylamine (3.37 g, 33 mmol, 4.6 mL) added slowly (T < 25 °C). The solution was then heated at 120 °C for 2.5 h and the excess phosphorous oxychloride removed in vacuo. The brown residue was triturated with 100 mL iced water and extracted two times with ethyl acetate. The combined organic layers were dried over magnesium sulfate, filtered and the solvent was evaporated. The resulting residue was mixed with chloroform and the remaining solid removed by filtration. The solvent was again removed and the last step repeated with cyclohexane. After evaporation of the solvent, 3.18 g (59%) of **6** was obtained as a yellow solid. ^{13}C NMR (75.5 MHz, $CDCl_3$): 164.1 (1C, C_q), 155.0 (1C, C_q), 130.5 (1C, CH), 128.9 (2C, CH), 128.1 (1C, C_q), 126.5 (2C, CH), 99.5 (1C, CH). ^{1}H NMR: 7.77–7.74 (m, 2H, CH), 7.47–7.45 (m, 3H, CH), 6.47 (s, 1H, CH).

Isoxazole (7a) [23]**.** Malonaldehyde tetraethyl acetal (22.03 g, 0.1 mol) was added over a 30 min period to hydroxylamine hydrochloride (7.64 g, 0.11 mol) in water (50 mL) at 70 °C. Heating was continued for 3 h and the resulting mixture distilled at 95 °C and a mixture of isoxazole, alcohol and water collected. The distillate was added dropwise to a solution of cadmium chloride (18.30 g) in water (15 mL). The resulting precipitate was filtered, washed with a little cold water and dried. The resulting solid was then suspended in water, heated to boiling and a mixture of isoxazole and water was obtained on distillation. The distillate (two phases) was extracted with ether, dried over magnesium sulfate and filtered. After evaporation of the solvent, 2.97 g (43%) of **7a** was obtained as a colorless liquid. ^{13}C NMR (75.5 MHz, $CDCl_3$): 157.4 (1C, CH), 148.7 (1C, CH), 103.2 (1C, CH). ^{1}H NMR (300 MHz, $CDCl_3$): 8.36 (s, 1H, CH), 8.19 (s, 1H, CH), 6.26 (s, 1H, CH).

5-Methylisoxazole (7b). A mixture of acetylacetaldehyde (30.0 g, 0.227 mol), diethylamine (17.40 g, 0.238 mol, 24.6 mL) and methanol (70 mL) was heated at 65 °C for 1 h. Hydroxylamine hydrochloride (16.50 g, 0.238 mol) of in water (50 mL) was then added dropwise and heating was continued for 2 h. The solution was cooled to rt, extracted with ether, dried over magnesium sulfate and filtered. The solvent was evaporated and the residue fractionated (78–80 °C, 270 mbar) to yield 4.94 g (26%) of **7b** as a colorless liquid. ^{13}C NMR (75.5 MHz, $CDCl_3$): 168.4 (1C, C_q), 150.1 (1C, CH), 100.5 (1C, CH), 11.6 (1C, CH_3). ^{1}H NMR (300 MHz, $CDCl_3$): 8.02 (s, 1H, CH), 5.88 (s, 1H, CH), 2.33 (s, 3H, CH_3).

3-Methylisoxazole (7c) [24]**.** A solution of **2** (20.80 g, 0.12 mol) and *p*-toluenesulfonic acid (2.0 g) in chloroform (200 mL) was refluxed for 2 h. The resulting mixture was cooled to rt, washed with aqueous sodium bicarbonate and extracted several times with chloroform. The combined organic phases were washed several times with water, dried over magnesium sulfate, filtered and evaporated in vacuo to give 3.89 g (39%) of **7c** as a colorless liquid. ^{13}C NMR (75.5 MHz, $CDCl_3$): 158.4 (1C, C_q), 157.9 (1C, CH), 104.8 (1C, CH), 10.9 (1C, CH_3). ^{1}H NMR (300 MHz, $CDCl_3$): 8.22 (s, 1H, CH), 6.11–6.10 (d, 1H, ^3J = 0.9 Hz, CH), 2.24 (s, 3H, CH_3).

3,5-Dimethylisoxazole (7d) [25]**.** A solution of 2,4-pentanedione (100.10 g, 1 mol, 103.2 mL) and hydroxylamine hydrochloride (74.70 g, 1.075 mol) in water (150 mL) and ethanol (100 mL) was refluxed for 90 min. The mixture was cooled to rt, poured onto ice (200 mL) and extracted four times with dichloromethane. The combined organic phases were dried over magnesium sulfate, filtered and evaporated. The resulting dark mixture was fractionated (141 °C) to yield 77.5 g (80%) of **7d** as a colorless liquid. ^{13}C NMR (75.5 MHz, $CDCl_3$): 168.2 (1C, C_q), 159.0 (1C, C_q), 101.6 (1C, CH), 11.1 (1C, CH_3), 10.4 (1C, CH_3). ^{1}H NMR (300 MHz, $CDCl_3$): 5.76 (s, 1H, CH), 2.317 (s, 3H, CH_3), 2.19 (s, 3H, CH_3).

3,4,5-Trimethylisoxazole (7e) [26]**.** A mixture of **3 (**20.55 g, 0.18 mol), hydroxylamine hydrochloride (12.50 g, 0.18 mol) and water (80 mL) was stirred at rt for 24 h. The solution was then extracted three times with chloroform and the combined organic layers were dried over magnesium sulfate and filtered. After removal of the solvent, the residue was distilled (165 °C) to yield 13.0 g (65%) of **7e** as a colorless liquid. ^{13}C NMR (75.5 MHz, $CDCl_3$): 163.4 (1C, C_q), 159.0 (1C, C_q), 108.2 (1C, C_q), 9.9 (1C, CH_3), 9.2 (1C, CH_3), 5.8 (1C, CH_3). ^{1}H NMR (300 MHz, $CDCl_3$): 2.01 (s, 3H, CH_3), 1.91 (s, 3H, CH_3), 1.61 (s, 3H, CH_3).

3,5-Diphenylisoxazole (7f) [25]**.** A solution of **4** (4.49 g, 20 mmol) and hydroxylamine hydrochloride (1.74 g, 20 mmol) in water (30 mL) and ethanol (20 mL) was refluxed for 90 min. The mixture was cooled to rt, poured onto ice (50 mL) and extracted two times with dichloromethane. The combined organic phases were dried over magnesium sulfate, filtered and evaporated. The resulting solid was recrystallized from ether to yield 4.09 g (92%) of **7f** as colorless crystals. ^{13}C NMR (75.5 MHz, $CDCl_3$): 170.3 (1C, C_q), 162.9 (1C, C_q), 130.1 (1C, CH), 129.9 (1C, CH), 129.0 (1C, C_q), 128.9 (2C, CH), 128.8 (2C, CH), 127.4 (1C, C_q), 126.7 (2C, CH), 125.7 (2C, CH), 97.4 (1C, CH). ^{1}H NMR (300 MHz, $CDCl_3$): 7.90–7.84 (m, 4H, CH), 7.52 (m, 6H, CH), 6.83 (s, 1H, CH).

3-Phenyl-5-Methoxy-isoxazole (7g) [22]**.** A solution of **6** (2.88 g, 16 mmol) and sodium methoxide (7.78 g, 144 mmol) in methanol (40 mL) and THF (40 mL) was heated under reflux for 63 h and then concentrated. The residue was poured in iced water (100 mL), extracted with ether and washed with aqueous sodium carbonate to neutralize hydrochloric acid. The organic layer was dried over magnesium sulfate followed by removal of the solvent. The remaining solid was recrystallized from warm cyclohexane (50 °C) to yield 1.57 g (56%) of **7g** as yellow crystals. ^{13}C NMR (75.5 MHz, $CDCl_3$): 174.4 (1C, C_q), 163.9 (1C, C_q), 129.8 (1C, CH), 129.3 (1C, C_q), 128.6 (2C, CH), 126.2 (2C, CH), 75.1 (1C, CH), 58.7 (1C, CH_3). ^{1}H NMR: 7.75–7.72 (m, 2H, CH), 7.42–7.39 (m, 3H, CH), 5.51 (s, 1H, CH), 3.96 (s, 3H, CH_3).

3-Phenyl-5-(trimethylsilyloxy)isoxazole (7h) [27]**.** To 2.72 g (25 mmol, 3.2 mL) of chlorotrimethylsilane, was added a mixture of **5 (**3.22 g, 20 mmol) and hexamethyldisilazane (7.26 g, 45 mmol, 9.5 mL). The solution was heated at 120 °C for 30 min and then concentrated. The resulting product was unstable and therefore used immediately.

NMR-photolyses of isoxazoles 7a–h with aldehydes: General procedure. A solution of isoxazole (0.05 mmol) and aldehyde (0.1 M) in deuterated acetonitrile (0.5 mL) was transferred to a quartz NMR tube, degassed with argon and irradiated in a photo reactor (LZ-C4, 300 nm) for 6 h. The mixture was examined before and after irradiation by ^{1}H NMR spectroscopy.

Photocycloaddition reactions of 7e with aryl substituted aldehydes: General procedure. A solution of **7e** (2.22 g, 20 mmol) and the corresponding aldehyde (20 mmol) in acetonitrile (200 mL) was transferred to a quartz vessel, mixed with potassium carbonate (0.28 g, 10 mol %) and degassed with nitrogen. The mixture was stirred and irradiated in a Rayonet photochemical reactor (RPR 208, lamps centered 300 nm) at −10 °C for 48–72 h. The resulting yellow solution was concentrated (35 °C) and extracted three times with ether. The combined organic layers were dried over magnesium sulfate and the solvent was evaporated. The solid residue was mixed with a little ethanol, stirred for 30 min, filtered and recrystallized at −10 °C from ethanol.

***exo*-1,4,5-trimethyl-6-phenyl-2,7-dioxa-3-aza-bicyclo[3.2.0]hept-3-en (9a).** Yield: 50%. ^{13}C NMR (500 MHz, CD_3CN): 163.6 (1C, CN), 138.9 (1C, Ar-C), 129.3 (2C, Ar-C), 128.9 (1C, Ar-C), 126.2 (2C, Ar-C), 115.6 (1C, OCO), 86.4 (1C, CO), 63.7 (1C, C_q), 19.1 (1C, CH_3), 11.1 (1C, CH_3), 10.2 (1C, CH_3). ^{1}H NMR (500 MHz, CD_3CN): 7.45–7.35 (m, 5H, ^3J = 7.6 Hz, ^3J = 7.0 Hz, Ar-CH), 5.59 (s, 1H, CH), 2.05 (s, 3H, CH_3CN), 1.60 (s, 3H, CH_3), 0.78 (s, 3H, CH_3). Anal. calcd. for $C_{13}H_{15}NO_2$: C 71.87, H 6.96, N 6.45. Found: C 71.67, H 6.98, N 6.40. Colorless needles, unit cell parameters: a = 9.3804(6), b = 14.8345(10), c = 9.080(6), β = 116.646(3), space group $P2_1/c$.

***exo*-1,4,5-trimethyl-6-(4'-methylphenyl)-2,7-dioxa-3-aza-bicyclo[3.2.0]hept-3-en (9b).** Yield: 35%. ^{13}C NMR (75.5 MHz, CD_3CN): 163.7 (1C, CN), 138.8 (1C, Ar-C), 136.1 (1C, Ar-C), 130.0 (2C, Ar-C), 126.4 (2C, Ar-C), 115.6 (1C, OCO), 86.6 (1C, CO), 63.8 (1C, C_q), 21.1 (1C, CH_3), 19.2 (1C, CH_3), 11.1 (1C, CH_3), 10.3 (1C, CH_3). ^{1}H NMR (300 MHz, CD_3CN): 7.26–7.24 (m, 4H, Ar-CH), 5.55 (s, 1H, CH), 2.35 (s, 3H, Ar-CH_3), 2.03 (s, 3H, CH_3CN), 1.60 (s, 3H, CH_3), 0.79 (s, 3H, CH_3). Anal. calcd. for $C_{14}H_{17}NO_2$: C 72.70, H 7.41, N 6.06. Found: C 72.71, H 7.45, N 6.08. Colorless needles, unit cell parameters: a = 17.196(2), b = 5.9199(4), c = 12.807(2), β = 109.944(4), space group $P2_1/c$.

***exo*-1,4,5-trimethyl-6-(3'-methylphenyl)-2,7-dioxa-3-aza-bicyclo[3.2.0]hept-3-en (9c).** Yield: 65%. ^{13}C NMR (75.5 MHz, CD_3CN): 163.7 (1C, CN), 139.3 (1C, Ar-C), 139.0 (1C, Ar-C), 129.7 (1C, Ar-C), 129.3 (1C, Ar-C), 126.9 (1C, Ar-C), 123.4 (1C, Ar-C), 115.7 (1C, OCO), 86.6 (1C, CO), 63.8 (1C, C_q), 21.4 (1C, CH_3), 19.2 (1C, CH_3), 11.1 (1C, CH_3), 10.3 (1C, CH_3). ^{1}H NMR (300 MHz, CD_3CN): 7.35–7.13 (m, 4H,

Ar-CH), 5.54 (s, 1H, CH), 2.37 (s, 3H, Ar-CH_3), 2.04 (s, 3H, CH_3CN), 1.60 (s, 3H, CH_3), 0.79 (s, 3H, CH_3). Anal. calcd. for $C_{14}H_{17}NO_2$: C 72.70, H 7.41, N 6.06. Found: C 72.55, H 7.39, N 6.09. Colorless needles, unit cell parameters: a = 13.3045(8), b = 6.9356(6), c = 17.5348(10), β = 129.284(3), space group $P2_1/c$.

References

1. Griesbeck, A. G. In *Handbook of Organic Photochemistry and Photobiology;* Horspool, W. M.; Song, P.-S., Eds.; CRC Press: Boca Raton, FL, 1995; pp 550 and 755.
2. Griesbeck, A. G.; Mauder, H.; Stadtmüller, S. *Acc. Chem. Res.* **1994,** *27,* 70–75. doi:10.1021/ar00039a002
3. Griesbeck, A. G.; Buhr, S.; Fiege, M.; Schmickler, H.; Lex, J. *J. Org. Chem.* **1998,** *63,* 3847–3854. doi:10.1021/jo971767l
4. Kutateladze, A. G. *J. Am. Chem. Soc.* **2001,** *123,* 9279–9282. doi:10.1021/ja016092p
5. Griesbeck, A. G.; Abe, M.; Bondock, S. *Acc. Chem. Res.* **2004,** *37,* 919–928. doi:10.1021/ar040081u
6. Bach, T. *Synthesis* **1998,** 683–703. doi:10.1055/s-1998-2054
7. Schreiber, S. L.; Hoveyda, A. H.; Wu, H. J. *J. Am. Chem. Soc.* **1983,** *105,* 660–661. doi:10.1021/ja00341a077
8. Griesbeck, A. G.; Fiege, M.; Lex, J. *Chem. Commun.* **2000,** 589–590. doi:10.1039/b000578i
9. Bondock, S.; Griesbeck, A. G. *Monatsh. Chem.* **2006,** *137,* 765–777. doi:10.1007/s00706-006-0474-4
10. Griesbeck, A. G.; Bondock, S.; Lex, J. *J. Org. Chem.* **2003,** *68,* 9899–9906. doi:10.1021/jo034830h
11. Griesbeck, A. G.; Bondock, S.; Lex, J. *Org. Biomol. Chem.* **2004,** *2,* 1113–1115. doi:10.1039/b401990c
12. Fuentes, J. A.; Maestro, A.; Testera, A. M.; Báñez, J. M. *Tetrahedron: Asymmetry* **2000,** *11,* 2565–2577. doi:10.1016/S0957-4166(00)00225-1
13. Scott, M. S.; Luckhurst, C. A.; Dixon, D. J. *Org. Lett.* **2005,** *7,* 5813–5816. doi:10.1021/ol052333c
14. Büchi, G.; Vederas, J. C. *J. Am. Chem. Soc.* **1972,** *94,* 9128–9132. doi:10.1021/ja00781a023
15. Kobayashi, T.; Kubota, T.; Ezumi, K.; Utsunomiya, C. *Bull. Chem. Soc. Jpn.* **1982,** *55,* 3915–3919. doi:10.1246/bcsj.55.3915
16. Singh, B.; Ullman, E. F. *J. Am. Chem. Soc.* **1967,** *89,* 6911–6916. doi:10.1021/ja01002a018
17. The crystallographic data for the isoxazole photoadducts **9a**, **9b**, and **9c** have been deposited with the Cambridge Crystallographic Data Centre as supplementary publications no. CCDC-795107 (**9a**), CCDC-795108 (**9b**), CCDC-795109 (**9c**).
18. Bouas-Laurent, H.; Dürr, H. *Pure Appl. Chem.* **2001,** *73,* 639–665. doi:10.1351/pac200173040639
19. Torssell, K.; Zeuthen, O. *Acta Chem. Scand.* **1978,** *32B,* 118–124. doi:10.3891/acta.chem.scand.32b-0118
20. Johnson, A. W.; Markham, E.; Price, R. *Org. Synth.* **1962,** *42,* 75–76.
21. Moreno-Mañas, M.; Pérez, M.; Pleixats, R. *Tetrahedron* **1994,** *50,* 515–528. doi:10.1016/S0040-4020(01)80773-0
22. Micetich, R. G.; Chin, C. G. *Can. J. Chem.* **1970,** *48,* 1371–1376. doi:10.1139/v70-226
23. Tarsio, P. J.; Nicholl, L. *J. Org. Chem.* **1957,** *22,* 192–193. doi:10.1021/jo01353a027
24. Sharma, S. C.; Torssell, K. *Acta Chem. Scand.* **1979,** *33B,* 379–383. doi:10.3891/acta.chem.scand.33b-0379
25. Fitton, A. O.; Smalley, R. K. *Practical Heterocyclic Chemistry;* Academic Press: London, 1968; pp 28–29.
26. Micetich, R. G.; Shaw, C. C.; Hall, T. W.; Spevak, P.; Fortier, R. A.; Wolfert, P.; Foster, B. C.; Bains, B. K. *Heterocycles* **1985,** *23,* 571–583. doi:10.3987/R-1985-03-0571
27. Ohba, Y.; Hishiwaki, T.; Akagi, H.; Nori, M. *J. Chem. Res., Miniprint* **1984,** 2254–2262.

License and Terms

Beilstein Journal of Organic Chemistry

Application of the diastereoselective photodeconjugation of α,β-unsaturated esters to the synthesis of gymnastatin H

Ludovic Raffier and Olivier Piva*

Full Research Paper

Open Access

Address:
Université Lyon 1, UMR 5246 CNRS, Institut de Chimie et de Biochimie Moléculaire et Supramoléculaire, 69622 Villeurbanne, France

Email:
Olivier Piva* - piva@univ-lyon1.fr

* Corresponding author

Keywords:
amide; diastereoselective protonation; dienol; isomerisation; Wittig reaction

Beilstein J. Org. Chem. **2011,** *7,* 151–155.
doi:10.3762/bjoc.7.21

Received: 31 October 2010
Accepted: 04 January 2011
Published: 02 February 2011

This article is part of the Thematic Series "Photocycloadditions and photorearrangements"

Guest Editor: A. G. Griesbeck

Abstract

The asymmetric synthesis of gymnastatin H has been achieved by using the photoisomerisation of a conjugated ester to its β,γ-unsaturated isomer through the protonation of a in situ generated dienol as key step. Thanks to diacetone D-glucose used as a chiral alkoxy group, the protonation occurred well onto one of the two diastereotopic faces with very high yields and selectivities. Moreover, by this way the configuration of the C-6 centre of the target molecule was controlled.

Introduction

The photodeconjugation of α,β-unsaturated esters **1** – which bear at least one hydrogen atom on γ-position – allows a straightforward access to β,γ-unsaturated isomers **2** [1]. This reaction was first reported by Jorgenson [2,3] and has been extensively studied by different groups in a mechanistical point of view. For example, Weedon et al. were able to trap an intermediate species identified as a photodienol (its formation resulting from a [1,5]-sigmatropic rearrangement). It was shown that the efficiency of the isomerisation process is highly dependent on the nature of the solvent and on the presence of various additives (e.g., amines) which could catalyse the reketonisation of the transient dienol [4] (Scheme 1).

Despite the potential interest in β,γ-unsaturated acid derivatives, until recently only a few applications of this photochemical transformation in total synthesis appeared in the literature.

However, the scope of the photochemical isomerisation has been greatly enhanced thanks to the development of diastereo- and enantioselective versions. Starting from α-substituted esters **3** in the presence of a catalytic amount of an enantiomerically pure bicyclic amino alcohol **4** – derived from camphor –, the protonation of the prochiral photodienol can be achieved with an ee up to 91% [5]. This value is one of the highest values observed for an enantioselective protonation transformation

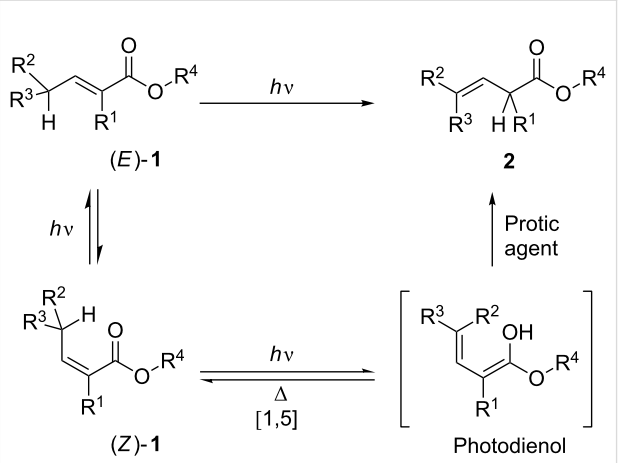

Scheme 1: Principle of the photodeconjugation process.

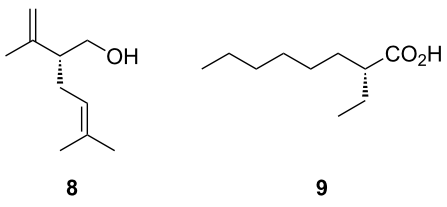

Figure 1: Natural products prepared by photodeconjugation.

reaction. However, as the selectivities were highly dependent on the substrate, an alternative diastereoselective version has been developed. By using cheap and commercially available diacetone D-glucose (DAG-OH) as chiral alkoxy group and dimethylamino alcohol as additive, a selective protonation of one of the two diastereotopic faces of the transient dienol was achieved which lead to esters **7** with a d.r. better than 97.5:2.5 [6] (Scheme 2). This transformation allowed the formation of a new allylic stereogenic centre and found already a direct application to the asymmetric synthesis of different natural products including *(R)*-lavandulol (**8**), *(R)*-arundic acid (**9**) and 2-fluoroacids or lactones [7-9] (Figure 1).

Filamentous fungi are the source of a wide range of secondary metabolites which possess very promising biological activities. Among them, gymnastatins **10** constitute a family of compounds isolated from *Gymnascella dankaliensis* which grows in symbiosis with the marine sponge *Halichondria japonica* [10] (Figure 2).

Gymnastatins **10** possess a common unsaturated fatty acid residue connected to a tyrosine subunit. These compounds have been reported to exhibit antibacterial activity and cytotoxities against cultured P388 cancer cells. Interestingly, the same acid chain with an *R*-configuration has been identified in other structures like dankastatins [11] isolated from the same source, aranorosin (**11**) isolated from *Pseudoarachniotus roseus* [12] and manumycin C (**12**) isolated from *Streptomyces parvulus* [13]. Different groups have investigated the synthesis of gymnastatins **10a**–**c** [14-16], compounds **11** [17] and **12** [18]. In most cases, the lateral acid chain was prepared starting from *(R)*-2-methyloctanal by iterative Wittig reactions to build the

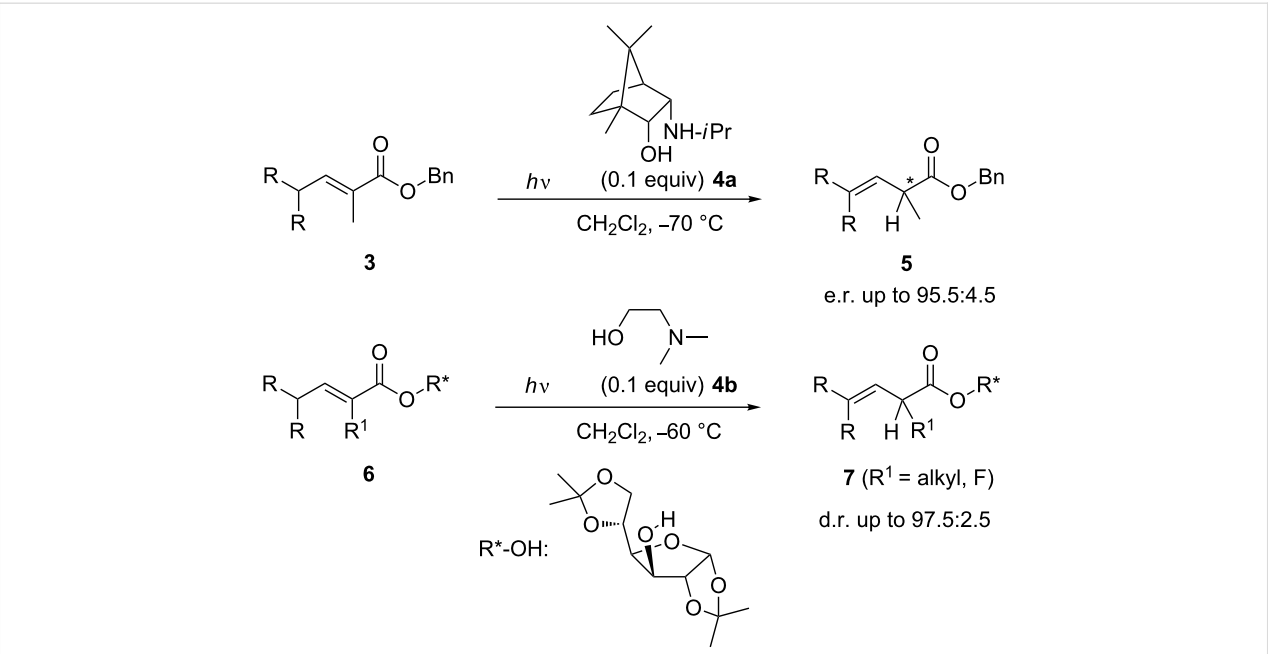

Scheme 2: Enantio- and diastereoselective photodeconjugation reactions.

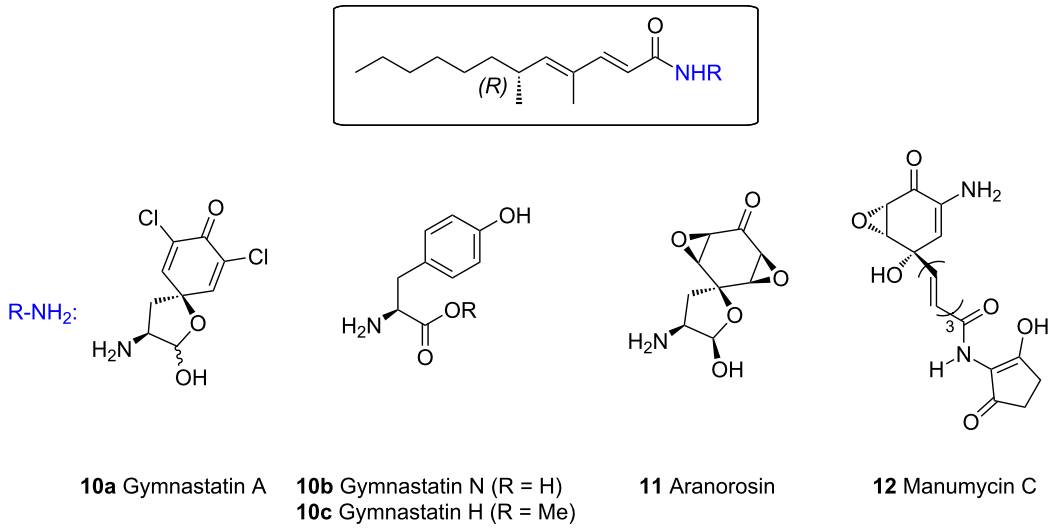

10a Gymnastatin A **10b** Gymnastatin N (R = H) **10c** Gymnastatin H (R = Me) **11** Aranorosin **12** Manumycin C

Figure 2: Natural amides possessing the same (6*R*)-fatty acid side chain.

dienoate chain. The configuration at the C-2 carbon atom of this precursor was controlled by using a diastereoselective alkylation of an acyl oxazolidinone. In some cases, a Claisen condensation took place and afforded a β-ketoamide in noticeable amounts diminishing the overall yield of the sequence [15]. In this context, we have considered an alternative synthetic route to the fatty acid common to all gymnastatins according to a photoisomerisation–diastereoselective protonation sequence involving catalytic amounts of an achiral organocatalyst (e.g., amino alcohol **4b**). Our goal was to describe the first de novo total synthesis of gymnastatin H (**10c**).

Results and Discussion

Ethyl ester **14,** readily prepared from hexanal by a Wittig–Horner reaction, was saponified and esterified under DCC activation with commercially available diacetone D-glucose (Scheme 3). Irradiation of **16** at 254 nm in methylene chloride at −60 °C delivered the β,γ-unsaturated ester **17** in 90% yield as an inseparable mixture of *E*- and *Z*-isomers. Hydrogenation of the double bond lead to the saturated ester **18** for which a 95:5 diastereomeric ratio was measured by ^{1}H NMR spectroscopy. Next, a two-step sequence delivered 2-methyloctanal (**20**) in 58% overall yield. The configuration of the newly created centre was first assigned as *R* by applying a model we disclosed earlier and was confirmed by comparison with optical rotation values published in the literature [19]. Aldehyde **20** was submitted to a Wittig condensation with phosphorane **13b** at reflux of toluene to deliver ester **21** only as the *E*-isomer. It should be pointed out that the Wadsworth–Emmons variant using 2-phosphonatoester **13a** led mainly to the *Z*-isomer, a phenomenon which was already observed with α-substituted aldehydes [20]. The reduction of the ethyl ester into the corresponding allylic alcohol **22** followed by the oxidation with Dess–Martin periodinane (DMP) [21] afforded aldehyde **23** which was converted into the known ethyl ester *(E,E)*-**24** by a subsequent Wittig–Horner reaction. The comparison of the optical rotation with literature data confirmed the (*R*) configuration at the C-6 carbon. By saponification under mild conditions, **24** was converted into carboxylic acid **25** which was implicated into a free-epimerising amidation procedure with HOBt [22] and the readily available *O*-protected tyrosine derivative **26**. Finally, the TBS group of the amino ester moiety was removed under standard conditions to deliver compound **10c**. The measured spectroscopic data were identical to those reported for gymnastatin H [10]. Interestingly, the optical rotation of the synthetic product showed a higher value ($[\alpha]_D^{25}$ = +104 (0.3, $CHCl_3$)) than those measured for the isolated natural product ($[\alpha]_D^{25}$ = +42.3 (0.76, $CHCl_3$)). Similar discordances have been already observed in the case of gymnastatin N and were shown to be a consequence of a partial epimerisation at the C-2’ carbon of the natural compound's amino ester subunit [15].

Conclusion

In conclusion, we have achieved the total synthesis of (6*R*)-gymnastatin H in 14 steps and 4.3% overall yield by using a highly diastereoselective photodeconjugation of a diacetone D-glucose ester as key step (de >95%). Now, work is underway to prepare parent structures that either possess an opposite configuration on the stereogenic centre or a modified geometry of the two double bonds. Furthermore, the biological activities of these novel structures are going to be studied.

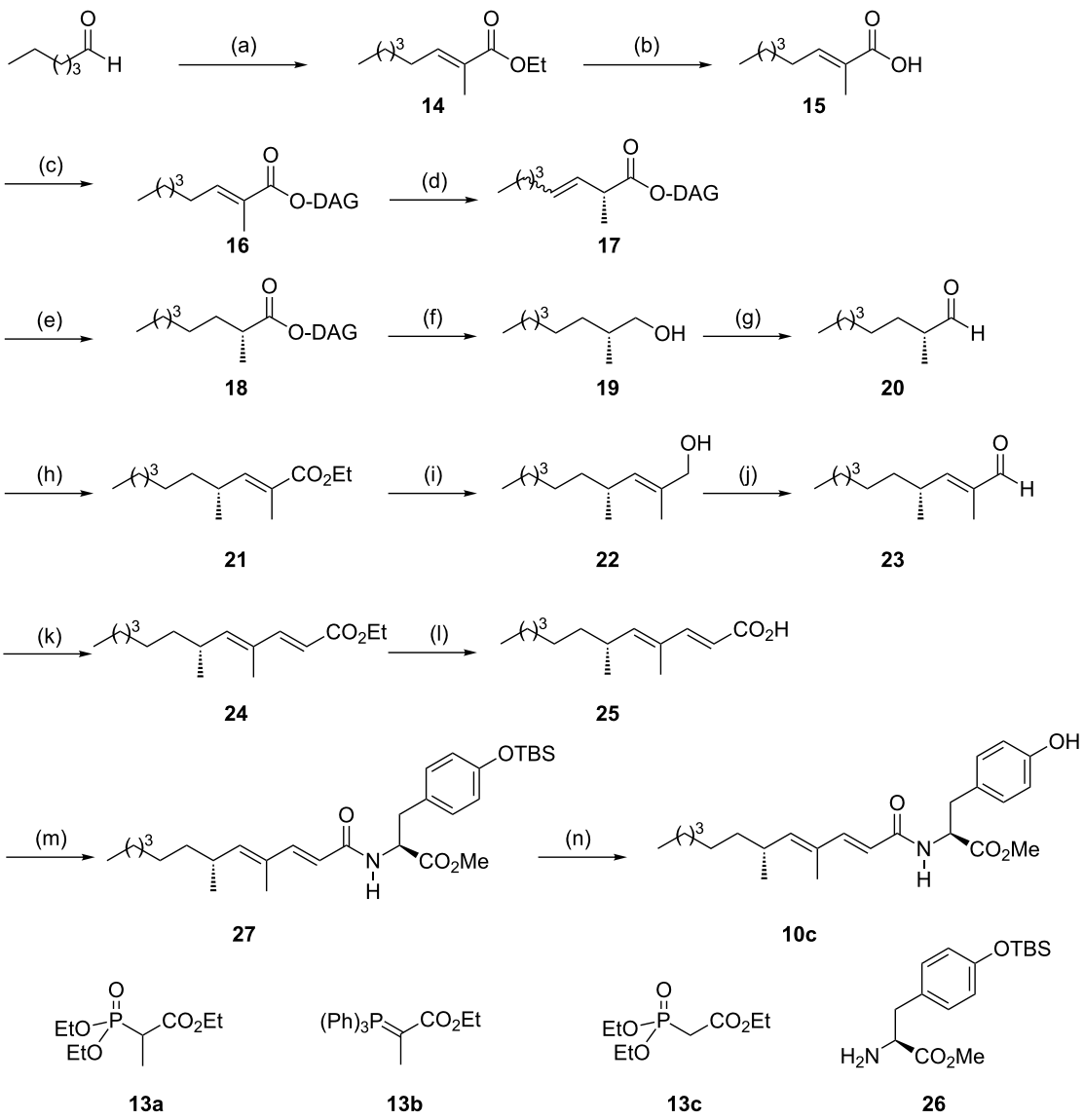

Scheme 3: Reagents and conditions: (a) NaH, **13a**, THF, 25 °C, 83%. (b) KOH, EtOH/H_2O (95/5), Δ, 97% (*E*/*Z*: 90/10). (c) DAG-OH, DCC, DMAP, CH_2Cl_2, 0 °C then rt, 76%. (d) *hv* (254 nm), **4b** (0.3 equiv), CH_2Cl_2, −60 °C, 90%. (e) H_2 (1 atm), PtO_2 (cat.), Et_2O, 99%. (f) $LiAlH_4$, Et_2O, 0 °C, 83%. (g) DMP, CH_2Cl_2, 0 °C, 70%. (h) **13b**, PhMe, 80 °C, 80% (*E*-only). (i) Dibal-H (2 equiv), THF, 0 °C, 99%. (j) DMP, CH_2Cl_2, 0 °C, 75%. (k) **13c**, NaH, THF, rt, 60%. (l) LiOH, MeOH, THF, H_2O, 70%. (m) **26**, DCC, HOBt, CH_2Cl_2, 57%. (n) TBAF, THF, 0 °C, 96%.

Supporting Information

Supporting Information File 1

Full experimental and spectral data for compounds **10c**, **14**–**27**.
[http://www.beilstein-journals.org/bjoc/content/supplementary/1860-5397-7-21-S1.pdf]

Acknowledgements

L. R. thanks the “Ministère de l’Enseignement Supérieur et de la Recherche“ for a PhD grant. We are grateful to the Université Lyon 1, CNRS and “Région Rhône-Alpes“ for financial support (programme Cible).

References

1. Piva, O. Photodeconjugation of enones and carboxylic acid derivatives. In *CRC Handbook of Organic Photochemistry and Photobiology,* 2nd ed.; Horspool, W.; Lenci, F., Eds.; CRC Press: Boca Raton, 2004; pp 70-1–70-18.
2. Jorgenson, M. J. *J. Chem. Soc., Chem. Commun.* **1965,** 137–138. doi:10.1039/c19650000137
3. Jorgenson, M. J.; Patumtevapibal, S. *Tetrahedron Lett.* **1970,** *11,* 489–492. doi:10.1016/0040-4039(70)89007-4

4. Duhaime, R. M.; Weedon, A. C. *J. Am. Chem. Soc.* **1987,** *109,* 2479–2483. doi:10.1021/ja00242a038
5. Piva, O.; Pete, J.-P. *Tetrahedron Lett.* **1990,** *31,* 5157–5160. doi:10.1016/S0040-4039(00)97830-4
6. Piva, O.; Pete, J.-P. *Tetrahedron: Asymmetry* **1992,** *3,* 759–768. doi:10.1016/S0957-4166(00)80517-0
7. Piva, O. *J. Org. Chem.* **1995,** *60,* 7879–7883. doi:10.1021/jo00129a030
8. Pelotier, B.; Holmes, T.; Piva, O. *Tetrahedron: Asymmetry* **2005,** *16,* 1513–1520. doi:10.1016/j.tetasy.2005.02.011
9. Bargiggia, F.; Dos Santos, S.; Piva, O. *Synthesis* **2002,** 427–437. doi:10.1055/s-2002-20028
10. Amagata, T.; Minoura, K.; Numata, A. *J. Nat. Prod.* **2006,** *69,* 1384–1388. doi:10.1021/np0600189
11. Amagata, T.; Tanaka, M.; Yamada, T.; Minoura, K.; Numata, A. *J. Nat. Prod.* **2008,** *71,* 340–345. doi:10.1021/np070529a
12. Fehlhaber, H. W.; Kogler, H.; Mukhopadhyay, T.; Vijayakumar, E. K. S.; Ganguli, B. N. *J. Am. Chem. Soc.* **1988,** *110,* 8242–8244. doi:10.1021/ja00232a050
13. Buzzetti, F.; Gaümann, E.; Hütter, R.; Keller-Schierlein, W.; Neipp, L.; Prelog, V.; Zähner, H. *Pharm. Acta Helv.* **1963,** *38,* 871–874.
14. Gurjar, M. K.; Bhaket, P. *Heterocycles* **2000,** *53,* 143–149. doi:10.3987/COM-99-8745
15. Phoon, C. W.; Somanadhan, B.; Hui Heng, S. C.; Ngo, A.; Ng, S. B.; Butler, M. S.; Buss, A. D.; Sim, M. M. *Tetrahedron* **2004,** *60,* 11619–11628. doi:10.1016/j.tet.2004.09.046
16. Murayama, K.; Tanabe, T.; Ishikawa, Y.; Nakamura, K.; Nishiyama, S. *Tetrahedron Lett.* **2009,** *50,* 3191–3194. doi:10.1016/j.tetlet.2009.01.156
17. Wipf, P.; Kim, Y.; Fritch, P. C. *J. Org. Chem.* **1993,** *58,* 7195–7203. doi:10.1021/jo00077a050
18. Alcaraz, L.; Macdonald, G.; Ragot, J.; Lewis, N. J.; Taylor, R. J. K. *Tetrahedron* **1999,** *55,* 3707–3716. doi:10.1016/S0040-4020(98)00879-5
19. Goldstein, S. W.; Overman, L. E.; Rabinowitz, M. H. *J. Org. Chem.* **1992,** *57,* 1179–1190. doi:10.1021/jo00030a026
20. Nagaoka, H.; Kishi, Y. *Tetrahedron* **1981,** *37,* 3873–3888. doi:10.1016/S0040-4020(01)93261-2
21. Zhdankin, V. V.; Stang, P. J. *Chem. Rev.* **2002,** *102,* 2523–2584. doi:10.1021/cr010003+
22. Lygo, B. 1-Hydroxybenzotriazol. In *Activating agents and protection groups;* Pearson, A.; Roush, W. J., Eds.; J. Wiley & Sons Ltd.: New York, 1999; p 220.

License and Terms

Beilstein Journal of Organic Chemistry

Formation of macrocyclic lactones in the Paternò–Büchi dimerization reaction

Junya Arimura[1], Tsutomu Mizuta[1], Yoshikazu Hiraga[1] and Manabu Abe[*1,2]

Letter

Open Access

Address:
[1]Department of Chemistry, Graduate School of Science, Hiroshima University (HIRODAI), 1-3-1 Kagamiyama, Higashi-Hiroshima, Hiroshima 739-8526, Japan and [2]Japan Science and Technology Agency, CREST, 5 Sanbancho, Chiyodaku, Tokyo, 102-0075, Japan

Email:
Junya Arimura - m095523@hiroshima-u.ac.jp;
Tsutomu Mizuta - mizuta@sci.hiroshima-u.ac.jp;
Yoshikazu Hiraga - yhiraga@sci.hiroshima-u.ac.jp;
Manabu Abe* - mabe@hiroshima-u.ac.jp

* Corresponding author

Keywords:
furans; macrocyclic lactone; oxetane; Paternò–Büchi reaction; photochemical reaction

Beilstein J. Org. Chem. **2011,** *7,* 265–269.
doi:10.3762/bjoc.7.35

Received: 11 November 2010
Accepted: 02 February 2011
Published: 28 February 2011

This article is part of the Thematic Series "Photocycloadditions and photorearrangements"

Guest Editor: A. G. Griesbeck

Abstract

Furan-2-ylmethyl 2-oxoacetates **1a**,**b**, in which the furan ring and the carbonyl moiety were embedded intramolecularly, were synthesized from commercially available furan-2-ylmethanol and their photochemical reaction ($h\nu > 290$ nm) was investigated. Twelve-membered macrocyclic lactones **2a**,**b** with C_i symmetry including two oxetane-rings, which are the Paternò–Büchi dimerization products, were isolated in ca. 20% yield. The intramolecular cyclization products, such as 3-alkoxyoxetane and 2,7-dioxabicyclo[2.2.1]hept-5-ene derivatives, were not detected in the photolysate.

Findings

Photochemical [2 + 2] cycloaddition reaction of alkenes with carbonyls, so-called Paternò–Büchi reaction [1-13], is one of the most efficient methods for preparing synthetically useful four-membered heterocyclic compounds, i.e., oxetanes. The Paternò–Büchi reaction of furan with a triplet carbonyl, such as n,π* triplet benzophenone, produces regioselectively 2-alkoxyoxetanes **2OX** (Scheme 1). The regioselective formation is rationalized by the relative stability of the intermediary triplet biradicals, **BR** versus **BR'**, and also by the relative nucleophilicity of the furan-ring carbons, i.e., C1 versus C2 (Scheme 1) [14-18].

Biradical **BR**, in principle, possess two resonance forms, i.e., 1,4-biradical form and 1,6-biradical form. The 1,4-biradical form affords oxetane **2OX** after the intersystem crossing (ISC). Alternatively, 2,7-dioxabicyclo[2.2.1]hept-5-ene **OBH** would be formed from the 1,6-biradical form. The regioisomeric oxetane **3OX** should be formed via the regioisomeric biradical

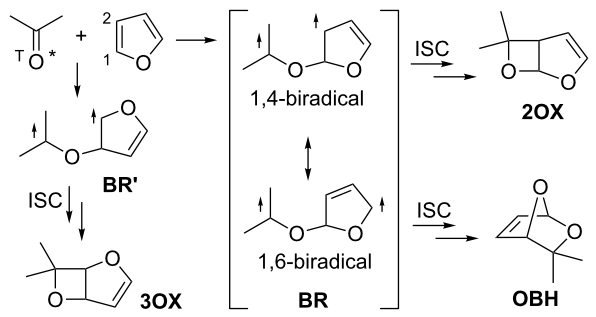

Scheme 1: Reaction of furan with triplet excited carbonyls, regioselectivity.

BR'. Biradical **BR** is energetically more stable than **BR'**, because **BR** can undergo radical delocalization. The electrophilic oxygen of the excited carbonyl should preferably interact with more nucleophilic C1 carbon to give selectively the biradical **BR**. Thus, only the 2-alkoxyoxetane **2OX** has been observed in the Paternò–Büchi reactions reported so far [19-27]. Thus, in this study, furan-2-ylmethyl 2-oxoacetates **1a**,**b** and 2-(furan-2-yl)ethyl 2-oxo-2-phenylacetate **1c** [28] were synthesized, in which the furan ring and the carbonyl moiety are connected intramolecularly, and their photochemical reactions were investigated to see whether the reaction proceeds intramolecularly to produce the 3-alkoxyoxetane derivative **A** and/or the dioxabicyclo[2.2.1]hept-5-ene derivative **B**, or intermolecularly to give the 2-alkoxyoxetane derivative **C** (Scheme 2).

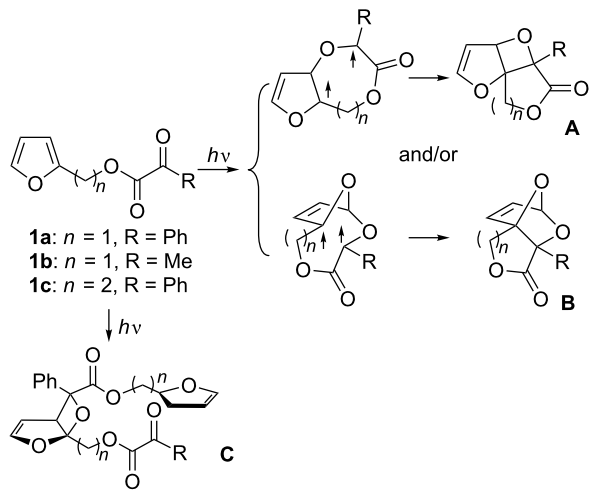

Scheme 2: Possible pathways for the photochemical reaction of furan derivatives **1a–c**.

Compounds **1a**–**c** [28] were synthesized from furan-2-ylmethanol or furan-2-ylethanol [29] (Scheme 3). Compound **1a** (R = Ph) was irradiated in degassed benzene with a high-pressure Hg lamp with a Pyrex filter (Scheme 3). Interestingly, the

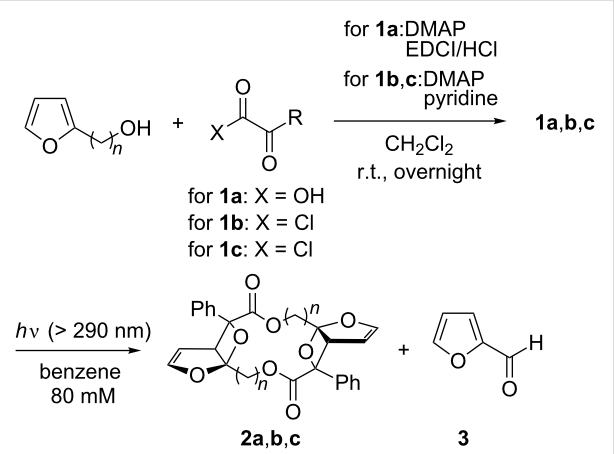

Scheme 3: Synthesis and the photochemical reaction of furan-2-ylmethyl 2-oxoacetates **1a**,**b**.

Paternò–Büchi dimer product **2a** (R = Ph), which possesses C_i symmetry, was obtained as the major product and contains the biologically important macrocyclic lactone structure [30-33]. The structure of **2a** was unequivocally determined by the X-ray crystallographic analysis (Figure 1). The one-step preparation of the highly functionalized twelve-membered macrocyclic lactone is synthetically attractive. Intramolecular products, such as compounds **A** and **B**, were not detected in the photolysate, although intramolecular cyclization products are known to be products in the photoreaction of 3-substituted furan derivatives [11,21]. Furan-2-carbaldehyde (**3**) was the only assignable product during the photochemical reaction, which was monitored by ^{1}H NMR spectroscopy (Figure 2). The intermolecular Paternò–Büchi reaction product, i.e., **C** in Scheme 2, was also not observed in the photolysate. This result suggests that the

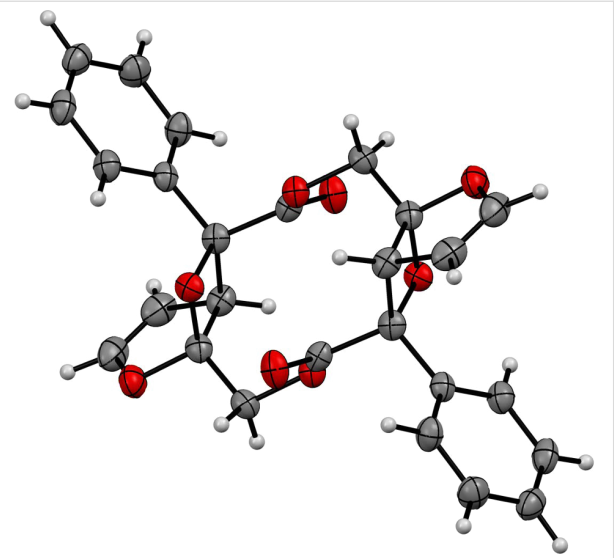

Figure 1: X-ray crystal structure of the macrocyclic lactone **2a**.

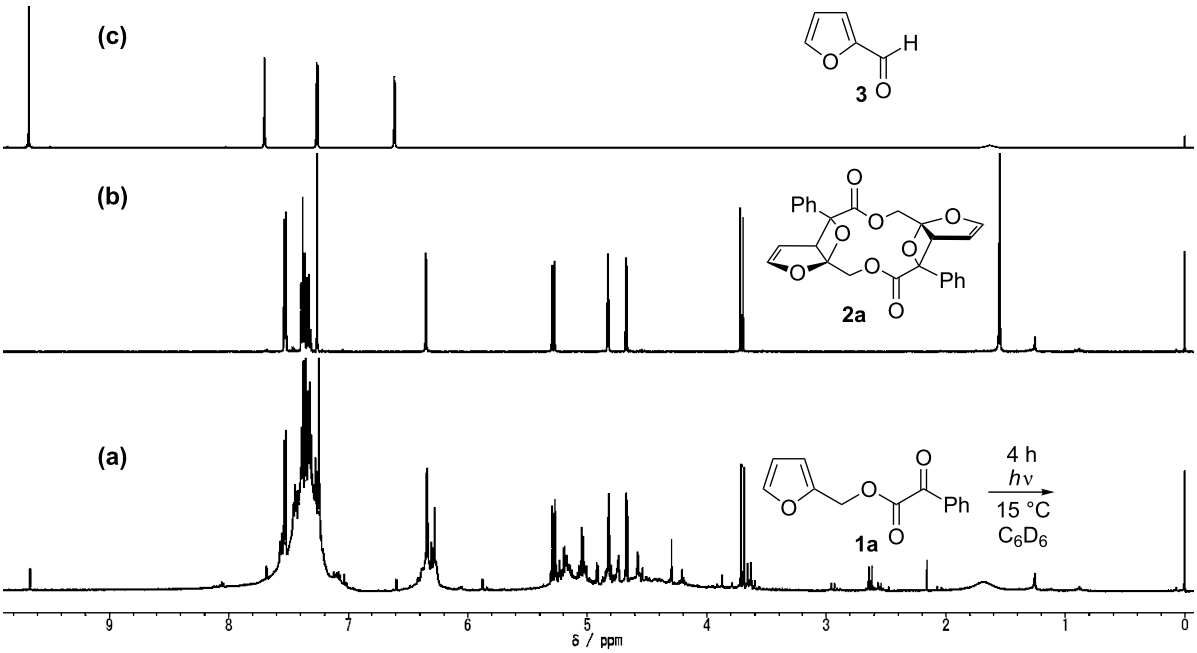

Figure 2: ^{1}H NMR spectra (500 MHz) for (a) the photolysate of **1a** after 4 h irradiation in degassed and dried C_6D_6 solution, (b) for isolated macrocyclic lactone **2a**, and (c) for furan-2-carbaldehyde (**3**).

intramolecular Paternò–Büchi reaction of **C** is faster than the first intermolecular Paternò–Büchi reaction of **1a**. The photoreaction of **1b** (R = Me) gave **2b** and **3** in 25% and 18%, respectively (Scheme 3). The dimerization product **2c** was not observed in the reaction of **1c**. Only polymeric products were present in the photolysate. Although the dimerization is sensitive to the chain-length, the Paternò–Büchi dimerization reaction could in future be applicable to the synthesis of a variety of macrocyclic lactones.

To investigate the effects of concentration, solvent, and temperature on the formation of **2a**, the photochemical reaction of **1a** was conducted under the variety of conditions (Table 1). The yield of intermolecular product **2a** was expected to be improved when the concentration of **1a** was increased; however, no concentration effect was observed (entry 2). Under the reaction conditions, the formation of polymeric products increased as evidenced by ^{1}H NMR analysis of the photolysate. Even with low concentrations of **1a** (entry 3), the intramolecular photoproducts **A** and **B** were not detected by ^{1}H NMR (500 MHz). To investigate the medium effect on the formation of **2a**, the photochemical reaction of **1a** was performed in several solvents (entries 4–6). The yield of **2a** decreased with increasing solvent polarity; 16% in toluene (entry 4) and 10% in CH_3CN (entry 6). Temperature had no effect on the yield of **2a** (entries 7–9).

In summary, the intramolecular products such as **A** and **B** were not observed in the photochemical reaction of furan derivatives

Table 1: Formation of **2a** in the photochemical reaction of **1a** under the various conditions[a].

entry	solvent	concentration of **1a** (mM)	temperature (°C)	yield of **2a** (%)[b]
1	benzene	80	15	18
2	benzene	800	15	8
3	benzene	8	15	17
4	toluene	80	15	16
5	CH_2Cl_2	80	15	10
6	CH_3CN	80	15	10
7	benzene	80	50	5
8	toluene	80	−35	18
9	toluene	80	−75	14

[a]The photochemical reactions of **1a** were performed for 4 h with a high-pressure Hg lamp (300 W) with a Pyrex filter under a dry nitrogen atmosphere in dried and degassed solvent. [b]The yields of **2a** were determined on the basis of ^{1}H NMR (500 MHz) peak areas; error ± 3%. Dimethyl fumarate was used as an internal standard.

1a,**b**, but interestingly the Paternò–Büchi dimers **2a**,**b** with the C_i symmetry, i.e., macrocyclic lactones, were isolated in ca. 20% yield. The results indicate that the intramolecular reactions, which produce 3-alkoxyoxetanes and 2,7-dioxabicyclo[2.2.1]hept-5-ene (Scheme 1 and Scheme 2), are slower than the intermolecular reaction which leads to the preferential formation of 2-alkoxyoxetane **C** which is followed by a second Paternò–Büchi reaction to give the observed macrocyclic lactones **2**. This finding should stimulate future experimental

and computational studies on the mechanistically and synthetically fascinating formation of macrocyclic lactone derivatives.

Experimental

NMR and MS measurements were made using JEOL JMN-LA500 and Thermo Fisher Scientific LTD Orbitrap XL spectrometers, respectively, at the Natural Science Center for Basic Research and Development (N-BARD), Hiroshima University.

The furan derivatives **1a**–**c** (129 mg, 0.561 mmol) were dissolved in benzene (7.0 ml) and the degassed reaction mixture was irradiated with a high-pressure Hg lamp (300 W, $h\nu$ > 290 nm) with a Pyrex filter. After 13 h, the solvent was removed in vacuo and dimethyl fumarate added as an internal standard. ^{1}H NMR (500 MHz, $CDCl_3$) was measured to determine the ratio of products. After the photoreaction, the residue was purified by repeated column chromatography and PTLC (hexane–EtOAc = 2:1) to give **2a**,**b** as colorless crystals.

2a: ^{1}H NMR (500 MHz, $CDCl_3$) δ 7.55–7.51 (m, 4H), 7.40–7.31 (m, 6H), 6.35 (dd, J = 3.1, 1.1 Hz, 2H), 5.28 (dd, J = 12.5, 0.9 Hz, 2H), 4.82 (dt, J = 3.0, 0.9 Hz, 2H), 4.67 (dd, J = 3.0, 1.1 Hz, 2H), 3.71 (d, J = 12.5 Hz, 2H); ^{13}C NMR (125 MHz, $CDCl_3$): δ 171.6 (C), 148.7 (CH), 136.0 (CH), 128.6 (CH), 128.4 (CH), 125.7 (CH), 112.6 (C), 102.1 (CH), 90.7 (C), 61.4 (CH2), 55.2 (CH); HRMS (ESI) *m/z* calcd for $C_{26}H_{20}O_8Na$ $(M + Na)^+$ 483.10504, found 483.10526.

2b: ^{1}H NMR (500 MHz, $CDCl_3$): δ 6.66 (dd, J = 3.0, 1.2 Hz, 2H), 5.23 (dt, J = 3.0, 0.8 Hz, 2H), 5.14 (dd, J = 12.5, 0.8 Hz, 2H), 4.27 (dd, J = 3.0, 1.2 Hz, 2H), 3.77 (d, J = 12.5 Hz, 2H), 1.57 (s, 6H); ^{13}C NMR (125 MHz, $CDCl_3$): δ 173.3 (C), 149.8 (CH), 112.7 (C), 101.3 (CH), 88.1 (C), 61.5 (CH_2), 53.1 (CH), 21.2 (CH_3); HRMS (ESI) *m/z* calcd for $C_{16}H_{16}O_8Na$ $(M + Na)^+$ 359.07374, found 359.07391.

Supporting Information

Supporting Information File 1

Experimental section for preparation of compounds **1a**–**c**, the detail of the X-ray structure of compound **2a**, and ^{1}H NMR and ^{13}C NMR spectra for compounds **2a**,**b**.
[http://www.beilstein-journals.org/bjoc/content/supplementary/1860-5397-7-35-S1.pdf]

Supporting Information File 2

X-Ray crystallographic data for compound **2a**.
[http://www.beilstein-journals.org/bjoc/content/supplementary/1860-5397-7-35-S2.cif]

Acknowledgements

M. A. acknowledges financial support in the form of a Grant-in-Aid for Scientific Research on Innovative Areas "π-Space" (No 21108516), the Scientific Research (B) (No. 19350021), and Tokuyama Science Foundation.

References

1. Paternò, E.; Chieffi, G. *Gazz. Chim. Ital.* **1909,** *39,* 341–361.
2. Büchi, G.; Inman, C. G.; Lipinsky, E. S. *J. Am. Chem. Soc.* **1954,** *76,* 4327–4331. doi:10.1021/ja01646a024
3. Yang, N. C.; Nussim, M.; Jorgenson, M. J.; Murov, S. *Tetrahedron Lett.* **1964,** *5,* 3657–3664. doi:10.1016/S0040-4039(01)89388-6
4. Arnold, D. R. The Photocycloaddition of Carbonyl Compounds to Unsaturated Systems: The Syntheses of Oxetanes. In *Advances in Photochemistry;* Noyes, W. A.; Hammond, G. S.; Pitts, J. N., Eds.; John Wiley & Sons, Inc.: Hoboken, NJ, USA, 1968; Vol. 6, pp 301–349. doi:10.1002/9780470133361.ch4
5. Carless, H. A. J. In *Synthetic Organic Photochemistry;* Horspool, W. M., Ed.; Plenum Press: New York, 1984; pp 425–487.
6. Griesbeck, A. G. Photochemical Oxetane Formation: Intermolecular Reactions. In *CRC Handbook of Organic Photochemistry and Photobiology;* Horspool, W. M.; Song, P.-S., Eds.; CRC Press: Boca Raton, 1995; pp 522–535.
7. Griesbeck, A. G. In *CRC Handbook of Organic Photochemistry and Photobiology;* Horspool, W. M.; Song, P.-S., Eds.; CRC Press: Boca Raton, 1995; pp 550–559.
8. Griesbeck, A. G.; Bondock, S. Oxetane Formation: Stereocontrol. In *CRC Handbook of Organic Photochemistry and Photobiology,* 2nd ed.; Horspool, W. M.; Lenci, F., Eds.; CRC Press: Boca Raton, 2004; chapter 59.
9. Griesbeck, A. G.; Bondock, S. Oxetane Formation: Intermolecular Additions. In *CRC Handbook of Organic Photochemistry and Photobiology,* 2nd ed.; Horspool, W. M.; Lenci, F., Eds.; CRC Press: Boca Raton, 2004; chapter 60.
10. Abe, M. Photochemical Oxetane Formation: Addition to Heterocycles. In *CRC Handbook of Organic Photochemistry and Photobiology,* 2nd ed.; Horspool, W. M.; Lenci, F., Eds.; CRC Press: Boca Raton, 2004; chapter 62.
11. Porco, J. A.; Schreiber, S. L. The Paternò–Büchi Reaction. In *Comprehensive Organic Synthesis;* Trost, B. M.; Fleming, I., Eds.; Pergamon Press: Oxford, 1991; Vol. 2, pp 151–192. doi:10.1016/B978-0-08-052349-1.00123-2
12. Bach, T. *Synthesis* **1998,** 683–703. doi:10.1055/s-1998-2054
13. Hei, X.-M.; Song, Q.-H.; Li, X.-B.; Tang, W.-J.; Wang, H.-B.; Guo, Q.-X. *J. Org. Chem.* **2005,** *70,* 2522–2527. doi:10.1021/jo048006k
14. Abe, M.; Kawankami, T.; Ohata, S.; Nozaki, K.; Nojima, M. *J. Am. Chem. Soc.* **2004,** *126,* 2838–2846. doi:10.1021/ja039491o
15. Griesbeck, A. G.; Abe, M.; Bondock, S. *Acc. Chem. Res.* **2004,** *37,* 919–928. doi:10.1021/ar040081u
16. Abe, M. *J. Chin. Chem. Soc. (Taipei, Taiwan)* **2008,** *55,* 479–486.
17. Abe, M. Chapter 7. Formation of a Four-Membered Ring: Oxetanes. In *Handbook of Synthetic Photochemistry;* Albini, A.; Fagnoni, M., Eds.; Wiley-VCH: Weinheim, 2009; pp 217–239. doi:10.1002/9783527628193.ch7
18. Shima, K.; Sakurai, H. *Bull. Chem. Soc. Jpn.* **1966,** *39,* 1806–1808. doi:10.1246/bcsj.39.1806
19. Whipple, E. B.; Evanega, G. R. *Tetrahedron* **1968,** *24,* 1299–1310. doi:10.1016/0040-4020(68)88081-0

20. Jarosz, S.; Zamojski, A. *Tetrahedron* **1982,** *38,* 1447–1451. doi:10.1016/0040-4020(82)80228-7
21. Schreiber, S. L.; Hoveyda, A. H.; Wu, H.-J. *J. Am. Chem. Soc.* **1983,** *105,* 660–661. doi:10.1021/ja00341a077
22. Cantrell, T. S.; Allen, A. C.; Ziffer, H. *J. Org. Chem.* **1989,** *54,* 140–145. doi:10.1021/jo00262a032
23. Hambalek, R.; Just, G. *Tetrahedron Lett.* **1990,** *31,* 5445–5448. doi:10.1016/S0040-4039(00)97868-7
24. Griesbeck, A. G.; Buhr, S.; Fiege, M.; Schmickler, H.; Lex, J. *J. Org. Chem.* **1998,** *63,* 3847–3854. doi:10.1021/jo971767l
25. Hu, S.; Neckers, D. C. *J. Chem. Soc., Perkin Trans. 2* **1999,** 1771–1778. doi:10.1039/a901092k
26. D'Auria, M.; Racioppi, R.; Romaniello, G. *Eur. J. Org. Chem.* **2000,** 3265–3272. doi:10.1002/1099-0690(200010)2000:19<3265::AID-EJOC3265>3.0.CO;2-6
27. Zhang, Y.; Xue, J.; Gao, Y.; Fun, H.-K.; Xu, J.-H. *J. Chem. Soc., Perkin Trans. 1* **2002,** 345–353. doi:10.1039/B109697D
28. Howard, B. E.; Woerpel, K. A. *Tetrahedron* **2009,** *65,* 6447–6453. doi:10.1016/j.tet.2009.05.066
29. Loiseau, F.; Simone, J.-M.; Carcache, D.; Bobal, P.; Neier, R. *Monatsh. Chem.* **2007,** *138,* 121–129. doi:10.1007/s00706-006-0578-x
30. Miyauchi, H.; Ikematsu, C.; Shimazaki, T.; Kato, S.; Shinmyozu, T.; Shimo, T.; Somekawa, K. *Tetrahedron* **2008,** *64,* 4108–4116. doi:10.1016/j.tet.2008.02.005
31. Denmark, S. E.; Muhuhi, J. M. *J. Am. Chem. Soc.* **2010,** *132,* 11768–11778. doi:10.1021/ja1047363
32. Wang, X.; Porco, J. A., Jr. *J. Am. Chem. Soc.* **2003,** *125,* 6040–6041. doi:10.1021/ja034030o
33. Molander, G. A.; Dehmel, F. *J. Am. Chem. Soc.* **2004,** *126,* 10313–10318. doi:10.1021/ja047190o

License and Terms

Beilstein Journal of Organic Chemistry

Photoinduced homolytic C–H activation in *N*-(4-homoadamantyl)phthalimide

Nikola Cindro[1], Margareta Horvat[1], Kata Mlinarić-Majerski[1], Axel G. Griesbeck[2] and Nikola Basarić[*1]

Full Research Paper

Open Access

Address:
[1]Department of Organic Chemistry and Biochemistry, Ruđer Bošković Institute, Bijenička cesta 54, 10 000 Zagreb, Croatia and [2]Department of Chemistry, University of Cologne, Greinstr. 4, Cologne D-50939, Germany

Email:
Nikola Basarić[*] - nbasaric@irb.hr

* Corresponding author

Keywords:
homoadamantanes; photoinduced H-abstraction; phthalimides

Beilstein J. Org. Chem. **2011,** *7,* 270–277.
doi:10.3762/bjoc.7.36

Received: 29 October 2010
Accepted: 27 January 2011
Published: 02 March 2011

This article is part of the Thematic Series "Photocycloadditions and photorearrangements".

Guest Editor: A. G. Griesbeck

Abstract

N-(4-homoadamantyl)phthalimide (**5**) on excitation and population of the triplet excited state underwent intramolecular H-abstractions and gave products **6** and **7**. The major product, *exo*-alcohol **6** was a result of the regioselective δ H-abstraction and the stereoselective cyclization of the 1,5-biradical. Minor products **7** were formed by photoinduced γ H-abstractions, followed by ring closure to azetidinols and ring enlargement to azepinediones. The observed selectivity to *exo*-alcohol **6** was explained by the conformation of **5** and the best orientation and the availability of the δ-H for the abstraction.

Introduction

Since the pioneering work of Ciamican and Paterno [1,2], the photochemistry of ketones has been intensively studied [3-6]. One important chemical pathway for the deactivation of ketones from the electronically excited states is photoinduced H-abstraction [7]. Intermolecular photoinduced H-abstraction leads principally to the reduction of the ketone [8-12], whereas intramolecular H-abstraction [13,14] leads to cyclization [15-17] or fragmentation, the so called Norish type II reaction [18-20]. The photochemistry of phthalimide derivatives is often similar to that of simple ketones [21-33]. For example, phthalimide derivatives in the electronically excited state abstract H-atoms from alcohols to give reduction products [34]. Furthermore, suitably substituted phthalimides deactivate from the excited state by intramolecular H-abstractions to yield cyclization products, often benzazepinone derivatives [35-37]. Therefore, photoinduced homolytic C–H activation by phthalimide derivatives can, in principle, be used in organic synthesis for the preparation of benzazepinones [21,25,33].

In continuation of our interest in the Majerski's laboratory in the functionalization and transformation of cage molecules [38-48] as well as the preparation of biologically active compounds

[49], we turned our attention to adamantylphthalimides [50-52]. Recently, in cooperation with the group of Griesbeck we discovered a photoinduced domino reaction of adamantylphthalimide that involves two consecutive γ H-abstractions and leads to a complex methanoadamantane benzazepinone **2** (Scheme 1) [51]. The mechanism of the photoinduced domino reaction was investigated and it was found that it probably takes place from a higher excited triplet state or the singlet state [52]. Herein, we report the synthesis and photochemistry of a phthalimide derivative of homoadamantane **5**. The research was conducted to investigate the availability of different C–H bonds in the homoadamantane skeleton for the homolytic activation, that is, abstraction by the phthalimide. The research was, furthermore, sparked by the discovery that numerous polyazaheterocyclic adamantane derivatives show antiviral activity [53-55]. Thus, photoproducts derived from **5** may also exhibit antiviral activity, although that is yet to be substantiated.

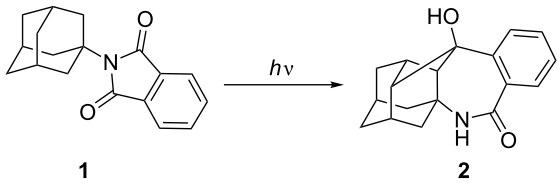

Scheme 1: Photoinduced domino reaction of adamantylphthalimide.

Investigation of the distances between the carbonyl groups of the phthalimide moiety and the H-atoms of the homoadamantane skeleton revealed that there are principally two γ H-atoms (with respect to the carbonyl of the phthalimide) and one δ H-atom available for the abstraction (see Scheme 4 and the Experimental for the notation of atoms). The distances between the carbonyl and γ H-atoms at the positions 3 and 5 of the homoadamantane skeleton are 3.52 and 2.52 Å, respectively, whereas distance to the δ H-atom at the position 2 is 2.37 Å. The calculated distances suggest that phthalimide **5** in the excited state should primarily give rise to products derived from the abstraction of the γ H-atom from position 5 and the δ H-atom from position 2 in the homoadamantane skeleton.

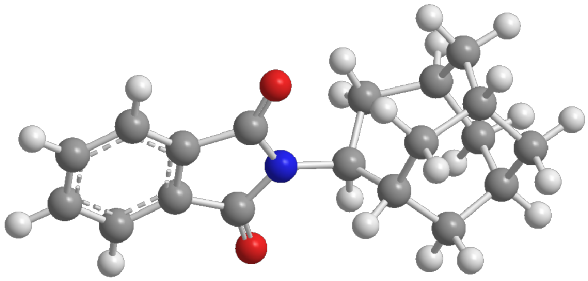

Figure 1: Molecular structure of **5**, the geometry optimization was performed by use of DFT B3LYP/6-31G.

Results and Discussion

The synthesis of homoadamantylphthalimide **5** started from homoadamantanone **3** which is easily prepared by the ring enlargement of adamantanone with diazomethane, generated in situ from *N*-methyl-*N*-nitroso-*p*-toluenesulfonamide (Diazald®) [56]. Homoadamantanone **3** was first reduced to the alcohol **4** [57-59] and subsequently converted to homoadamantyl phthalimide **5** in moderate yield via the Mitsunobu protocol [60] (Scheme 2).

To get more insight into the availability of H-atoms in the homoadamantane skeleton for the abstraction by the phthalimide, molecular modeling was performed. The geometry of **5** was optimized by DFT B3LYP/6-31G method (Figure 1) [61].

Irradiation of **5** was performed in CH_3CN, CH_3CN–H_2O (3:1), acetone and acetone–H_2O (3:1) and gave three products, i.e., the *exo*-alcohol **6**, and the azepinediones *syn*-**7** and *anti*-**7** (Scheme 3). In all investigated solvents, *exo*-alcohol **6** was the major product. For example, when the irradiation was performed in acetone–H_2O for 4 h (see the Experimental), the ratio of the isolated starting phthalimide **5** and the photoproducts **6** and **7** was 10:8:6. However, prolonged irradiation in acetone–H_2O (18 h) gave only alcohol **6** which was isolated in 53% yield. Products **7** decomposed on prolonged irradiation. The photochemical reaction was more efficient in solvent system containing acetone rather than CH_3CN. After 18 h irradiation in acetone–H_2O, complete conversion of **5** was achieved, whereas under the same photolysis conditions in

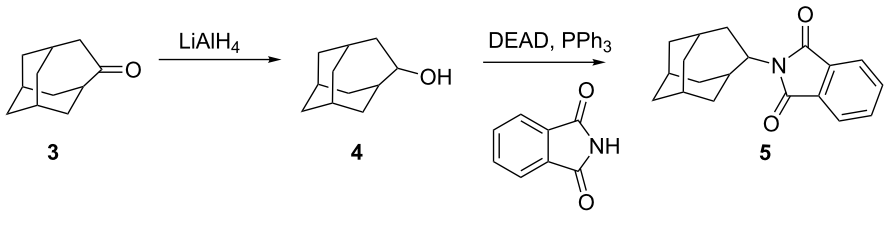

Scheme 2: Synthesis of homoadamantylphthalimide **5**.

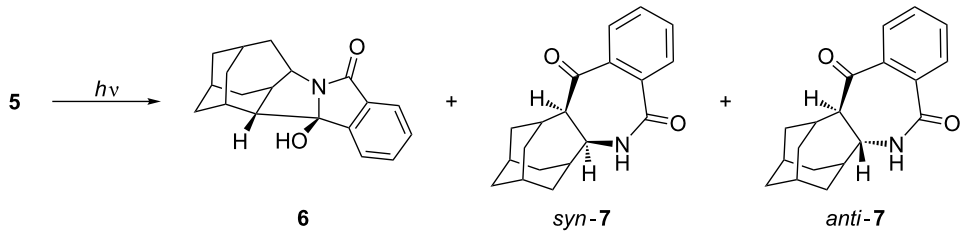

Scheme 3: Products after irradiation of **5**.

$CH_3CN–H_2O$, 72% of unreacted **5** was recovered. This finding is in accordance with acetone acting as a triplet sensitizer and the anticipated triplet state reactivity of the phthalimide in the H-abstraction reactions. Furthermore, the addition of H_2O as a protic solvent also increased the reactivity of the phthalimide, based on the conversion of the starting material under the same irradiation conditions. Thus, after 1 h photolysis of **5** in acetone, only 5% of **5** was converted to products, whereas after photolysis in acetone–H_2O, a 60% conversion was achieved. This suggests that phthalimide in the triplet excited state, in a protic solvent, undergoes H-abstraction to give products with ten times higher quantum yields than in an aprotic solvent. Such a finding is in accordance with previous reports for phthalimides and is probably due to a switching of the relative order of the singlet and the triplet excited states of the phthalimide [54,62,63].

The structures of photoproducts was determined by spectroscopic methods. In the ^{1}H NMR spectrum of **6**, in the aromatic region, 4 well-resolved signals are present, indicating the loss of symmetry of the aromatic part of the molecule (compared to the symmetry in **5**). Similarly, in the aromatic part of the ^{13}C NMR spectrum, 4 doublets are present. In the aliphatic part of the ^{13}C spectrum, 6 doublets and 5 triplets are observed and one quaternary C at δ 98.13 ppm. All of these features are in agreement with the molecular structure of **6**. The structure is further supported by 2D NMR wherein all the observed interactions are in agreement with the structure (for HMBC see the Experimental). The *exo*-stereochemistry of the product was established from the NOESY spectrum where an NOE interaction between the H-7 and H-10, and the H-7 and H-15 were present (for the notation of atoms see the Experimental). Assignment of the structure to azepinone products **7** was straightforward from the corresponding NMR spectra. In the ^{1}H NMR spectra they display the characteristic broad N–H singlets at 6.4 and 6.0 ppm. Furthermore, in the aliphatic part of the ^{13}C NMR spectra, 6 doublets and 5 triplets are present, in accord with the proposed structures. However, from their spectra we were unable to assign the *syn*- or the *anti*-stereochemistry to the isolated products **7**. In the NOESY spectra of both isolated compounds, an NOE interaction was observed between the H-atoms at the position 1 and 11 (for the notation of atoms see the Experimental), which precluded unambiguous assignment of the stereochemistry to the isomers **7**.

According to the above product study, a mechanism for the photochemical transformation of **5** can be proposed. On excitation (direct or sensitized) the triplet state of **5** is populated and undergoes intramolecular H-abstraction. The abstraction of the δ H-atom of the homoadamantane (Scheme 4) is probably the fastest since this H-atom is closest to the carbonyl of the phthalimide moiety. Although two γ H-atoms are available for the abstraction, and it is generally known that γ H-atoms are more readily abstracted [7,13,14], the conformation of the molecule is probably the most important factor that directs the selective δ-abstraction. The δ-abstraction gives rise to a 1,5-biradical (**1,5BR**) that undergoes stereoselective cyclization to furnish the major product, *exo*-alcohol **6**. The observed selectivity of the 1,5-cyclization is in line with the stability of the product formed. According to B3LYP calculations [61], *exo*-**6** is 15 kJ/mol more stable than *endo*-**6**. However, the reason for the observed selectivity is probably due to the preferred motion in which the half-filled orbitals of **1,5BR** overlap after ISC, and induce ring-closure.

Two γ H-atoms in **5** are in the proximity to the carbonyl and, in principle, available for abstraction. However, the H-atom at the ethylene bridge of the homoadamantane skeleton (position 5) is closer to the carbonyl, and therefore, more readily abstracted. Abstraction gives a 1,4-biradical (**1,4BR**) that cyclizes to azetidinol intermediates **AZT1** and **AZT2**. Azetidinols undergo subsequent ring enlargement to furnish products *anti*-**7** and *syn*-**7**, respectively. The ratio of the isolated compounds **7** is 5:1. However, no assignment of their stereochemistry was made from their spectra. Nevertheless, the cyclization of **1,4BR** is probably selective giving more **AZT2**, and product *syn*-**7** from the subsequent ring enlargement. The reason for the suspected selectivity becomes evident from the inspection of the structure of **1,4BR** where ring closure to the azetidinol probably takes place preferably from the upper side giving **AZT2**. The other approach (rear side) is sterically more demanding and results in a less stable trans-configuration on the azetidinol intermediate

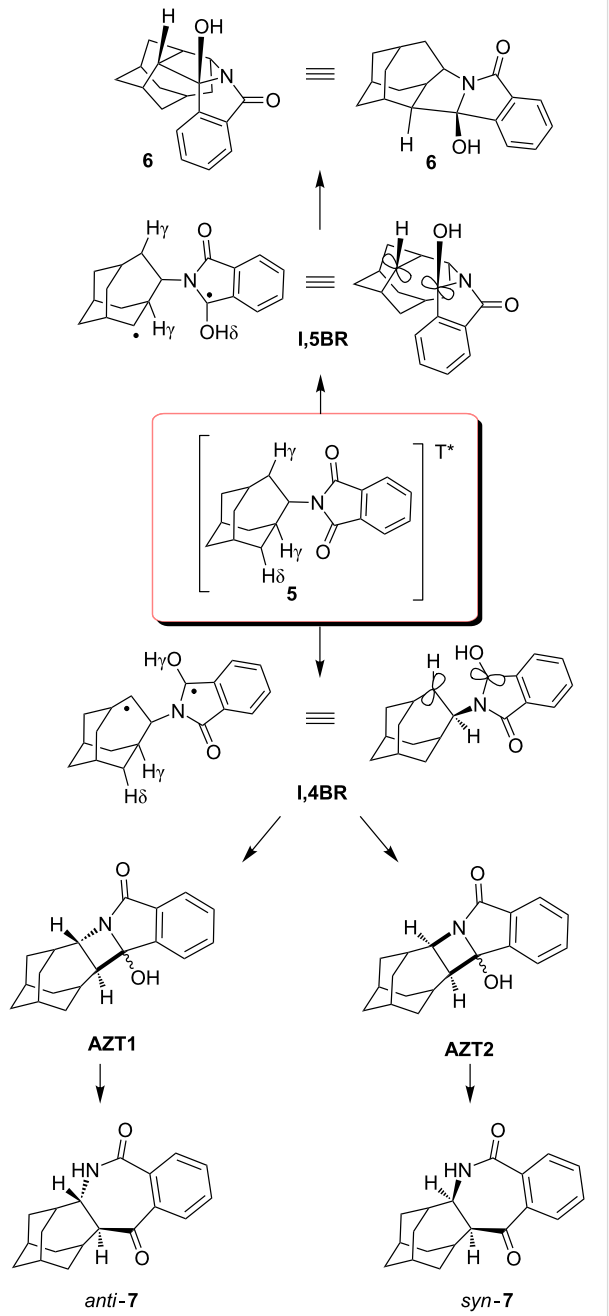

Scheme 4: Proposed mechanism for the photochemical transformation of **5**.

AZT1. Consequently, we suspect that the major isomer **7** has the *syn*-configuration, whereas the minor isomer has the *anti*-configuration.

Conclusion

N-(4-homoadamantyl)phthalimide (**5**) was synthesized and its photochemistry investigated. On excitation and population of the triplet state, **5** undergoes intramolecular homolytic C–H activation and gives products **6** and **7**. The major product of the photochemical reaction is exo-alcohol **6** formed *via* regioselective δ H-abstraction and stereoselective cyclization of the 1,5-biradical. The observed selectivity is due to the conformation of **5** where the δ H-atom is the closest to the carbonyl of the phthalimide moiety. Minor products **7** are formed by photoinduced γ H-abstraction, followed by ring closure to azetidinols and ring enlargement to azepinediones. High selectivity and high isolable yield of **6** in the photoreaction of **5** makes this photoinduced C–H activation useful in the synthesis of very complex derivatives with the homoadamantane skeleton with potential antiviral activity for which otherwise tedious multi-step synthesis would be required.

Experimental

General

^{1}H and ^{13}C NMR spectra were recorded on a Bruker Spectrometer at 300 or 600 MHz. All NMR spectra were measured in $CDCl_3$ using tetramethylsilane as a reference. High-resolution mass spectra (HRMS) were measured on an Applied Biosystems 4800 Plus MALDI TOF/TOF instrument. Melting points were obtained using an Original Kofler apparatus and are uncorrected. IR spectra were recorded on Perkin Elmer M-297 and ABB Bomem M-102 spectrophotometers. Solvents were purified by distillation. 4-Homoadamantanone (**3**) was prepared in the laboratory according to a known procedure [56]. Phthalimide, triphenylphosphine, lithium aluminum hydride (LAH) and diethyl azodicarboxylate (DEAD) were obtained from commercial sources. All photochemical experiments were performed in a Rayonet photochemical reactor equipped with 300 nm lamps.

4-Homoadamantanol (**4**)

To a suspension of LAH (3.00 g, 78.95 mmol) in dry THF (100 mL), was added a solution of 4-homoadamantanone (**3**, 1.00 g, 6.08 mmol) in THF (50 mL). The suspension was heated under reflux for 24 h. After the reaction was complete and cooled (ice bath), LAH was carefully destroyed by the slow addition of H_2O. The resulting precipitate was removed by filtration and washed with diethyl ether (3 × 30 mL). The combined organic solution was dried over anhydrous $MgSO_4$. After filtration and removal of the solvent under vacuum, compound **4** [57-59] was isolated in 99% yield (998 mg) and used in the next step without further purification.

N-(4-homoadamantyl)phthalimide (**5**)

4-Homoadamantanol (**4**, 1.00 g, 6.06 mmol), phthalimide (1.23 g, 8.35 mmol) and DEAD (2.00 mL, 12.64 mmol) were dissolved in dry THF (60 mL) in a three necked round bottomed flask. To the resulting mixture, a solution of triphenylphosphine (2.00 g, 7.63 mmol) in THF (60 mL) was added over a

1 h period. The reaction mixture was stirred at rt in the dark and under a nitrogen atmosphere for 12 h. After the reaction was complete, the solvent was evaporated, and the crude product purified by column chromatography on silica gel with hexane–CH_2Cl_2 (1:1) as eluent. Pure **5** (622 mg, 35%) was obtained as a crystalline product.

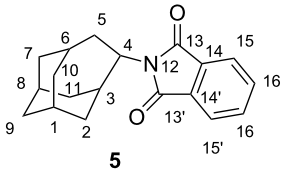

5

Colorless crystals, mp 110–111 °C; ^{1}H NMR ($CDCl_3$, 300 MHz, δ/ppm) 7.84–7.77 (m, 2H), 7.72–7.66 (m, 2H), 4.61 (t, 1H, *J* = 9.5 Hz, H-4), 2.60–2.50 (m, 1H), 2.45 (d, 1H, *J* = 14.1 Hz), 2.22–2.03 (m, 3 H), 1.98–1.85 (m, 5H), 1.80–1.62 (m, 3H), 1.60–1.52 (m, 3H); ^{13}C NMR ($CDCl_3$, 75 MHz, δ/ppm) 170.00 (s, 2C, C-13 and C-13'), 133.60 (d, 2C, C-15 and C-15' or C-16 and C-16'), 131.96 (s, 2C, C-14 and C-14'), 122.82 (d, 2C, C-15 and C-15' or C-16 and C-16') 56.97 (d, C-4), 40.10 (t, C-2 or C-10), 39.74 (t, C-2 or C-10), 39.56 (d, C-3), 36.64 (t, C-5), 35.58 (t, C-11), 33.99 (t, C-7 or C-9), 31.53 (t, C-7 or C-9), 29.44 (d, C-1), 27.18 (d, C-6), 27.17 (d, C-8); IR (KBr) ν/cm^{-1} 2910, 2850, 1765, 1707, 1375, 1350, 1323, 1114, 1084, 1070, 710; HRMS (MALDI), calculated for $C_{19}H_{22}NO_2$ 296.1645, observed 296.1644.

General procedure for semi-preparative photolysis of *N*-(4-homoadamantyl)phthalimide (**5**)

Phthalimide **5** (10 mg, 0.034 mmol) was dissolved in 20 mL of the appropriate solvent, CH_3CN, CH_3CN–H_2O (3:1), acetone or acetone–H_2O (3:1) in a quartz cuvette. The solutions were purged with N_2 for 20 min and irradiated in a Rayonet at 300 nm for 1 h. The solvent was removed on a rotary evaporator and ^{1}H NMR spectrum of the crude photolysis mixture recorded to determine the ratio of the products.

Preparative photolysis of *N*-(4-homoadamantyl)-phthalimide (**5**)

A Pyrex vessel was filled with a solution of *N*-(4-homoadamantyl)phthalimide (**5**) (100 mg, 0.338 mmol) in acetone–H_2O (3:1, 200 mL). The solution was irradiated in a Rayonet photoreactor at 300 nm for 4 h. During irradiation the reaction mixture was continuously purged with argon and cooled with a finger-condenser with tap water. After irradiation, the solvent was removed on a rotary evaporator. Unreacted **5** (42%) was recovered by column chromatography on silica gel with 5% MeOH-CH_2Cl_2 as eluent. The photoproducts were isolated by repeated preparative thin layer chromatography with the use of the following solvent mixtures: 5% MeOH-CH_2Cl_2, 30% diethyl ether-CH_2Cl_2, ethyl acetate–diethyl ether–CH_2Cl_2 (1:1:3) and hexane–ethyl acetate–diethyl ether–CH_2Cl_2 (1:2:2:5).

1-aza-9-hydroxyhexacyclo [10.7.0.1^{13,17}.0^{3,8}.0^{10,15}.0^{11,19}]eicosa-3,5,7-trien-2-one (**6**)

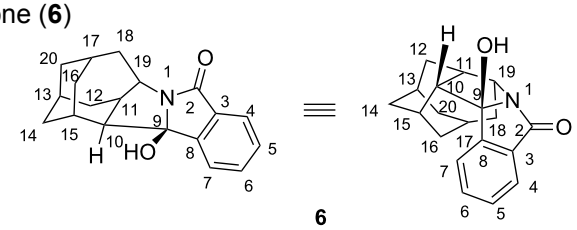

6

33 mg (33%); Colorless crystals; mp 183–185 °C; ^{1}H NMR ($CDCl_3$, 300 MHz, δ/ppm) 7.71 (td, 1H, *J* = 1.0 7.5 Hz, H-4), 7.61 (dt, 1H, *J* = 1.0, 7.5 Hz, H-6), 7.54 (td, 1H, *J* = 1.0, 7.5 Hz, H-7), 7.46 (dt, 1H, *J* = 1.0, 7.5 Hz, H-5), 4.35 (t(dd), 1H, *J* = 7.3 Hz, H-19), 2.70 (t(dd), 1H, *J* = 5.8 Hz, H-10), 2.60 (d, 1H, *J* = 14 Hz, H-16), 2.38 (br s, 1H, H-15), 2.11–2.22 (m, 3H, 2H-18, H-13), 2.03 (q, 1H, *J* = 6.9 Hz, H-11), 1.88–1.98 (m, 2H, H-17 and H-20), 1.70–1.88 (m, 3H, H-16, H-14 and H-12), 1.55–1.62 (m, 3H, H-14 and H-12), 1.43 (d, *J* = 13 Hz, H-20); ^{13}C NMR ($CDCl_3$, 75 MHz, δ/ppm) 177.27 (s, C-2), 151.77 (s, C-8), 133.65 (d, C-6), 131.38 (s, C-3), 129.52 (d, C-5), 123.95 (d, C-4), 122.24 (d, C-7), 98.13 (s, C-9), 64.31 (d, C-19), 48.19 (d, C-10), 42.21 (d, C-11), 40.94 (t, C-18), 40.38 (t, C-20), 35.62 (t, C-14), 32.69 (t, C-16), 31.17 (d, C-13), 30.62 (t, C-12), 27.93 (d, C-15), 26.89 (d, C-17); IR (KBr) ν/cm^{-1} 3300, 2980, 2902, 1694, 1605, 1464, 1433, 1338, 1320, 1297, 1231, 1125, 1053; HRMS (MALDI), calculated for $C_{19}H_{22}NO_2$ 296.1645, observed 296.1649.

Important HMBC interactions: H-19 and C-6, C-2, C-9, C-10; H-17 and C-19; H-16 and C-14, C-20; H-15 and C-9; H-12 and C-19; H-10 and C-19, C-8; H-4 and C-2, C-8; H-6 and C-8; H-7 and C-9; Important NOE interactions: H-7 and H-15; H-17 and H-10.

rel-(1*R*,11*S*)-2-azapentacyclo [9.7.0.1^{12,16}.1^{14,18}.0^{4,9}]eicosa-4,6,8-trien-3,10-dione (*syn*-**7**) and *rel*-(1*S*,11*S*)-2-azapentacyclo [9.7.0.1^{12,16}.1^{14,18}.0^{4,9}]eicosa-4,6,8-trien-3,10-dione (*anti*-**7**)

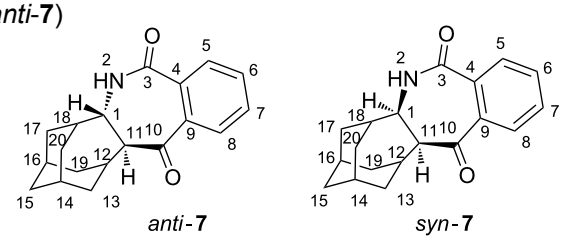

anti-**7** *syn*-**7**

21 mg (21%); colorless crystals, mp 244–245 °C; ^{1}H NMR ($CDCl_3$, 300 MHz, δ/ppm) 7.90–7.85 (m, 1H), 7.62–7.54 (m, 2H), 7.33–3.28 (m, 1H), 6.02 (br s, 1H, NH), 4.43 (m, H-1), 3.09 (d, 1H, *J* = 8.0 Hz, H-11), 3.04 (m, 1H, H-12), 2.44 (m (ddd), 1H, H-18), 2.18 (s, 1H, H-13), 2.08–1.93 (m, 4H, H-14, H-15, H-19 and H-17 or H-20), 1.89–1.83 (m, 2H, H-17 and H-20), 1.75 (d, 1H, H-13), 1.68–1.57 (m, 3H, 2 H-15 and H-20 or H-17), 1.38 (d, *J* = 12 Hz, H-19); ^{13}C NMR ($CDCl_3$, 75 MHz, δ/ppm) 132.30 (d, 1C), 130.38 (d, 1C), 128.71 (d, 1C), 125.40 (d, 1C), 67.21 (d, C-11), 54.32 (d, C-1), 41.42 (t, C-19), 35.50 (t, C-15), 34.72 (d, C-18), 32.75 (t, C-17 or C-20), 32.69 (t, C-17 or C-20), 30.78 (t, C-13), 28.61 (d, C-12), 27.09 (d, C-16 or C-14), 27.05 (d, C-16 or C-14), quarternary C-signals were not detected; IR (KBr) ν/cm^{-1} 3424, 2922, 2856, 1703, 1658, 1561, 1384, 1275, 1096, 801; HRMS (MALDI), calculated for $C_{19}H_{22}NO_2$ 296.1645, observed 296.1646.

Important COSY interactions: NH and H-1, H-1 and H-11, H-1 and H-18. Important NOE interaction: H-1 and H-11, H-1 and H-18, NH and H-17, H-11 and H-19 [64].

4 mg (4%); colorless crystals, mp 229–231 °C; ^{1}H NMR ($CDCl_3$, 300 MHz, δ/ppm) 8.12 (dd, 1H, *J* = 1.2, 7.6 Hz, H-5 or H-8), 8.06 (dd, 1H, *J* = 1.2, 7.6 Hz , H-5 or H-8), 7.72–7.60 (m, 2H, H-6 and H-7), 6.49 (br s, 1H, NH), 3.92 (t, 1H, *J* = 7.5 Hz, H-1), 3.00 (t, 1H, *J* = 5.4 Hz, H-12), 2.95 (d, 1H, *J* = 8.8 Hz, H-11), 2.17–1.82 (m, 7H, H-18, 2 H-13, H-14, H-17, H-16, H-19), 1.63–1.40 (m, 6H, 2 H-15, H-17, 2 H-20, H-19); ^{13}C NMR ($CDCl_3$, 75 MHz, δ/ppm) 133.01 (d, C-5 or C-8), 131.66 (d, C-5 or C-8), 130.81 (d, C-6 or C-7), 129.48 (d, C-6 or C-17), 67.33 (d, C-11), 58.49 (d, C-1), 40.43 (t, C-17 or C-19), 38.73 (t, C-17 or C-19), 36.00 (d, C-18), 35.78 (t, C-20), 32.06 (t, C-15), 30.36 (d, C-12), 30.18 (t, C-13), 26.48 (d, C-14 or C-16), 26.17 (d, C-14 or C-16), quarternary C-signals were not detected due to small quantity of the sample; IR (KBr) ν/cm^{-1} 3159, 3057, 2899, 2851, 1681, 1658, 1595, 1441, 1403, 1275, 1266, 1011, 786, 756; HRMS (MALDI), calculated for $C_{19}H_{22}NO_2$ 296.1645, observed 296.1646. Important NOE interaction: H-1 and H-11, H-1 and H-18, NH and H-20 [64].

Supporting Information

Supporting Information File 1

Supporting information contains ^{1}H and ^{13} C NMR spectra of compounds **5**–**7** and atomic coordinates for **5** and **6** calculated by B3LYP/6-31G.
[http://www.beilstein-journals.org/bjoc/content/supplementary/1860-5397-7-36-S1.pdf]

Acknowledgements

These materials are based on work financed by the National Foundation for Science, Higher Education and Technological Development of the Republic of Croatia (NZZ grant no. 02.05/25), the Ministry of Science Education and Sports of the Republic of Croatia (grant No. 098-0982933-2911).

References

1. Ciamician, G. *Science* **1912,** *36,* 385–394. doi:10.1126/science.36.926.385
2. Paterno, E.; Chieffi, G. *Gazz. Chim. Ital.* **1909,** *39,* 341–361.
3. Wagner, P. J. *Acc. Chem. Res.* **1971,** *4,* 168–177. doi:10.1021/ar50041a002
4. Mattay, J.; Griesbeck, A. G. *Photochemical Key Steps in Organic Synthesis: An Experimental Course Book;* Wiley-VCH: Weinheim, 1994; pp 11–118.
5. Lenci, F.; Horspool, W., Eds. *CRC Handbook of Organic Photochemistry and Photobiology;* CRC Press: Boca Raton, FL, 2004.
6. Griesbeck, A. G.; Mattay, J., Eds. *Synthetic Organic Photochemistry;* Marcel Dekker: New York, 2005.
7. Wagner, P. J.; Park, B.-S. In *Organic Photochemistry;* Padwa, A., Ed.; Marcel Dekker: New York, 1991; Vol. 11, pp 227–366.
8. Simonaitis, R.; Cowell, G. W.; Pitts, J. N., Jr. *Tetrahedron Lett.* **1967,** *38,* 3751–3754. doi:10.1016/S0040-4039(01)89786-0
9. Cohen, S. G.; Chao, H. M. *J. Am. Chem. Soc.* **1968,** *90,* 165–173. doi:10.1021/ja01003a029
10. Cohen, S. G.; Green, B. *J. Am. Chem. Soc.* **1969,** *91,* 6824–6829. doi:10.1021/ja01052a048
11. Lewis, F. D. *Tetrahedron Lett.* **1970,** *11,* 1373–1376. doi:10.1016/S0040-4039(01)97973-0
12. Lewis, F. D.; Magyar, J. G. *J. Org. Chem.* **1972,** *37,* 2102–2107. doi:10.1021/jo00978a010
13. Wagner, P. J. In *Synthetic Organic Photochemistry;* Griesbeck, A. G.; Mattay, J., Eds.; Molecular and Supramolecular Photochemistry, Vol. 12; Marcel Dekker: New York, 2005; pp 11–39.
14. Wessig, P.; Mühling, O. In *Synthetic Organic Photochemistry;* Griesbeck, A. G.; Mattay, J., Eds.; Molecular and Supramolecular Photochemistry, Vol. 12; Marcel Dekker: New York, 2005; pp 41–87.
15. Yang, N. C.; Yang, D.-D. H. *J. Am. Chem. Soc.* **1958,** *80,* 2913–2914. doi:10.1021/ja01544a092
16. Wagner, P. J. *Acc. Chem. Res.* **1989,** *22,* 83–91. doi:10.1021/ar00159a001
17. Wagner, P. J. Yang Photocyclization: Coupling of Biradicals Formed by Intramolecular Hydrogen Abstraction of Ketones. In *CRC Handbook of Organic Photochemistry and Photobiology;* Lenci, F.; Horspool, W., Eds.; CRC Press: Boca Raton, FL, 2004; Chapter 58.
18. Barltrop, J. A.; Coyle, J. D. *J. Am. Chem. Soc.* **1968,** *90,* 6584–6588. doi:10.1021/ja01026a002
19. Wagner, P. J.; Klán, P. Norrish Type II Photoelimination of Ketones: Cleavage of 1,4-Biradicals Formed by γ-Hydrogen Abstraction. In *CRC Handbook of Organic Photochemistry and Photobiology;* Lenci, F.; Horspool, W., Eds.; CRC Press: Boca Raton, FL, 2004; Chapter 52.
20. Hasegawa, T. Norrish Type II Processes of Ketones: Influence of Environment. In *CRC Handbook of Organic Photochemistry and Photobiology;* Lenci, F.; Horspool, W., Eds.; CRC Press: Boca Raton, FL, 2004; Chapter 55.
21. Kanaoka, Y. *Acc. Chem. Res.* **1978,** *11,* 407–413. doi:10.1021/ar50131a002

22. Mazzocchi, P. H. In *Organic Photochemistry;* Padwa, A., Ed.; Marcel Dekker: New York, 1981; Vol. 5, pp 421–471.
23. Coyle, J. D. In *Synthetic Organic Photochemistry;* Horspool, W. M., Ed.; Plenum Press: New York, 1984; pp 259–284.
24. Mauder, H.; Griesbeck, A. G. In *CRC Handbook of Organic Photochemistry and Photobiology;* Horspool, W. M.; Song, P.-S., Eds.; CRC Press: Boca Raton, FL, 1995; pp 513–521.
25. Griesbeck, A. G. *Liebigs Ann.* **1996,** *1996,* 1951–1958. doi:10.1002/jlac.199619961202
26. Griesbeck, A. G. *Chimia* **1998,** *52,* 272–283.
27. Oelgemöller, M.; Griesbeck, A. G. *J. Photochem. Photobiol., C: Photochem. Rev.* **2002,** *3,* 109–127. doi:10.1016/S1389-5567(02)00022-9
28. Yoon, U. C.; Mariano, P. S. *Acc. Chem. Res.* **2001,** *34,* 523–533. doi:10.1021/ar010004o
29. Oelgemöller, M.; Griesbeck, A. G. Photoinduced Electron-Transfer Processes of Phthalimides. In *CRC Handbook of Organic Photochemistry and Photobiology;* Lenci, F.; Horspool, W., Eds.; CRC Press: Boca Raton, FL, 2004; Chapter 84.
30. Yoon, U. C.; Mariano, P. S. The Photochemistry of Silicon-Substituted Phthalimides. In *CRC Handbook of Organic Photochemistry and Photobiology;* Lenci, F.; Horspool, W., Eds.; CRC Press: Boca Raton, FL, 2004; Chapter 85.
31. McDermott, G.; Yoo, D. J.; Oelgemöller, M. *Heterocycles* **2005,** *65,* 2221–2257. doi:10.3987/REV-05-601
32. Yoon, U. C.; Mariano, P. S. In *Organic Photochemistry and Photophysics;* Ramamurthy, V.; Schanze, K., Eds.; CRC Press, Taylor & Francis Group: Boca Raton, FL, 2006; pp 179–206.
33. Horvat, M.; Mlinarić-Majerski, K.; Basarić, N. *Croat. Chem. Acta* **2010,** *83,* 179–188.
34. Kanaoka, Y.; Koyama, K. *Tetrahedron Lett.* **1972,** 4517–4520. doi:10.1016/S0040-4039(01)94356-4
35. Kanaoka, Y.; Migita, Y.; Koyama, K.; Sato, Y.; Nakai, H.; Mizoguchi, T. *Tetrahedron Lett.* **1973,** *14,* 1193–1196. doi:10.1016/S0040-4039(01)95793-4
36. Kanaoka, Y.; Nagasawa, C.; Nakai, H.; Sato, Y.; Ogiwara, H.; Mizoguchi, T. *Heterocycles* **1975,** *3,* 553–556. doi:10.3987/R-1975-07-0553
37. Griesbeck, A. G.; Mauder, H. *Angew. Chem., Int. Ed.* **1992,** *31,* 73–75. doi:10.1002/anie.199200731
38. Mlinarić-Majerski, K.; Pavlović, D.; Milinković, V.; Kojić-Prodić, B. *Eur. J. Org. Chem.* **1998,** 1231–1236. doi:10.1002/(SICI)1099-0690(199806)1998:6<1231::AID-EJOC1231>3.0.CO;2-1
39. Mlinarić-Majerski, K.; Veljković, J.; Marchand, A. P.; Ganguly, B. *Tetrahedron* **1998,** *54,* 11381–11386. doi:10.1016/S0040-4020(98)00680-2
40. Mlinarić-Majerski, K.; Kragol, G. *Eur. J. Org. Chem.* **1999,** 1401–1406. doi:10.1002/(SICI)1099-0690(199906)1999:6<1401::AID-EJOC1401>3.0.CO;2-S
41. Mlinarić-Majerski, K.; Veljković, J.; Kaselj, M. *Croat. Chem. Acta* **2000,** *73,* 575–584.
42. Klaić, L.; Veljković, J.; Mlinarić-Majerski, K. *Synth. Commun.* **2002,** *32,* 89–97. doi:10.1081/SCC-120001513
43. Mlinarić-Majerski, K.; Veljković, J.; Kaselj, M.; Marchand, A. P. *Eur. J. Org. Chem.* **2004,** 2923–2927. doi:10.1002/ejoc.200400121
44. Šafar-Cvitaš, D.; Savin, B.; Mlinarić-Majerski, K. *Croat. Chem. Acta* **2004,** *77,* 619–625.
45. Mlinarić-Majerski, K.; Margeta, R.; Veljković, J. *Synlett* **2005,** 2089–2091. doi:10.1055/s-2005-871967
46. Basarić, N.; Molčanov, K.; Matković, M.; Kojić-Prodić, B.; Mlinarić-Majerski, K. *Tetrahedron* **2007,** *63,* 7985–7996. doi:10.1016/j.tet.2007.05.066
47. Mlinarić-Majerski, K.; Kragol, G.; Šumanovac Ramljak, T. *Synlett* **2008,** 405–409. doi:10.1055/s-2008-1032054
48. Vujasinović, I.; Veljković, J.; Molčanov, K.; Kojić-Prodić, B.; Mlinarić-Majerski, K. *J. Org. Chem.* **2008,** *73,* 9221–9227. doi:10.1021/jo801143s
49. Horvat, Š.; Mlinarić-Majerski, K.; Glavaš-Obrovac, L.; Jakas, A.; Veljković, J.; Marczi, S.; Kragol, G.; Roščić, M.; Matković, M.; Milostić-Srb, A. *J. Med. Chem.* **2006,** *49,* 3136–3142. doi:10.1021/jm051026+
50. Basarić, N.; Horvat, M.; Franković, O.; Mlinarić-Majerski, K.; Neudörfl, J.; Griesbeck, A. G. *Tetrahedron* **2009,** *65,* 1438–1443. doi:10.1016/j.tet.2008.12.010
51. Basarić, N.; Horvat, M.; Mlinarić-Majerski, K.; Zimmermann, E.; Neudörfl, J.; Griesbeck, A. G. *Org. Lett.* **2008,** *10,* 3965–3968. doi:10.1021/ol801362x
52. Horvat, M.; Görner, H.; Warzecha, K.-D.; Neudörfl, J.; Griesbeck, A. G.; Mlinarić-Majerski, K.; Basarić, N. *J. Org. Chem.* **2009,** *74,* 8219–8231. doi:10.1021/jo901753z
53. Lundahl, K.; Schut, J.; Schlatmann, J. L. M. A.; Paerels, G. B.; Paters, A. *J. Med. Chem.* **1972,** *15,* 129–132. doi:10.1021/jm00272a003
54. Kolocouris, N.; Foscolos, G. B.; Kolocouris, A.; Marakos, P.; Pouli, N.; Fytas, G.; Ikeda, S.; De Clercq, E. *J. Med. Chem.* **1994,** *37,* 2896–2902. doi:10.1021/jm00044a010
55. Kolocouris, N.; Kolocouris, A.; Foscolos, G. B.; Fytas, G.; Neyts, J.; Padalko, E.; Balzarini, J.; Snoeck, R.; Andrei, G.; De Clercq, E. *J. Med. Chem.* **1996,** *39,* 3307–3318. doi:10.1021/jm950891z
56. von Rague Schleyer, P.; Funke, E.; Liggero, S. H. *J. Am. Chem. Soc.* **1969,** *91,* 3965–3967. doi:10.1021/ja01042a058
57. Nordlander, J. E.; Wu, F. Y.-H.; Jindal, S. P.; Hamilton, J. B. *J. Am. Chem. Soc.* **1969,** *91,* 3962–3964. doi:10.1021/ja01042a057
58. Black, R. M.; Gill, G. B. *J. Chem. Soc. C* **1970,** 671–676. doi:10.1039/J39700000671
59. Majerski, K.; Majerski, Z. *Tetrahedron Lett.* **1973,** *14,* 4915–4918. doi:10.1016/S0040-4039(01)87371-8
60. Sen, S. E.; Roach, S. L. *Synthesis* **1995,** 756–758. doi:10.1055/s-1995-4012
61. *Gaussian 98;* Gaussian, Inc.: Pittsburgh, PA, 2001. Note: Calculated for the gas phase.
62. Griesbeck, A. G.; Görner, H. *J. Photochem. Photobiol., A: Chem.* **1999,** *129,* 111–119. doi:10.1016/S1010-6030(99)00180-X
63. Görner, H.; Griesbeck, A. G.; Heinrich, T.; Kramer, W.; Oelgemöller, M. *Chem.–Eur. J.* **2001,** *7,* 1530–1538. doi:10.1002/1521-3765(20010401)7:7<1530::AID-CHEM1530>3.0.CO;2-L
64. Plausible stereochemistry of the molecule is assigned according to the reaction mechanism. No unambigous assignment could be made from the NMR spectra.

Beilstein Journal of Organic Chemistry

Effects of anion complexation on the photoreactivity of bisureido- and bisthioureido-substituted dibenzobarrelene derivatives

Heiko Ihmels* and Jia Luo

Full Research Paper

Open Access

Address:
Organic Chemistry II, University of Siegen, Adolf-Reichwein-Str. 2, D-57068 Siegen, Germany

Email:
Heiko Ihmels* - ihmels@chemie.uni-siegen.de

* Corresponding author

Keywords:
dibenzobarrelenes; dibenzosemibullvalenes; di-π-methane rearrangement; supramolecular photochemistry; (thio)urea derivatives

Beilstein J. Org. Chem. **2011,** *7,* 278–289.
doi:10.3762/bjoc.7.37

Received: 11 November 2010
Accepted: 04 February 2011
Published: 04 March 2011

This article is part of the Thematic Series "Photocycloaddition and photorearrangement".

Guest Editor: A. G. Griesbeck

Abstract

Bisureido- and a bisthioureido-substituted dibenzobarrelene derivative were synthesized and the photoreactivity of two representative examples were studied. Direct irradiation of the ureido-substituted derivative induces a di-π-methane rearrangement to the corresponding dibenzosemibullvalene derivative, whereas the thioureido-substituted derivative is almost photoinert. Complexes of the latter derivative with chloride, carboxylates, or sulfonate anions, however, are efficiently transformed to the dibenzosemibullvalene product upon irradiation, presumably by suppressing the self-quenching of the thiourea units in the complex. The association of the ureido-substituted dibenzobarrelene derivative with (*S*)-mandelate and irradiation of this complex led to the formation of the dibenzosemibullvalene with moderate stereoselectivity (68:32 er). In contrast, the thioureido derivative showed no such effect upon complexation of chiral anions.

Introduction

The control of the selectivity of a photoreaction by supramolecular interactions has recently received much attention [1-3]. For example, chiral receptors have been employed that associate with photoreactive substrates, leading to a distinct preferential conformation of the latter and/or to a limited exposure of the substrate to other reagents due to the shielding effect of the receptor. Because of the restricted freedom of movement or availability of reactive sites within this assembly, mono- and bimolecular photoreactions may proceed through one preferential pathway resulting in regio- or stereoselective product formation. Indeed, this approach has been employed to carry out stereoselective photoreactions, for example [2 + 2] cycloaddition [4], [4 + 4] photocycloaddition [5], Norrish–Yang cyclization [6], and [6π] photocyclization [7]. Asymmetric photoreactions have also been carried out with very good stereoselectivities in organized or constrained media [8-10]. For

example, photoactive substrates may be accommodated as guest molecules in chiral host systems, such as suitably modified cucurbiturils [11-15], self-assembled cages [16] and bowls [17], liquid crystals [18], chiral crystals [19-23], or cyclodextrins (CDs) [24-26] in such a way that the chiral environment within the binding site has an influence on preferential reaction pathways, thus inducing stereoselective photoreactions.

Along these lines, the di-π-methane (DPM) rearrangement [27,28] of dibenzobarrelene (dibenzobicyclo[2.2.2]octatriene) (**1a**) and its derivatives has been shown to be an appropriate model reaction for the assessment of substituent effects on the selectivity of organic photoreactions (Scheme 1) [29,30]. The photoreactivity of dibenzobarrelene derivatives is multiplicity-dependent: The direct irradiation of **1a** leads to the dibenzocyclooctatetraene **3a** in a singlet reaction that occurs via an initial [2 + 2] cycloaddition followed by a [4 + 2] retro-Diels–Alder reaction [27-30]. In the presence of a triplet sensitizer, e.g., acetone or benzophenone, a triplet-state di-π-methane rearrangement is induced. Thus, in the initial reaction step connection between one vinyl and one benzo carbon atom takes place, i.e., a so called vinyl–benzo bridging, that leads to the intermediate biradical **BR1a** [29]. Subsequent rearomatization with the formation of the intermediate **BR2a** and intramolecular radical recombination gives the dibenzosemibullvalene **2a** as the reaction product. Notably, the DPM rearrangement of dibenzobarrelene derivatives such as **1b**, that carry substituents other than hydrogen atoms at the vinyl positions, leads to the formation of two enantiomeric dibenzosemibullvalenes **2b** and *ent*-**2b**. As indicated in Scheme 1, the two enantiomers originate from different vinyl–benzo bridging pathways in the first reaction step (path a or b). Note that the same two enantiomers are formed upon initial vinyl–benzo bridging with the other benzene unit.

Stereoselective DPM rearrangements of dibenzobarrelene derivatives have been reported in special media, such as chiral mesoporous silica [31] or ionic-liquids [32]; however, most examples for stereoselective DPM rearrangements of dibenzobarrelene derivatives have been observed in the solid-state. For example, the achiral derivative **1b** crystallizes in the chiral space group $P2_12_12_1$, and irradiation of the chiral crystals gives dibenzosemibullvalene **2b** with a high enantiomeric excess, >95% ee [33]. Since achiral molecules crystallize only very rarely in chiral space groups, the ionic chiral auxiliary strategy was developed by Scheffer et al. which allows to influence the stereoselectivity of solid-state photoreactions by chiral counter ions [34]. This is accomplished by providing the chromophore

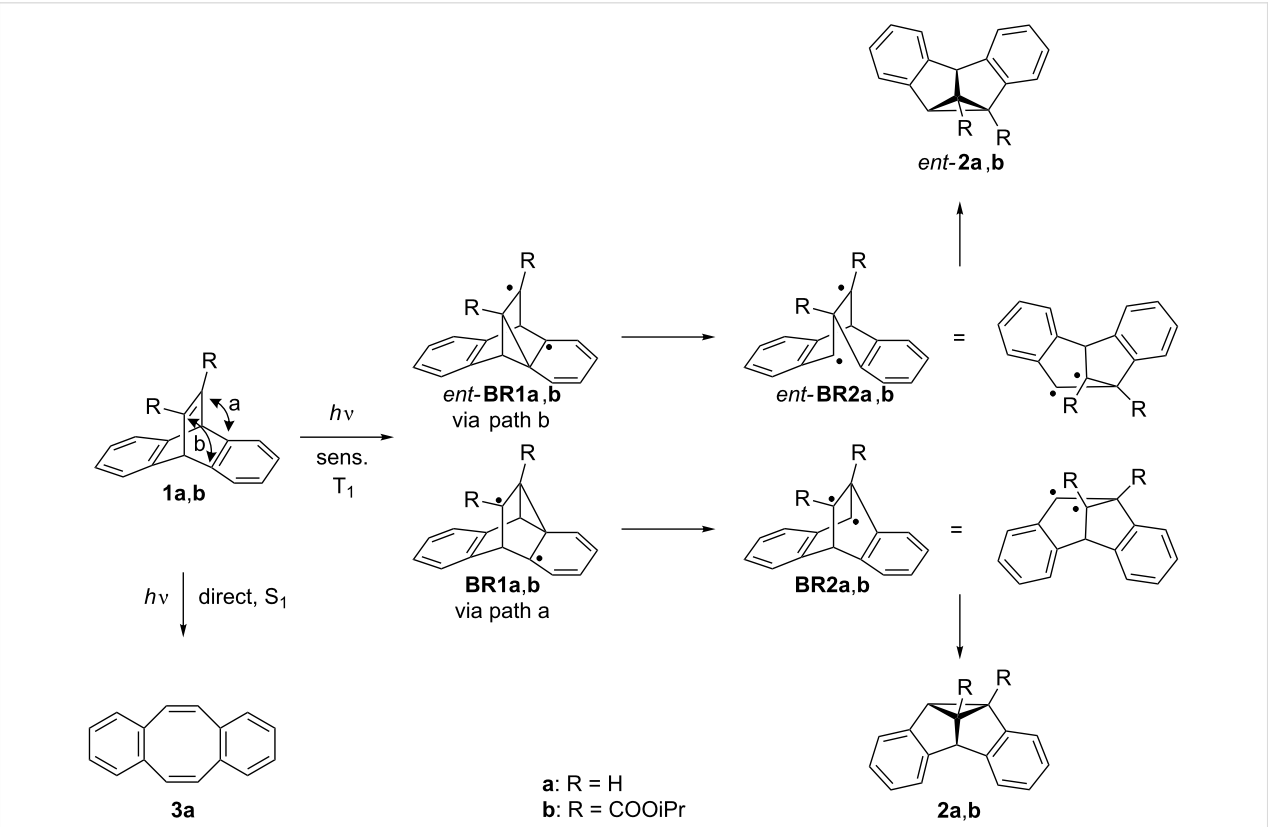

Scheme 1: Photorearrangements of dibenzobarrelenes **1a** and **1b**.

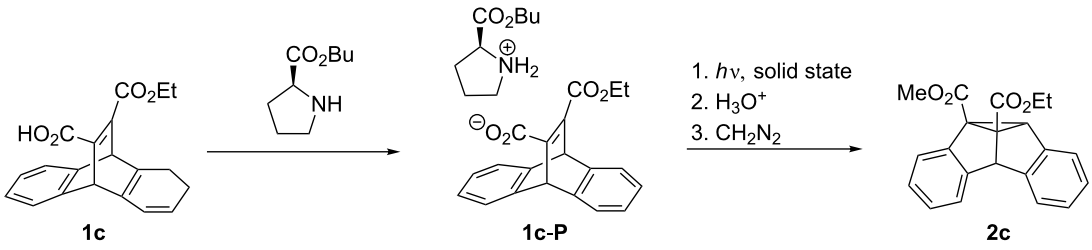

Scheme 2: Stereoselective DPM rearrangement of chiral salts in the solid-state.

under investigation with a carboxylic acid functionality and then by attaching a chiral, enantiomerically pure amine by salt formation. An optically active salt is obtained, which consequently crystallizes in a chiral space group. The irradiation of these salts in the solid-state leads to enantiomerically enriched photoproducts. This approach has been successfully applied to the carboxy-substituted dibenzobarrelene derivative **1c** which forms the chiral ammonium carboxylate **1c-P** with (*S*)-proline (Scheme 2). After irradiation, acidic workup and subsequent esterification with diazomethane, the dibenzosemibullvalene **2c** was obtained with high enantiomeric excess (>95% ee) [35,36].

Interestingly, several asymmetric photoreactions have been conducted with remarkable enantioselectivity in homogeneous solution, whereas reports of asymmetric di-π-methane rearrangements in solutions are relatively rare. Chiral auxiliaries attached as ester or amide functionalities at the vinylic positions of dibenzobarrelene induce only low enantioselectivities in the DPM rearrangement in solution [37]; and the ionic auxiliary strategy, which generates impressive enantioselectivity in the solid-state, fails to induce any stereoselectivity in DPM rearrangements in solution. Considering these observations, it remains a challenge to develop a method to accomplish stereoselective DPM rearrangements of dibenzobarrelene derivatives in homogenous solutions. Therefore, we intended to study whether supramolecular interactions of chiral additives with achiral dibenzobarrelenes may be used to influence the photoreactivity of the latter in solution. For that purpose the dibenzobarrelene chromophore was functionalized with ureido or thioureido substituents, since these functionalities are strong hydrogen bonding donors, which may associate with (chiral) anions [38,39]. Moreover, the versatile use of urea and thiourea derivatives in organocatalysis has been demonstrated in several examples [40-44]. Herein, we report the synthesis of ureido- and thioureido-substituted dibenzobarrelene derivatives **1e–i**, along with first studies of their photochemical properties in the absence and in the presence of anions.

Results

The bisureido- and bisthioureido-substituted dibenzobarrelene derivatives **1e–i** were synthesized by the reaction of the known bis(diaminomethyl)-substituted derivative of dibenzobarrelene **1d** [45] with a slight excess of the corresponding isocyanate or isothiocyanate (Scheme 3). The resulting products precipitated

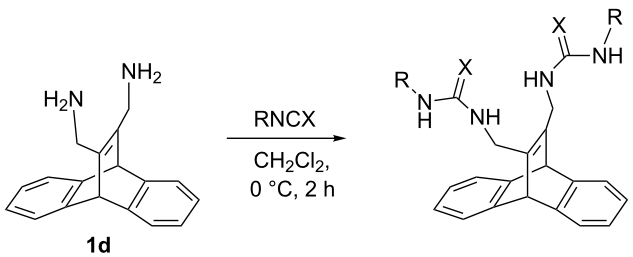

1e: R = *n*-Bu, X = O (79%)
1f : R = Ph, X = O (72%)
1g: R = 4-*n*-butylphenyl, X = O (76%)
1h: R = 3,5-$(CF_3)_2C_6H_3$, X = O (82%)
1i : R = 3,5-$(CF_3)_2C_6H_3$, X = S (86%)

Scheme 3: Synthesis of ureido- and thioureido-substituted dibenzobarrelene derivatives **1e–i**.

from the reaction mixture and were isolated in good yields (72–86%) by direct filtration, except for the thioureido-substituted derivative **1i**, which was crystallized from ethyl acetate to give crystals containing one molecule of ethyl acetate as indicated by ^{1}H NMR spectroscopy and elemental analysis. All products were fully characterized by ^{1}H and ^{13}C NMR spectroscopy, mass spectrometry, and elemental analysis. The solubility of the dibenzobarrelene derivatives **1e–g** is very low in most organic solvents (e.g., <5 mg/l in acetonitrile at 20 °C). In contrast, the 3,5-bis(trifluoromethyl)phenyl-substituted derivatives **1h** and **1i** have significantly improved solubility in organic solvents; i.e., compound **1h** has good solubility in acetone, acetonitrile and alcohols, while thiourea **1i** dissolves in most polar organic solvents.

Because of their favorable solubility in organic solvents, the dibenzobarrelene derivatives **1h** and **1i** were used for the systematic photochemical studies. In both acetone and acetonitrile, irradiation of the bisureido-substituted derivative **1h** gave the dibenzosemibullvalene **2h** as the major photoproduct (Scheme 4). After irradiation of dibenzobarrelene **1h** in acetone solution, product **2h** was isolated in 60% yield by crystallization directly from the reaction mixture. The structural assignment of **2h** was based on the characteristic ^{1}H NMR shifts of the two singlets for the protons at C*8b* (3.22 ppm) and C*4b* (4.63 ppm). Irradiation of compound **1h** through a quartz filter ($\lambda > 254$ nm) resulted in rapid conversion of **1h**. The photolysate contained ca. 60% of **2h**, as determined by ^{1}H NMR spectroscopic analysis. The byproducts could not be identified. In contrast, no byproducts were formed when the irradiation was carried out through Duran glass ($\lambda > 310$ nm); however, in this case a longer irradiation time was required . For example, after irradiation of a solution of **1h** in acetonitrile (10^{-3} M) through Duran glass for 8 h, TLC analysis still indicated the presence of the starting material, whereas in acetone solution full conversion was observed after 3 h irradiation under otherwise identical conditions. The reaction was significantly faster in the presence of anions: The irradiation of a solution of **1h** and two molar equiv of tetrabutylammonium chloride (TBAC) in acetonitrile for 3 h (10^{-3} M, $\lambda > 310$ nm) led to complete conversion, and the semibullvalene **2h** was obtained in 84% yield after column chromatography. Similar results were obtained in the presence of carboxylate or sulfonate salts.

The irradiation of the bisthioureido-substituted dibenzobarrelene derivative **1i** in various organic solvents did not induce the DPM rearrangement, even in acetone, as indicated by TLC and ^{1}H NMR spectroscopic analysis of the reaction mixture. Instead, ^{1}H NMR spectroscopic analysis revealed slow decomposition of the dibenzobarrelene derivative **1i** upon irradiation with no formation of distinct photoproducts. In contrast, the irradiation of compound **1i** in the presence of 2 molar equiv of either tetrabutylammonium chloride (TBAC) or tetrabutylammonium (*S*)-camphor-10-sulfonate (**SCS**) in acetonitrile for 4–6 h converted the dibenzobarrelene **1i** into the dibenzosemibullvalene **2i** (Scheme 4), as indicated by the characteristic singlets of the dibenzosemibullvalene structure in the ^{1}H NMR spectrum (*8b*-H: 3.43 ppm; *4b*-H: 4.76 ppm, in acetone). The dibenzosemibullvalene **2i** was obtained in 52% yield by filtration through a column of silica gel and subsequent crystallization. The dibenzosemibullvalenes **2h** and **2i** were identified and fully characterized by ^{1}H NMR and ^{13}C NMR spectroscopy, elemental analysis and/or mass spectrometry.

To assess whether the influence of the anions on the photoreactivity of the dibenzobarellenes is caused by complex formation, the propensity of the urea and thiourea functionalities to associate with anions was investigated by spectrophotometric titrations of selected tetrabutylammonium salts with derivatives **1h** and **1i** (Figure 1). Upon the addition of TBAC, a slight change of the absorption bands of the urea derivative **1h** was observed with the exception of the absorption maxima at

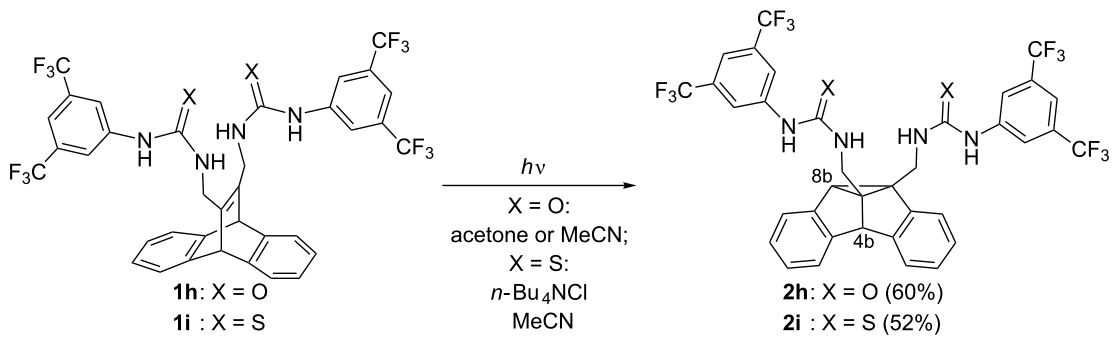

Scheme 4: Di-π-methane rearrangements of ureido- and thioureido-substituted dibenzobarrelene derivatives **1h** and **1i**.

280 nm which remained essentially unaffected during the titration. The latter absorption band was assigned to the dibenzobarrelene unit, by comparison with the absorption of the resembling dibenzobarrelene derivative **1d** [45]. This observation indicates that the complexation of the chloride anion has no significant influence on the dibenzobarrelene chromophore, but rather on the trifluoromethyl-substituted phenyl substituents. The absorption of the thioureido-substituted derivative **1i** changed significantly upon the addition of the sulfonate salt **SCS**. Specifically, the absorption maximum at 272 nm was red shifted by ca. 15 nm, along with an overall increase of the absorption. In addition, an isosbestic point at 248 nm was observed during the titration process, which indicates an equilibrium between two different absorbing species, i.e., the free and complexed ligand. Because of the predominant absorption of the arylthiourea unit, it was not possible to assess the influence of complexation on the dibenzobarrelene chromophore. The binding isotherms from the spectrophotometric titration were fitted to a 1:1 stoichiometry and the resulting binding constants of the complexes were determined to be K_b = 1.1 × 10^4 M^{-1} for **1h**-TBAC and K_b = 1.8 × 10^4 M^{-1} for **1i-SCS** (Figure 1). In addition, it was observed that the ^{1}H NMR spectroscopic signals of the NH protons of **1h** (from 6.63 and 9.34 to 7.66 and 10.20) as well as the one of the methine proton (from 4.54 to 4.35) and of the OH proton (from 5.22 to 5.14) of the mandelate were significantly shifted upon the addition of (*S*)-mandelate (**SMD**) [in $(CD_3)_2SO$)]. The corresponding Job plot confirms the 1:1 complex between **1h** and **SMD** (Supporting Information File 1). Moreover, complex formation was confirmed by a weak NOE effect, as determined by ROESY NMR experiments, between the protons in the ortho position of the phenyl group of the mandelate and the bis(trifluoro)phenyl groups of **1h**.

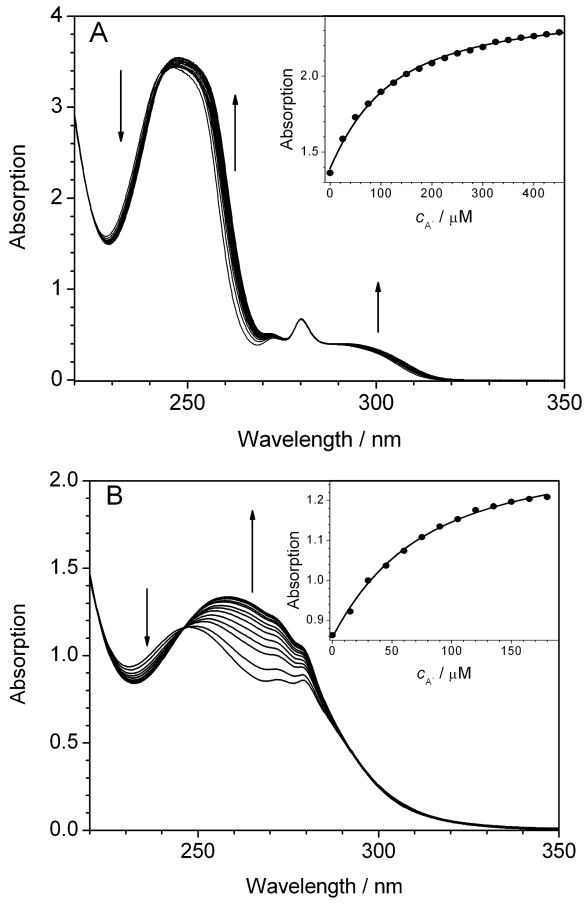

Figure 1: Photometric titration of A) tetrabutylammonium chloride (TBAC) to **1h** ($c_{\mathbf{1h}}$ = 50 μM) and of B) tetrabutylammonium (10*S*)-camphorsulfonate (**SCS**) to **1i** ($c_{\mathbf{1i}}$ = 30 μM). Arrows indicate the changes of the absorption with increasing concentration of the salt. Inset: Plot of the absorbance at 260 nm vs $c_{\mathbf{TBAC}}$ (A) and at 272 nm vs $c_{\mathbf{SCS}}$ (B); straight line represents the fit of the isotherm to a 1:1 stoichiometry.

Since it was demonstrated that the ureido- and thioureido-substituted dibenzobarrelene derivatives **1h** and **1i** associate with anions, experiments were carried out to assess whether a stereoselective DPM rearrangement of **1h** may be induced by a bound chiral anion. The initial experiments were performed with (*S*)-mandelate (**SMD**). Thus, a complex of the dibenzobarrelene **1h** with **SMD** was irradiated in acetone solution at different concentrations and with varied host–guest ratios (Table 1, entries 1–5). The enantiomeric ratio (er) of the dibenzosemibullvalene product was determined by ^{1}H NMR spectroscopy with **SMD** as chiral shift reagent, as it turned out that this additive induces a significant separation of the protons of the enantiomers of **2h** (Supporting Information File 1). The absolute configuration of the products was not determined. The photoreaction proceeded rapidly with full conversion in 4–6 hours with moderate stereoselectivity (68:32 er) in the presence of 1.1 molar equiv of the chiral mandelate. Variations of the host–guest ratio ($c_{\mathbf{1h}}$:c_{anion} = 1:0.5, 1:2.1, 1:5) led to a decrease of the stereoselectivity. In addition, changes in the concentration of the dibenzobarrelene **1h** did not have a significant influence on the stereoselectivity of the reaction. Based on these results, the following experiments were carried out with a concentration of 0.25 mM for the dibenzobarrelene derivative **1h** and 1.1 molar equiv of the chiral additive (Table 1, entries 6–10). Notably, the (*R*)-enantiomer of mandelate induced the same extent of stereoselectivity with the reverse ratio of products. For comparison, the photoreaction of dibenzobarrelene **1h** was performed in the presence of other chiral anions, namely (*R*)-thiazolidine-4-carboxylate (**RTZ**), (*S*)-camphor-10-sulfonate (**SCS**), (*R*)-carnitine (**RCN**), and (2*S*)-1-[(benzyloxy)carbonyl]-2-pyrrolidinecarboxylate (**SCP**) (Figure 2). In each case, the induced stereoselectivity was significantly lower than that induced by (*S*)-mandelate.

Table 1: DPM rearrangements of dibenzobarrelene **1h** in the presence of chiral anions.

Entry	Solvent[a]	Anion[b]	c_{1h} / mM	c_{1h}:c_{anion}	er[c]
1	Acetone	**SMD**	0.25	1:0.5	45:55
2	Acetone	**SMD**	0.25	1:1.1	32:68
3	Acetone	**SMD**	0.50	1:1.1	33:67
4	Acetone	**SMD**	0.50	1:2.1	41:59
5	Acetone	**SMD**	0.50	1:5.0	47:53
6	Acetone	**RMD**	0.25	1:1.1	67:33
7	Acetone	**RTZ**	0.25	1:1.1	59:41
8	Acetone	**SCS**	0.25	1:1.1	44:56
9	Acetone	**SCP**	0.25	1:1.1	53:47
10	MeCN-MeOH 1:1	**RCN**	0.25	1:1.1	47:53
11	Acetonitrile	**SMD**	0.25	1:1.1	40:60
12	Methanol	**SMD**	0.25	1:1.1	48:52
13	Ethanol	**SMD**	0.25	1:1.1	49:51
14	2-Propanol	**SMD**	0.25	1:1.1	50:50
15	Acetone-THF 1:9	**SMD**	0.25	1:1.1	45:55
16	Acetone-EtOAc 1:9	**SMD**	0.25	1:1.1	35:65
17	Acetone-Benzene 1:9	**SMD**	0.25	1:1.1	44:56

[a]Conditions described in the Experimental Section; amount of **2h** in reaction mixture: >90% in all cases. [b]Except for **SCN** used as tetrabutylammonium salts. [c]er = enantiomeric ratio, determined by ^{1}H NMR spectroscopic analysis with 5 molar equiv of **SMD** as the shift reagent; estimated error: ±3% of the given data. Each measurement was carried out twice to ensure the reproducibility.

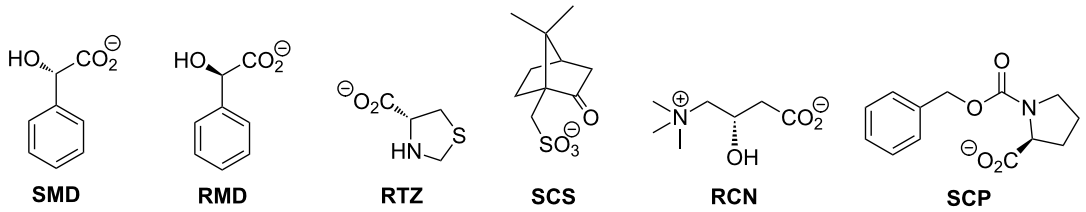

Figure 2: Structures of chiral additives employed in DPM rearrangements.

The influence of the solvent on the DPM rearrangement of compound **1h** was also investigated in the presence of (*S*)-mandelate (Table 1, entries 11–17). The low solubility of **1h** in non-polar solvents required the addition of 10% acetone as co-solvent to give a homogeneous solution. Notably, a small but significant stereoselectivity of the DPM rearrangement of **1h** was only observed in acetone or ethyl acetate/acetone (32:68 and 35:65 er), whereas in acetonitrile (40:60 er), THF (45:55 er) or MeOH, EtOH or 2-PrOH (50:50 er) the DPM rearrangement of compound **1h** proceeds with very low or no selectivity.

In additional experiments, the photoreactions of the thioureido-substituted dibenzobarrelene derivative **1i** were studied with chiral mandelate, camphorsulfonate and binaphthyl phosphonate in a variety of solvents including acetone, acetonitrile, ethyl acetate, dichloromethane, and benzene. Although the DPM rearrangement of the dibenzobarrelene **1i** took place readily upon irradiation and the semibullvalene photoproducts were isolated by column chromatography in very good yields, none of these products proved to be enantiomerically enriched, as determined by ^{1}H NMR experiments with **SMD** as the chiral shift reagent.

Discussion

It is well established that the regio- and stereoselectivity of a photoreaction may be induced by the selective preorganization of the substrates by hydrogen bonding between neutral organic functionalities with an appropriate substitution pattern or by complexation of crown-ether units to cationic guest molecules [1-3]. In contrast, the selective anion recognition has not been employed systematically to influence the photochemical properties of a substrate, although such supramolecular recep-

tor–anion interactions have been used in the organocatalysis of ground-state reactions [40-44]. It should be noted that the supramolecular interactions between anions and ureido- or thioureido-substituted fluorophores have been used elegantly for the fluorimetric detection of the anion [46], and the photophysical background has been evaluated in detail [47], but the influence of the binding event on the photochemical properties has not been assessed. In this regard, the studies of the photoreactivity of the dibenzobarrelene derivatives **1h** and **1i** provide useful initial information about the potential of anion-controlled photoreactions.

The fact that the DPM rearrangement of ureido-substituted dibenzobarrelene derivative **1h** takes place even without external sensitizers suggests that an efficient intersystem crossing (ISC) process exists for the excited chromophore **1h** that directs the photoreaction predominately to the triplet pathway. The 3,5-bis(trifluoromethyl)phenyl substituent may be responsible for the ISC, because *m*-bis(trifluoromethyl)benzene has an ISC quantum yield of $\Phi_{ISC} = 0.12$ ($\lambda_{ex} = 254$ nm) in the gas phase, and the latter compound is able to sensitize a triplet-state *E/Z*-isomerization of alkenes [48]. On the other hand, the thioureido-substituted dibenzobarrelene derivative **1i** does not undergo a DPM rearrangement upon direct irradiation, despite the potentially sensitizing 3,5-bis(trifluoromethyl)phenyl substituents. Notably, not even the commonly employed sensitizer acetone is capable of inducing the DPM rearrangement of **1i**. Considering the different photophysical and photochemical properties of the carbonyl and thiocarbonyl chromophores [49], it may be that a similar difference exists between urea and thiourea functionalities. Thiocarbonyl groups usually have high ISC rates, but they are also prone to self-quenching [49] and act as efficient quenchers for triplet reactions [50]. Thus, in analogy to the properties of the thiocarbonyl chromophore, it is proposed that the thioureido functionality in **1i** quenches the triplet excited-state, most likely by the intramolecular self-quenching of the two proximate thiourea groups. Interestingly, upon association of the thiourea units with anions, the DPM reactivity of compound **1i** is regained. This observation is consistent with the shorter reaction time of the DPM rearrangement of the ureido-substituted derivative **1h** upon association with anions. Since the photometric titrations clearly indicate complex formation, it may be assumed that the decreased reaction times are due to restricted molecular flexibility of the ureido- and thioureido substituents within the complex. Specifically, the deactivation of the excited-state by conformational relaxation is suppressed upon complex formation leading to increased quantum yields of the photoreaction. Nevertheless, in the case of the thioureido-substituted derivative **1i** additional effects need to be considered to explain the drastic change of the photochemical properties. Apparently, the quenching effect of the thioureido substituents on the triplet reaction is no longer effective after the association with anions. Presumably, the complexed anions affect the properties of the C=S bond in **1i**, leading to changes in excited-state reactivity, as has been shown for hydrogen bonded thiocarbonyl compounds in a theoretical study [51]. For comparison, it should be noted that the ISC rate constant of the thioureido-substituted anthracene **4** (Figure 3), $k_{ISC} = 1.1 \times 10^9\ s^{-1}$ (CH_3CN), even decreases by one order of magnitude upon association with acetate [27]. In that case, however, the absorption of the anthracene and the (trifluoromethyl)phenylthiourea part are well separated and the anthracene is excited selectively at lower energy. Moreover, as there is only one thioureido substituent attached to the anthracene in **4**, self-quenching can only take place in a bimolecular process, which is negligible at the low concentration employed in these experiments.

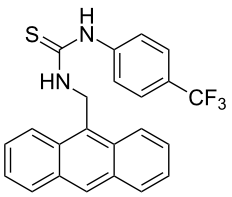

4

Figure 3: Structure of anthracene–thiourea conjugate **4**.

It was demonstrated that the complexation of chiral carboxylates by the ureido substituents of the dibenzobarrelene derivative **1h** may be employed, in principle, to induce a stereoselective DPM rearrangement. The lack of stereoselectivity in competitive protic solvents, namely alcohols, indicates the relevance of the hydrogen bonding between the anion and the urea group for chiral induction. As the best selectivities were observed in the presence of 1 molar equiv of the mandelate ion, it may be deduced that the stereoselectivity of the reaction mainly originates from a 1:1 complex between **1h** and the mandelate **SMD** (**1h-SMD**) (Figure 4), thus resembling known complexes, in which a bisurea receptor uses all four NH hydrogen for chelating hydrogen bonding to carboxylate in a 1:1 complex [52-54]. The fact that mandelate induces a significantly higher selectivity than the other employed anions may be explained by additional interactions of the hydroxy or phenyl substituent of the mandelate with the bis(trifluoromethyl)phenyl substituent or with the ureido substituent. Presumably, in complex **1h-SMD** one initial vinyl–benzo bridging (pathway a or b) is preferred due to steric or conformational restraints; however, this effect is only small, but significant, as indicated by the moderate stereoselectivity (68:32 er).

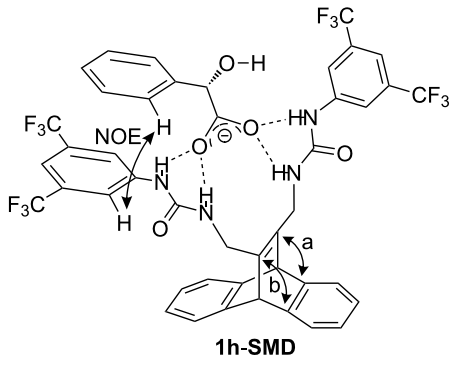

Figure 4: Proposed structure of the complex between **1h** and mandelate **SMD**.

At present, the reason for the lack of stereoselectivity of the DPM rearrangement of the thioureido-substituted dibenzobarrelene **1i** upon complexation of chiral anions is not clear. Nevertheless, it has been shown that neighboring aryl substituents decrease the anion-binding ability of thiourea derivatives because of the steric repulsion between the ortho-substituents and the sulfur atom [55]. This effect may also suppress the formation of a stable 1:1 complex between the chelating thioureido functionalities in **1i** and anions, such that an inducing effect of the anion on the photoreaction of the dibenzobarrelene is not operative.

Conclusion

In summary, it was demonstrated that the photochemical properties of the bisureido- and bisthioureido-substituted dibenzobarralene derivatives **1h** and **1i** may be influenced by complex formation with appropriate anions. In general, the photoreactivity of the substrates is significantly increased upon association with anions. Specifically, the DPM rearrangement of the thioureido derivative **1i** to give the dibenzosemibullvalene **2i** can only be performed successfully when the self-quenching of the triplet state is suppressed by complex formation. At the same time it was shown in preliminary experiments that the association of chiral carboxylates with **1h** induces a stereoselective DPM rearrangement. So far, the selectivities are very low; however, these observations demonstrate that anion-controlled stereoselective DPM rearrangements may be accomplished in principle. Therefore, it is proposed that this methodology may be optimized in future studies, thus providing a complementary tool to perform stereoselective photoreactions based on supramolecular interactions.

Experimental

General remarks: The NMR spectra were recorded on a Bruker Avance 400 (^{1}H NMR: 400 MHz; ^{13}C NMR: 100 MHz) and a Varian NMR system 600 (^{1}H NMR: 600 MHz; ^{13}C NMR: 150 MHz). ^{1}H NMR chemical shifts are relative to tetramethylsilane (δ_{TMS} = 0.00 ppm), and ^{13}C NMR chemical shifts refer to either the signal of tetramethylsilane (δ_{TMS} = 0.00 ppm) or the solvent signals [$(CD_3)_2CO$: 29.8 ppm, $(CD_3)_2SO$: 39.5 ppm]. Absorption spectra were recorded on a Varian 100 Bio spectrometer at 25 °C. Melting points were determined on a Büchi 510K and are uncorrected. Mass spectra were recorded on a Hewlett-Packard HP 5968 (EI) and a Finnigan LCQ Deca instrument (ESI). Elemental analyses were performed on a KEKA-tech EuroEA combustion analyzer by Mr. H. Bodenstedt, Organic Chemistry I, University of Siegen. TLC analyses were performed on silica-gel sheets (Macherey-Nagel Polygram Sil G/UV$_{254}$). Unless otherwise mentioned, commercially available chemicals were reagent grade and were used without further purification. Tetrabutylammonium hydroxide in MeOH (1.0 M) and (*S*)-camphor-10-sulfonic acid were obtained from Aldrich. (*R*)-Mandelic acid and (*S*)-mandelic acid were obtained from Fluka. (*R*)-Thiazolidine-4-carboxylic acid and (2*S*)-1-[(benzyloxy)carbonyl]-2-pyrrolidinecarboxylic acid were obtained from Acros. (*R*)-Carnitine was obtained from Alfa-Aesar. Preparative column chromatography was performed on MN Silica Gel 60 M (particle size 0.04–0.063 mm, 230–440 mesh).

Irradiations were performed with a TQ150 middle-pressure mercury lamp (Heraeus, UV-Consulting Peschl), which was placed inside a quartz cooling tube. The reaction mixture was placed ca. 10–15 cm in front of the lamp.

General procedure for the preparation of bisurea- and bisthiourea derivatives of dibenzobarrelene (GP1): The isocyanate or isothiocyanate derivative (1.1 molar equiv) was added to a stirred solution of 11,12-bis(aminomethyl)-9,10-dihydro-9,10-ethenoanthracene (**1d**, 0.45–10.0 mmol) [45] in CH_2Cl_2 (3 mL/mmol) at 0 °C. A white or pale yellow solid precipitated shortly after the addition of iso(thio)cyanate. The mixture was stirred for 2 h at room temperature, and the solid collected by filtration or recrystallization directly from the reaction mixture depending on the solubility of the product.

11,12-Bis(*N*'-*n*-butylureidomethyl)-9,10-dihydro-9,10-ethenoanthracene (1e): Prepared from dibenzobarrelene **1d** (554 mg, 2.00 mmol) according to **GP1**, collected by filtration and dried in vacuo. Yield 732 mg (1.77 mmol, 79%), white powder, mp > 320 °C (dec.). ^{1}H NMR [400 MHz, $(CD_3)_2SO$]: δ 0.88 (t, *J* = 7 Hz, 6H, CH_3), 1.23–1.34 (m, 8H, CH_2), 2.95–2.99 (m, 4H, C*H*$_2$NH), 3.83 (d, *J* = 7 Hz, 4H, C*H*$_2$C=C), 5.08 (s, 2H, CH), 5.83–5.85 (m, 4H, NH), 6.91, 7.22 (AA'BB'-system, 8H, CH_{ar}). ^{13}C NMR [100 MHz, $(CD_3)_2SO$]: δ 14.1

(CH_3), 19.9 (CH_2), 32.6 (CH_2), 38.0 (CH_2), 53.1 (CH), 122.9 (CH_{ar}), 124.5 (CH_{ar}), 143.3 (C_q), 146.6 (C_q), 158.6 (C=O). Anal. Calcd for $C_{34}H_{28}N_4O_2$ (460.6): C, 73.01; H, 7.88; N, 12.16. Found: C, 73.25; H, 7.95; N, 12.04.

11,12-Bis(*N*'-phenylureidomethyl)-9,10-dihydro-9,10-ethenoanthracene (1f): Prepared from dibenzobarrelene **1d** (131 mg, 0.50 mmol) according to **GP1** and collected by filtration and obtained as a white powder (179 mg, 0.36 mmol, 72%), mp 309–312 °C (dec.). ^{1}H NMR [400 MHz, $(CD_3)_2SO$]: δ 4.07 (d, J = 5 Hz, 4H, CH_2), 5.15 (s, 2H, CH), 6.37 (t, J = 5 Hz, 2H, NH), 6.90–6.93 (m, 6H, CH_{ar}), 7.20–7.41 (m, 12H, CH_{ar}), 8.29 (s, 2H, NH). ^{13}C NMR [100 MHz, $(CD_3)_2SO$]: δ 37.9 (CH_2), 53.3 (CH), 118.3 (CH_{ar}), 121.5 (CH_{ar}), 123.0 (CH_{ar}), 124.6 (CH_{ar}), 129.0 (CH_{ar}), 140.8 (C_q), 143.5 (C_q), 146.5 (C_q), 155.8 (C=O). MS (EI): m/z = 500 [M^+]. Anal. Calcd for $C_{34}H_{28}N_4O_2$ (500.6): C, 76.78; H, 5.64; N, 11.19. Found: C, 76.68; H, 5.67; N, 11.12.

11,12-Bis[*N*'-(4-*n*-butylphenyl)ureidomethyl]-9,10-dihydro-9,10-ethenoanthracene (1g): Prepared from dibenzobarrelene **1d** (0.12 g, 0.45 mmol) according to **GP1**, collected by filtration and dried in vacuo. White amorphous solid, yield 0.21 g (0.34 mmol, 76%), mp > 320 °C. ^{1}H NMR [400 MHz, $(CD_3)_2SO$]: δ 0.89 (t, J = 7 Hz, 6H, CH_3), 1.26–1.55 (m, 8H, $CH_2CH_2CH_3$), 2.47–2.50 (m, 4H, $PhCH_2CH_2$, partly overlapped with the solvent signal), 3.97 (d, J = 6 Hz, 4H, $C{=}CCH_2$), 5.14 (s, 2H, CH), 6.06 (t, J = 6 Hz, 2H, NH), 6.90–6.92 (m, 4H, CH_{ar}), 7.03–7.05 (m, 4H, CH_{ar}), 7.25–7.29 (m, 8H, CH_{ar}), 8.42 (s, 2H, NH). ^{13}C NMR [100 MHz, $(CD_3)_2SO$]: δ 14.2 (CH_3), 22.1 (CH_2), 33.7 (CH_2), 34.5 (CH_2), 37.9 (CH_2), 53.3 (CH), 118.4 (CH_{ar}), 123.0 (CH_{ar}), 124.6 (CH_{ar}), 128.8 (CH_{ar}), 135.3 (CH_{ar}), 138.4 (C_q), 143.5 (C_q), 146.5 (C_q), 155.9 (C=O). MS (EI): m/z (%) = 613 [M^+]. Anal. Calcd for $C_{40}H_{44}N_4O_2$ (612.8): C, 78.40; H, 7.24; N, 9.14. Found: C, 78.12; H, 7.25; N, 9.09.

11,12-Bis{*N*'-[3,5-bis(trifluoromethyl)phenyl]ureidomethyl}-9,10-dihydro-9,10-ethenoanthracene (1h): Prepared from dibenzobarrelene **1d** (0.13 g, 0.50 mmol) according to **GP1**. After filtration of the precipitate, the product was purified by recrystallization from CH_2Cl_2/hexane and obtained as a white solid (0.33 g, 0.41 mmol, 82%), mp > 300 °C. ^{1}H NMR [400 MHz, $(CD_3)_2CO$]: δ 4.18 (d, J = 4 Hz, 4H, CH_2), 5.25 (s, 2H, CH), 6.43 (br s, 2H, NH), 6.86 (m, 4H, CH_{ar}), 7.27 (m, 4H, CH_{ar}), 7.51 (s, 2H, CH_{ar}), 8.03 (br s, 4H, CH_{ar}), 8.64 (br s, 2H, NH). ^{13}C NMR [100 MHz, $(CD_3)_2CO$]: δ 38.3 (CH_2), 53.3 (CH), 113.9 (CH_{ar}), 117.7 (CH_{ar}), 122.4 (CH_{ar}), 123.0 (CH_{ar}), 124.6 (CH_{ar}), 125.1 (CH_{ar}), 130.7 (CH_{ar}), 131.1 (CH_{ar}), 142.7 (C_q), 143.4 (C_q), 146.4 (C_q), 155.4 (C=O). UV (MeCN): λ_{max} (log ε) = 229 (4.49), 246 (4.86), 272 (4.01), 280 (4.13). MS (ESI$^-$): m/z (%) = 771 (100) [M − H]$^-$. Anal. Calcd for $C_{36}H_{24}F_{12}N_4O_2$ (772.6): C, 55.97; H, 3.13; N, 7.25. Found: C, 55.58; H, 2.85; N, 7.04.

11,12-Bis{*N*'-[3,5-(bistrifluoromethyl)phenyl]thioureidomethyl}-9,10-dihydro-9,10-ethenoanthracene (1i): Prepared from dibenzobarrelene **1d** (0.13 g, 0.50 mmol) according to **GP1** and obtained by recrystallization from CH_2Cl_2/hexane as a white solid (0.34 g, 0.43 mmol, 86%), mp > 300 °C. ^{1}H NMR [600 MHz, $(CD_3)_2CO$]: δ 4.66 (d, J = 4 Hz, 4H, CH_2), 5.36 (s, 2H, CH), 6.92 (m, 4H, CH_{ar}), 7.30–7.32 (m, 4H, CH_{ar}), 7.73 (m, 4H, CH_{ar} overlapped with NH), 8.25–8.26 (m, 4H, CH_{ar}), 9.57 (br s, 2H, NH). ^{13}C NMR [150 MHz, $(CD_3)_2CO$]: δ = 43.4 (CH_2), 54.2 (CH), 117.9 (CH_{ar}), 121.5 (CH_{ar}), 123.6 (CH_{ar}), 125.3 (CH_{ar}), 127.0 (CH_{ar}), 132.0 (CH_{ar}), 142.4 (C_q), 144.1 (C_q), 146.8 (C_q), 182.4 (C=O). UV (MeCN): λ_{max} (log ε) = 230 (4.49), 246 (4.59), 272 (4.46), 280 (4.47). MS (ESI): m/z (%) = 803 (100) [M − H]$^-$. Anal. Calcd for $C_{36}H_{24}F_{12}N_4S_2$ (804.7): C, 53.73; H, 3.01; N, 6.96; S, 7.97. Found: C, 53.58; H, 2.79; N, 6.84; S, 7.97.

General procedure for the synthetic photolysis in solution (GP2): Solutions of the substrate (10^{-3}–10^{-2} mol/l) were placed in a Duran flask (acetone) or quartz test tube (other solvents), and argon gas was bubbled carefully through the solution for at least 20 min. The solution was irradiated for 4–15 h with stirring until the starting material was fully converted as determined by TLC or ^{1}H NMR spectroscopic analysis. After evaporation of the solvent in vacuo, the photolysate was analyzed by ^{1}H NMR spectroscopy. In preparative experiments, the photoproduct was isolated by recrystallization or column chromatography.

4b,8b-Dihydro-8c,8e-bis{*N*'-[3,5-bis(trifluoromethyl)phenyl]ureidomethyl}dibenzo[*a*,*f*]cyclopropa[*c*,*d*]pentalene (2h): Prepared by irradiation of **1h** (48.0 mg, 0.06 mmol) in acetone solution according to **GP2** and obtained as white crystals (29.0 mg, 0.04 mmol, 60%), mp 246–247 °C. ^{1}H NMR [600 MHz, $(CD_3)_2CO$]: δ 3.22 (s, 1H, CH), 3.78 (dd, J = 15, 6 Hz, 1H, CH_2), 3.82 (dd, J = 15, 6 Hz, 1H, CH_2), 3.94 (dd, J = 15, 6 Hz, 1H, CH_2), 4.44 (dd, J = 15, 6 Hz, 1H, CH_2), 4.63 (s, 1H, CH), 6.42 (t, J = 5 Hz, 1H, NH), 6.53 (t, J = 5 Hz, 1H, NH), 6.99–7.05 (m, 4H, CH_{ar}), 7.21–7.25 (m, 3H, CH_{ar}), 7.36–7.38 (m, 1H, CH_{ar}), 7.49 (s, 2H, CH_{ar}), 8.09 (s, 2H, CH_{ar}), 8.13 (s, 2H, CH_{ar}), 8.75 (s, 1H, NH), 8.81 (s, 1H, NH). ^{13}C NMR [150 MHz, $(CD_3)_2CO$]: δ 41.3 (CH_2), 41.4 (CH_2), 46.7 (CH), 53.3 (C_q), 58.8 (C_q), 67.4 (CH), 115.6 (CH_{ar}), 115.6 (CH_{ar}), 115.6 (CH_{ar}), 115.7 (CH_{ar}), 119.3 (CH_{ar}), 119.3 (CH_{ar}), 123.4 (CH_{ar}), 123.4 (CH_{ar}), 124.5 (CH_{ar}), 124.6 (C_q), 125.8 (CH_{ar}), 126.3 (C_q), 126.4 (CH_{ar}), 126.6 (CH_{ar}), 128.1 (CH_{ar}), 128.2 (CH_{ar}),

128.3 (CH_{ar}), 128.5 (CH_{ar}), 133.2 (C_q), 133.2 (C_q), 133.4 (C_q), 133.4 (C_q), 139.9 (CH_{ar}), 140.1 (CH_{ar}), 144.4 (C_q), 144.6 (C_q), 151.8 (C_q), 152.8 (C_q), 156.7 (C=O), 157.2 (C=O). MS (ESI): *m*/*z* (%) = 771 (100) $[M - H]^-$. An analytical sample was obtained by recrystallization from ethyl acetate/hexane and contained one equiv of ethyl acetate as the lattice solvent. Anal. Calcd for $C_{36}H_{24}F_{12}N_4O_2$·EtOAc (860.7): C, 55.82; H, 3.75; N, 6.51. Found: C, 55.93; H, 3.51; N, 6.45.

4b,8b-Dihydro-8c,8e-bis{*N*'-[3,5-bis(trifluoromethyl)phenyl]thioureidomethyl}dibenzo[*a*,*f*]cyclopropa[*c*,*d*]pentalene (2i): Prepared by photoreaction of **1i** (0.20 g, 0.25 mmol) in acetonitrile solution in the presence of 2 molar equiv of ammonium chloride according to **GP2**. After the irradiation the inorganic components were removed by column filtration (SiO_2; EtOAc/hexane 1/2, v/v), and the residue was recrystallized from ethyl acetate/hexane to give light yellow crystals (104 mg, 0.13 mmol, 52%), mp 181–182 °C. ^{1}H NMR [600 MHz, $(CD_3)_2CO$]: δ 1.20 (t, *J* = 7 Hz, 3H, CH_3), 3.43 (s, 1H, CH), 4.05 (q, *J* = 7 Hz, 2H, CH_2), 4.22 (d, *J* = 13 Hz, 1H, NHC*H*HC), 4.29 (d, *J* = 13 Hz, 1H, NHC*H*HC), 4.48 (d, *J* = 13 Hz, 1H, NHCH*H*C), 4.74 (d, *J* = 13 Hz, 1H, NHCH*H*C), 4.76 (s, 1H, CH), 7.00–7.09 (m, 5H, CH_{ar}), 7.24–7.28 (m, 3H, CH_{ar}), 7.36–7.38 (m, 1H, CH_{ar}), 7.67 (s, 2H, CH_{ar}), 7.81 (s, 1H, NH), 7.89 (s, 1H, NH), 8.23 (s, 2H, CH_{ar}), 8.32 (s, 2H, CH_{ar}), 9.45 (s, 1H, NH), 9.53 (s, 1H, NH). ^{13}C NMR [150 MHz, $(CD_3)_2CO$)]: δ 14.5 (CH_3), 20.8 (CH_2), 44.2 (CH_2), 45.2 (CH_2), 50.3 (C_q), 57.2 (CH), 59.7 (CH), 65.1 (C_q), 116.5 (CH_{ar}), 116.7 (c), 121.5 (CH_{ar}), 121.6 (CH_{ar}), 122.1 (CH_{ar}), 122.5 (CH_{ar}), 123.8 (CH_{ar}), 124.3 (CH_{ar}), 124.3 (CH_{ar}), 124.9 (CH_{ar}), 126.4 (CH_{ar}), 126.4 (CH_{ar}), 126.6 (CH_{ar}), 126.9 (CH_{ar}), 130.6 (CH_{ar}), 130.6 (CH_{ar}), 130.8 (CH_{ar}), 130.9 (CH_{ar}), 131.1 (C_q), 131.1 (C_q), 137.6 (C_q), 137.7 (C_q), 141.8 (C_q), 142.0 (C_q), 149.9 (C_q), 150.8 (C_q), 181.4 (C=S), 181.8 (C=S), two C_q signals are overlapped in the aromatic region. MS (ESI): *m*/*z* (%) = 803 (100) $[M - H]^-$. Anal. Calcd for $C_{36}H_{24}F_{12}N_4S_2$·EtOAc (892.8): C, 53.81; H, 3.61; N, 6.28; S, 7.18. Found: C, 54.03; H, 3.28; N, 6.32; S, 7.09.

Preparation of the tetrabutylammonium salts of chiral acids: The tetrabutylammonium salts of the chiral carboxylates **SMD**, **RMD**, **RTZ**, and **SCP** were prepared by the neutralization of the corresponding chiral acids with tetrabutylammonium hydroxide (1.0 M in MeOH) [56]. The resulting salts were used as 0.1 M stock solutions in acetone.

The tetrabutylammonium salt of (S)-camphor-10-sulfonate **SCS** was prepared according to the literature procedure [57], and used as 0.1 M stock solution in the respective solvent required for the experiment.

Photoreaction of dibenzobarrelene derivatives 1h and 1i in the presence of chiral anions: The dibenzobarrelene derivatives **1h** or **1i** (50 µmol) were dissolved in a stock solution (0.55 mL of 0.1 M stock solution, 55 µmol, 1.1 equiv) of the chiral tetrabutylammonium salt, and the solvent was removed in vacuo. The resulting residue was re-dissolved in the solvent of choice (200 mL). Argon gas was bubbled through the solution for 20 min to remove residual oxygen from the solvent. The reaction container (DURAN, λ > 310 nm) was placed ca. 15 cm in front of the light source, and the solution was irradiated for 3–4 h (TLC control). The solvent was removed in vacuo and the major photoproduct purified by column chromatography (SiO_2; hexane:acetone:ethyl acetate = 4:1:1, v/v/v). The photoproduct was analyzed by ^{1}H NMR spectroscopy in the presence of 5 equiv of tetrabutylammonium **SMD** as chiral shift reagent. The enantiomeric ratio of the semibullvalene mixture was determined by the integration of the aromatic proton signals from each isomer (δ in the range of 8.4–8.7 ppm), and by the integration of the NH and cyclopropane CH signals. Each spectroscopic measurement was repeated twice to ensure the reproducibility.

Supporting Information

^{1}H NMR and ^{13}C NMR spectra of compounds **1e**–**i** and **2h**–**i**; ^{1}H NMR spectra of **2h** with (*S*)-mandelate (**SMD**) at different molar ratios and corresponding Job plot; ^{1}H NMR spectra of **2h** with (*S*)-mandelate (**SMD**) as chiral shift reagent.

Supporting Information File 1

Supporting Information for: Effects of anion complexation on the photoreactivity of bisureido- and bisthioureido-substituted dibenzobarrelene derivatives.
[http://www.beilstein-journals.org/bjoc/content/supplementary/1860-5397-7-37-S1.pdf]

Acknowledgements

We thank the Deutsche Akademische Austauschdienst for a fellowship to Dr. Jia Luo (DAAD-Abschluss-Stipendium), and Ms. Stephanie Müller and Dr. Maoqun Tian, University of Siegen, for assistance during the preparation of this manuscript.

References

1. Svboda, J.; König, B. *Chem. Rev.* **2006,** *106,* 5413–5430. doi:10.1021/cr050568w
2. Wessig, P. *Angew. Chem., Int. Ed.* **2006,** *45,* 2168–2171. doi:10.1002/anie.200503908

3. Müller, C.; Bach, T. *Aust. J. Chem.* **2008,** *61,* 557–564. doi:10.1071/CH08195
4. Bach, T.; Bergmann, H.; Harms, K. *Angew. Chem., Int. Ed.* **2000,** *39,* 2302–2304. doi:10.1002/1521-3773(20000703)39:13<2302::AID-ANIE2302>3.0.CO;2-6
5. Bach, T.; Bergmann, H.; Harms, K. *Org. Lett.* **2001,** *3,* 601–603. doi:10.1021/ol007004t
6. Bach, T.; Aechtner, T.; Neumüller, B. *Chem.–Eur. J.* **2002,** *8,* 2464–2475. doi:10.1002/1521-3765(20020603)8:11<2464::AID-CHEM2464>3.0.CO;2-S
7. Bach, T.; Grosch, B.; Strassner, T.; Herdtweck, E. *J. Org. Chem.* **2003,** *68,* 1107–1116. doi:10.1021/jo026602d
8. Liu, R. S. H.; Hammond, G. S. *Acc. Chem. Res.* **2005,** *38,* 396–403. doi:10.1021/ar040246z
9. Inoue, Y.; Ramamurthy, V., Eds. *Chiral Photochemistry;* Marcel Dekker: New York, 2004.
10. Ramamurthy, V., Ed. *Photochemistry in Organized and Constrained Media,* 1st ed.; Wiley-VCH: Weinheim, 1991.
11. Pemberton, B. C.; Barooah, N.; Srivatsava, D. K.; Sivaguru, J. *Chem. Commun.* **2010,** *46,* 225–227. doi:10.1039/b920605a
12. Maddipatla, M. V. S. N.; Kaanumalle, L. S.; Natarajan, A.; Pattabiraman, M.; Ramamurthy, V. *Langmuir* **2007,** *23,* 7545–7554. doi:10.1021/la700803k
13. Wang, R.; Yuan, L.; Macartney, D. H. *J. Org. Chem.* **2006,** *71,* 1237–1239. doi:10.1021/jo052136r
14. Wu, X.-L.; Luo, L.; Lei, L.; Liao, G.-H.; Wu, L.-Z.; Tung, C.-H. *J. Org. Chem.* **2008,** *73,* 491–494. doi:10.1021/jo701998e
15. Yang, C.; Mori, T.; Origane, Y.; Ko, Y. H.; Selvapalam, N.; Kim, K.; Inoue, Y. *J. Am. Chem. Soc.* **2008,** *130,* 8574–8575. doi:10.1021/ja8032923
16. Karthikeyan, S.; Ramamurthy, V. *Tetrahedron Lett.* **2005,** *46,* 4495–4498. doi:10.1016/j.tetlet.2005.04.115
17. Yoshizawa, M.; Klosterman, J. K.; Fujita, M. *Angew. Chem., Int. Ed.* **2009,** *48,* 3418–3438. doi:10.1002/anie.200805340
18. Ishida, Y.; Kai, Y.; Kato, S.-Y.; Misawa, A.; Amano, S.; Matsuoka, Y.; Saigo, K. *Angew. Chem.* **2008,** *120,* 8365–8369. doi:10.1002/ange.200803242
19. Tanaka, K.; Toda, F. *Chem. Rev.* **2000,** *100,* 1025–1074. doi:10.1021/cr940089p
20. Braga, D.; Grepioni, F. *Angew. Chem.* **2004,** *116,* 4092–4102. doi:10.1002/ange.200301721
21. Matsumoto, A. *Top. Curr. Chem.* **2005,** *254,* 263–305. doi:10.1007/b10100
22. Scheffer, J. R. *Can. J. Chem.* **2001,** *79,* 349–357. doi:10.1139/cjc-79-4-349
23. Ihmels, H.; Scheffer, J. R. *Tetrahedron* **1999,** *55,* 885–907. doi:10.1016/S0040-4020(98)01019-9
24. Ke, C.; Yang, C.; Liang, W.; Mori, T.; Liu, Y.; Inoue, Y. *New J. Chem.* **2010,** *34,* 1323–1329. doi:10.1039/c0nj00131g
25. Yang, C.; Ke, C.; Fujita, K.; Yuan, D.-Q.; Mori, T.; Inoue, Y. *Aust. J. Chem.* **2008,** *61,* 565–568. doi:10.1071/CH08143
26. Lu, R.; Yang, C.; Cao, Y.; Wang, Z.; Wada, T.; Jiao, W.; Mori, T.; Inoue, Y. *Chem. Commun.* **2008,** 374–376. doi:10.1039/b714300a
27. Zimmerman, H. E.; Armesto, D. *Chem. Rev.* **1996,** *96,* 3065–3112. doi:10.1021/cr910109c
28. Armesto, C.; Ortiz, M. J.; Agarrabeitia, A. R. Di-π-Methane Rearrangement. In *Synthetic Organic Photochemistry;* Griesbeck, A.; Mattay, J., Eds.; *Molecular and Supramolecular Photochemistry*, Vol. 12; Marcel Dekker: New York, 2005; pp 161–181.
29. Zimmerman, H. E.; Sulzbach, H. M.; Tollefson, M. B. *J. Am. Chem. Soc.* **1993,** *115,* 6548–6556. doi:10.1021/ja00068a011
30. Scheffer, J. R.; Yang, J. The Photochemistry of Dibenzobarrelene (9,10-Ethenoanthracene) and Its Derivatives. In *CRC Handbook of Organic Photochemistry and Photobiology,* 1st ed.; Horspool, W. M.; Song, P.-S., Eds.; CRC Press: New York, 1995; pp 204–221.
31. Benitez, M.; Bringmann, G.; Dreyer, M.; Garcia, H.; Ihmels, H.; Waidelich, M.; Wissel, K. *J. Org. Chem.* **2005,** *70,* 2315–2321. doi:10.1021/jo047878j
32. Ding, J.; Desikan, V.; Han, X.; Xiao, T. L.; Ding, R. F.; Jenks, W. S.; Armstrong, D. W. *Org. Lett.* **2005,** *7,* 335–337. doi:10.1021/ol047599i
33. Evans, S. V.; Garcia-Garibay, M.; Omkaram, N.; Scheffer, J. R.; Trotter, J.; Wireko, F. *J. Am. Chem. Soc.* **1986,** *108,* 5648–5650. doi:10.1021/ja00278a060
34. Gamlin, J. N.; Jones, R.; Leibovitch, M.; Patrick, B.; Scheffer, J. R.; Trotter, J. *Acc. Chem. Res.* **1996,** *29,* 203–209. doi:10.1021/ar950165q
35. Gudmundsdottir, A. D.; Scheffer, J. R. *Tetrahedron Lett.* **1990,** *31,* 6807–6810. doi:10.1016/S0040-4039(00)97177-6
36. Garcia-Garibay, M.; Scheffer, J. R.; Trotter, J.; Wireko, F. *J. Am. Chem. Soc.* **1989,** *111,* 4985–4986. doi:10.1021/ja00195a066
37. Chen, J.; Garcia-Garibay, M.; Scheffer, J. R. *Tetrahedron Lett.* **1989,** *30,* 6125–6128. doi:10.1016/S0040-4039(01)93321-0
38. Amendola, V.; Esteban-Gómez, D.; Fabbrizzi, L.; Licchelli, M. *Acc. Chem. Res.* **2006,** *39,* 343–353. doi:10.1021/ar050195l
39. Amendola, V.; Fabbrizzi, L.; Mosca, L. *Chem. Soc. Rev.* **2010,** *39,* 3889–3915. doi:10.1039/b822552b
40. Etzenbach-Effers, K.; Berkessel, A. *Top. Curr. Chem.* **2010,** *291,* 1–27. doi:10.1007/128_2009_3
41. Grondal, C.; Jeanty, M.; Enders, D. *Nat. Chem.* **2010,** *2,* 167–178. doi:10.1038/nchem.539
42. Takemoto, Y. *Org. Biomol. Chem.* **2005,** *3,* 4299–4306. doi:10.1039/b511216h
43. Connon, S. J. *Chem.–Eur. J.* **2006,** *12,* 5418–5427. doi:10.1002/chem.200501076
44. Zhang, Z.; Schreiner, P. R. *Chem. Soc. Rev.* **2009,** *38,* 1187–1198. doi:10.1039/b801793j
45. Scheffer, J. R.; Ihmels, H. *Liebigs Ann./Recl.* **1997,** 1925–1929. doi:10.1002/jlac.199719970919
46. Li, A.-F.; Wang, J.-H.; Wang, F.; Jiang, Y.-B. *Chem. Soc. Rev.* **2010,** *39,* 3729–3745. doi:10.1039/b926160p
47. Del Giacco, T.; Carlotti, B.; De Solis, S.; Barbafina, A.; Elisei, F. *Phys. Chem. Chem. Phys.* **2010,** *12,* 8062–8070. doi:10.1039/b927442a
48. Gray, D.; Philips, D. *J. Chem. Phys.* **1973,** *58,* 3216–3220. doi:10.1063/1.1679644
49. Maciejewski, A.; Steer, R. P. *Chem. Rev.* **1999,** *93,* 67–98. doi:10.1021/cr00017a005
50. Ramesh, V.; Ramnath, N.; Ramamurthy, V. *J. Photochem.* **1983,** *23,* 141–148. doi:10.1016/0047-2670(83)80056-2
51. Zhao, G.-J.; Han, K.-L. *ChemPhysChem* **2008,** *9,* 1842–1846. doi:10.1002/cphc.200800371
52. Hamann, B. C.; Branda, N. R.; Rebek, J., Jr. *Tetrahedron Lett.* **1993,** *34,* 6837–6840. doi:10.1016/S0040-4039(00)91808-2
53. Formica, M.; Fusi, V.; Macedi, E.; Paoli, P.; Piersanti, G.; Rossi, P.; Zappia, G.; Orlando, P. *New J. Chem.* **2008,** *32,* 1204–1214. doi:10.1039/b719342d

54. Gale, P. *Acc. Chem. Res.* **2006,** *39,* 465–475. doi:10.1021/ar040237q
55. Brooks, S. J.; Edwards, P. R.; Gale, P. A.; Light, M. E. *New J. Chem.* **2006,** 65–70. doi:10.1039/b511963d
56. Kawamura, K.; Nagano, H.; Okuwaki, A. *Sep. Sci. Technol.* **2005,** *40,* 2761–2771. doi:10.1080/01496390500326503
57. Olszewska, T.; Gdaniec, M.; Polonski, T. *J. Org. Chem.* **2008,** *73,* 4859–4864. doi:10.1021/jo8004809

License and Terms

Beilstein Journal of Organic Chemistry

Supramolecular FRET photocyclodimerization of anthracenecarboxylate with naphthalene-capped γ-cyclodextrin

Qian Wang[1,2], Cheng Yang[*1], Gaku Fukuhara[1], Tadashi Mori[1], Yu Liu[2] and Yoshihisa Inoue[*1]

Full Research Paper

Open Access

Address:
[1]Department of Applied Chemistry, Osaka University, 2-1 Yamada-oka, Suita 565-0871, Japan and [2]Department of Chemistry and State Key Laboratory of Elemento-Organic Chemistry, Nankai University Tianjin, 300071 (China)

Email:
Cheng Yang[*] - c.yang@chem.eng.osaka-u.ac.jp;
Yoshihisa Inoue[*] - inoue@chem.eng.osaka-u.ac.jp

* Corresponding author

Keywords:
anthracenecarboxylic acid; capped γ-cyclodextrin; FRET sensitization; photochirogenesis; photocyclodimerization

Beilstein J. Org. Chem. **2011,** *7,* 290–297.
doi:10.3762/bjoc.7.38

Received: 06 December 2010
Accepted: 04 February 2011
Published: 07 March 2011

This article is part of the Thematic Series "Photocycloadditions and photorearrangements" and is dedicated to the memory of Prof. Hiroshi Sakurai and Prof. Tadao Hakushi.

Guest Editor: A. G. Griesbeck

Abstract

γ-Cyclodextrin (CD) derivatives with a naphthalene moiety anchored to one or two of the glucose units of the CD were synthesized in order to investigate the effects of flexible and rigid capping upon complexation, as well as Förster resonance energy transfer (FRET) and photochirogenic behavior of anthracenecarboxylate (AC) moieties. UV–vis, circular dichroism and fluorescence spectral studies revealed that two AC molecules are simultaneously included in the modified γ-CD cavity to form a right-handed screw and also that the naphthalene cap efficiently transfers the singlet energy to AC included in the CD cavity via the FRET mechanism. Compared to native γ-CD, the modified γ-CDs showed much higher first association constants (K_1) but relatively lower second association constants (K_2) for AC, leading to two-fold larger overall affinities (K_1K_2). Photocyclodimerization of AC with these modified γ-CDs produced more head-to-head (HH) dimers in much better enantiomeric excesses (ee) for *anti*-HH dimer compared to native γ-CD. Interestingly, FRET excitation further enhanced the chemical and optical yields of *anti*-HH dimer up to 36% and 35% ee, for which the highly efficient FRET sensitization within the CD cavity, minimizing the "contamination" from the achiral "outside" photoreaction, is responsible. FRET sensitization also enabled us to achieve the catalytic photocyclodimerization of AC with a sub-equivalent amount of chiral supramolecular host.

Introduction

Chiral photochemistry, often characterized by low optical yields, remains a great challenge for chemists [1-3]. This situation reflects primarily the difficulty in efficiently transferring the stereochemical information of the chiral source to the substrate in the electronically excited state. Thus, a supramolecular approach in chiral photochemistry could be a promising strategy

for critically controlling the stereochemical outcome via intimate, long-lasting contacts with the photosubstrate through noncovalent interactions in the ground state [4-11]. The geometrical and functional complementarity and the subsequent induced fit between chiral host and guest substrate should play a crucial role in determining the stereochemical fate of chiral photoreaction, and therefore the design of chiral host is considered to be one of the most important aspects for manipulating stereoselectivity in supramolecular photochirogenesis.

We have recently focused our attention on enantiodifferentiation in the photocyclodimerization of anthracenecarboxylate (AC) as a representative bimolecular photochirogenic system for the elucidation of the factors and mechanism that control supramolecular photochirogenesis [12-22]. Photocyclodimerization of AC leads to the formation of four stereoisomeric cyclodimers **1**–**4**, of which *syn*-head-to-tail (HT) **2** and *anti*-head-to-head (HH) **3** are chiral (Scheme 1). This chiral photoreaction turned out to be an ideal benchmark system for

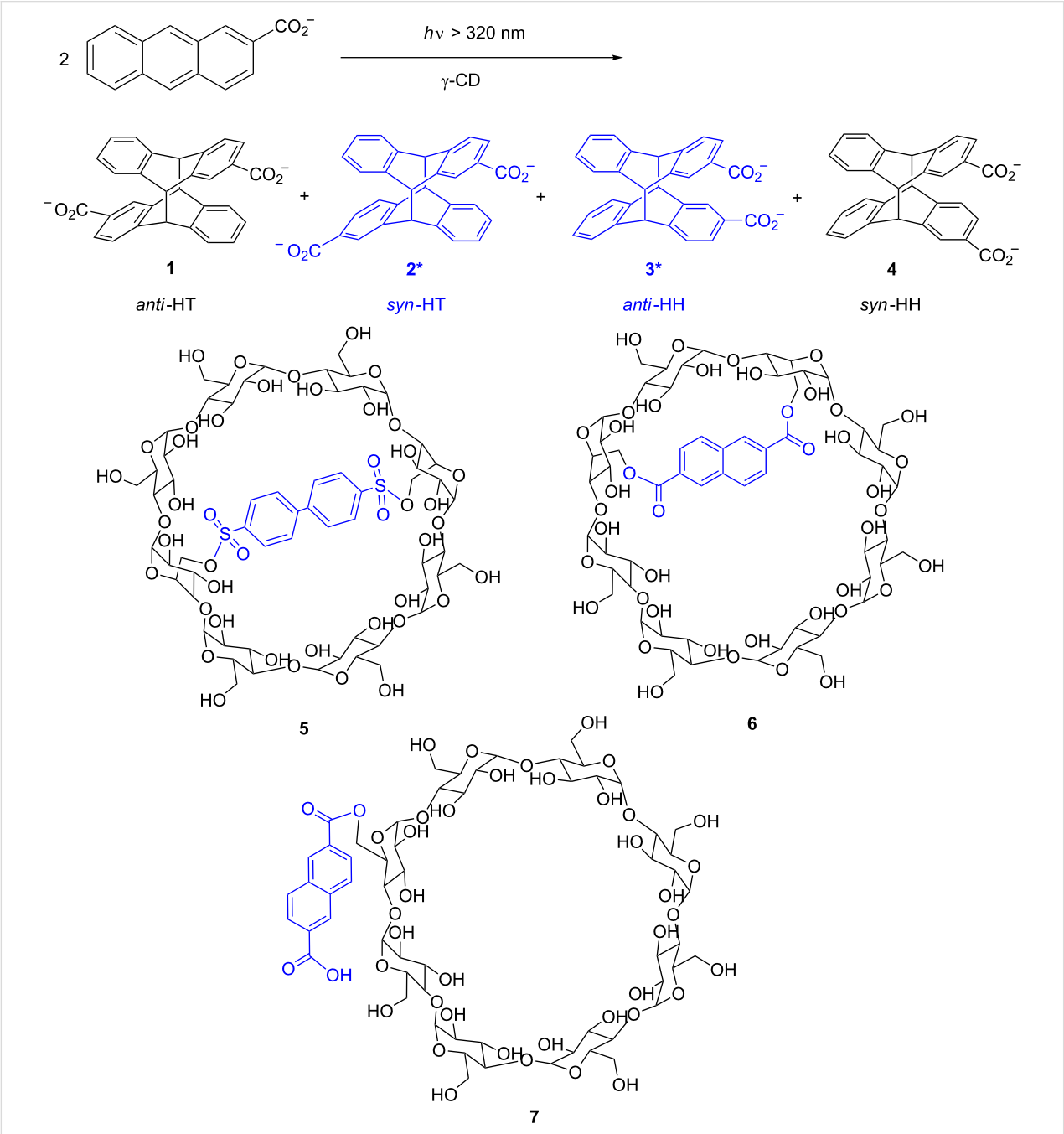

Scheme 1: Biphenyl-capped (**5**), naphthalene-capped (**6**), and naphthalene-appended γ-cyclodextrin (**7**).

exploring and comparing the performance of various chiral hosts, such as cyclodextrins (CDs), proteins and chiral hydrogen-bonding templates. γ-CD can significantly accelerate the photocyclodimerization of AC by forming a 1:2 host–guest complex with AC in aqueous solutions [12]. Altering the chiral environment of γ-CD by rim modification is a convenient, yet effective, tool for manipulating the stereoselectivity of AC photocyclodimerization. In our previous studies, we have shown that a capping modification of γ-CD causes a dramatic switching of stereoselectivity in AC photodimerization [12,22]. Thus, by using native γ-CD the chiral cyclodimer **2** is obtained in 41% enantiomeric excess (ee), whereas biphenyl-capped γ-CD **5** yields antipodal **2** in −57% ee (Scheme 1) [22]: Where the positive/negative sign of ee indicates a higher yield of first/second eluted enantiomer detected on the chiral HPLC analysis. These observations prompted us to design and synthesize a more rigidly capped $6^A,6^C$-(2,6-naphthalenedicarboxyl)-γ-CD **6**. This modification further enabled us to trigger the photocyclodimerization via Förster resonance energy transfer (FRET) sensitization.

Results and Discussion

Naphthalene-capped γ-CD **6** was synthesized by the reaction of $6^A,6^C$-ditosyl-γ-CD [23] with disodium 2,6-naphthalenedicarboxylate in DMSO. An attempt to synthesize the regioisomeric $6^A,6^D$-(2,6-naphthalenedicarboxyl)-γ-CD by reacting $6^A,6^D$-ditosyl-γ-CD with disodium 2,6-naphthalenedicarboxylate was unsuccessful, presumably due to the longer distance between the A and D glucose units to be bridged by the 2,6-naphthalenedicarboxylate unit. For the purposes of comparison, naphthalene-appended γ-CD **7** was synthesized by reacting γ-CD with 2,6-naphthalenedicarboxylic acid. Modified γ-CD **7** was found to be sparingly soluble in water, probably due to the intermolecular aggregation of **7** by successive penetration of the naphthalene moiety into the cavity of another CD. The solubility of **7** was significantly enhanced by adding sodium carbonate. In contrast, capped γ-CD **6** showed a much higher solubility in water, as the naphthalene cap can hardly interact with another CD.

The complexation behavior of AC with modified γ-CDs **6** and **7** was investigated by UV–vis, circular dichroism and fluorescence spectral studies. As shown in Figure 1, the addition of **7** to an aqueous solution of AC (0.2 mM) caused an evident bathochromic shift of the ^1L_a band of AC, which is probably due to the stacking complexation of two AC molecules in a single γ-CD cavity.

Modified γ-CDs **6** and **7** showed moderate circular dichroism signals in the naphthalene-absorbing region. As shown in Figure 2, naphthalene-appended γ-CD **7** at 0.2 mM concentration gave a bisignate circular dichroism signal even in the absence of AC. As the intensity (Δε) decreased at lower concentrations, this bisignate signal is thought to be a real exciton couplet arising from the self-aggregation of **7**, where the included naphthalene chromophores are arranged in a right-handed screw [24]. As can be seen from Figure 3, naphthalene-capped γ-CD **6** gave only weak induced circular dichroism signals at the ^1L_a and ^1B_b bands of the naphthalene chromophore, the intensity of which was not concentration-dependent.

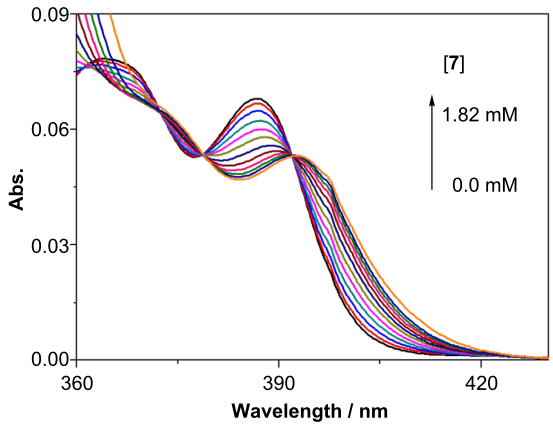

Figure 1: UV–vis spectral changes of 0.2 mM AC upon increasing the concentration of **7** in pH 9 phosphate buffer at 25 °C.

The addition of AC (0–0.26 mM) to the above solutions of **7** or **6** (0.2 mM) produced a strong positive exciton couplet at the ^1B_b transition of AC (Figure 2 and Figure 3) which overwhelmed the inherent signals. The positive couplet observed indicates the right-handed helical conformation of the two AC molecules in the γ-CD cavity [24].

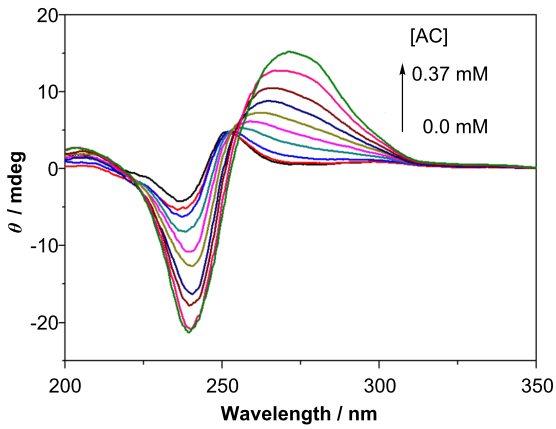

Figure 2: Circular dichroism spectra of **7** (0.2 mM) in the presence of 0, 0.0083, 0.025, 0.048, 0.071, 0.093, 0.13, 0.16, 0.22, 0.27 and 0.37 mM AC in pH 9 phosphate buffer at 20 °C.

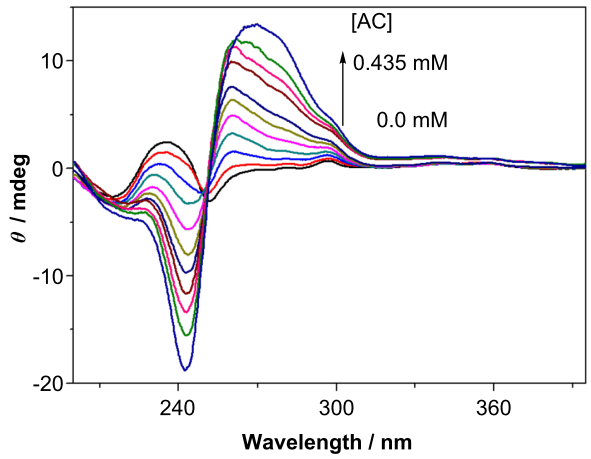

Figure 3: Circular dichroism spectra of **6** (0.2 mM) in the presence of 0, 0.0083, 0.025, 0.048, 0.071, 0.093, 0.11, 0.15, 0.18, 0.21 and 0.26 mM AC in pH 9 phosphate buffer at 20 °C.

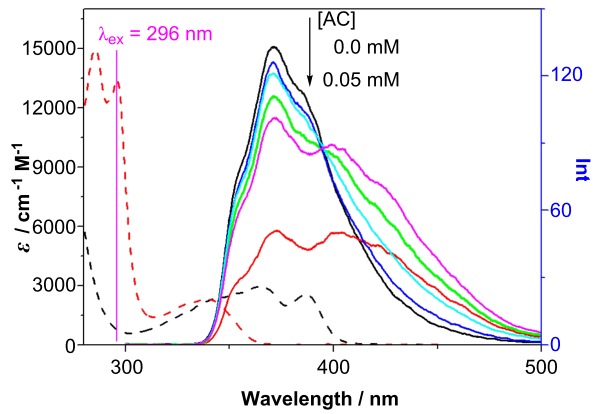

Figure 4: UV–vis spectra of AC (black dashed line) and **7** (red dashed line) and fluorescence spectra of **7** (0.02 mM) in the presence of 0.0, 0.0041, 0.0125, 0.025, 0.0375 and 0.05 mM AC in pH 9 phosphate buffer at 20 °C. λ_{ex} = 296 nm.

Fluorescence spectral behavior was examined at a lower host concentration in order to observe the fluorescence from both the 1:1 and 1:2 complexes with AC. Upon the addition of AC (0–0.05 mM) to a solution of **7** (0.02 mM), the naphthalene fluorescence at 373 nm was gradually reduced in intensity with an accompanying increase of AC fluorescence at 426 nm (Figure 4). The reduction of fluorescence intensity amounted to 27% at an AC concentration of 0.0375 mM, even although the absorbance of 0.0375 mM AC is only 11% of 0.02 mM naphthalene at the excitation wavelength (296 nm) and the internal filter effect of AC at 350–400 nm is negligible (absorbance <0.1). Considering the nice spectral overlap of the naphthalene fluorescence with the AC absorption (Figure 4), we conclude that Förster resonance energy transfer (FRET) is operating from naphthalene-appended **7** to AC residing in the cavity. Further addition of AC up to 0.05 mM caused a global decrease of the fluorescence of both **7** and AC, which can be rationalized by the increased formation of a 1:2 complex at the higher AC concentration, leading to efficient FRET and photocyclodimerization in the cavity.

Nonlinear least-squares fits of the UV–vis spectral titration data to the stepwise 1:2 complexation model gave binding constants for each step: K_1 = 1050 M^{-1} and K_2 = 18600 M^{-1} for **6** and K_1 = 620 M^{-1} and K_2 = 22300 M^{-1} for **7** at 25 °C. When compared to the corresponding values reported for native γ-CD (K_1 = 182 M^{-1} and K_2 = 56700 M^{-1}) [12], the first binding constant was enhanced by a factor of 3.5–5.8 by introducing the naphthalene moiety, whilst the second binding constant was reduced by a factor of 2.5–3.0, thus making the overall binding constant (K_1K_2) approximately twice as high. It is known that the small K_1 for native γ-CD is due to the oversized cavity which cannot provide tight contacts for a single AC molecule. Only when a second AC is introduced into the same cavity, are close contacts possible for two AC molecules with γ-CD walls thus leading to a much larger K_2. We attribute the enhanced K_1 values for **6** and **7** to the increased hydrophobicity of the naphthalene-modified γ-CD cavity. On the contrary, the naphthalene moieties reduce the K_2 values, probably due to steric hindrance and the restricted conformation and orientation available for ACs in the cavity. The higher overall affinities (K_1K_2) for **6** and **7** than for native γ-CD indicate the positive effect of aromatic modification on AC complexation.

An aqueous buffer solution (pH 9) of AC (0.4 mM) and modified γ-CD (2 mM) was photoirradiated at 360 nm with a Xenon lamp fitted with a band-pass filter. The product distribution and the ee of chiral photodimers, both determined by chiral HPLC, are shown in Table 1. As a general tendency, the HH dimers were preferred by introducing the aromatic substituents. Thus, the HH/HT ratio was dramatically enhanced from 0.12 for native γ-CD to 0.4–1.0 for biphenyl- or naphthalene-modified γ-CDs **5**–**7**. In particular, the use of the capped γ-CD **6** led to the preferential formation of chiral **3** in 34% yield at 0 °C. The increased hydrophobicity around the primary rim of these modified γ-CDs favors inclusion of the non-polar aromatic part of AC near the primary portal and the polar carboxylate part near the secondary portal to give the HH-oriented precursor complex. In contrast, the HT-oriented precursor complex, in which one of AC's carboxylate is positioned at the primary rim, should be less stable due to increased hydrophobicity, leading to the switching of product population to HH dimers.

Closer examination of the product distributions revealed the contrasting behavior of the *anti/syn* ratio in HT versus HH

Table 1: Photocyclodimerization of 2-anthracenecarboxylate (AC) in the presence of native and modified γ-cyclodextrins (CDs)[a].

host	λ/nm[b]	CD/AC[c]	*T*/°C	relative yield/%[d]				HH/HT[e]	*anti/syn*		ee/%[d,f]	
				1	**2**	**3**	**4**		**1/2**	**3/4**	**2**	**3**
γ-CD[g]	365	5	0	43	46	6	5	0.12	0.9	1.2	41	−1
5[h]	365	5	0	39	28	20	13	0.49	1.4	1.5	−58	−14
6	360	5	35	40	30	23	7	0.43	1.3	3.3	16	18
		5	20	38	29	25	9	0.51	1.3	2.8	20	21
		5	10	34	25	30	11	0.69	1.4	2.7	23	25
		5	0	29	23	34	13	0.90	1.3	2.6	29	30
		0.3	0	36	33	22	9	0.45	1.1	2.4	15	18
	300	5	0	27	22	36	15	1.04	1.2	2.4	28	35
		0.3	0	28	26	32	14	0.85	1.1	2.3	24	30
7	360	5	35	39	33	15	13	0.39	1.2	1.2	26	−1
		5	25	39	33	15	14	0.40	1.2	1.1	33	4
		5	15	37	35	15	13	0.39	1.1	1.2	28	−5
		5	0	37	34	14	14	0.39	1.1	1.0	37	−4
	300	5	0	39	30	14	17	0.45	1.3	0.8	32	−5

[a]Irradiated in pH 9 aqueous buffer at 0–35 °C with a Xenon lamp fitted with a band-pass filter; [AC] = 0.4 mM (fixed); [CD] = 0.12 or 2 mM. [b]Irradiation wavelength. [c]Host–guest ratio. [d]Relative yield and ee determined by chiral HPLC on a tandem column of Intersil ODS-2 (GL Science) and Chiralcel OJ-R (Daicel); error in ee: ±0.7%. [e](**3**+**4**)/(**1**+**2**). [f]Positive/negative ee sign corresponds to the excess of the first/second-eluted enantiomer, respectively. [g]Ref [12]. [h]Ref [20].

dimers. As can be seen from the *anti/syn* ratios for the HT and HH dimers shown in Table 1, the modifications of γ-CD only slightly alter the **1**/**2** ratio from 0.9 for native γ-CD to 1.1–1.4 for **5**–**7**. In sharp contrast, the **3**/**4** ratio was more susceptible to rim modification, in particular rigid capping was enhanced from 1.2 for native γ-CD to 1.5 for biphenyl-capped **5** and even to 2.3–3.3 for naphthalene-capped **6**, but was practically unaffected at 1.0–1.2 for naphthalene-appended **7**. These results are quite reasonable, as the electrostatic repulsion of the carboxylate anions of two ACs in the CD cavity should be stronger in an HH-oriented complex than in an HT-oriented one due to the shorter inter-anion distance in the former. In summary, naphthalene-capping greatly enhances the formation of HH, in particular *anti*-HH, dimers as a combined effect of increased hydrophobicity and electrostatic repulsion.

The hydrophobic modifications at the primary rim reduced the ee of chiral HT dimer **2**, suggesting that the achiral substituent introduced altered the chiral environment of γ-CD cavity. In this context, it is interesting to note that naphthalene-capped **6** and naphthalene-appended **7** give **2** in 29% and 37% ee, respectively, which are only slightly smaller than that obtained with native γ-CD (41% ee), whereas biphenyl-capped **5** gave antipodal **2** in −58% ee under comparable conditions (Table 1). Molecular model examinations indicated that the biphenyl group, attached to the A and D glucose units of γ-CD **5**, covers half of the primary rim. In the HT-oriented precursor complex of AC with **5**, one of the carboxylate groups is inevitably exposed to the bulk water through the narrowed primary rim, leading to a highly restricted conformation, which significantly differs from the original one achieved in the native γ-CD cavity. In contrast, the naphthalene moiety is anchored to only one glucose unit in **7** or to the A and C glucose units in **6**, leaving a larger opening for the carboxylate tail of the AC and more freedom for the HT-oriented AC pair in the cavity, a situation similar to native γ-CD. Based on these considerations, we may conclude that the steric restriction caused by the capping group, rather than its rigidity, is the real cause of the chirality switching observed for **5**.

Interestingly, the use of naphthalene-capped **6** greatly improved the chemical and optical yields of **3**, while native γ-CD, biphenyl-capped **5**, and naphthalene-appended **7** afforded almost racemic or antipodal **3** in much smaller chemical and optical yields. The HH-oriented AC pair in a complex precursor to **3** is likely to conceal the hydrophobic anthracene moiety inside the cavity with the carboxylate groups being exposed to the bulk water near the secondary rim of γ-CD. The enhanced chemical and optical yields observed for **3** should reflect the totally altered chiral environment, which favors the formation of one of the diastereomeric HH-oriented precursor complexes in the modified CD cavity of **6**. By lowering the temperature to 0 °C, the system was optimized to give *anti*-HH **3** in 34% yield with an ee of 30%, which is much higher than the corresponding values obtained with native or any other capped γ-CDs so far examined in aqueous solutions [20,22].

We further examined indirect FRET excitation (intramolecular photosensitization) of AC included in host **6**. Mechanistically, FRET excitation of AC is highly advantageous from the photochirogenic point of view, since the static energy transfer to an AC molecule accommodated in the CD cavity is much faster and more efficient than the dynamic energy transfer to an AC in bulk solution (even if it exists), thus minimizing the unfavorable achiral "outside" photoreaction. Irradiation of an aqueous solution containing 0.4 mM AC and 2 mM **6** was performed at 300 nm, where 98.5% of the incident light was absorbed by the naphthalene moiety of **6** and therefore it is possible to examine the effects of FRET excitation on the distribution and ee of cyclodimers. As can be seen from Table 1, FRET excitation at 300 nm gave **3** in 36% yield and 35% ee, both of which are appreciably higher than the corresponding values obtained upon direct AC excitation at 360 nm. The enhanced stereoselectivity is attributed to the smaller contribution of the photoreaction outside the CD cavity, where the HT dimers are favored and chiral **2** and **3** produced should be racemic. To the best of our knowledge, this is the first example of FRET sensitization applied to photochirogenesis.

In supramolecular photochirogenesis, an excess amount of the chiral host is often the prerequisite for minimizing contamination from undesirable racemic photoreactions occurring outside chiral host. In the present system, it is likely that only AC that is included in the CD cavity can be FRET-sensitized by naphthalene, since the FRET efficiency is inversely proportional to the sixth power of donor–acceptor distance. We expected therefore that the AC photocyclodimerization could be catalyzed even with a sub-equivalent amount of the chiral FRET host. Indeed, the FRET-sensitized photocyclodimerization of AC with 0.3 equiv of **6** gave dimer **3** in 32% yield and 30% ee, which are only slightly decreased from the original 36% yield and 35% ee obtained with 5 equiv of **6** (Table 1). In contrast, the chemical yield of **3** was reduced from 34% to 22% and the ee from 30% to 18% upon direct AC excitation at 360 nm.

Conclusion

In the present work, naphthalene-appended and -capped γ-CDs were synthesized to investigate the effects of naphthalene capping and of FRET excitation on the complexation and supramolecular photochirogenic behavior of AC. Compared to native γ-CD, the naphthalene-modified γ-CDs showed 3.5–5.8 fold larger first binding constants and 2.5–3.0 fold smaller second binding constants, which resulted in roughly two-fold larger overall affinities, due to increased cavity hydrophobicity. Fluorescence spectral examination revealed that the FRET from the excited naphthalene on CD rim to AC included in the CD cavity is operative upon excitation of the naphthalene chromophore at 296 nm. Circular dichroism spectral studies revealed that the two AC molecules are arranged in a right-handed screw sense in the CD cavity. Direct excitation at 360 nm of AC accommodated in the cavity of modified γ-CD afforded HH cyclodimers (despite electrostatic repulsion between the HH-oriented carboxylate anions of the AC) in combined yields of up to 51%, which is much higher than that (11%) obtained with native γ-CD. In particular, both the chemical and optical yields of HH dimer **3** were significantly enhanced from 6% to 34% and from −1% ee to 30% ee by introducing a naphthalene-cap to γ-CD. More interestingly, FRET sensitization by exciting the naphthalene-cap of **6** at 300 nm afforded HH dimer **3** in a further enhanced yield of 36% with an ee of 35%. In the FRET sensitization**,** the high stereoselectivity was maintained even when the host/guest ratio was reduced to 0.3, thus achieving catalytic supramolecular photochirogenesis.

Experimental

General. FAB mass spectra were measured on a JEOL JMS-DX303 mass spectrometer. NMR spectra were recorded on a Bruker DRX-600 or a JEOL JNM-EX 400 spectrometer. UV–vis, fluorescence, and circular dichroism spectra were recorded in a UNISOKU USP-203CD cryostat with a JASCO V-560 spectrophotometer, JASCO FP-6500 luminescence spectrometer, and JASCO J-810 spectropolarimeter, respectively. Photoirradiation was performed in a UNISOKU USP-203 cryostat with an appropriate interference filter for 300 nm or 360 nm. Irradiated samples were subjected to chiral HPLC analysis on a tandem column of Intersil ODS-2(GL Science) and Chiralcel OJ-R (Daicel) with a 36:64 mixture of acetonitrile and water as eluent [12].

Syntheses of modified γ-CDs 6 and 7. For **6**: 6^A,6^C-ditosyl-γ-CD (321 mg, 0.2 mmol) and disodium 2,6-naphthalenedicarboxylate (52 mg, 0.2 mmol) were dissolved in 10 mL DMSO, and the mixture heated at 90 °C for 3 d. After cooling, the solution was concentrated to 0.5 mL under vacuum, trifluoroacetic acid added and the solution added dropwise to 30 mL acetone to give a precipitate. The precipitate was collected by filtration and purified by reverse-phase chromatography to give pure **6** (15.3 mg, 5.2% yield). ^{1}H NMR (400 MHz, D_2O): δ 8.14 (1H, s), 8.02 (1H, s), 7.78 (1H, d, J = 8.4 Hz), 7.69 (1H, d, J = 8.6 Hz), 7.62 (2H, d, J = 8.6 Hz), 4.97 (7H, m), 4.88 (2H, m), 4.79 (2H, m), 4.39 (2H, m), 4.31 (1H, m,), 4.18 (1H, m), 3.99–3.64 (13H, m), 3.63–3.31 (19H, m), 3.13 (4H, m), 2.56 (1H, d, J = 11.0 Hz,), 2.39 (1H, d, J = 11.1 Hz,), 2.27 (1H, d, J = 11.2 Hz,), 2.21 (1H, m), 1.60 (1H, br). ^{13}C NMR (150 MHz, D_2O): δ 167.85, 166.52, 133.85, 133.41, 132.71, 132.25, 131.98, 129.86, 129.50, 128.72, 125.94, 125.38, 102.36, 102.01, 101.84, 101.75, 101.67, 101.53, 81.21, 80.70, 80.07, 79.74, 74.86, 73.57, 73.26, 72.99, 72.81, 72.69, 72.61, 72.49, 72.31, 72.06, 71.94, 71.83, 71.68, 71.53, 71.22, 70.55, 68.13, 66.09, 60.23, 60.04, 59.91, 59.83,

58.52. HR–FAB-MS: Calc. for [**6**+Na]$^+$, $C_{60}H_{86}NaO_{42}$ 1499.43, found: 1499.43.

For **7**: 2,6-naphthalenedicarboxylic acid (216 mg, 1 mmol) and γ-CD (1296 mg, 1 mmol) were dissolved in 10 mL DMF, to which DCC (310 mg, 1.5 mmol) and HOBT (54 mg, 0.4 mmol) were added and the solution stirred at room temperature for 2 d. The reaction mixture was poured into 150 mL dry acetone to give a white precipitate. The precipitate was collected by filtration, dissolved in 10% aqueous methanol and then subjected to reverse–phase HPLC separation to give **7** (194 mg, 13% yield). ^{1}H NMR (600 MHz, 4:1 DMSO-d_6–D_2O): δ 8.58 (1H, d, J = 12.4 Hz,), 8.54 (1H, s), 8.13 (1H, dd, J = 8.5, 2.6 Hz,), 8.10 (1H, d, J = 8.5 Hz,), 7.99 (1H, d, J = 8.8 Hz), 7.96 (1H, d, J = 8.6 Hz,), 4.93 (1H, d, J = 3.3 Hz), 4.89 (1H, d, J = 3.3 Hz), 4.83 (6H, m), 4.64 (1H, m), 4.36 (1H, m), 3.66–3.52 (24H, m), 3.52–3.39 (14H, m), 3.38–3.26 (18H, m). ^{13}C NMR (150 MHz, 4:1 DMSO-d_6–D_2O) δ 167.71, 166.09, 149.51, 137.12, 134.64, 130.64, 130.49, 129.11, 126.42, 126.01, 124.42, 102.84, 102.01, 101.81, 82.30, 81.25, 81.17, 81.12, 81.04, 80.73, 73.30, 73.07, 72.97, 72.70, 72.47, 72.39, 69.46, 64.89, 60.22, 60.08, 59.89. HR–FAB-MS: Calc. for [**7**+Na]$^+$, $C_{60}H_{86}NaO_{43}$ 1517.44, found: 1517.45.

Supporting Information

Supporting Information File 1

NMR and HR–MS data of compounds **6** and **7**.
[http://www.beilstein-journals.org/bjoc/content/supplementary/1860-5397-7-38-S1.pdf]

Acknowledgements

This work was supported by JST (CY and YI), JSPS (YI). QW thanks the Student Exchange Support Program of JASSO for financial support for her stay in Japan.

References

1. Inoue, Y. *Chem. Rev.* **1992,** *92,* 741–770. doi:10.1021/cr00013a001
2. Inoue, Y.; Ramamurthy, Y., Eds. *Chiral Photochemistry; Molecular and Supramolecular Photochemistry;* Marcel Dekker: New York, 2004; Vol. 11. doi:10.1201/9780203026342
3. Griesbeck, A. G.; Meierhenrich, U. J. *Angew. Chem., Int. Ed.* **2002,** *41,* 3147–3154. doi:10.1002/1521-3773(20020902)41:17<3147::AID-ANIE3147>3.0.CO;2-V
4. Yang, C.; Inoue, Y. Supramolecular Photochirogenesis with Cyclodextrin. In *Cyclodextrin Materials Photochemistry, Photophysics and Photobiology;* Douhal, A., Ed.; Elsevier: Amsterdam, 2006; pp 241–265. doi:10.1016/B978-044452780-6/50012-7
5. Inoue, Y. *Nature* **2005,** *436,* 1099–1100. doi:10.1038/4361099a
6. Bauer, A.; Westkämper, F.; Grimme, S.; Bach, T. *Nature* **2005,** 1139–1140. doi:10.1038/nature03955
7. Inoue, Y.; Dong, F.; Yamamoto, K.; Tong, L.-H.; Tsuneishi, H.; Hakushi, T.; Tai, A. *J. Am. Chem. Soc.* **1995,** *117,* 11033–11034. doi:10.1021/ja00149a037
8. Lu, R.; Yang, C.; Cao, Y.; Wang, Z.; Wada, T.; Jiao, W.; Mori, T.; Inoue, Y. *Chem. Commun.* **2008,** 374–376. doi:10.1039/b714300a
9. Sivaguru, J.; Natarajan, A.; Kaanumalle, L. S.; Shailaja, J.; Uppili, S.; Joy, A.; Ramamurthy, V. *Acc. Chem. Res.* **2003,** *36,* 509–521. doi:10.1021/ar020269i
10. Aechtner, T.; Dressel, M.; Bach, T. *Angew. Chem., Int. Ed.* **2004,** *43,* 5849–5851. doi:10.1002/anie.200461222
11. Nishioka, Y.; Yamaguchi, T.; Kawano, M.; Fujita, M. *J. Am. Chem. Soc.* **2008,** *130,* 8160–8161. doi:10.1021/ja802818t
12. Nakamura, A.; Inoue, Y. *J. Am. Chem. Soc.* **2003,** *125,* 966–972. doi:10.1021/ja016238k
13. Wada, T.; Nishijima, M.; Fujisawa, T.; Sugahara, N.; Mori, T.; Nakamura, A.; Inoue, Y. *J. Am. Chem. Soc.* **2003,** *125,* 7492–7493. doi:10.1021/ja034641g
14. Nakamura, A.; Inoue, Y. *J. Am. Chem. Soc.* **2005,** *127,* 5338–5339. doi:10.1021/ja050704e
15. Nishijima, M.; Wada, T.; Mori, T.; Pace, T. C. S.; Bohne, C.; Inoue, Y. *J. Am. Chem. Soc.* **2007,** *129,* 3478–3479. doi:10.1021/ja068475z
16. Yang, C.; Mori, T.; Origane, Y.; Ko, Y. H.; Selvapalam, N.; Kim, K.; Inoue, Y. *J. Am. Chem. Soc.* **2008,** *130,* 8574–8575. doi:10.1021/ja8032923
17. Ke, C.; Yang, C.; Mori, T.; Wada, T.; Liu, Y.; Inoue, Y. *Angew. Chem., Int. Ed.* **2009,** *48,* 6675–6677. doi:10.1002/anie.200902911
18. Yang, C.; Fukuhara, G.; Nakamura, A.; Origane, Y.; Fujita, K.; Yuan, D.-Q.; Mori, T.; Wada, T.; Inoue, Y. *J. Photochem. Photobiol., A: Chem.* **2005,** *173,* 375–383. doi:10.1016/j.jphotochem.2005.04.017
19. Yang, C.; Nakamura, A.; Fukuhara, G.; Origane, Y.; Mori, T.; Wada, T.; Inoue, Y. *J. Org. Chem.* **2006,** *71,* 3126–3136. doi:10.1021/jo0601718
20. Yang, C.; Nakamura, A.; Wada, T.; Inoue, Y. *Org. Lett.* **2006,** *8,* 3005–3008. doi:10.1021/ol061004x
21. Yang, C.; Nishijima, M.; Nakamura, A.; Mori, T.; Wada, T.; Inoue, Y. *Tetrahedron Lett.* **2007,** *48,* 4357–4360. doi:10.1016/j.tetlet.2007.04.104
22. Yang, C.; Mori, T.; Inoue, Y. *J. Org. Chem.* **2008,** *73,* 5786–5794. doi:10.1021/jo800533y
23. Fujita, K.; Yamamura, H.; Imoto, T.; Fujioka, T.; Mihashi, K. *J. Org. Chem.* **1988,** *53,* 1943–1947. doi:10.1021/jo00244a018
24. Nakanishi, K.; Berova, N. *Circular dichroism–principles and applications;* Wiley-VCH: New York, 2000.

Beilstein Journal of Organic Chemistry

Photoinduced electron-transfer chemistry of the bielectrophoric *N*-phthaloyl derivatives of the amino acids tyrosine, histidine and tryptophan

Axel G. Griesbeck*, Jörg Neudörfl and Alan de Kiff

Full Research Paper

Open Access

Address:
University of Cologne, Department of Chemistry, Organic Chemistry, Greinstr. 4, D-50939 Köln, Germany; Fax: +49(221)470 5057

Email:
Axel G. Griesbeck* - griesbeck@uni-koeln.de

* Corresponding author

Keywords:
amino acids; decarboxylation; electron transfer; photochemistry; phthalimides

Beilstein J. Org. Chem. **2011,** *7,* 518–524.
doi:10.3762/bjoc.7.60

Received: 26 November 2010
Accepted: 22 March 2011
Published: 26 April 2011

This article is part of the Thematic Series "Photocycloadditions and photorearrangements".

Guest Editor: A. G. Griesbeck

Abstract

The photochemistry of phthalimide derivatives of the electron-rich amino acids tyrosine, histidine and tryptophan **8**–**10** was studied with respect to photoinduced electron-transfer (PET) induced decarboxylation and Norrish II bond cleavage. Whereas exclusive photodecarboxylation of the tyrosine substrate **8** was observed, the histidine compound **9** resulted in a mixture of histamine and preferential Norrish cleavage. The tryptophan derivative **10** is photochemically inert and shows preferential decarboxylation only when induced by intermolecular PET.

Introduction

Phthalimides are versatile electron acceptors in photoinduced electron-transfer (PET) reactions. N-Alkylated phthalimides typically absorb in the 295 nm region with extinction coefficients around 10^3. The quantum yields for intersystem crossing Φ_{ISC} significantly change with the substitution on the imide nitrogen, e.g., $\Phi_{ISC} = 0.5$ for *N*-isobutylphthalimide and $\Phi_{ISC} < 0.01$ for *N*-arylphthalimides [1]. If necessary, the population of the triplet state is also possible by sensitization, e.g., with triplet sensitizers such as acetone or benzophenone. With a triplet energy E_T of 293–300 kJ mol^{-1} and a ground-state reduction potential E^0 of −1.85 V vs Fc/Fc$^+$, electronically excited phthalimides are potent electron acceptors [2]. The rich photochemistry of this chromophore has recently been reviewed [3,4]. Intramolecular hydrogen abstraction is an archetype process for electronically excited carbonyl groups (Norrish type II reaction). The 1,4-biradicals formed by γ-CH transfer can undergo several subsequent reactions, among which are secondary H transfer, cyclization, or fragmentation. The excited imido

group is at the same time an efficient electron acceptor and can be reduced by numerous donor groups.

As a model compound for neutral aliphatic amino acids, the photophysical and photochemical properties of *N*-phthaloylvaline methyl ester (**1**) have been studied by nanosecond laser flash photolysis (λ_{exc} = 248 or 308 nm) [5]. The quantum yield of fluorescence is low ($\Phi_F = 10^{-2}$), whereas that of phosphorescence at −196 °C is large (0.5). The triplet properties of **1** at room temperature and in ethanol at low temperatures are known: Triplet acetone, acetophenone and xanthone in acetonitrile are quenched by **1** via energy transfer; the rate constant is almost diffusion-controlled and somewhat smaller for benzophenone. The sole product from the photolysis of **1** is the double hydrogen transfer product **2**. On the other hand, phthaloyl derivatives of C-unprotected α-amino acids (e.g., derivatives of Gly, Ala, Val, Ile, Phe) undergo efficient photodecarboxylation to yield the corresponding amines, β-amino acids are converted to benzazepines, and γ-amino acids to benzopyrrolizidines (Scheme 1). For example, the glutamic acid derivative **3** resulted in the formation of a diastereoisomeric mixture of benzopyrrolizidinones **4** [6]. For a specific system, *N*-phthaloyl methionine (**5**), we have detected bielectrophoric behavior in that the electron transfer from the thioether group competes efficiently with decarboxylation when the reaction is triplet-sensitized [7]. Photodecarboxylation is followed by PET cyclization to give **6**, whereas the lactone **7** originates from PET-induced sulfur oxidation and radical ion trapping without subsequent decarboxylation. Similar effects were observed for the cysteine and *S*-methyl cysteine derivatives [8].

Other proteinogenic amino acids that, in principle, should also be able to show bielectrophoric behavior with aromatic side chains similar to phenylalanine are tyrosine, histidine and tryptophan. The photochemistry of the phthalimide derivatives of these three amino acids are described in this publication.

Results

Synthesis of phthalimide substrates

The C-unprotected *N*-phthaloyl amino acids **8**–**10** were available from tyrosine, histidine, and tryptophan (Figure 1). The phthalimide derivatives were prepared either by thermal reaction of phthalic anhydride with the corresponding amino acids or by the Nefkens procedure [9]. The latter procedure yields enantiomerically pure products (by optical rotation), whereas the thermal method leads to partial epimerization.

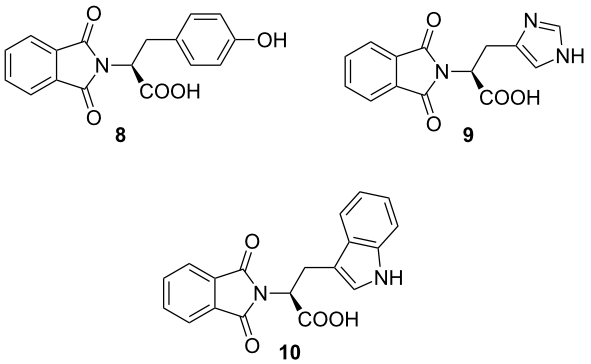

Figure 1: Phthalimides from tyrosine **8**, histidine **9** and tryptophan **10**.

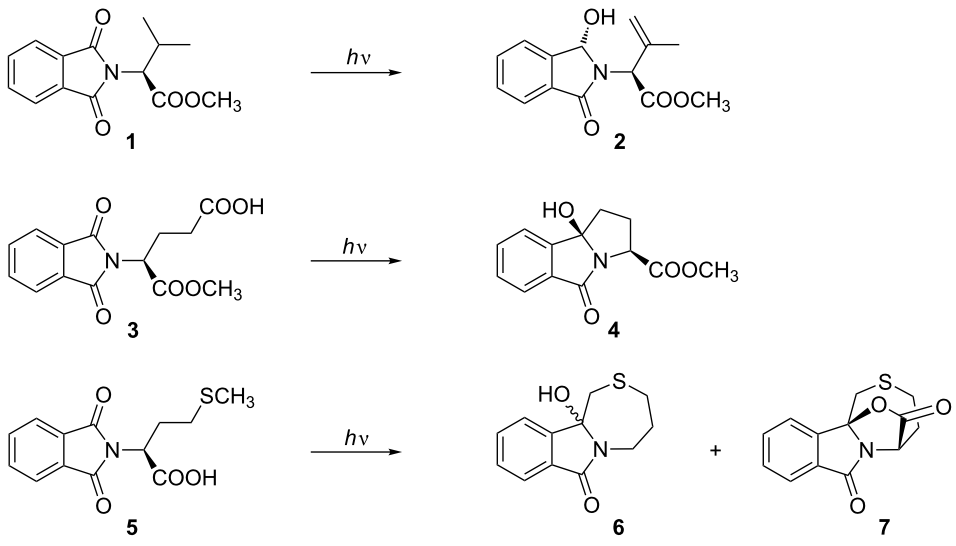

Scheme 1: Three phthalimide/amino acid model reactions: Norrish II process of **1**, PET decarboxylation of **3**, PET competition of **5**.

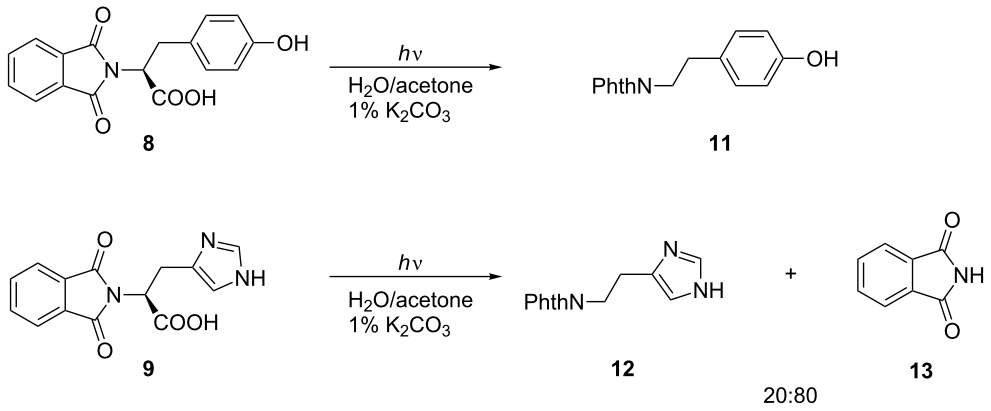

Scheme 2: PET decarboxylation/photocleavage of **8** and **9**.

Photochemistry of the tyrosine and histidine derivatives **8** and **9**

The colorless phthalimides from tyrosine and histidine **8** and **9**, respectively, were photochemically active and gave decarboxylation and cleavage products. In contrast to photolysis in pure acetone [10], irradiation of the tyrosine substrate **8** in basic water/acetone resulted solely in the decarboxylation product **11**. Under identical conditions, the histidine derivative **9** resulted in a 1:4 mixture of phthaloyl histamine **12** and phthalimide (**13**) (Scheme 2). In both cases, the photolyses were clean processes and the products were isolated in high yields after complete conversion. The tyramine derivative **11** was isolated by crystallization in near quantitative yield.

Photochemistry of the tryptophan derivative **10**

In contrast to all other – colorless – phthalimides of the proteinogenic amino acid series, the tryptophan derivative **10** is bright yellow. This compound, which we crystallized and whose solid-state structure was determined by X-ray diffraction analysis (Figure 2) [11], has also been described in literature as a yellow compound [12,13]. The color is not the consequence of any impurity and did not vanish after several recrystallizations and, more importantly, was also observed for the methyl ester and the decarboxylation product, the *N*-phthaloyl tryptamine (**14**). Compound **10** represents a donor–*ethylene bridge*–acceptor situation and intramolecular electron transition (ET) is feasible. The UV spectra of the three substrates **8**–**10** (Figure 3) showed in fact two major absorption peaks for **8** and **10** at 280 and 300 nm, whereas the histidine derivative **9** only exhibits the typical phthalimide absorption at λ_{max} = 282 nm. The red-shifted absorption of **10** has a tailing that explains the color of this compound and derivatives as CT state absorption

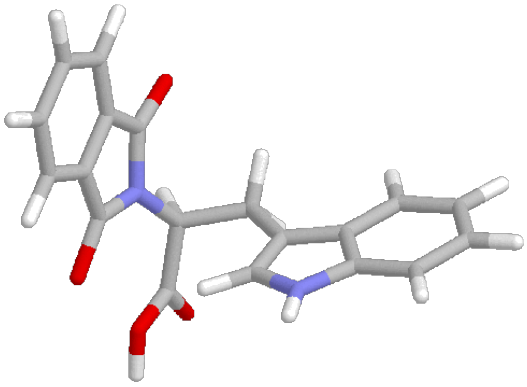

Figure 2: Structure of the tryptophan derivative **10** in the crystal.

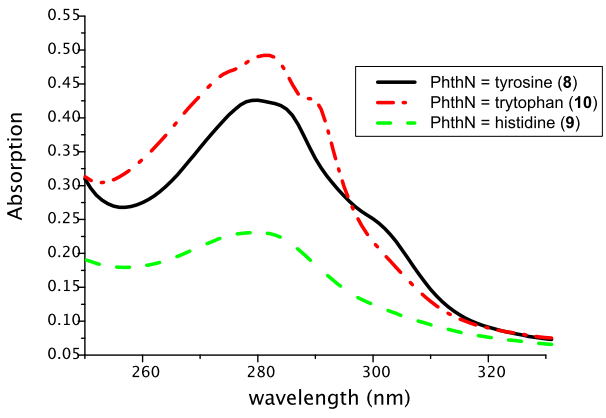

Figure 3: UV–vis absorption spectra of compounds **8**–**10** (c = 2 × 10^{-4} in CH_3OH).

and is additionally red-shifted by 10 nm on changing the solvent from ether to acetonitrile or methanol, respectively. It is remarkable that under solid-state conditions the molecular conformation of **10** in the crystal lattice is synclinal with respect to the indole and the phthalimide groups as well as for the indole and the carboxy groups, indicating a ground-state electronic interaction between the donor indole and the acceptor phthalimide (Figure 2). Such interactions also in solution phase would facilitate decay processes from the excited singlet or triplet state. This concept has also been described by Gawronski et al. from exciton CD Cotton effects that have been measured for a series of bichromophoric systems based on phthalimide–linker–donor triades [12]. Concerning the photochemistry of **10**, a remarkable difference to all other phthalimide derivatives occurred: Neither direct excitation nor triplet (acetone, benzophenone) sensitized conditions led to substrate conversion even after prolonged irradiation. Only the use of the PET catalyst 2,4,6-triphenylpyrylium tetrafluoroborate enabled quantitative conversion to give a 4:1 mixture of the decarboxylation product, *N*-phthaloyl typtamine (**14**) and the cleavage product **13** (Scheme 3).

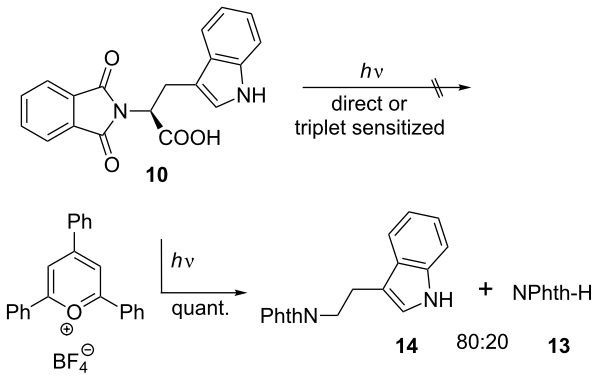

Scheme 3: Direct, triplet-sensitized and ET-sensitized photochemistry of **10**.

Additionally, the fluorescence spectra (Figure 4) indicated a charge-transfer excited-state formation from the tyrosine and tryptophan derivatives, **8** and **10**, respectively, by showing dual emission at 310 and 370 nm.

Discussion

Two reaction modes were observed with the phthalimides **8**–**10**: (a) Norrish type II cleavage of the central N–C bond to give the N-unsubstituted phthalimide **13**, and (b) photochemical decarboxylation. Analysis of the energetics of the PET between the phthalimide acceptor (see Introduction) and the arene donor side chains of the corresponding amino acid leads to the conclusion that PET is exergonic with $\Delta G = -0.1$ to -0.3 V for all cases: The redox potentials of the three amino acids tryptophan,

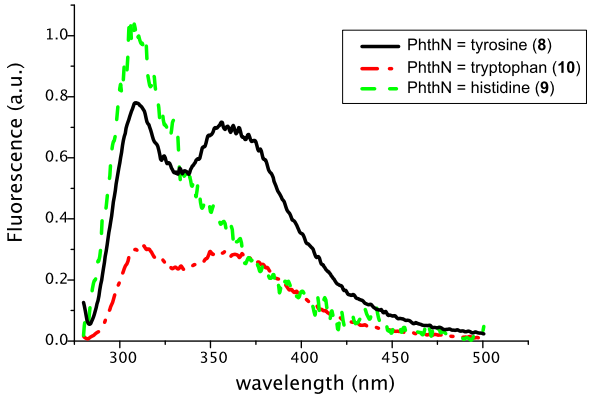

Figure 4: Fluorescence spectra of compounds **8**–**10** ($c = 6 \times 10^{-5}$ in CH_3OH).

histidine and tyrosine are reported to be 1.02 V [14], 1.17 V [15] and 0.93 V [16].

Due to this narrow redox potential window, similar electron-transfer properties can be expected. Among the amino acids investigated herein, tryptophan is described in biological electron-transfer processes as the most active hole transport molecule [17]. Thus, it can be concluded that the excited charge-transfer state from **10**, as can be interpreted from its fluorescence spectrum, is rapidly deactivated radiatively as well as non-radiatively by back electron transfer (BET). In contrast to **10**, electron transfer from the electronically excited tyrosine compound **8** is followed by oxidation of the carboxyl anion and subsequent decarboxylation to give *N*-phthaloyl tyramine (**11**). If BET from the radical cation state of **10** can be retarded (i.e., produced by an intermolecular PET), the corresponding decarboxylation proceeds to give *N*-phthaloyl tryptamine (**14**) (Scheme 3). The histidine derivative **9** is expected to undergo PET with oxidation of the aryl group with the lowest efficiency and thus a Norrish II process (γ-hydrogen transfer with subsequent central bond cleavage) prevails here (Scheme 4). This process, which was also detected as the minor pathway for the histidine case can, of course, also be described as an electron-transfer induced process followed by α-deprotonation.

Conclusion

The photochemistry of three bielectrophoric phthaloyl derivatives of tyrosine (**8**), histidine (**9**) and tryptophan (**10**) follows two distinct pathways, fragmentation and decarboxylation. Both routes can be described as initiated by electron transfer. Intramolecular transfer in the tyrosine substrate **8** leads to efficient decarboxylation whereas for the tryptophan substrate **10** this process can only be initiated by intermolecular electron transfer suggesting efficient back electron transfer in the photoexcited substrate.

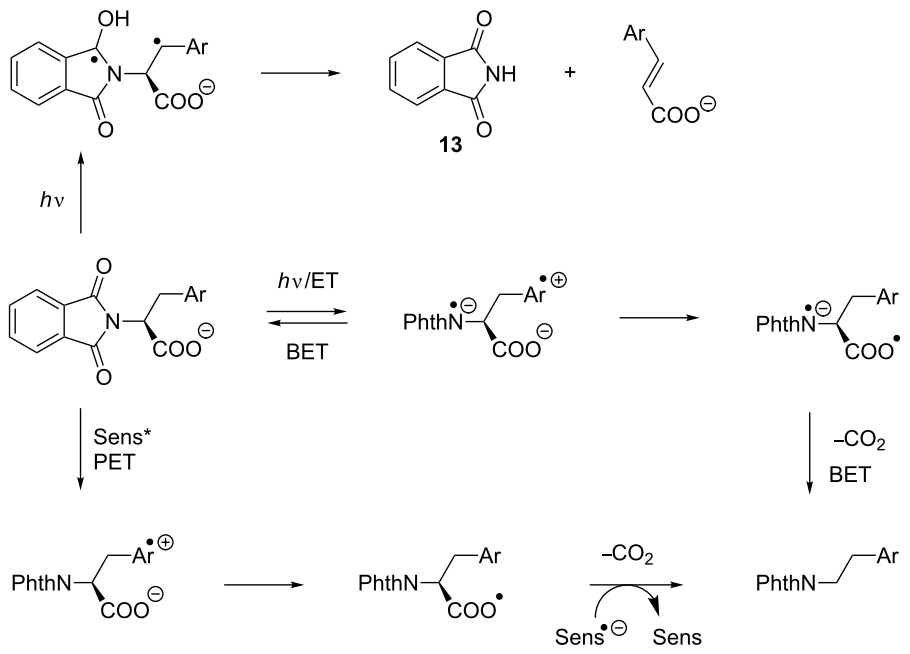

Scheme 4: Mechanistic scenario.

Experimental

Synthesis of *N*-phthaloyl tyrosine (8) [18]. A well ground mixture of 2.00 g (13 mmol) of L-tyrosine and 2.45 g (13 mmol) of phthalic anhydride were added to a 10 mL flask with a magnetic stirring bar. The flask was heated in an oil bath, stirred at 150–160 °C for 20 min and then the mixture was allowed to cool to room temperature. Recrystallization of the crude solid material from ethanol gave 3.67 g of *N*-phthaloyl tyrosine (**8**) (88%) as colorless needles; mp 161–163 °C (lit. 162–164 °C); $[\alpha]_D^{20}$ −183.8 (*c* 1.0, EtOH) (lit. −182.4); ^{1}H NMR (300 MHz, DMSO-d_6): δ (ppm) = 3.22 (dd, 2H, J_1 = 13.6 Hz, J_2 = 11.8 Hz), 5.01 (dd, 1H, J_1 = 11.9 Hz, J_2 = 5.0 Hz), 6.53 (d, 1H, *J* = 8.5 Hz), 6.91 (d, *J* = 8.5 Hz), 7.84 (s, 4H), 9.14 (s, COOH). ^{13}C NMR (75 MHz, DMSO-d_6): δ (ppm) = 33.1 (t, 1C), 53.2 (s, 1C), 115.1 (d, 2C), 123.4 (d, 2C), 127.2 (s, 1C), 129.7 (d, 2C), 130.8 (s, 2C), 134.9 (d, 2C), 155.8 (s, 1C), 167.1 (s, 2C), 170.2 (s, 1C).

Synthesis of *N*-phthaloyl histidine (9) [19]. L-histidine 3.0 g (14 mmol) and 1.52 g (14 mmol) of Na_2CO_3 were dissolved in 100 mL water and 3.14 g (14 mmol) of *N*-carbethoxy phthalimide was added to the solution. The mixture was allowed to stir at room temperature for 2 h. After acidification with 2 M HCl, the solvent was removed under reduced pressure. The colorless residue was heated under reflux in 10 mL MeOH for 20 min. After cooling, the residue was removed by filtration and washed with 100 mL MeOH to give 3.40 g of *N*-phthaloyl histidine (**9**) (83%) as a colorless solid; mp >260 °C; ^{1}H NMR (300 MHz, DMSO-d_6): δ (ppm) = 3.37 (d, 2H, *J* = 6.6 Hz, H 7), 4.91 (dd, 1H, J_1 = 9.5 Hz, J_2 = 6.5 Hz), 6.81 (s, 1H), 7.73 (s, 1H), 7.84 (s, 4H). ^{13}C NMR (75 MHz, DMSO-d_6): δ (ppm) = 33.1 (t, 1C), 53.2 (s, 1C), 115.1 (d, 2C), 123.4 (d, 2C), 127.2 (s, 1C), 129.7 (d, 2C), 130.8 (s, 2C), 134.9 (d, 2C), 155.8 (s, 1C), 167.1 (s, 2C), 170.2 (s, 1C).

Synthesis of *N*-phthaloyl tryptophan (10) [18]. A mixture of 2 g (9.8 mmol) of L-tryptophan and 1.04 g (9.8 mmol) of Na_2CO_3 was dissolved in 100 mL of water. To this solution, 2.15 g (9.8 mmol) of *N*-carbethoxy phthalimide were added. The mixture was stirred at room temperature for 1 h. After filtration the solution was acidified with 2 M HCl and the precipitate collected. Recrystallization from aqueous acetone gave 3.12 g of *N*-phthaloyl tryptophan (**10**) (95%) as yellow needles; mp 170 °C; $[\alpha]_D^{20}$ −247.5 (*c* 1.0, EtOH) (lit: −249.6); ^{1}H NMR (300 MHz, DMSO-d_6): δ (ppm) = 3.55–3.62 (m, 2H), 5.13 (dd, 1H, J_1 = 10 Hz, J_2 = 6.7 Hz), 6.89 (t, 1H, *J* = 7.3 Hz), 7.00 (t, 1H, *J* = 8 Hz), 7.49 (d, 1H, *J* = 8.1 Hz), 7.26 (d, 1H, *J* = 8.2 Hz), 7.80 (s, 4H), 10.74 (s, COOH). ^{13}C NMR (75 MHz, DMSO-d_6): δ (ppm) = 24.1 (t, 1C), 52.7 (d, 1C), 109.8 (s, 1C), 111.5 (d, 1C), 117.9 (d, 1C), 118.5 (d, 1C), 121.0 (d, 1C), 123.4 (d, 2C), 126.9 (s, 1C), 130.9 (s, 2C), 134.9 (d, 2C), 136.1 (s, 1C), 167.2 (s, 2C), 170.4 (s, 1C).

Photolysis of *N*-phthaloyl tyrosine (8). A water-cooled solution ($c = 2.1 \times 10^{-3}$ mol/l) of **8** and 0.5 equiv K_2CO_3 in 100 mL of an acetone/water mixture (1:1) was irradiated at 300 nm

(lamps: 8 × 3000 Å, 800 W, 300 ± 10 nm) for 12 h under a nitrogen atmosphere. The product was removed by filtration and washed with water to give 396 mg of *N*-phthaloyl tyramine (**11**) (95%) as a colorless solid; mp 171–174 °C; ^{1}H NMR (300 MHz, DMSO-d_6): δ (ppm) = 2.77 (t, 2H, *J* = 7.5 Hz), 3.73 (t, 2H, *J* = 7.5 Hz), 6.59 (d, 2H, *J* = 8.5 Hz), 6.92 (d, 2H, *J* = 8.5 Hz), 7.82 (s, 2H), 7.83 (s, 2H). ^{13}C NMR (75 MHz, DMSO-d_6): δ (ppm) = 32.9 (t, 1C), 40.3 (t, 1C), 115.5 (d, 2C), 123.0 (d, 2C), 127.0 (s, 1C), 129.4 (d, 2C, C8/C8'), 131.5 (s, 2C), 134.4 (d, 2C), 157.2 (s, 1C), 167.7 (s, 2C).

Photolysis of *N*-phthaloyl histidine (9). A water-cooled solution ($c = 2.1 \times 10^{-3}$ mol/l) of **9** and 0.5 equiv K_2CO_3 in 100 mL of an acetone/water mixture (1:1) was irradiated at 300 nm (lamps: 8 × 3000 Å, 800 W, 300 ± 10 nm) under a nitrogen atmosphere. After 24 h the solution was acidified with 2 M HCl and the solvent was removed under reduced pressure. The product composition [*N*-phthaloyl histamine (**12**)/phthalimide (**13**)] was determined by ^{1}H NMR spectroscopy.

12: 20% (by ^{1}H NMR); mp 173–175 °C; ^{1}H NMR (300 MHz, DMSO-d_6): δ (ppm) = 2.91 (t, 2H, *J* = 6.6 Hz), 3.88 (t, 2H, *J* = 6.6 Hz), 6.79 (s, 1H), 7.70 (s, 1H), 7.80 (s, 4H). ^{13}C NMR (75 MHz, DMSO-d_6): δ (ppm) = 24.0 (t, 1C), 37.9 (d, 1C, C5), 116.1 (d, 1C), 123.1 (d, 2C), 131.1 (s, 2C), 132.9 (d, 1C), 134.5 (d, 2C), 138.4 (s, 1C), 167.9 (s, 2C, C4/C4').

13: 80% (by ^{1}H NMR); ^{1}H NMR (300 MHz, DMSO-d_6): δ (ppm) = 7.75 (s, 4H). ^{13}C NMR (75 MHz, DMSO-d_6): δ (ppm) = 123.0 (d, 2C), 132.1 (s, 2C), 134.7 (d, 2C), 167.2 (s, 2C).

Photolysis of *N*-phthaloyl tryptophan (10). A 100 mL solution (c = 0.01 mol/l) of **10** and 5.4×10^{-3} mmol 2,4,6-triphenylpyrylium tetrafluoroborate in acetonitrile was irradiated at 350 nm (RPR-3500 Å lamp: 6 × 3500 Å, 400 W, 350 ± 25 nm) for 4 d under a nitrogen atmosphere. After removal of the solvent under reduced pressure, the ratio of products was determined by ^{1}H NMR spectroscopy. Silica gel flash chromatography (cyclohexane/ethylacetate) of the residue afforded *N*-phthaloyl tryptamine (**14**) as a yellow solid and phthalimide (**13**) as a colorless solid.

14: 80% (by ^{1}H NMR); mp 173–175 °C; ^{1}H NMR (300 MHz, acetone-d_6): δ (ppm) = 3.13 (t, 2H, *J* = 7.7 Hz), 3.95 (t, 2H, *J* = 7.7 Hz), 7.01 (t, 1H, *J* = 7.4 Hz), 7.09 (t, 1H, *J* = 7.8 Hz), 7.20 (s, 1H), 7.37 (d, 1H, *J* = 7.9 Hz), 7.67 (d, 1H, *J* = 87.7 Hz), 7.81 (s, 4H). ^{13}C NMR (75 MHz, acetone-d_6): δ (ppm) = 24.2 (t, 1C), 38.4 (t, 1C), 111.4 (d, 1C), 118.3 (d, 1C), 118.7 (d, 1C), 121.3 (d, 1C), 122.9 (d, 2C), 127.6 (s, 1C), 132.3 (s, 2C), 134.1 (d, 2C), 135.9 (s, 1C), 167.9 (s, 2C).

Acknowledgements

We thank the Deutsche Forschungsgemeinschaft (DFG) for project funding.

References

1. Warzecha, K.-D.; Görner, H.; Griesbeck, A. G. *J. Phys. Chem. A* **2006,** *110,* 3356–3363. doi:10.1021/jp055878x
2. Wintgens, V.; Valat, P.; Kossanyi, J.; Biczok, L.; Demeter, A.; Bérces, T. *J. Chem. Soc., Faraday Trans.* **1994,** *90,* 411–421. doi:10.1039/ft9949000411
3. Yoon, U. C.; Mariano, P. S. *Acc. Chem. Res.* **2001,** *34,* 523–532. doi:10.1021/ar010004o
4. Griesbeck, A. G.; Hoffmann, N.; Warzecha, K.-D. *Acc. Chem. Res.* **2007,** *40,* 128–140. doi:10.1021/ar068148w
5. Griesbeck, A. G.; Görner, H. *J. Photochem. Photobiol., A: Chem.* **1999,** *129,* 111–119. doi:10.1016/S1010-6030(99)00180-X
6. Griesbeck, A. G.; Nerowski, F.; Lex, J. *J. Org. Chem.* **1999,** *64,* 5213–5217. doi:10.1021/jo990390b
7. Griesbeck, A. G.; Mauder, H.; Müller, I.; Peters, K.; Peters, E.-M.; von Schnering, H. G. *Tetrahedron Lett.* **1993,** *34,* 453–456. doi:10.1016/0040-4039(93)85100-B
8. Griesbeck, A. G.; Hirt, J.; Kramer, W.; Dallakian, P. *Tetrahedron* **1998,** *54,* 3169–3180. doi:10.1016/S0040-4020(98)00063-5
9. Nefkens, G. H. L.; Tesser, G. I.; Nivard, R. J. F. *Recl. Trav. Chim. Pays-Bas* **1960,** *79,* 688–698. doi:10.1002/recl.19600790705
10. Griesbeck, A. G.; Henz, A.; Hirt, J.; Ptatschek, V.; Engel, T.; Löffler, D.; Schneider, F. W. *Tetrahedron* **1994,** *50,* 701–714. doi:10.1016/S0040-4020(01)80787-0
11. The crystallographic data for the tryptophan derivative **10** has been deposited with the Cambridge Crystallographic Data Centre as supplementary publication no. CCDC-784387.
12. Gawronski, J.; Kazmierczak, F.; Gawronska, K.; Skowronek, P.; Waluk, J.; Marczyk, J. *Tetrahedron* **1996,** *52,* 13201–13214. doi:10.1016/0040-4020(96)00795-8
13. Casimir, J. R.; Guichard, G.; Briand, J.-P. *J. Org. Chem.* **2002,** *67,* 3764–3768. doi:10.1021/jo016347h
14. Harriman, A. *J. Phys. Chem.* **1987,** *91,* 6102–6104. doi:10.1021/j100308a011
15. Navaratnam, S.; Parsons, B. J. *J. Chem. Soc., Faraday Trans.* **1998,** *94,* 2577–2581. doi:10.1039/a803477j
16. Cordes, M.; Köttgen, A.; Jasper, C.; Jacques, O.; Boudebous, H.; Giese, B. *Angew. Chem., Int. Ed.* **2008,** *47,* 3461–3463. doi:10.1002/anie.200705588
17. Giese, B.; Wang, M.; Stoltz, M.; Müller, P.; Graber, M. *J. Org. Chem.* **2009,** *74,* 3621–3625. doi:10.1021/jo900375f
18. Zeng, Q.; Liu, Z.; Li, B.; Wang, F. *Amino Acids* **2004,** *27,* 183–186. doi:10.1007/s00726-004-0109-1
19. Auterhoff, H.; Hansen, J.-G. *Pharmazie* **1970,** *25,* 336–340.

Beilstein Journal of Organic Chemistry

The arene–alkene photocycloaddition

Ursula Streit and Christian G. Bochet*

Review

Open Access

Address:
Department of Chemistry, University of Fribourg, Chemin du Musée 9, CH-1700 Fribourg, Switzerland

Email:
Ursula Streit - ursula.streit@unifr.ch; Christian G. Bochet* - christian.bochet@unifr.ch

* Corresponding author

Keywords:
benzene derivatives; cycloadditions; Diels–Alder; photochemistry

Beilstein J. Org. Chem. **2011,** *7,* 525–542.
doi:10.3762/bjoc.7.61

Received: 07 January 2011
Accepted: 23 March 2011
Published: 28 April 2011

This article is part of the Thematic Series "Photocycloadditions and photorearrangements".

Guest Editor: A. G. Griesbeck

Abstract

In the presence of an alkene, three different modes of photocycloaddition with benzene derivatives can occur; the [2 + 2] or *ortho*, the [3 + 2] or *meta*, and the [4 + 2] or *para* photocycloaddition. This short review aims to demonstrate the synthetic power of these photocycloadditions.

Introduction

Photocycloadditions occur in a variety of modes [1]. The best known representatives are undoubtedly the [2 + 2] photocycloaddition, forming either cyclobutanes or four-membered heterocycles (as in the Paternò–Büchi reaction), whilst excited-state [4 + 4] cycloadditions can also occur to afford cyclooctadiene compounds. On the other hand, the well-known thermal [4 + 2] cycloaddition (Diels–Alder reaction) is only very rarely observed photochemically (vide infra). Photocycloadditions are not limited to simple alkenes, and even the thermally very stable benzene core has been shown to become quite reactive upon excitation with photons. It can be converted into benzvalene [2,3] and fulvene when excited to its first excited-state, or to Dewar benzene [4,5] via excitation to its second excited-state (Scheme 1) [6].

In the presence of an alkene, three different modes of photocycloaddition with benzene derivatives can occur, viz. the [2 + 2] or *ortho*, the [3 + 2] or *meta*, and the [4 + 2] or *para* photocycloaddition (Scheme 2). The descriptors *ortho*, *meta* and *para* only indicate the connectivity to the aromatic ring, and do not have any implication with regard to the reaction mechanism. This article aims at giving a didactic insight in the synthetic power of these photocycloadditions. While the field of *meta* photocycloadditions has been the focus of a series of excellent reviews, the *ortho* and *para* variants have only been reviewed in a more broad fashion.

In this article we will first discuss the *meta*, *ortho* and *para* modes, which we will call classical photocycloadditions of

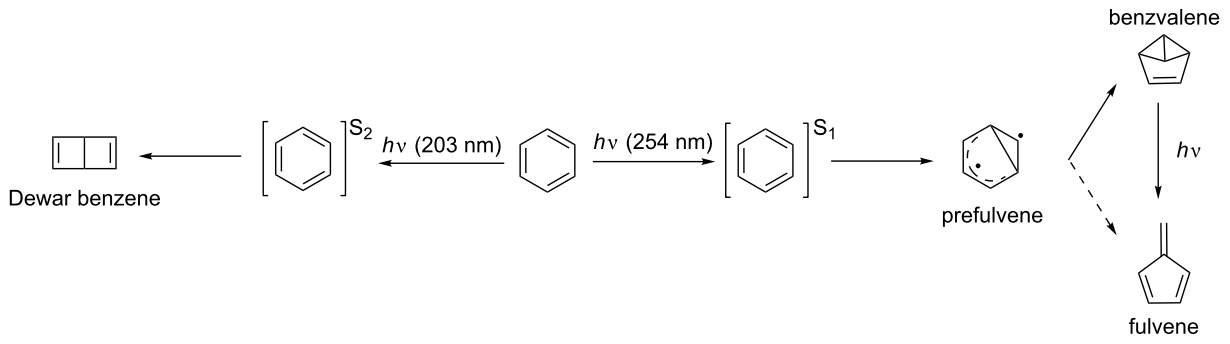

Scheme 1: Photochemistry of benzene.

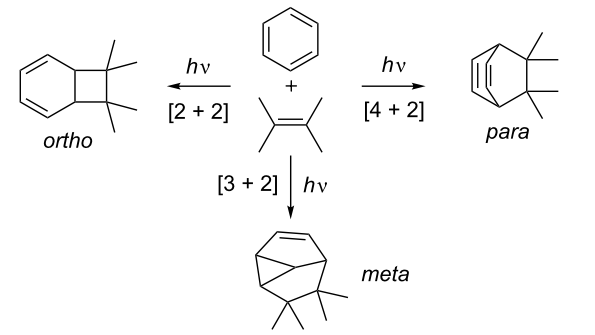

Scheme 2: Three distinct modes of photocycloaddition of arenes to alkenes.

alkenes with arenes. The last part includes a related class of cycloadditions with arenes, where the aromaticity on the final compounds is restored. In this review, we will call this class "non-classical" photocycloadditions.

Review

Classical photocycloaddition of alkenes to arenes

While the *meta* photocycloaddition of benzene is very well documented in the literature and has been used many times in organic synthesis, the *ortho* and particularly the *para* photocycloadditions have not received as much attention since both types occur rarely and are usually low yield reactions. However, also in these two cases, the complexity of the products is considerably increased with respect to that of the reactants, as a new ring and up to four new stereocenters are formed.

The first "classical" [2π + 2π] photocycloaddition of benzene was described by Angus and Bryce-Smith in 1959 [7]. However, Ayer, Bradford and Büchi had obtained similar *ortho* products some four years earlier and recorded their findings in a patent [8]. The *meta* photocycloaddition was discovered in 1966 independently and almost simultaneously by Wilzbach and Kaplan [9] at Argonne, and by Bryce-Smith, Gilbert and Orger [10] at Reading. The *para* mode was the last to be discovered fifteen years later, again by Wilzbach and Kaplan [11]. Subsequently, considerable effort has been invested in an attempt to understand and further develop benzene photocycloadditions. This has resulted in some very spectacular results, among which is the application of the *meta* photocycloaddition in the total synthesis of natural products, particularly by Wender [12]. The field has been reviewed on several occasions mainly by Cornelisse [13], Mattay [14,15], Wender [16], Hoffmann [17] and de Keukeleire [18] with a focus on the *meta* mode.

Excited-states involved

Photocycloadditions of arenes with alkenes are usually triggered by the photoexcitation of the arene moiety. If the first excited singlet state of benzene is involved ($^1B_{2u}$, excited at 254 nm in a electric dipole forbidden transition, ε = 20.4), only the *meta* mode is allowed to occur in a concerted fashion according to molecular orbital symmetry rules [19,20]. Concerted *ortho* and *para* photocycloadditions of olefins are forbidden to occur from the first excited-state, but they are formally allowed from the second excited-state of benzene ($^1B_{1u}$). The fact that *ortho* and *para* cycloadducts are nevertheless observed to be formed can be explained if charge transfer processes are invoked, if reaction occurs in a non-concerted fashion (where the Woodward–Hoffmann rules do not apply), or from the second singlet excited-state. However, more recent computational work using a VB description of the structures has shown that such cycloadditions can take place from the S_1 excited-state without barrier through a conical intersection, which is common to all three cycloadducts [21], at least for the benzene/ethylene system.

Quenching and sensitizing experiments were carried out to elucidate the spin state of the excited species involved. Mattay has shown that the quantum yield of the photocycloaddition of

1,3-dioxoles with benzene is halved for all three occurring modes (*ortho*, *meta* and *para*) if the reaction is carried out under an atmosphere of xenon rather than argon [22]. Xenon accelerates the singlet–triplet intersystem crossing by the heavy-atom effect, and thus decreases the singlet excited-state lifetime of the arene. Mattay considered this as direct proof that the addition of benzene to 1,3-dioxoles takes place primarily via the singlet excited-state of benzene. Ferree et al. had earlier provided evidence that the *meta* photocycloaddition occurs from the singlet excited-state; they observed that 6-phenyl-2-hexene undergoes cis–trans isomerization upon sensitizing with acetone and benzophenone, whereas the photocycloaddition to the *meta* product could only be triggered via direct irradiation [23].

Mode selectivity

Photocycloadditions are usually atom-economical, meaning that all atoms of the starting material end up in the final compound. Furthermore, photocycloadditions of alkenes with arenes are "step-economical", as the complexity can be increased considerably in a single step. With these unprecedented possibilities to efficiently create diverse molecules with high complexity, synthetic applications should abound. One should, however, keep in mind, as Wender wrote some years ago, that*: "Any reaction with the potential to produce a highly complex product also has the potential to provide a highly complex product mixture, if its selectivity is not controlled"* [12]. Control of mode-, regio- and stereoselectivity is absolutely crucial if one aims at obtaining defined photocycloadducts in relevant yields.

The mode selectivity is predicted by the electronic properties of the two reaction partners involved. The (simplified) Weller equation determines whether or not electron transfer will occur from an excited-state (Equation 1) [24,25]. For the reaction of an excited aromatic moiety with an alkene, this means that if the change in free energy, determined by the Weller equation, is negative.

$$\Delta G^{\mathrm{ET}} = E^{\mathrm{ox}}_{\frac{1}{2}}(\mathrm{D}) - E^{\mathrm{red}}_{\frac{1}{2}}(\mathrm{A}) - \Delta E_{\mathrm{excit}} + \Delta E_{\mathrm{coul}} \qquad (1)$$

with ΔG^{ET} = free enthalpy of the radical ion pair formation, $\Delta E_{\mathrm{excit}}$ = excitation energy of the chromophore, ΔE_{coul} = coulomb interaction energy of the radical ions and $E^{\mathrm{ox\ or\ red}}_{\frac{1}{2}}$ = half wave potential of donor and acceptor.

If electron transfer pathways dominate, substitution reactions are found to prevail. However, if the electron transfer is endergonic, *ortho* photocycloaddition can be observed. Mattay also observed that when ΔG^{ET} rises above 1.5 eV, *meta* photocycloadditions prevail (Scheme 3) [24].

However, these limits are not very sharp and a lack of mode selectivity may be observed in borderline regions (Scheme 4) [26]. These findings are consistent with the proposal that *ortho* photocycloadditions are the major reaction pathway when a certain degree of charge transfer is involved.

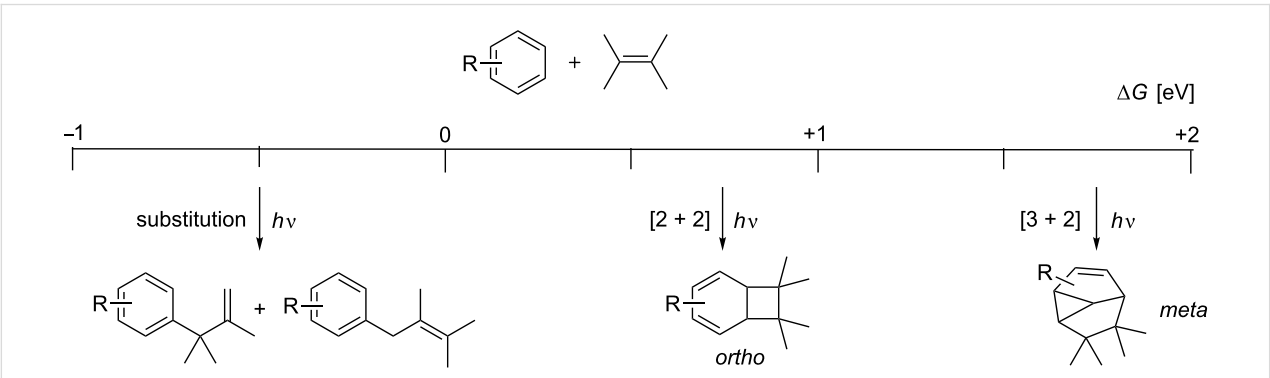

Scheme 3: Mode selectivity with respect of the free enthalpy of the radical ion pair formation.

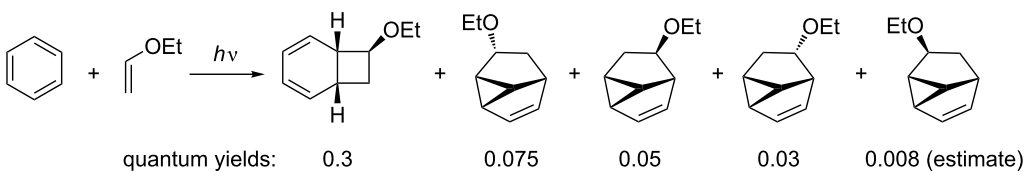

Scheme 4: Photocycloaddition shows lack of mode selectivity.

Meta photocycloadditions

Mechanism

The *meta* photocycloaddition reaction was extensively reviewed in 1993 by Cornelisse [13], who gave also a summary of mechanistic suggestions and debates up to that date. The now commonly accepted mechanism of this reaction involves the excitation of the benzene moiety to its first excited-state ($^1B_{2u}$) and subsequent formation of an exciplex with the alkene moiety (Scheme 5).

The occurrence of such exciplexes has been detected by emission spectroscopy [22,27]. The two new sigma C–C bonds are formed concertedly from the exciplex. The reaction is thought to proceed through a slightly polarized intermediate, which explains the observed regioselectivity when the arene is disymmetrically substituted. While the bridging carbon atom is slightly positively charged, the termini of the allylic moiety carry a partial negative charge. It was shown that the formation of the sigma bonds is the rate determining step, as isotope effects were only observed when the addition occurred directly at the deuterium-substituted site [28]. On the other hand, it was also proposed that a biradical intermediate is involved in this photocycloaddition mechanism. Nevertheless, all attempts to trap a biradical or a zwitterionic intermediate have so far been unsuccessful. A very clever plan to test whether a biradical intermediate is indeed involved was carried out by Reedich and Sheridan [29]: By incorporating a diazo group into the last formed bond of the cyclopropyl ring in the *meta* photocycloadduct [30], they would be able to see whether the biradical formed by the extrusion of nitrogen gave the same products as the *meta* photocycloaddition (Scheme 6).

This was indeed the case, as very similar ratios of the two distinct stereoisomers **C** and **D** were found to be formed from the diazo compounds **A** and **B** as well as from the photocycloaddition of *o*-xylene to cyclopentadiene. This finding seems to indicate that a biradical structure is indeed involved in the *meta* photocycloaddition pathway; however, whether this biradical is an intermediate with a well-defined half-life or whether it is only just a transitory species remains so far unclear [31].

Regioselectivity

The *meta* photocycloaddition reaction creates a compound containing up to six new stereocenters in a single step from planar achiral starting materials. If substituents are added to the arene and the complexity of the olefin is increased, a great

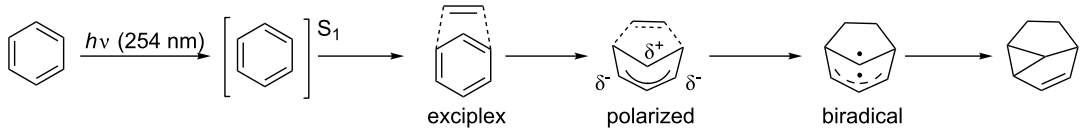

Scheme 5: Mechanism of the *meta* photocycloaddition.

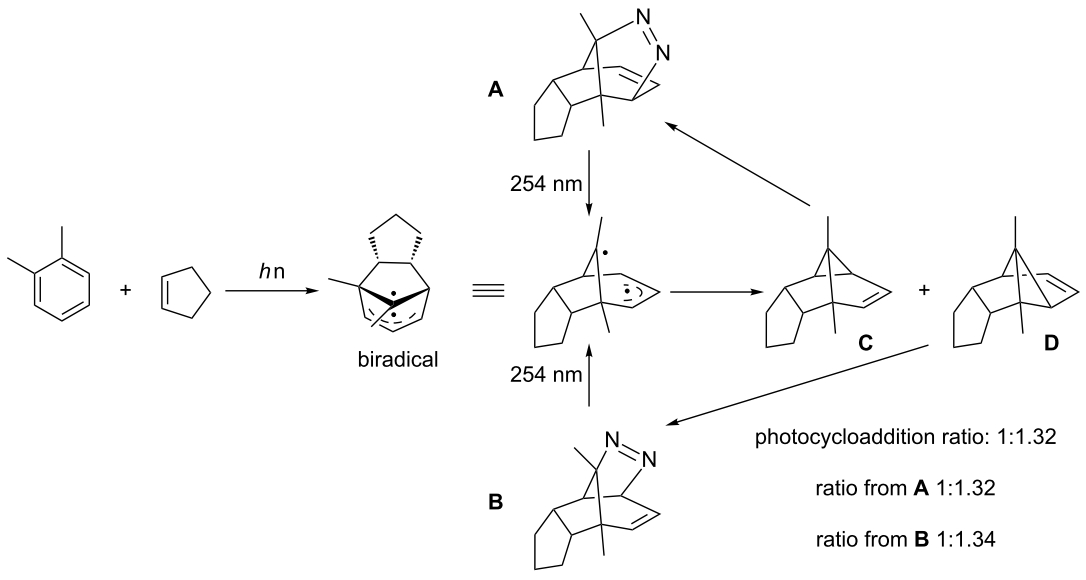

Scheme 6: Evidence of biradiacal involved in *meta* photocycloaddition by Reedich and Sheridan.

diversity of products can be created. However, not all of these products are accessible via such a photocycloaddition, as many possibilities can be ruled out due to the intrinsic selectivity of the reaction.

There are two distinct regioselectivities involved in the *meta* photocycloaddition. The first is with regard to the substitution pattern on the aromatic ring. The influence of electron donating and electron withdrawing substituents on the reactivity is mainly on the polarized intermediate shown in Scheme 5. While electron donating substituents are usually known to direct the addition towards the 2,6-mode, they therefore end up on the positively polarized one-carbon bridge, whilst electron withdrawing substituents trigger a 2,4-addition and end up at one of the negatively polarized carbon atoms on the three-membered bridge (Scheme 7) [13,18].

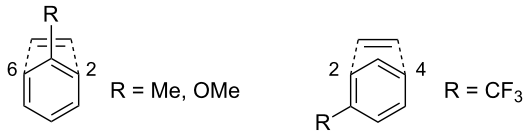

Scheme 7: Regioselectivity with electron withdrawing and electron donating substituents.

A second possibility to obtain different regioisomers occurs in the last step of the reaction. The recombination of the biradical may afford regioisomers when unsymmetrical olefins or additional substituents on the aromatic moiety are involved (Scheme 8).

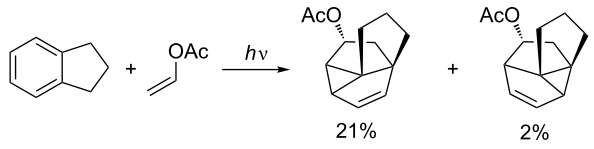

Scheme 8: Closure of cyclopropyl ring affords regioisomers.

However, *meta* photocycloadditions usually show a lack of regioselectivity at this stage of reaction, and thus mixtures of compounds are often isolated [32].

Stereoselectivity

If the olefin contains substituents, an issue of stereoselectivity is added to the regioselectivity. The addition can either occur from the *exo* or *endo* exciplex to the aromatic moiety (Scheme 9).

The observed preference for *endo* photocycloaddition [34-36] has been rationalized by secondary orbital overlap, which supports attack on the olefin from the *endo* position [37].

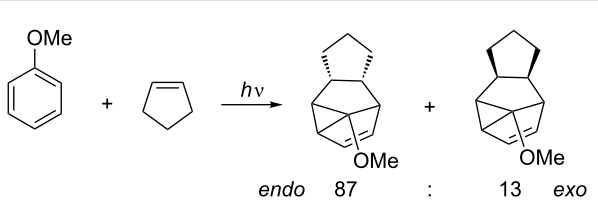

Scheme 9: *Endo* versus *exo* product in the photocycloaddition of pentene to anisole [33].

An excellent example for such intermolecular selectivity was published a few years ago by Piet et al. (Scheme 10) [38].

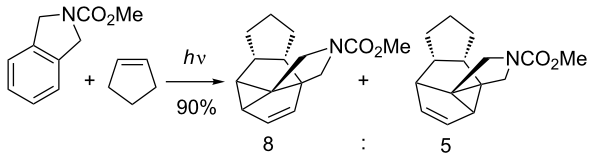

Scheme 10: Regio- and stereoselectivity in the photocycloaddition of cyclopentene with a protected isoindoline.

They observed a very selective *endo* 1,3-photocycloaddition across the substituent on the aromatic moiety in the reaction of cyclopentene with a protected isoindoline. This reaction has been reported to produce very high yields; however, the lack of regioselectivity in the biradical cyclopropane formation gives the two regioisomers in a ratio of 8:5.

Intramolecular reactions

The first intramolecular *meta* photocycloaddition was reported in 1969 by Morrison and Ferree [39]. The intramolecular reaction was shown to be very efficient when three atoms tethers were employed, but the quantum yield drops considerably when four atoms tethers are involved [40], apart from some exceptional cases when the freedom of the tether is restricted and a suitable conformation can be found [41]. The influence of the incorporation of oxygen in the tether has been reviewed by de Keukeleire [42].

The selectivities mentioned above may change in intramolecular reactions. In this mode, the *endo* approach of the alkene cannot be achieved without introducing significant strain, which usually outweighs secondary orbital interactions, and thus *exo* rather than *endo* adducts are obtained [40].

In the intramolecular mode, either 2,6- or 1,3-addition to the tether can be observed (Scheme 11) [43].

1,3-Addition is usually observed selectively when electron donating groups are attached to the aromatic moiety *ortho* to the

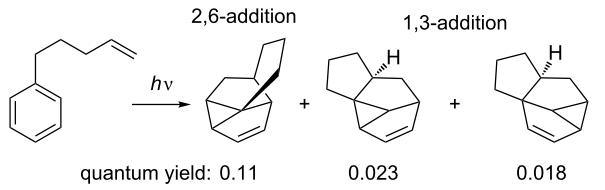

Scheme 11: 2,6- and 1,3-addition in intramolecular approach.

tether or if the olefin contains additional cis substituents; this is due to repulsion of the substituents on the olefin with the hydrogen atoms of the tether in the *exo*-addition which prevents the 2,6-addition mode. Intramolecular *meta* photocycloadditions that occur at positions 1,3 relative to the tether may give either a linear or an angular isomer (Scheme 12) [44].

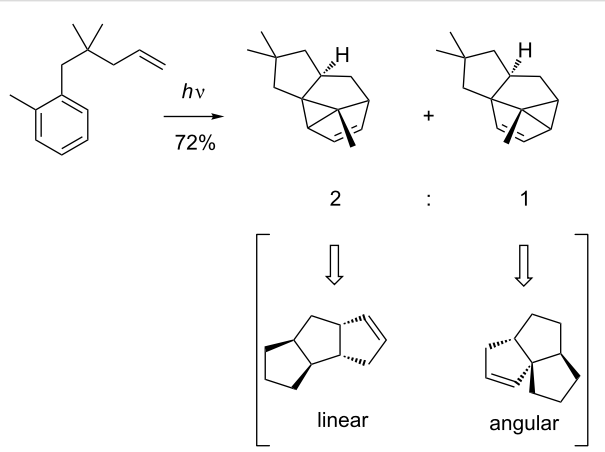

Scheme 12: Linear and angularly fused isomers can be obtained upon intramolecular 1,3-addition.

Calculations of the relative stabilities are a useful tool to predict the selectivity. If no additional substituents are present, the linear compounds are slightly more stable [40]. However, some examples show that this selectivity can be changed [45]. The linear and angular isomer names are derived from the opening of the cyclopropane ring to afford linearly and angularly fused triquinanes.

Asymmetric *meta* photocycloadditions

The *meta* photocycloaddition has the potential to convert planar (thus achiral) molecules into three-dimensional chiral molecules. It is therefore not surprising that many attempts have been made to render this process enantioselective. The main strategy in this perspective is the introduction of a chiral center directly on the tether in an intramolecular photocycloaddition, and to carry out the reaction in a diastereoselective way. The best known example of this approach was implemented in the total synthesis of (±)-α-cedrene published by Wender et al. in 1981 (Scheme 13) [46].

Following this very elegant and highly efficient synthesis, the *meta* photocycloaddition attracted much interest in the field of total synthesis of natural products. In addition, studies aimed at understanding and predicting the diastereoselectivity of this photocycloaddition were undertaken. For example, the group of Sugimura has shown that chiral 2,4-pentanediol tethers are very efficient for face recognition (Scheme 14) [47,48].

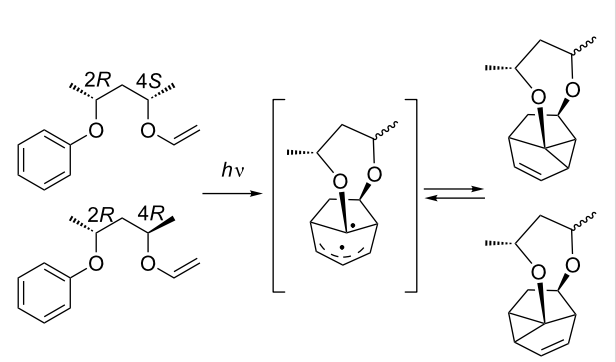

Scheme 14: Asymmetric *meta* photocycloaddition introduced by chirality of tether at position 2.

The chirality at the position 2 of the tether completely directs the diastereoselectivity. Compounds having a 2*R* configuration react uniquely at the *si* face of the vinyl group, leading to the *R* configuration at the newly formed stereocenter. However, the reaction lacks regioselectivity in the formation of the cyclopropane ring, and both regioisomers are obtained. A similar ap-

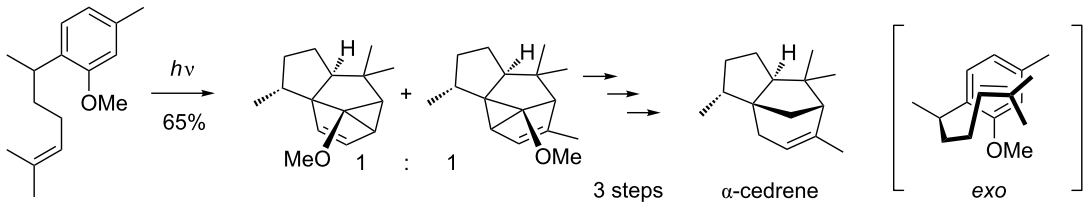

Scheme 13: Synthesis of α-cedrene via diastereoselective *meta* photocycloaddition.

proach has been published by Morales et al. who observed diastereoselectivity by the introduction of a chiral center α to the aromatic moiety on the tether [49]. Some diastereoselective approaches where the chiral induction is at position 3 of the tether have also been reported [50,51]. The diastereoselectivity observed is then due to steric interactions [51].

A completely different approach to an asymmetric *meta* photocycloaddition was made by Van der Eycken. He showed that *meta* photocycloaddition carried out in an chiral cavity (β-cyclodextrin) affords the photocycloaddition product in 17% ee (Scheme 15) [52].

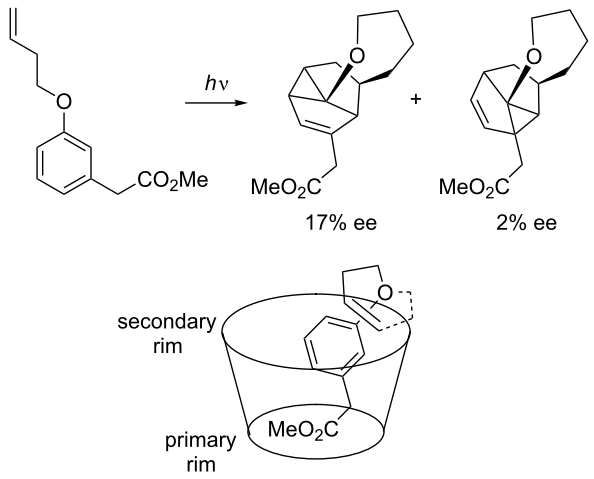

Scheme 15: Enantioselective *meta* photocycloaddition in β-cyclodextrin cavity.

Further diversification

Meta photocycloaddition can be considered as very regio- and stereoselective if the appropriate substituents are chosen. The only reaction step notoriously lacking regioselectivity is the closing of the cyclopropane ring. Therefore, in many examples, the isolation of the two regioisomers of the *meta* photocycloaddition is described. However, a possibility to interconvert one compound into the other by thermal [53] as well as photochemical [47,54] means was found (Scheme 16).

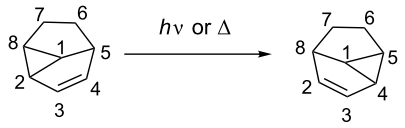

Scheme 16: Vinylcyclopropane–cyclopentene rearrangement.

The numerous applications of *meta* photocycloaddition in total syntheses show that this reaction can be a very efficient tool to access polycyclic natural compounds. However, the cores directly obtained are usually not useful as such, and cleavage of the cyclopropyl ring must be carried out to access naturally occurring polycyclic systems. Many investigations have already been achieved by different research groups to diversify the molecules accessible by this synthetic route: The cyclopropyl ring of the *meta* product is opened to give either bicyclo[3.3.0]octane or bicyclo[3.2.1]octane derivatives (Scheme 17).

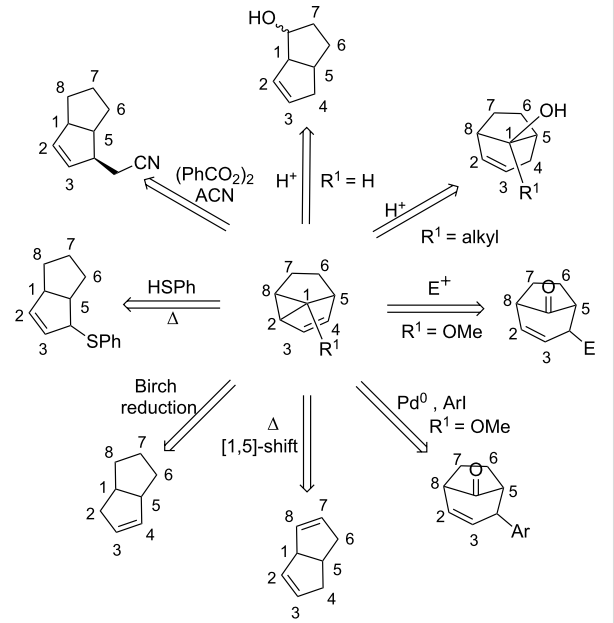

Scheme 17: Further diversification possibilities of the *meta* photocycloaddition product.

Acidolysis of *meta* photocycloaddition compounds has been studied by Gilbert [55]. He observed that the cyclopropane ring opens upon protonation of the double bond. If the *meta* photocycloaddition product contains a substituent at position 1, ring opening affords bicyclo[3.2.1]octane derivatives, whilst if no substituent is present at position 1, a hexahydropentalene is the preferred product of ring opening. Other electrophiles also have the tendency to add to the double bond. Wender has shown in his total synthesis of (±)-α-cedrene, that bromine readily adds and triggers the opening of the cyclopropane ring [46]. Rearrangement of the resulting allylic bromide to the more stable regioisomer at this stage occurs readily and debromination can be achieved on treatment with tributyltin hydride. Penkett has shown that 3-chloroperbenzoic acid (*m*-CPBA) can take the role of an electrophile in the epoxidation of the double bond [56] and also demonstrated that the *meta* photocycloaddition products containing a methoxy group at position 1 can be converted in a Heck-type reaction [57,58]. The intermediate palladium σ-complex, formed by insertion, opens the cyclopropane ring and arylated bicyclo[3.2.1]octane derivatives are

obtained. Thermolysis of the *meta* photocycloaddition product results in [1,5]-sigmatropic shifts. The shift can either be a shift of a hydrogen [54] or a carbon [59] atom to afford tetrahydropentalenes.

There are also radical approaches to the opening of the cyclopropyl ring. Under Birch reaction conditions, the cyclopropane ring can be reduced to the hexahydropentalene [45,60,61]. Radicals can also add to the double bond and induce the opening of the cyclopropane ring; for example, thiophenoxy radicals have been found to be very efficient for such reactions [44,62,63]. Another possibility to react radicals with *meta* photocycloadducts was demonstrated by Wender et al., who showed that acetonitrile radicals can be added to the olefin and open the cyclopropane ring to yield a hexahydropentalene [64].

Application in total synthesis

There are several reviews that describe a large number of applications of the *meta* photocycloaddition to the total synthesis of complex polycyclic molecules. A recent publication by Chappell and Russell discusses comprehensively and in detail many examples from α-cedrene and the following 25 years [40]. We will therefore focus on the most recent examples of total synthesis applications.

Several times, Fenestranes have been the targets of total synthesis by *meta* photocycloaddition reactions [65]. Penkett, described very recently an access to fenestranes in a single step (not counting the one-step preparation of the substrate) [66].

The reaction could also be carried out in a two step sequence. He observed that the starting material undergoes a selective 1,3-addition to one of the tethers. The subsequent cyclopropane ring closure gives mainly the linear fused *meta* product in 23% yield. The *meta* compounds and two rearranged *ortho* products were isolated from the reaction mixture in a combined yield of 60%. The major *meta* product can be converted into the fenestrane by further irradiation (Scheme 18). This second [3 + 2] addition reaction can be accelerated by the addition of sensitizers and could be quenched with piperylene. The proposed mechanism involves a homolytic cleavage of the cyclopropane ring to afford the linear triquinane biradical, which undergoes addition to the double bond. Wender achieved the total synthesis of fenestranes from *meta* photocycloaddition products some years earlier by cyclization using radicals in acetonitrile under reflux [67].

Another very recent application of the *meta* photocycloaddition has been published by Gaich and Mulzer [68]. They achieved the total synthesis of Penifulvin B and C in five steps after *meta* photocycloaddition (Scheme 19).

This first enantioselective total synthesis of the naturally occurring [5.5.5.6]fenestranes is highly efficient. The photocycloaddition occurs by an intramolecular 1,3-*exo* attack of the olefin to the aromatic moiety. The cyclopropane ring closure is, in this case, not regioselective at all, and leads to a 1:1 mixture of products. However, the undesired photocycloadduct can be converted to the desired compound via a thermal vinylcyclopropane–cyclopentene rearrangement. All obtained photocycloaddition compounds can be converted into the target by this means. The cyclopropane ring was opened by a Birch-type reduction. Oxidation of the primary alcohol and ozonolysis of the double bond afforded the hemiacetal after spontaneous cyclization. Subsequent oxidation and deprotection afforded the desired compound. In the same paper, the total synthesis of the naturally occurring epimer of Penifulvin B (Penifulvin C) was described, which was achieved by replacing the *trans*-olefin by the *cis*-olefin and following the same sequence of steps. One year earlier the same group accomplished the total synthesis of Penifulvin A via a *meta* photocycloaddition [69].

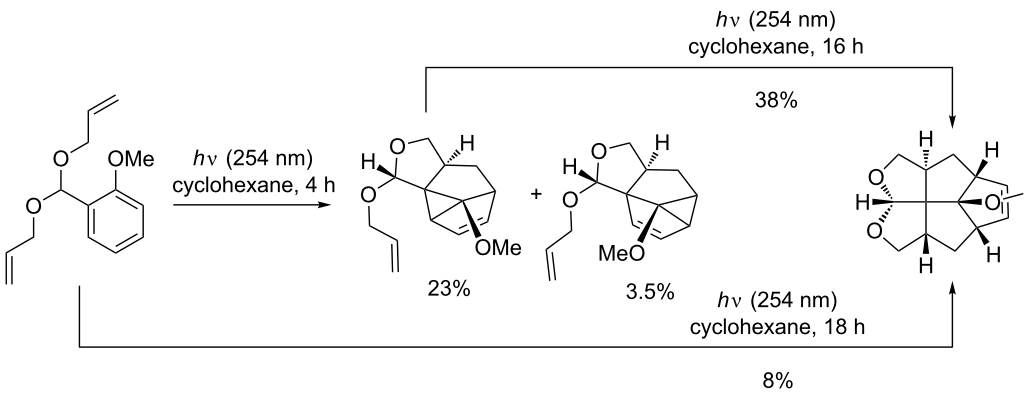

Scheme 18: Double [3 + 2] photocycloaddition reaction affording fenestrane.

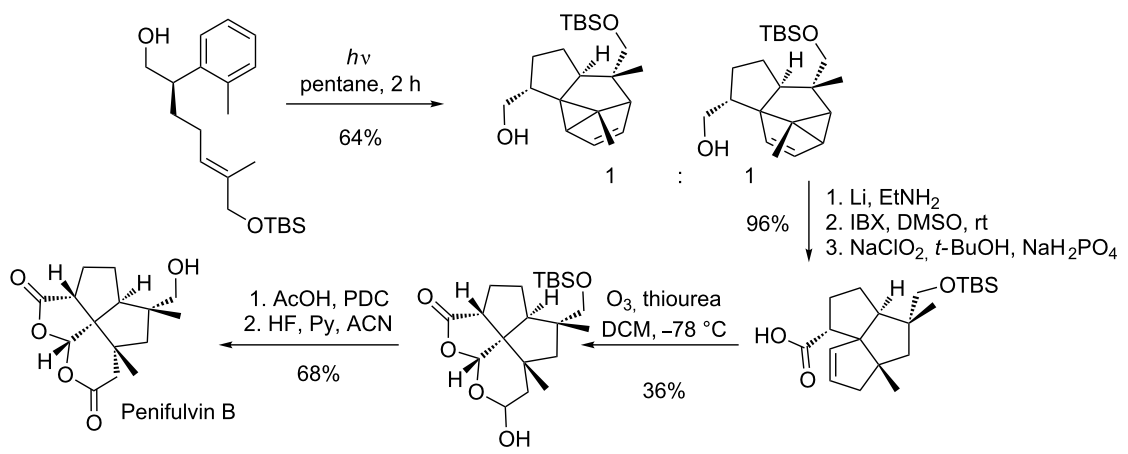

Scheme 19: Total synthesis of Penifulvin B.

Not only fenestranes are accessible from the *meta* photocycloaddition products. Wang and Chen have recently published an approach towards the core of Lancifodilactone F [70]. This triterpenoid contains three fused and one spiro cycle and is a very challenging target. Initial attempts to construct the fused seven-, six- and five-membered core were unsuccessful. Introduction of a trimethylsiloxy group on the tether and an oxygen substituent on the aromatic ring were crucial for the photocycloaddition to proceed in good yield (Scheme 20).

The additional tetrahydrofuran cycle helps to constrain the four unit tether. Only with these additional features does the cycloaddition step occur with a remarkable yield of 89%. The photocycloaddition occurs selectively 1,3-*exo* to the tether. The stereochemistry on the trimethylsiloxy substituent was shown to have no influence on the photochemistry, but it helped to direct the olefin group towards the arene moiety. The linear and angular fused compounds were elaborated to give a common intermediate containing the fused five-, six- and seven-membered ring pattern without further purification.

Ortho photocycloaddition

There is little data on the selectivity of the *ortho* photocycloaddition in the literature. However, Mattay discovered that the regioselectivity of the *ortho* photocycloaddition is dependent on the electronic properties of the two reaction partners [14]. He reported that 1,2-addition usually prevails when a high degree of charge transfer is involved in the exciplex (ΔG^{ET} below 0.5 eV). A substituent at position 1 stabilizes the charge which develops on the aromatic ring, and therefore favors the 1,2-ring closure of the intermediate (Scheme 21).

This selectivity is not very high and as the degree of charge transfer decreases, the selectivity decreases. The role of CT is

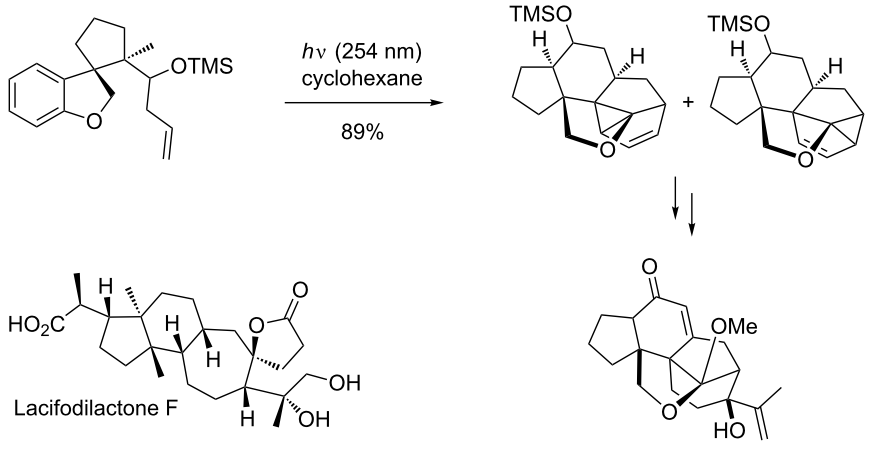

Scheme 20: Towards the total synthesis of Lacifodilactone F.

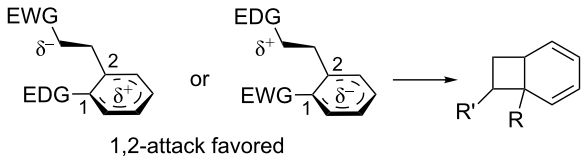

Scheme 21: Regioselectivity of *ortho* photocycloaddition in polarized intermediates.

also supported by the fact that regioselectivity is usually higher in polar solvents where charge separation is favored [71,72]. Substituted olefins may add in an *exo* or *endo* fashion. While electron-deficient alkenes give mixtures of both possible products, electron-rich compounds show stereoselectivity towards the *exo* products (Scheme 22) [73].

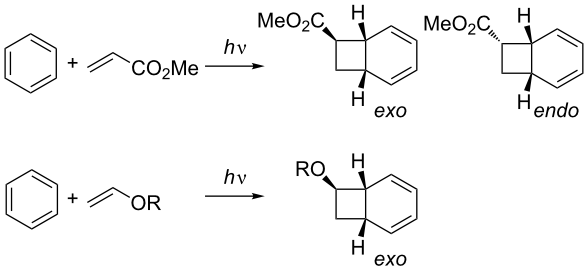

Scheme 22: *Exo* and *endo* selectivity in *ortho* photocycloaddition.

Ortho photocycloaddition can, however, also take place from the triplet excited-state by sensitization. The triplet excited-state is believed to have a higher biradical and less zwitterionic character [73]. *Ortho* photocycloaddition of triplet excited benzenes have been extensively studied by Wagner and his group. They investigated [2 + 2] photocycloadditions of alkanophenones, which occur from the triplet excited-state and via 1,4-biradicals [74-77]. The occurrence of such radicals has been proven by the insertion of a cyclopropyl radical trap in the olefin. Upon irradiation of this modified starting material, the *ortho* cycloadduct could no longer be isolated (Scheme 23) [78].

Naphthalenes are known to undergo preferably *ortho* photocycloadditions (Scheme 24), whilst higher arenes usually react with olefins in an [2 + 2], [4 + 2] or [4 + 4] cycloaddition mode.

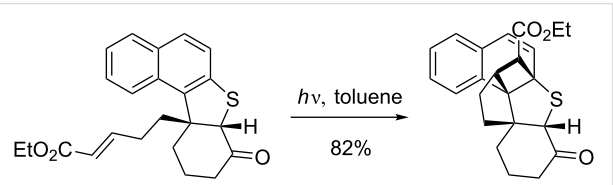

Scheme 24: Photocycloadditions to naphtalenes usually in an [2 + 2] mode [79].

The *ortho* photocycloaddition gives access to bicyclo-[4.2.0]octanes which usually undergo thermal electrocyclic ring opening to yield eight-membered ring systems (Scheme 25) [73,80].

Another possibility to further transform the intermediates are Diels–Alder cycloadditions of the dienes formed by the *ortho* photocycloaddition [81]. Furthermore, Scharf demonstrated that he could trigger a photochemical rearrangement to produce a *para* photocycloaddition product upon sensitization [82]. However, there also exists some examples where the [2 + 2] cycloadduct is stable enough to be isolated as such, and in good yield (Scheme 26) [83,84].

Ortho photocycloaddition is almost exclusively observed with alkynes. The photocycloaddition products usually undergo ring opening to cyclooctatetraenes [85] or to other rearrangement products [86] (Scheme 27).

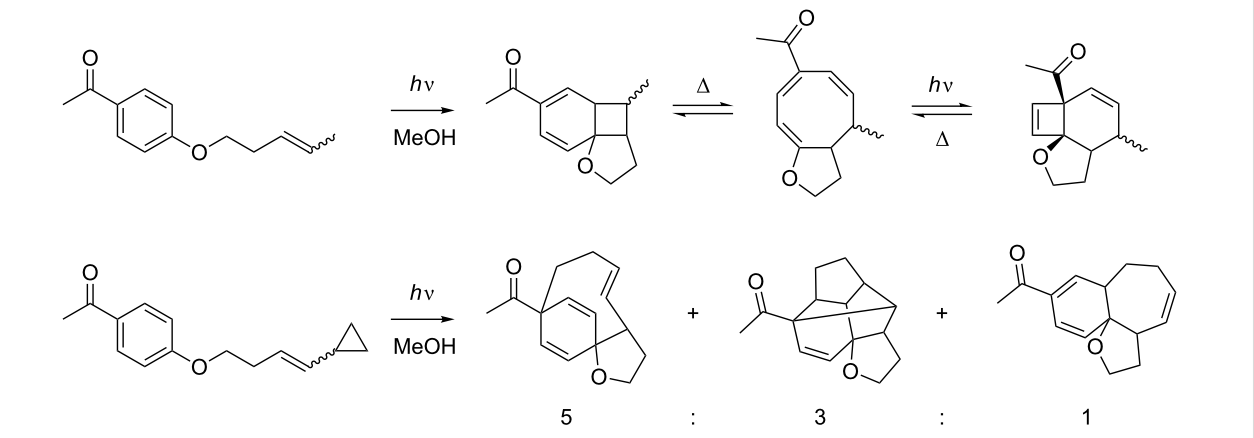

Scheme 23: *Ortho* photocycloaddition of alkanophenones.

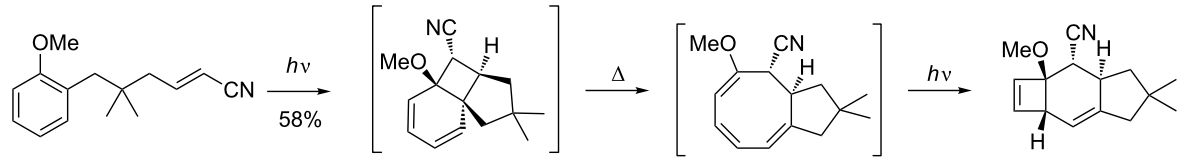

Scheme 25: *Ortho* photocycloaddition followed by rearrangements.

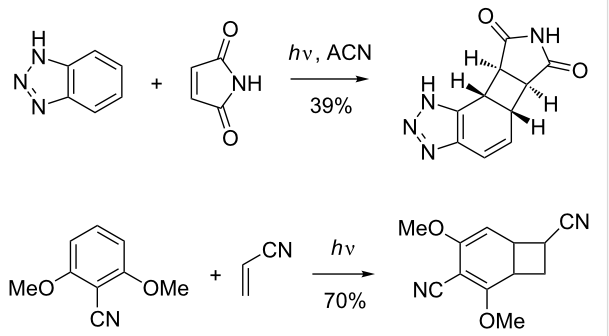

Scheme 26: Stable [2 + 2] photocycloadducts.

Ortho photocycloadducts are known to be very unstable as such. However, if they have the possibility to stabilize by rearrangement, products can be isolated often in high yield. A very good example of this was published by Kalena et al. some years ago [87] who observed that 2-alkenyl-7-hydroxy-4-chromanone could undergo *ortho* photocycloaddition to afford the tetracyclic compounds shown in Scheme 28.

The initial enol tautomerizes to the α,β-unsaturated ketone, which can be isolated in moderate yield. Anisole photocycloaddition precursors did not afford similar tetracyclic compounds under the same irradiation conditions. However, under slightly acidic conditions (chlorinated solvents or additional *p*-toluenesulfonic acid) the photocycloaddition to the same compound could be restored.

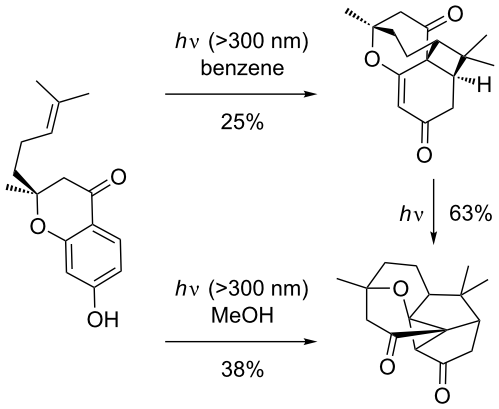

Scheme 28: Intramolecular *ortho* photocycloaddition and rearrangement thereof.

Some years later, the same group reported that irradiation of the same starting material in methanol instead of benzene afforded the compound apparently formed by *meta* photocycloaddition [88]. However this *meta* photocycloaddition product has some issues. Addition occurs 2,6 across an electron-withdrawing substituent; this is unfavorable in a direct [1,3]-addition (due to the polarization in the polarized intermediate; see the chapter on "*Meta* photocycloadditions"). Furthermore, Kalena et al. could show that the compound is also formed upon irradiation of the *ortho* photocycloadditon product under slightly different irradiation conditions.

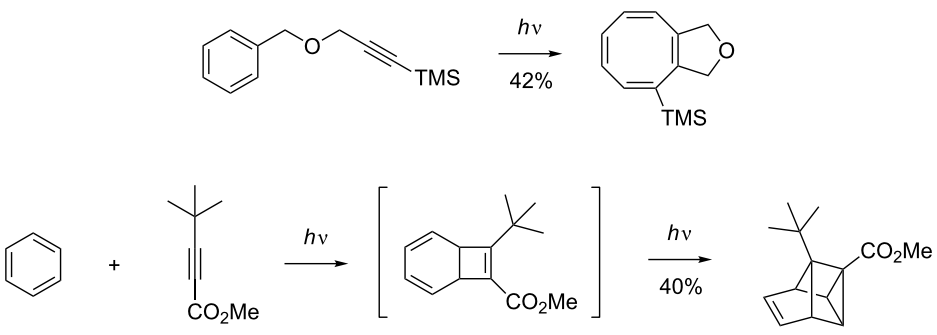

Scheme 27: *Ortho* photocycloadditions with alkynes.

A very unconventional [2 + 2] photocycloaddition to afford caged polycyclic structures has been recently described (Scheme 29) [89,90].

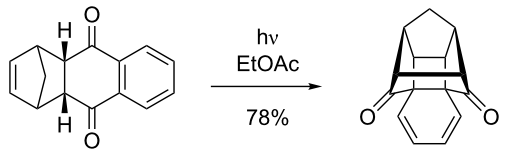

Scheme 29: Intramolecular *ortho* photocycloaddition to access propellanes.

By attaching the double bond very close to the aromatic moiety, the photocycloaddition leads to the desired cage compound in high yield. Surprisingly, the compound is fairly stable and can be recrystallized from hexane.

Para photocycloaddition

Para photocycloaddition giving access to bicyclo[2.2.2]octadiene systems by a formal Diels–Alder type reaction is very rare, and little is known about this mode. It is known that higher aromatics are more likely to undergo *para* cycloadditions [91], and that it is the main mode when allenes are involved [92]. A high yielding example of a *para* photocycloaddition with an allene has been published by Haddaway et al. (Scheme 30) [93].

If the irradiation is carried out in the presence of conjugated dienes or a second arene (usually higher aromatics), this photocycloaddition can also be carried out in a [4 + 4] mode to afford bicyclo[4.2.2]decatrienes and more complex homocycles [91,94,95].

In the non-sensitized irradiation of dianthryls, the [4 + 4] photocycloaddition [91] pathway is usually observed; upon sensitizing in the triplet excited-state, the [4 + 2] mode prevails (Scheme 31). Such [4 + 4] photocycloadditions have also been observed intermolecularly with very high yields [96].

There are few examples leading to *para* products in high yield. However, one example is the intramolecular photocycloaddition of a cinnamoylamide and a benzamide moiety (Scheme 32) [97]. This reaction is very efficient and leads to high yields of the bicyclo[2.2.2]octadiene derivative.

In this example, the cinnamoylamide is sensitized by benzil to its triplet excited-state. The proposed mechanism involves the reaction of the olefin with the ipso position of the aromatic ring affording a spiro biradical intermediate. Recombination of these radicals proceeds further until formation of the final compound. Some years later, Kohmoto showed that similar enamides linked to a naphthyl moiety underwent preferably *ortho* photocycloaddition if the naphthyl moiety is sensitized [98].

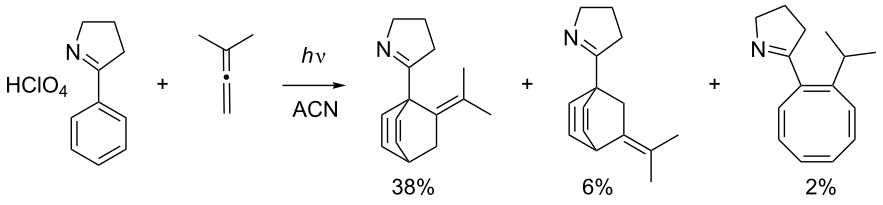

Scheme 30: *Para* photocycloaddition with allene.

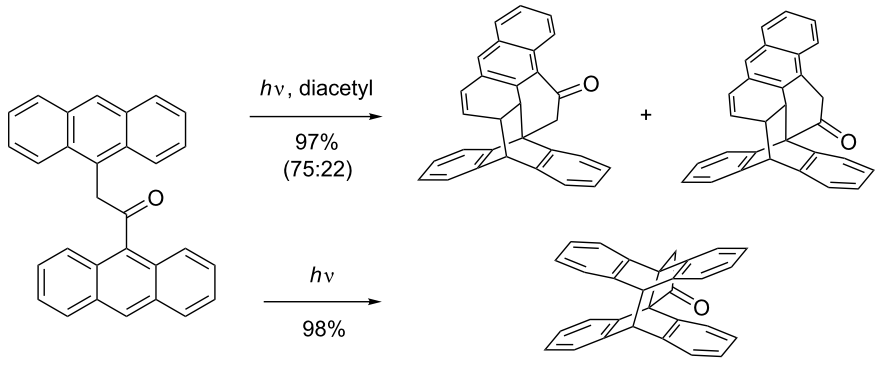

Scheme 31: Photocycloadditions of dianthryls.

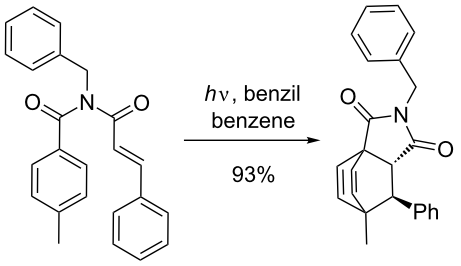

Scheme 32: Photocycloaddition of enone with benzene.

Irradiation of a naphthyl precursor containing only a two atom tether to the olefin afforded the *para* photocycloadduct (Scheme 33) [99].

However, Kalena et al. noted that the *para* product might also be derived from the *ortho* product upon further irradiation: The *para* product undergoes a sequence of ring opening/Michael addition of the solvent to give the final compound. However, neither the direct *ortho* nor the *para* product have been observed. The main changes from the previous papers of Kalena et al. were the replacement of the phenyl by a naphthyl group, and a two atom tether of the olefin. These two modifications are able to trigger different mode selectivity. As previously mentioned, the reaction with alkanophenones proceeds through a 1,4-biradical intermediate. The same reaction applied to this naphthyl derivative would lead initially to the formation of the four-membered ring. The five-membered ring will be preferred but the radical formed cannot recombine and fragments back to the starting material. Once the four-membered ring containing a primary exocyclic radical is formed, recombination either directly α to the carbonyl (construction of two fused cyclobutane ring systems) or delocalization of the radical to the *para* position can take place and the *para* product is formed.

Non-classical photocycloadditions of alkenes with arenes

Not only can the benzene moiety of arenes undergo cycloadditions upon exposure to light but, depending on the substitution pattern, other reactive sites may be involved. Carbonyl groups are also known to undergo different types of photochemistry. Thus, benzophenones, acetophenones and benzaldehydes are not only used as sensitizers but can, under specific circumstances, also be directly involved in photochemical reactions to form new structures.

Formation of benzoxepines

Sakamoto et al. reported that irradiation of *ortho* acylphenyl methacrylates can lead to photocycloaddition to afford benzoxepine structures in very high yield (Scheme 34) [100].

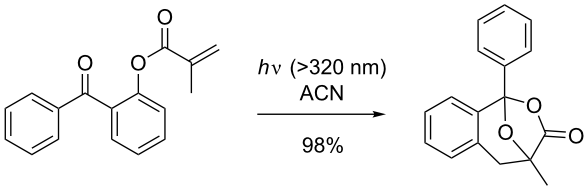

Scheme 34: Photocycloaddition described by Sakamoto et al.

This very unusual reaction involves the formation of a new aryl C–C bond and the loss of the aryl C–O bond, and is therefore clearly a rearrangement product. Furthermore, Sakamoto showed that this reaction was not limited to benzophenones, but also occurred with acetophenones, albeit in slightly lower yields. For this completely new reaction Sakamoto has proposed a mechanism involving a ζ-hydrogen abstraction to form a biradical intermediate (Scheme 35, **E**).

The resulting biradical cyclizes to form the spiro compound **F** upon recombination of the biradical. Re-aromatization affords the carboxylate **G**, which further attacks the carbonyl group. The alcohol intermediate **H** may cyclize by addition to the double bond to afford the final benzoxepine compound.

In the same year, a slightly different reaction was reported by Jones et al. [101] who triggered the formation of unusual photocycloaddition products by irradiation of *ortho* allyloxy-substituted anthraquinones (Scheme 36).

During their study on the photo-release of bioactive aldehydes, Jones et al. discovered that, under anaerobic conditions, the

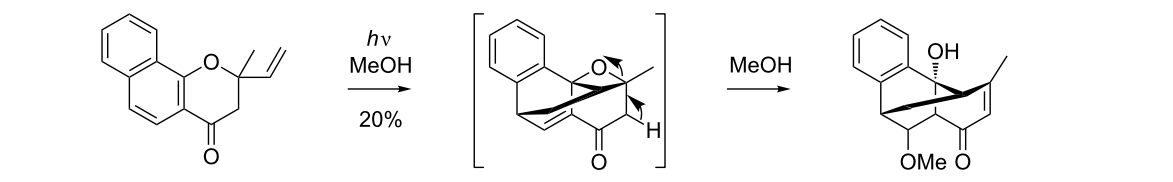

Scheme 33: Intramolecular photocycloaddition affording multicyclic compounds via [4 + 2].

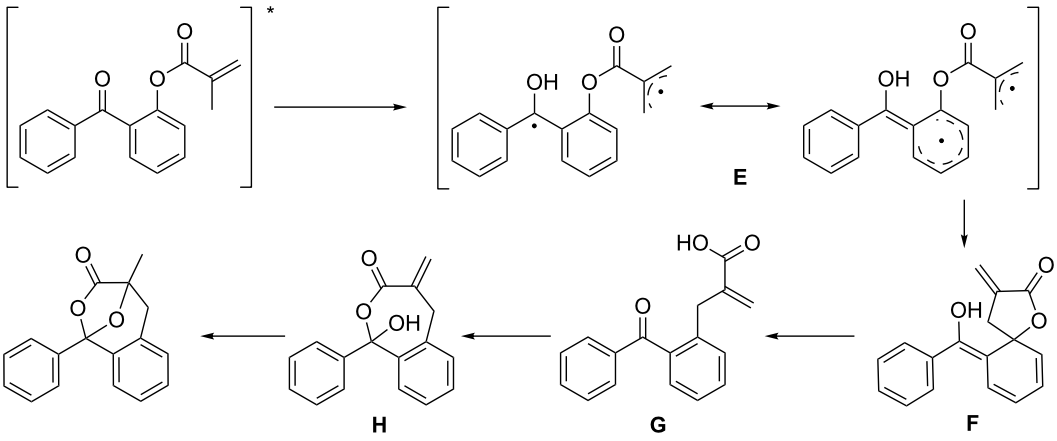

Scheme 35: Proposed mechanism by Sakamoto et al.

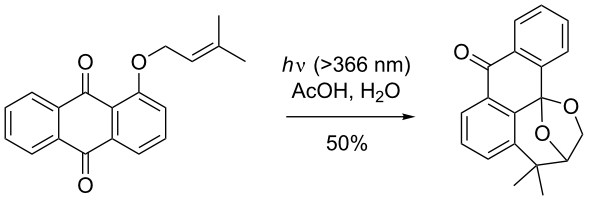

Scheme 36: Photocycloaddition described by Jones et al.

dihydroquinone intermediate loses water to form the zwitterionic structure (Scheme 37).

From this intermediate, cyclization can take place to form a spiro compound; further re-aromatization to form the enol, lactolization and cyclization explains the formation of the benzoxepine structure [101].

Griesbeck et al. reported the formation of benzoxepines from the benzophenone analogue upon irradiation at slightly lower

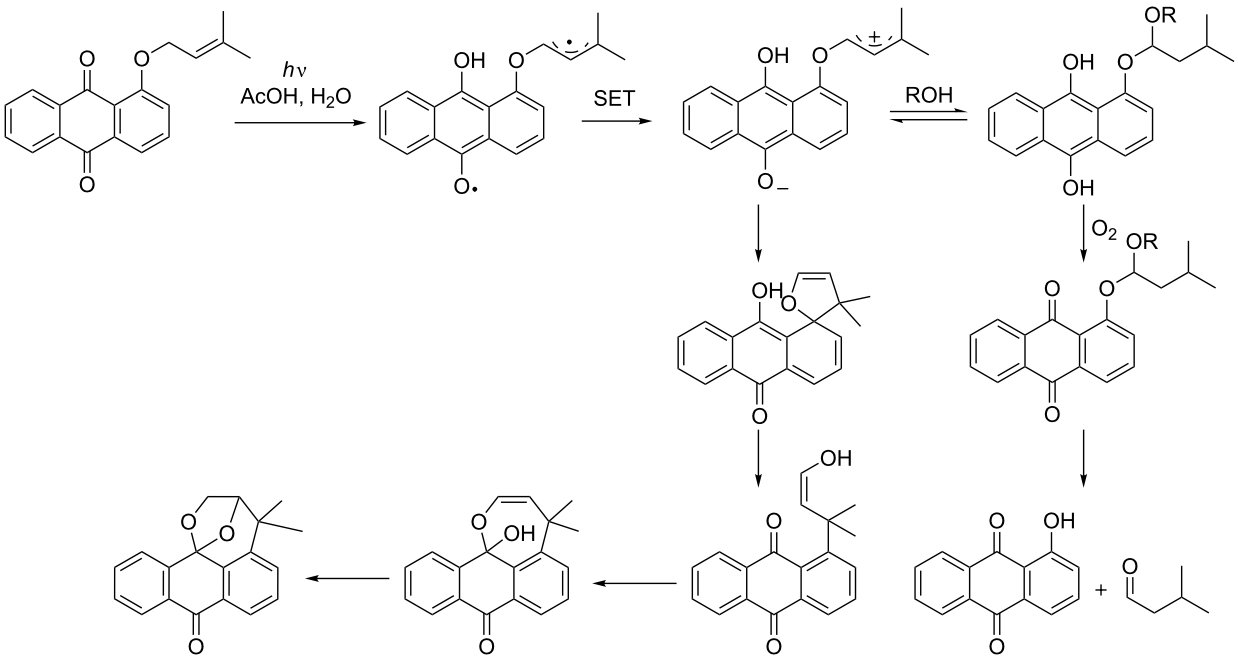

Scheme 37: Proposed mechanism for the formation of benzoxepine by Jones et al.

wavelengths [102]. The formation of the compound was observed in 50% yield, along with a diastereoisomeric mixture of dihydrobenzofurans in 40% yield (Scheme 38). Analogues of the dihydrobenzofuran formed upon irradiation of *ortho*-alkyloxyphenyl ketones have already been described in the literature and the reactions are known to take place via a δ-hydrogen abstraction by the ketone triplet, followed by cyclization of the 1,5-biradical intermediate [103].

Griesbeck et al. investigated the mechanism for this photocycloaddition, as he suggested that the mechanism proposed by Jones is unlikely, because the regiochemistry of proton catalyzed addition of alcohols to enols or enol ethers has the opposite regiochemistry to that observed in the product [102]. Furthermore, an electron transfer intermediate was ruled out, as the reaction is not thermodynamically feasible according to the Weller equation. Therefore, he proposed that the benzoxepine structure is achieved via a pseudo-Paternò–Büchi pathway (Scheme 39), while the dihydrobenzofurans arise from a Norrish-type II reaction and cyclization.

Griesbeck supports his proposed mechanism by flash laser photolysis, where a long lived (some seconds) intermediate with an UV absorption band at 380 nm was observed. This absorption band fits well with TD-DFT calculations. He proposes that re-aromatization of this intermediate takes place via a zwitterionic species or through a proton catalyzed pathway.

We recently found in our laboratories that the intramolecular photocycloaddition of allenylated salicylaldehydes affords a benzoxepine derivative and an apparent *para* photocycloadduct (Scheme 40) [104]. The product distribution is dependent on the substitution pattern of the aromatic core.

Introduction of bulky *tert*-butyl substituents at positions 3 and 5 on the aromatic ring yields up to 94% of the *para* photocycload-

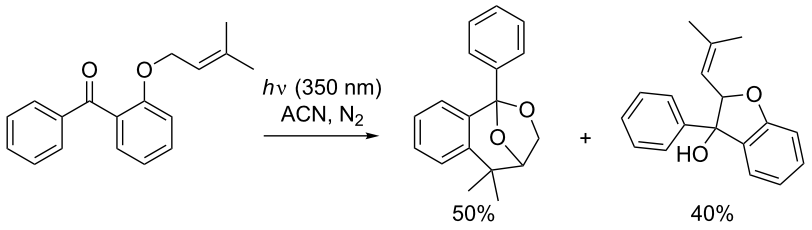

Scheme 38: Photocycloaddition observed by Griesbeck et al.

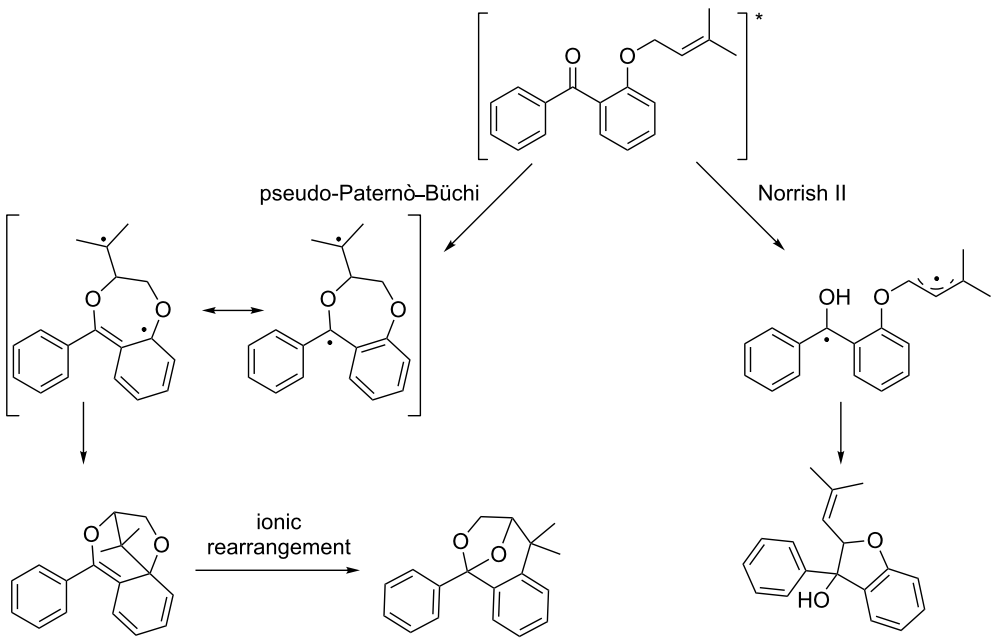

Scheme 39: Mechanism proposed by Griesbeck et al.

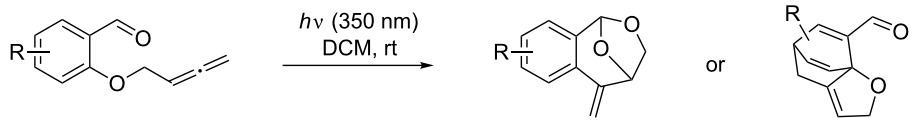

Scheme 40: Intramolecular photocycloaddition of allenes to benzaldehydes.

dition product, while other substituents gave yields of up to 44% of the benzoxepine compound. Pericyclic reaction mechanisms for these two photocycloadditions have been proposed, but no hard evidence has so far been obtained. The mechanism of this unprecedented reaction is currently under investigation in our laboratory.

Conclusion

In summary, we have described in this overview the applicability of the intriguing photocycloaddition of olefins with arenes. These reactions have been shown to afford compounds with a high increase in complexity in only one reaction step. We have discussed the diverse selectivities of the reaction, mechanisms as well as further modifications, and some of the most recent applications in total synthesis. Thus, while *meta* photocycloadditions have been exploited for over thirty years, *ortho* and, in particular, *para* photocycloadditions are uncommon and have consequently been less investigated. We have discussed these last two modes, which were exemplified by a few high yielding examples. Finally, we have reviewed the use and the reaction mechanism of the photocycloaddition of carbonyl substituted aromatics: Irradiation of *ortho* allyloxy, acrylic or allenyloxy substituted anthraquinones, benzophenones or benzaldehydes indeed give potentially interesting benzoxepines. There is little doubt that arene photochemistry will continue to help the synthetic chemist to assemble complex and challenging targets in the coming years.

References

1. Hoffmann, N. *Chem. Rev.* **2008,** *108,* 1052–1103. doi:10.1021/cr0680336
2. Wilzbach, K. E.; Ritscher, J. S.; Kaplan, L. *J. Am. Chem. Soc.* **1967,** *89,* 1031–1032. doi:10.1021/ja00980a053
3. Kaplan, L.; Willzbach, K. E. *J. Am. Chem. Soc.* **1968,** *90,* 3291–3292. doi:10.1021/ja01014a086
4. Van Tamelen, E. E.; Pappas, S. P. *J. Am. Chem. Soc.* **1962,** *84,* 3789–3791. doi:10.1021/ja00878a054
5. Van Tamelen, E. E.; Pappas, S. P. *J. Am. Chem. Soc.* **1963,** *85,* 3297–3298. doi:10.1021/ja00903a056
6. Harman, P. J.; Kent, J. E.; ODwyer, M. F.; Griffith, D. W. T. *J. Phys. Chem.* **1981,** *85,* 2731–2733. doi:10.1021/j150619a008
7. Angus, H. J.; Bryce-Smith, D. *Proc. Chem. Soc., London* **1959,** 326–327.
8. Ayer, D. E.; Bradfort, N. H.; Büchi, G. H. 1-Cyanobicyclo[4.2.0]octa-2,4-dienes and their synthesis. U.S. Patent 2,805,242, Sept 3, 1957.
9. Wilzbach, K. E.; Kaplan, L. *J. Am. Chem. Soc.* **1966,** *88,* 2066–2067. doi:10.1021/ja00961a052
10. Bryce-Smith, D.; Gilbert, A.; Orger, B. H. *Chem. Commun.* **1966,** 512–514. doi:10.1039/c19660000512
11. Wilzbach, K. E.; Kaplan, L. *J. Am. Chem. Soc.* **1971,** *93,* 2073–2074. doi:10.1021/ja00737a052
12. Wender, P. A.; Ternansky, R.; deLong, M.; Sigh, S.; Olivero, A.; Rice, K. *Pure Appl. Chem.* **1990,** *62,* 1597–1602. doi:10.1351/pac199062081597
13. Cornelisse, J. *Chem. Rev.* **1993,** *93,* 615–669. doi:10.1021/cr00018a002
14. Mattay, J. *J. Photochem.* **1987,** *37,* 167–183. doi:10.1016/0047-2670(87)85038-4
15. Mattay, J. *Angew. Chem., Int. Ed.* **2007,** *46,* 663–665. doi:10.1002/anie.200603337
16. Wender, P. A.; Dore, T. M. Intra- and Intermolecular Cycloadditions of Benzene Derivatives. In *CRC Handbook of Organic Photochemistry and Photobiology;* Horspool, W. M.; Song, P.-S., Eds.; CRC Press: Boca Raton, 1995; pp 280–290.
17. Hoffmann, N. *Synthesis* **2004,** 481–495. doi:10.1055/s-2004-815973
18. De Keukeleire, D.; He, S.-L. *Chem. Rev.* **1993,** *93,* 359–380. doi:10.1021/cr00017a017
19. Bryce-Smith, D. *J. Chem. Soc. D* **1969,** 806–808. doi:10.1039/C29690000806
20. van der Hart, J. A.; Mulder, J. J. C.; Cornelisse, J. *J. Photochem. Photobiol., A* **1995,** *86,* 141–148. doi:10.1016/1010-6030(94)03925-K
21. Clifford, S.; Bearpark, M. J.; Bernardi, F.; Olivucci, M.; Robb, M. A.; Smith, B. R. *J. Am. Chem. Soc.* **1996,** *118,* 7353–7360. doi:10.1021/ja961078b
22. Mattay, J.; Leismann, H.; Scharf, H.-D. *Mol. Photochem.* **1979,** *9,* 119–156.
23. Ferree, W., Jr.; Grutzner, J. B.; Morrison, H. *J. Am. Chem. Soc.* **1971,** *93,* 5502–5512. doi:10.1021/ja00750a033
24. Mattay, J. *Tetrahedron* **1985,** *41,* 2405–2417. doi:10.1016/S0040-4020(01)96636-0
25. Müller, F.; Mattay, J. *Chem. Rev.* **1993,** *93,* 99–117. doi:10.1021/cr00017a006
26. Gilbert, A.; Taylor, G. N.; Wahid bin Samsudin, M. *J. Chem. Soc., Perkin Trans. 1* **1980,** 869–876. doi:10.1039/p19800000869
27. Leismann, H.; Mattay, J.; Scharf, H.-D. *J. Am. Chem. Soc.* **1984,** *106,* 3985–3991. doi:10.1021/ja00326a016
28. De Vaal, P.; Lodder, G.; Cornelisse, J. *J. Phys. Org. Chem.* **1990,** *3,* 273–278. doi:10.1002/poc.610030411
29. Reedich, D. E.; Sheridan, R. S. *J. Am. Chem. Soc.* **1985,** *107,* 3360–3361. doi:10.1021/ja00297a059

30. Sheridan, R. S. *J. Am. Chem. Soc.* **1983,** *105,* 5140–5142. doi:10.1021/ja00353a052
31. Muller, P. *Pure Appl. Chem.* **1994,** *66,* 1077–1184. doi:10.1351/pac199466051077
32. Wender, P. A.; Dreyer, G. B. *J. Am. Chem. Soc.* **1982,** *104,* 5805–5807. doi:10.1021/ja00385a051
33. De Vaal, P.; Osselton, E. M.; Krijnen, E. S.; Lodder, G.; Cornelisse, R. *Recl. Trav. Chim. Pays-Bas* **1988,** *107,* 407–411. doi:10.1002/recl.19881070603
34. Ors, J. A.; Srinivasan, R. *J. Org. Chem.* **1977,** *42,* 1321–1327. doi:10.1021/jo00428a011
35. Merritt, V. Y.; Cornelisse, J.; Srinivasan, R. *J. Am. Chem. Soc.* **1973,** *95,* 8250–8255. doi:10.1021/ja00806a007
36. Mattay, J.; Rumbach, T.; Runsink, J. *J. Org. Chem.* **1990,** *55,* 5691–5696. doi:10.1021/jo00309a011
37. Houk, K. N. *Pure Appl. Chem.* **1982,** *54,* 1633–1650. doi:10.1351/pac198254091633
38. Piet, D.; De Bruijn, S.; Sum, J.; Lodder, G. *J. Heterocycl. Chem.* **2005,** *42,* 227–231. doi:10.1002/jhet.5570420208
39. Morrison, H.; Ferree, W. I. *J. Chem. Soc. D* **1969,** 268–269. doi:10.1039/C29690000268
40. Chappell, D.; Russell, A. T. *Org. Biomol. Chem.* **2006,** *4,* 4409–4430. doi:10.1039/B614011B
41. Boyd, J. W.; Greaves, N.; Kettle, J.; Russell, A. T.; Steed, J. W. *Angew. Chem., Int. Ed.* **2005,** *44,* 944–946. doi:10.1002/anie.200461661
42. De Keukeleire, D. *Aldrichimica Acta* **1994,** *27,* 59–69.
43. Gilbert, A.; Taylor, G. N. *J. Chem. Soc., Chem. Commun.* **1979,** 229–230. doi:10.1039/C39790000229
44. Baralotto, C.; Chanon, M.; Julliard, M. *J. Org. Chem.* **1996,** *61,* 3576–3577. doi:10.1021/jo960382k
45. Wender, P. A.; Von Geldern, T. W.; Levine, B. H. *J. Am. Chem. Soc.* **1988,** *110,* 4858–4860. doi:10.1021/ja00222a072
46. Wender, P. A.; Howbert, J. J. *J. Am. Chem. Soc.* **1981,** *103,* 688–690. doi:10.1021/ja00393a041
47. Sugimura, T.; Yamasaki, A.; Okuyama, T. *Tetrahedron: Asymmetry* **2005,** *16,* 675–683. doi:10.1016/j.tetasy.2004.11.086
48. Hagiya, K.; Yamasaki, A.; Okuyama, T.; Sugimura, T. *Tetrahedron: Asymmetry* **2004,** *15,* 1409–1417. doi:10.1016/j.tetasy.2004.03.017
49. Calderon Morales, R.; Lopez-Mosquera, A.; Roper, N.; Jenkins, P. R.; Fawcett, J.; García, M. D. *Photochem. Photobiol. Sci.* **2006,** *5,* 649–652. doi:10.1039/b602244h
50. Guo, X.-C.; Chen, Q.-Y. *J. Fluorine Chem.* **1999,** *97,* 149–156. doi:10.1016/S0022-1139(99)00042-1
51. Timmermans, J. L.; Wamelink, M. P.; Lodder, G.; Cornelisse, J. *Eur. J. Org. Chem.* **1999,** 463–470. doi:10.1002/(SICI)1099-0690(199902)1999:2<463::AID-EJOC463>3.0.CO;2-Z
52. Vízvárdi, K.; Desmet, K.; Luyten, I.; Sandra, P.; Hoornaert, G.; Van der Eycken, E. *Org. Lett.* **2001,** *3,* 1173–1175. doi:10.1021/ol0156345
53. Doering, W. von E.; Lambert, J. B. *Tetrahedron* **1963,** *19,* 1989–1994. doi:10.1016/0040-4020(63)85013-9
54. Wender, P. A.; Dreyer, G. B. *Tetrahedron* **1981,** *37,* 4445–4450. doi:10.1016/0040-4020(81)80011-7
55. Fenton, G. A.; Gilbert, A. *Tetrahedron* **1989,** *45,* 2979–2988. doi:10.1016/S0040-4020(01)80125-3
56. Avent, A. G.; Byrne, P. W.; Penkett, C. S. *Org. Lett.* **1999,** *1,* 2073–2075. doi:10.1021/ol991119j
57. Penkett, C. S.; Sims, R. O.; French, R.; Dray, L.; Roome, S. J.; Hitchcock, P. B. *Chem. Commun.* **2004,** 1932–1933. doi:10.1039/b404816d
58. Penkett, C. S.; Sims, R. O.; Byrne, P. W.; Kingston, L.; French, R.; Dray, L.; Berritt, S.; Lai, J.; Avent, A. G.; Hitchcock, P. B. *Tetrahedron* **2006,** *62,* 3423–3434. doi:10.1016/j.tet.2006.01.042
59. Srinivasan, R. *J. Am. Chem. Soc.* **1971,** *93,* 3555–3556. doi:10.1021/ja00743a059
60. Wender, P. A.; Ternansky, R. J. *Tetrahedron Lett.* **1985,** *26,* 2625–2628. doi:10.1016/S0040-4039(00)98120-6
61. Coates, R. M.; Ho, J. Z.; Klobus, M.; Zhu, L. *J. Org. Chem.* **1998,** *63,* 9166–9176. doi:10.1021/jo971579v
62. Wender, P. A.; Howbert, J. J. *Tetrahedron Lett.* **1983,** *24,* 5325–5328. doi:10.1016/S0040-4039(00)87859-4
63. Wender, P. A.; Dore, T. M. *Tetrahedron Lett.* **1998,** *39,* 8589–8592. doi:10.1016/S0040-4039(98)01965-0
64. Wender, P. A.; deLong, M. A. *Tetrahedron Lett.* **1990,** *31,* 5429–5432. doi:10.1016/S0040-4039(00)97864-X
65. Keese, R. *Chem. Rev.* **2006,** *106,* 4787–4808. doi:10.1021/cr050545h
66. Penkett, C. S.; Woolford, J. A.; Day, I. J.; Coles, M. P. *J. Am. Chem. Soc.* **2010,** *132,* 4–5. doi:10.1021/ja906163s
67. Wender, P. A.; Dore, T. M.; deLong, M. A. *Tetrahedron Lett.* **1996,** *37,* 7687–7690. doi:10.1016/0040-4039(96)01740-6
68. Gaich, T.; Mulzer, J. *Org. Lett.* **2010,** *12,* 272–275. doi:10.1021/ol902594b
69. Gaich, T.; Mulzer, J. *J. Am. Chem. Soc.* **2009,** *131,* 452–453. doi:10.1021/ja8083048
70. Wang, Q.; Chen, C. *Org. Lett.* **2008,** *10,* 1223–1226. doi:10.1021/ol800111j
71. Gilbert, A.; Yianni, P. *Tetrahedron* **1981,** *37,* 3275–3283. doi:10.1016/S0040-4020(01)92375-0
72. Gilbert, A.; Yianni, P. *Tetrahedron Lett.* **1982,** *23,* 255–256. doi:10.1016/S0040-4039(00)86801-X
73. Coxon, J. M.; Halton, B. *Organic Photochemistry,* 5th ed.; Cambridge University Press: Great Britain, 1987; pp 162–179.
74. Wagner, P. J. *Acc. Chem. Res.* **2001,** *34,* 1–8. doi:10.1021/ar000113n
75. Wagner, P. J.; Sakamoto, M.; Madkour, A. E. *J. Am. Chem. Soc.* **1992,** *114,* 7298–7299. doi:10.1021/ja00044a053
76. Wagner, P. J.; Nahm, K. *J. Am. Chem. Soc.* **1987,** *109,* 6528–6530. doi:10.1021/ja00255a058
77. Wagner, P. J.; Nahm, K. *J. Am. Chem. Soc.* **1987,** *109,* 4404–4405. doi:10.1021/ja00248a051
78. Cheng, K.-L.; Wagner, P. J. *J. Am. Chem. Soc.* **1994,** *116,* 7945–7946. doi:10.1021/ja00096a081
79. Dittami, J. P.; Nie, X. Y.; Nie, H.; Ramanathan, H.; Buntel, C.; Rigatti, S.; Bordmer, J.; Decosta, D. L.; Williard, P. *J. Org. Chem.* **1992,** *57,* 1151–1158. doi:10.1021/jo00030a022
80. Nuss, J. M.; Chinn, J. P.; Murphy, M. M. *J. Am. Chem. Soc.* **1995,** *117,* 6801–6802. doi:10.1021/ja00130a029
81. Mathew, T.; Tonne, J.; Sedelmeier, G.; Grund, C.; Keller, M.; Hunkler, D.; Knothe, L.; Prinzbach, H. *Eur. J. Org. Chem.* **2007,** 2133–2146. doi:10.1002/ejoc.200601075
82. Scharf, H.-D.; Leismann, H.; Erb, W.; Gaidetzka, H. W.; Aretz, J. *Pure Appl. Chem.* **1975,** *41,* 581–600. doi:10.1351/pac197541040581
83. Brooker-Milburn, K. I.; Wood, P. M.; Dainty, R. F.; Urquhart, M. W.; White, A. J.; Lyon, H. J.; Charmant, J. P. H. *Org. Lett.* **2002,** *4,* 1487–1489. doi:10.1021/ol025693y
84. Al-Jalal, N.; Gilbert, A. *Recl. Trav. Chim. Pays-Bas* **1990,** *109,* 21–25. doi:10.1002/recl.19901090104

85. Pirrung, M. C. *J. Org. Chem.* **1987,** *52,* 1635–1637. doi:10.1021/jo00384a057
86. Hanzawa, Y.; Paquette, L. *Synthesis* **1982,** 661–662. doi:10.1055/s-1982-29892
87. Kalena, G. P.; Pradhan, P.; Banerji, A. *Tetrahedron Lett.* **1992,** *33,* 7775–7778. doi:10.1016/0040-4039(93)88043-I
88. Kalena, G. P.; Pradhan, P.; Banerji, A. *Tetrahedron* **1999,** *55,* 3209–3218. doi:10.1016/S0040-4020(98)01134-X
89. Kotha, S.; Dipak, M. K. *Chem.–Eur. J.* **2006,** *12,* 4446–4450. doi:10.1002/chem.200501366
90. Kushner, A. S. *Tetrahedron Lett.* **1971,** *12,* 3275–3278. doi:10.1016/S0040-4039(01)97154-0
91. Becker, H.-D.; Hansen, L.; Andersson, K. *J. Org. Chem.* **1986,** *51,* 2956–2961. doi:10.1021/jo00365a019
92. Bryce-Smith, D.; Foulger, B. E.; Gilbert, A. *J. Chem. Soc., Chem. Commun.* **1972,** 664–665. doi:10.1039/C39720000664
93. Haddaway, K.; Somekawa, K.; Fleming, P.; Tossell, J. A.; Mariano, P. S. *J. Org. Chem.* **1987,** *52,* 4239–4253. doi:10.1021/jo00228a017
94. Yang, N. C.; Libman, J. *Tetrahedron Lett.* **1973,** *16,* 1409–1412. doi:10.1016/S0040-4039(01)95956-8
95. Berridge, J. C.; Bryce-Smith, D.; Gilbert, A. *Tetrahedron Lett.* **1975,** 2325–2326. doi:10.1016/0040-4039(75)80001-3
96. Kurata, H.; Kyusho, M.; Nishimae, Y.; Matsumoto, K.; Kawase, T.; Oda, M. *Chem. Lett.* **2007,** *36,* 540–541. doi:10.1246/cl.2007.540
97. Kishikawa, K.; Akimoto, S.; Kohmoto, S.; Yamamoto, M.; Yamada, K. *J. Chem. Soc., Perkin Trans. 1* **1997,** 77–84. doi:10.1039/A601710J
98. Kohmoto, S.; Miyaji, Y.; Tsuruoka, M.; Kishikawa, K.; Yamamoto, M.; Yamada, K. *J. Chem. Soc., Perkin Trans. 1* **2001,** 2082–2088. doi:10.1039/B100678I
99. Kalena, G. P.; Pradhan, P.; Puranik, V. S.; Banerji, A. *Tetrahedron Lett.* **2003,** *44,* 2011–2013. doi:10.1016/S0040-4039(03)00230-2
100. Nishio, T.; Sakurai, N.; Iba, K.; Hamano, Y.-I.; Sakamoto, M. *Helv. Chim. Acta* **2005,** *88,* 2603–2609. doi:10.1002/hlca.200590200
101. Brinson, R. G.; Hubbard, S. C.; Zuidema, D. R.; Jones, P. B. *J. Photochem. Photobiol., A* **2005,** *175,* 118–128. doi:10.1016/j.jphotochem.2005.03.027
102. Pérez-Ruiz, R.; Hinze, O.; Neudörfl, J.-M.; Blunk, D.; Görner, H.; Griesbeck, A. G. *Photochem. Photobiol. Sci.* **2008,** *7,* 782–788. doi:10.1039/b807889k
103. Wagner, P. J.; Meador, M. A.; Park, B.-S. *J. Am. Chem. Soc.* **1990,** *112,* 5199–5211. doi:10.1021/ja00169a031
104. Birbaum, F.; Neels, A.; Bochet, C. G. *Org. Lett.* **2008,** *10,* 3175–3178. doi:10.1021/ol800806a

License and Terms

Beilstein Journal of Organic Chemistry

Intraannular photoreactions in *pseudo*-geminally substituted [2.2]paracyclophanes

Henning Hopf*[1], Vitaly Raev[1] and Peter G. Jones[2]

Full Research Paper

Open Access

Address:
[1]Institut für Organische Chemie, Technische Universität Braunschweig, Hagenring 30, D-38106 Braunschweig, Germany, Fax: +49 531 / 391 5388 and [2]Institut für Anorganische und Analytische Chemie, Technische Universität Braunschweig, Hagenring 30, D-38106 Braunschweig, Germany, Fax: +49 531 / 391 5387

Email:
Henning Hopf* - H.Hopf@tu-bs.de; Peter G. Jones - p.jones@tu-bs.de

* Corresponding author

Keywords:
paracyclophanes; photoadditions; photoisomerizations; proximity effects; topochemical reaction control; vinylcyclopropanes; X-ray structural analysis

Beilstein J. Org. Chem. **2011,** *7,* 658–667.
doi:10.3762/bjoc.7.78

Received: 29 December 2010
Accepted: 12 May 2011
Published: 24 May 2011

This article is part of the Thematic Series "Photocycloadditions and photorearrangements". Photoactive cyclophanes, part 6. For part 5 see [1].

Guest Editor: A. G. Griesbeck

Abstract

The photoisomerization of the pseudo-*geminal* tetraene **11** furnishes the cyclooctadiene derivatives **13** and **15** with a completely new type of molecular bridge for a [2.2]paracyclophane which promise many interesting novel applications; the same is true for the photoisomerization of **22** to **23** and **24**. The structures of these new hydrocarbons were established by X-ray crystallography and spectroscopic analysis; among the noteworthy structural features of **13** and **15** are unusually long carbon–carbon single bonds (>1.64 Å).

Introduction

Photodimerizations of crystalline aromatic or olefinic compounds are among the oldest known organic photoreactions. In this type of reaction the crystal lattice locks the relative orientation of the substrate molecules or their photoreactive groups. If the orientation is favorable for reaction, reactivity increases. Unlike photochemistry in homogeneous solution, this often leads to highly selective formation of the photoproducts. Schmidt coined the term "topochemical principle" or "topochemistry" for (non)reactivity determined by a limiting distance between the reactive groups [2-4]. Although the model found widespread acceptance, many exceptions to the concept were known from the very beginning [5]. Later, AFM techniques enabled experimental elucidation of solid-state photochemistry. This showed that the supramolecular arrangement of molecules in the crystal plays a more important role for reaction control than the simple alignment of double bonds. Long-range molecular movements within crystals upon photochemical reaction and even topotactic single-crystal to single-crystal reactions were found, although the latter are rare. The subject has been comprehensively covered by recent reviews [6-8].

Reactions of inclusion complexes are a variation of the solid-state photochemistry topic [9]. Here, co-crystals of a host compound and the starting materials of a photochemical reaction are used and the supramolecular arrangement [10] may control the regio- and stereoselectivity of the photo-process. The enantioselective photochemical conversion of chiral crystals into optically active products has also been described [11]. Some approaches utilize zeolites as supramolecular hosts for photoreactions [12-14]. Internal complexation, or intracrystalline adsorption, occurs by diffusion of the guest into the channels and cavities of the zeolite crystal and is size- and shape-selective. Complexation of organic compounds may reversibly depend on temperature. The geometry of zeolite cavities restricts conformation and orientation of included guests and their reaction partners and leads to more selective reactions. In the absence of any low-energy electronic states of the zeolite, photoreaction occurs only with the included guest.

The common disadvantage of solid-state photoreactions is the difficulty in predicting and controlling reaction selectivity. It remains a challenge to find the suitable crystal, co-crystal, or inclusion complex for the desired regio- or stereoselective outcome of a given reaction. Therefore, an attractive strategy is to transfer the topochemical control from the solid state to a homogeneous solution using suitable templates. Such reactions are easier to analyze, design, and optimize.

Templated photochemistry in solution is possible if the photoreactive moieties can be brought into suitable positions for reaction. Such an arrangement may in principle be reached either by non-covalent bonding (e.g., hydrogen bonds) or by (cleavable) covalent bonds. The latter case can be realized if two (or more) reactive moieties are attached to a rigid scaffold, which is able to fix them in the correct position for reaction.

One such system is the generalized paracyclophane molecule **1** shown in Scheme 1. Here the distance between the benzene "decks" carrying the functional groups F^1 and F^2 can be adjusted both by the length of the two molecular bridges (variation of *m* and *n*), and by the relative orientation between these groups in terms of their relative positions in the aromatic subsystems. Although there will never be a continuum of intrafunctional distances, numerous spatial arrangements of F^1 and F^2 are possible, keeping in mind that, for example, the molecular bridges of **1** – with the number of carbon atoms held constant – can be modified by introducing functionality into this part of the molecule, making the bridges more rigid, and/or by exchanging the benzene rings of **1** for other aromatic or heteroaromatic subsystems. The two bridges do not have to be of the same length nor the aromatic nuclei of the same type.

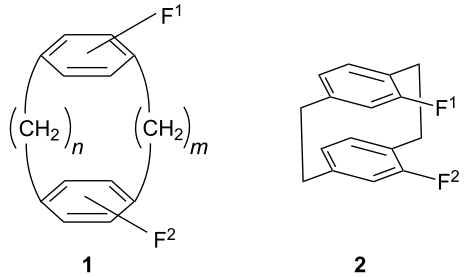

Scheme 1: [2.2]Paracyclophanes as scaffolds for intraannular photodimerization reactions in solution.

In our work we have so far concentrated our efforts on derivatives of [2.2]paracyclophane (**1**, $m = n = 2$) with the two functional groups usually in the so-called *pseudo*-geminal positions, that is, directly above each other as shown in **2**. The intraannular distance is approximately 3.1 Å in [2.2]paracyclophane and hence is less than the separation of the layers in graphite (3.4 Å) or between the base pairs of DNA (3.34 Å) [15]. In other words, the distance between the benzene rings of [2.2]paracyclophane and consequently of the two functional groups directly bonded to them is just slightly shorter than the length of a p-orbital, an ideal prerequisite for an intraannular reaction to take place should other factors, such as excessive strain, not prevent it. In principle, cyclophanes such as **1** are thus excellent model compounds for "molecular workbenches" [16-19] and we have already shown that certain *pseudo*-geminally substituted derivatives can be used as proxies for the crystal lattice in various solid-state reactions [20-22]. For example, on irradiation the unsaturated esters **3** photocyclize in excellent (up to quantitative) yield to the ladderane derivatives **4**. In this case the cyclophane moiety is the "order-generating" part of the molecule and the originally flexible, unsaturated chain remain attached to each other by stable C–C-bonds; altogether the process amounts to a stiffening (rigidization) of the molecules **3**. In the case of the bis amide **5** (Scheme 2), photodimerization to the corresponding cyclobutane derivative occurs readily, and the photoproduct can be saponified to the corresponding *pseudo*-geminal diamine and truxinic acid (**6**) in excellent yield, thus allowing its stereospecific synthesis. We believe that the use of the [2.2]paracyclophane scaffold as a removable spacer can be developed considerably further for the stereospecific synthesis of many other compounds.

Results and Discussion

However, the detailed stereochemical situation is in fact more complex, and the origin of the stereospecificity requires a more thorough analysis. For example, we have shown [22] by time-resolved photoelectron spectroscopy (TR-PES) that the *pseudo*-geminal divinyl derivative **7** can only react from its *anti*,*anti*-

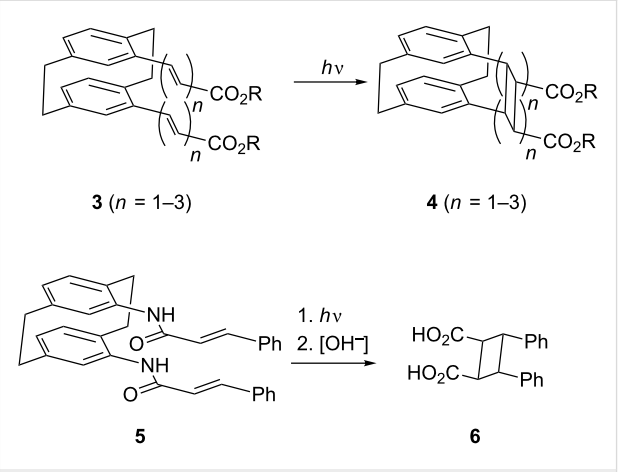

Scheme 2: Stereospecific intramolecular [2+2]photoadditions using [2.2]paracyclophane spacers.

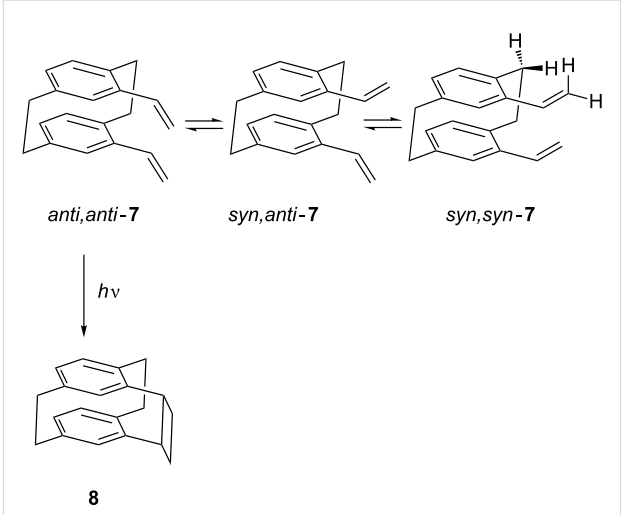

Scheme 3: Different conformations of *pseudo*-geminal divinyl[2.2]paracyclophane.

conformation (*anti* referring to the orientation of the vinyl substituent to the neighboring ethano bridge) to yield the cyclobutane derivative **8**. The *syn*,*anti*-conformation, which has been shown to be present as a conformer in the solid state by X-ray structural analysis does not photocyclize to **8**. Moreover, *syn*,*syn*-**7** is evidently too sterically hindered (by repulsion of the relevant hydrogen atoms as shown in Scheme 3) to be part of the conformational equilibrium.

Clearly, the situation is conformationally much more complex in cases such as the triene esters **3**, where several conformations could be present in the ground state. To investigate this phenomenon we decided to simplify our substrates structurally and chemically by omitting any functional groups. In this contribution we report on the results obtained with two hydrocarbons **11** (Scheme 4) and **22** (Scheme 8).

Bis-ene-al **10** was obtained in excellent yield (97%) as a mixture of three isomers (Scheme 4) in a ratio of 70:15:1; the isomers were isolated by column chromatography and their

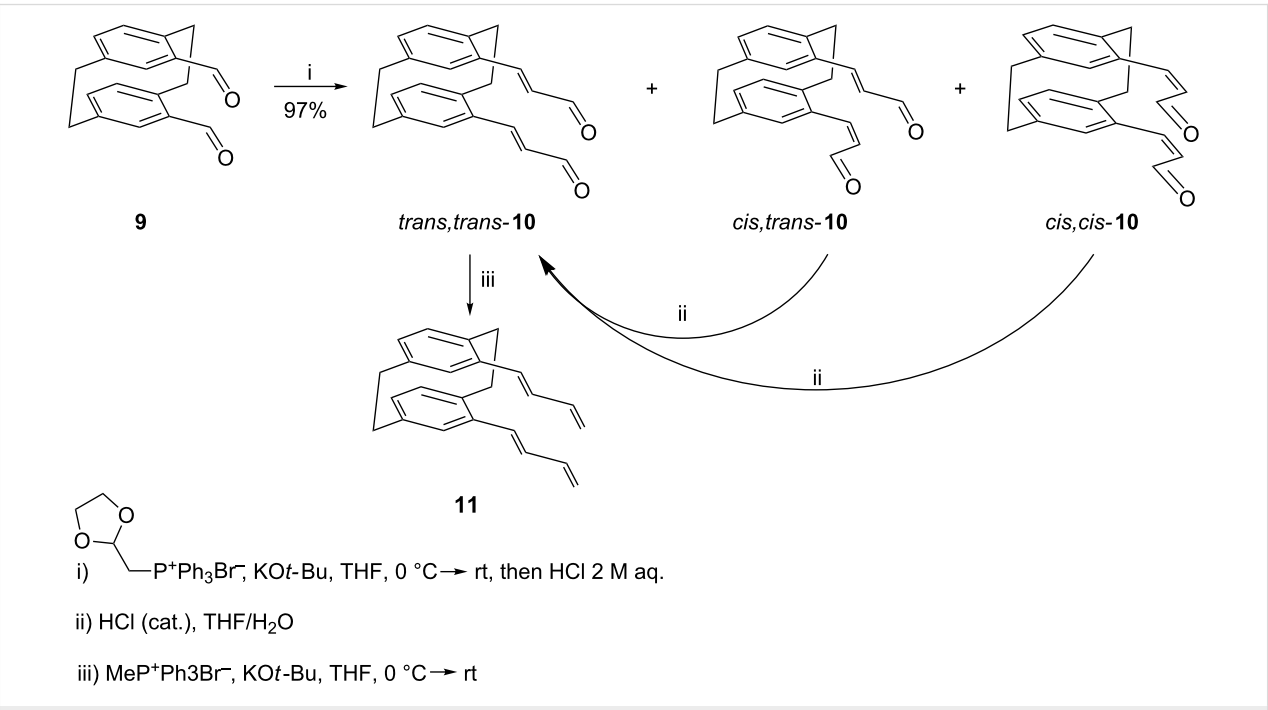

Scheme 4: Preparation of tetraene **11**.

structures were established from their spectroscopic data, especially from their NMR spectra (see Experimental). Treatment of the *cis,trans*- and *cis,cis*-isomers of **10** with hydrochloric acid in aqueous THF converted them into the thermodynamically most favorable *trans,trans*-isomer.

Bis-diene **11**, which was obtained in virtually quantitative yield from *trans,trans*-**10** by a Wittig olefination, appears to be unstable in the solid state at room temperature, but in the refrigerator at −20 °C or in dilute (~0.1 M) solution in dichloromethane or chloroform it can be stored in the dark for at least 3 months without any detectable decomposition or polymerization.

Irradiation of **11** with a halogen lamp (1 kW, 10 cm distance, water cooling) for 16 h gave a mixture of products (Scheme 5), which contained two isomers of a cycloocta-1,5-diene derivative, **13** (as the main product) and **15** (*syn*- and *anti*- position, respectively, relatively to the bridge) together with the divinylcyclobutane derivative **14** in moderate yield (total yield 70%, ratio **13**:**14**:**15** = 43:5:8 by ^{1}H NMR analysis). The expected ladderane **12** was not detected in the reaction mixture by NMR spectroscopy. Separation by column chromatography gave the pure divinylcyclobutane derivative **14**, but the cyclooctadienes were not separated from each other. Fractional crystallization of the mixture of cyclooctadienes from $CHCl_3$/MeOH mixture gave an analytically pure sample of **13**, which was characterized by single-crystal X-ray diffraction (Figure 1).

Further irradiation of compounds **13**, **14** and **15** did not lead to any detectable photoproducts.

The success in preparing cyclobutane derivative **4** (n = 1) from the corresponding cinnamophane diester **3** (n = 1, quantitative yield) led us to attempt to prepare the corresponding cyclobutane dialdehyde derivative **16** (Scheme 6). Unfortunately, although this was the only product after 2 h of irradiation with a halogen 1 kW lamp, it appeared to be very unstable even below 0 °C, although it was stable enough for NMR identification. Wittig olefination of the irradiated mixture gave the divinylcyclobutane derivative **14** as the sole product and was isolable by column chromatography.

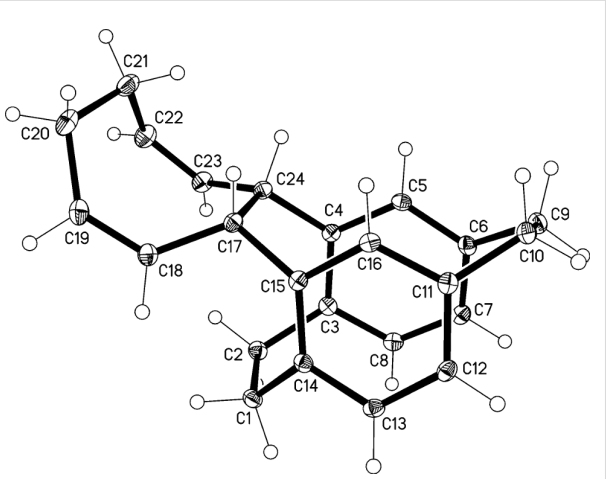

Figure 1: The molecule of compound **13** in the crystal. Ellipsoids correspond to 30% probability levels.

Interestingly, all three isomers of **10** (*trans,trans*-, *cis,trans*- and *cis,cis*-) under the above irradiation conditions furnish the same product: **16**. It is hence likely that a rapid photoequilibration process precedes the ring closure to the final product.

Attempts to crystallize **14** from boiling ethanol led to a mixture of **14** and the cyclooctadiene derivative **15**, which was separable by column chromatography. The divinylcyclobutane derivative **14** was completely converted into the cyclooctadiene derivative **15** within half an hour in boiling ethanol. The structure of **15** was confirmed by single-crystal X-ray analysis (Figure 2).

Molecules of **13** and **15** show common structural features. Despite the introduction of the new bridge C17–C24, the form of the original [2.2]paracyclophane is maintained to a considerable extent, with a flattened boat conformation of both six-membered rings (C4,5,7,8 and C12,13,15,16 remain essentially coplanar). However, the rings become significantly non-parallel (interplanar angles 14.4 and 13.4°, respectively). The new bridges C17–C24 are extremely long at 1.643(2) and 1.652(2) Å, respectively, even longer than the previously present bridges C1–C2 and C9–C10 at 1.57–1.60 Å. The steric crowding of **13** associated with the *syn* geometry is shown by,

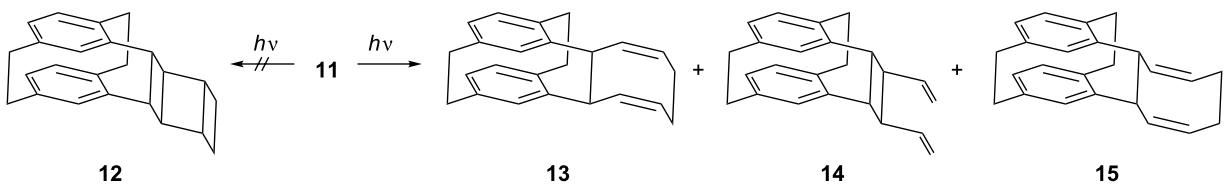

Scheme 5: Photolysis of tetraene **11**.

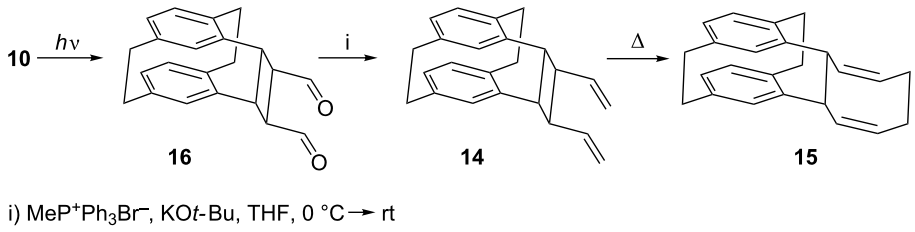

Scheme 6: Photolysis of *trans*,*trans*-dienal **10**.

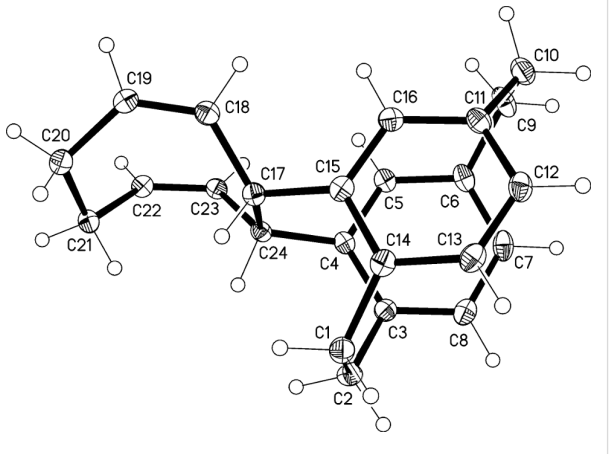

Figure 2: The molecule of compound **15** in the crystal. Ellipsoids correspond to 30% probability levels.

e.g., the short contact H18···H1A 1.91 Å; compound **15** has no intramolecular H···H < 2 Å.

Form the stereochemical viewpoint the above photocyclizations are quite complex. Not only can the *pseudo*-geminal substituents in principle adopt different conformations in the ground state, because of possible rotation around the various σ-bonds, but this situation becomes even more intricate when the substrates are photochemically excited. For example, on photoexcitation diradicals **17** (Scheme 7) should be the intermediates in conceivable *cis*–*trans*-isomerizations, e.g., **11**→**18**, and these diradicals could undergo very different subsequent reactions (in which, of course, it could also be of importance whether these intermediates are singlets or triplets).

To test for the possible formation of radical intermediates in the above photocyclizations, we decided to prepare the biscyclopropane analog of **11**, the bisvinylcyclopropane **19** (or one of its *cis*-isomers) and subject this presumably strained hydrocarbon to our photocyclization conditions. Of course, this system also has various options to react, among them the photoisomerization to a mono- or all-*cis*-diastereomer. If this process took place, it would involve the diradical **20**, which could isomerize to **21** with release of strain. The process could also occur a second time to provide a *pseudo*-geminally substituted [2.2]paracyclophane, now carrying two cyclopentenyl substituents. Should these ring-enlarged paracyclophanes

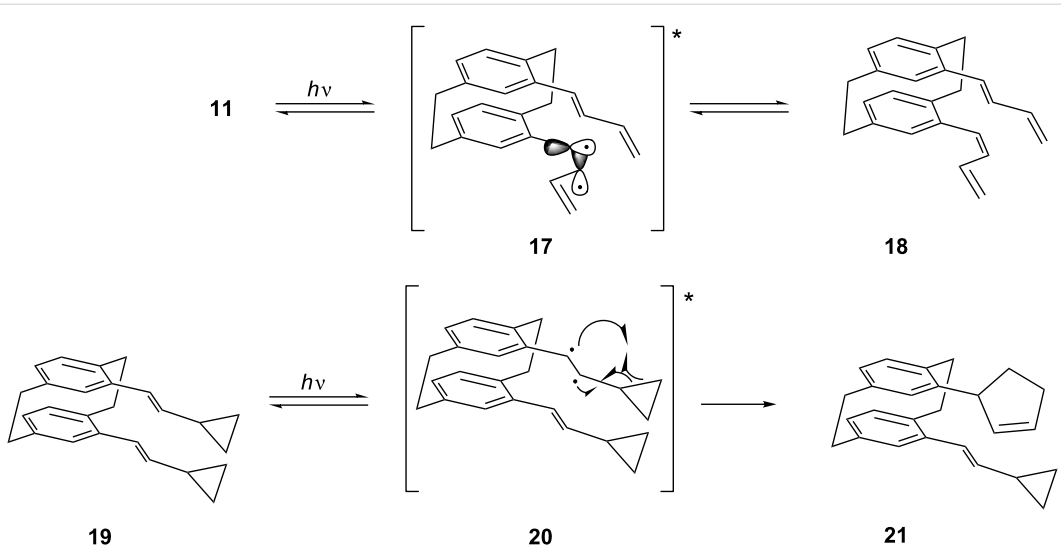

Scheme 7: *Cis*–*trans*-isomerizations of the double bonds of the *pseudo*-geminal cyclophanes **11** and **19**.

not be observed, this would not necessarily constitute a proof against diradical(oid) intermediates in these reactions. However, if derivatives such as **21** were among the photoproducts the involvement of radicals in the photoisomerizations would be indicated.

We therefore reacted the bis-aldehyde **9** with the ylide prepared from cyclopropylcarbinyl triphenylphosphonium bromide and obtained in quantitative yield a product mixture consisting of the three possible diastereomers *E*,*E*-, *E*,*Z*- and *Z*,*Z*-**22** (Scheme 8), the latter being the main product as is often observed in classical Wittig reactions (product ratio 1:13:31; analysis by ^{1}H NMR spectroscopy, see Experimental). The main product was separated by silica gel chromatography and its structure determined by X-ray crystallography (Figure 3).

The two independent molecules in the asymmetric unit are similar, with an r.m.s. deviation of 0.3 Å for all non-H atoms. As would be expected, the substituents are directed outwards from the ring systems. The non-bonded distances C17···C22 and C18···C23, across which bonds are to be formed are 3.34, 3.35 and 5.12, 4.93 Å; clearly the latter, in particular, can be reduced by suitable rotations.

Irradiation of *Z*,*Z*-**22** with a 1 kW halogen lamp in a Pyrex flask over 12 h (Scheme 8) gave only two [2 + 2] cycloaddition products: The hydrocarbons **23** and **24** in 3:5-ratio with a total yield of 70%. The isomers were separated by column chromatography and their structures established by NMR spectroscopy and single-crystal X-ray analysis (Figure 4 and Figure 5); no other products could be detected.

As for molecules **13** and **15**, but to a slightly lesser extent, the newly formed bridges C17–22 in **23** and **24** are significantly longer than a standard single bond at 1.612(2) and 1.614(2) Å, respectively. On the other side of the four-membered rings, the bond lengths C18–23 relax to 1.563(2) and 1.559(2) Å. The interplanar angles between the six-membered rings of the original [2.2]paracyclophane unit are 12.9 and 12.7°.

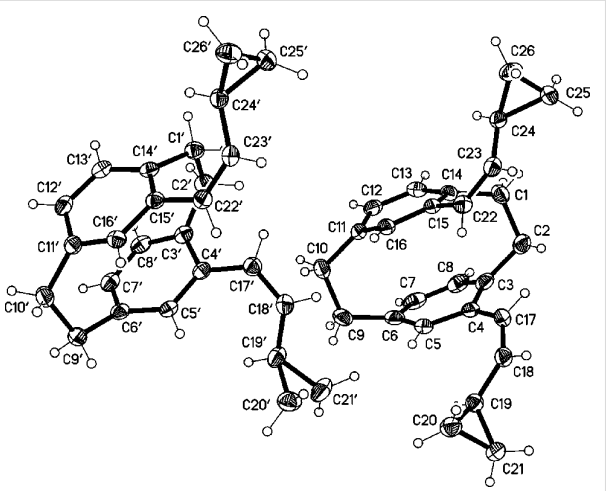

Figure 3: The two independent molecules of compound *Z*,*Z*-**22** in the crystal. Ellipsoids correspond to 50% probability levels.

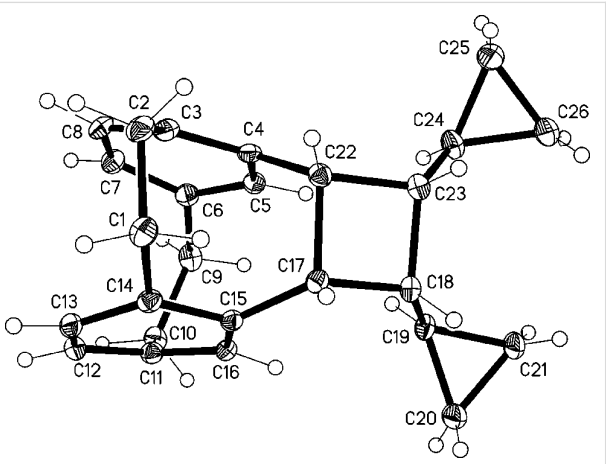

Figure 4: The molecule of compound **23** in the crystal. Ellipsoids correspond to 50% probability levels.

These results clearly show that the photocylization occurs from the conformation in which the two *pseudo*-geminal substituents are rotated away from the nearest ethano bridge (*anti*,*anti*-conformation). The conformation with both of these groups *syn*-

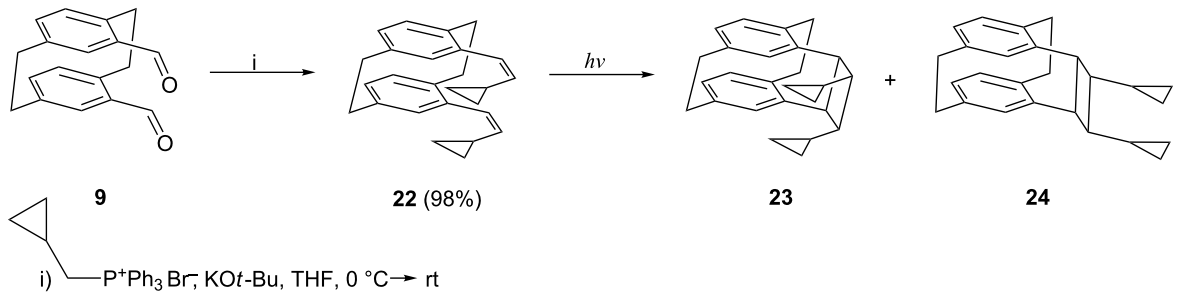

Scheme 8: Preparation of the vinylcyclopropanes **22**–**24**.

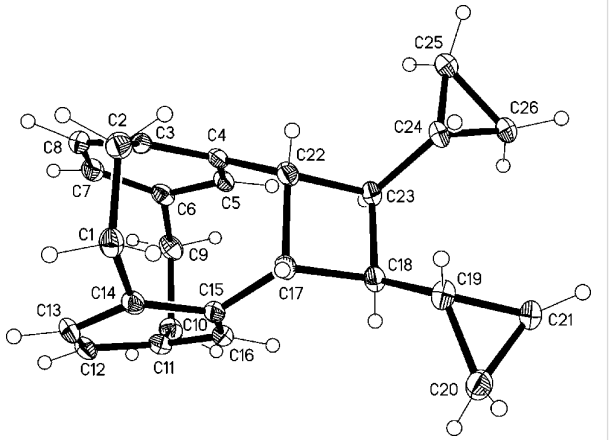

Figure 5: The molecule of compound **24** in the crystal. Ellipsoids correspond to 30% probability levels.

oriented towards this bridge, although in principle possible, is evidently not populated. Although in the crystalline state a *syn*,*anti*-conformation is preferred (Figure 3), no reaction takes place from this orientation on irradiation in solution. Since we have already demonstrated that a comparable situation prevails for the simplest compound studied in this series, hydrocarbon **7** (Scheme 3), we conclude that reaction from this *anti*,*anti*-conformation is the generally preferred reaction mode for derivatives of type **3** (Scheme 2). The production of **24**, however, proves that the stereochemical information contained in the first double bond (*E* or *Z*) can be lost in the course of the photochemical reaction. Whereas this *Z*→*E*-isomerization process must involve a diradical intermediate of type **17**, its lifetime is evidently too short to allow ring-expansion as depicted in Scheme 7. Whether this process might be induced thermally (vinylcyclopropane→cyclopentene rearrangement; [23]) is an open question.

Conclusion

Although the detailed mechanisms of the photoisomerization of the tetraene **11** to the cyclooctadiene-bridged cyclophanes **13** and **15** and the isomerization of **22** to **23** and **24** remain to be established, these processes allow the introduction of a completely new type of additional bridge into [2.2]paracyclophanes. For several of these new polycyclic molecules interesting preparative applications are conceivable, and we hope to report about them in the not too distant future.

Experimental

General: Melting points: Büchi 530 melting point apparatus, uncorrected. Thin layer chromatography (TLC): Macherey–Nagel Polygram SilG/UV254. Column chromatography: Merck Kieselgel 60 (70–230 mesh). IR: Perkin–Elmer 1420 or Nicolet 320 FT–IR spectrometer. ^{1}H and ^{13}C NMR: Bruker AC 200 (^{1}H) and 50.3 MHz (^{13}C) in $CDCl_3$, internal standards: TMS, δ = 0 ppm for ^{1}H, $CHCl_3$, δ = 77.05 ppm for ^{13}C spectroscopy. UV–vis: Beckman UV 5230 or Hitachi U 3300. The samples were degassed by the freeze, pump, and thaw technique. Irradiations were conducted with a high-pressure mercury lamp (150 W) or a halogen torch lamp (1 kW) using water cooling reactor.

Synthesis: (1,3-Dioxolan-2-ylmethyl)triphenylphosphonium bromide was prepared according to [24]; 4,15-diformyl[2.2]paracyclophane (**9**) was prepared according to [20] with a modified oxidation step (Swern oxidation rather than the Dess–Martin protocol); 4,15-bis[(*E*)-2-formylvinyl]-[2.2]paracyclophane (*trans,trans*-**10**) was prepared according to [20]; cyclopropylmethyltriphenylphosphonium bromide was purchased from ABCR; methyltriphenylphosphonium bromide was purchased from Acros. Reagents were used without further purification. Solvents used were of analytical grade; anhydrous THF was distilled from an $LiAlH_4$ dispersion with triphenylmethane as indicator.

4,15-Divinyl[2.2]paracyclophane (**7**): A freshly prepared solution of potassium *tert*-butoxide (4.26 g, 38.0 mmol) in anhydrous THF (50 mL) was added dropwise over 30 min to a cooled (ice/water bath), vigorously stirred dispersion of methyltriphenylphosphonium bromide (14.29 g, 40.0 mmol) in anhydrous THF (25 mL) under a N_2 atmosphere. The bath was removed and the mixture stirred for 2 h at ambient temperature, then re-cooled to 0 °C, after which a solution of **9** (2.64 g, 10.0 mmol) in anhydrous THF (30 mL) was added dropwise over 1 h. The mixture was left to stir in the melting ice/water bath overnight and sat. aq. Na_2SO_4 solution (25 mL) added with vigorous stirring. The mixture was stirred for 15 min and the organic layer decanted. The aqueous layer was washed with THF (3 × 20 mL, decanting), then the combined organic phases were dried over anhydrous Na_2SO_4, filtered and concentrated under reduced pressure to give a solid residue (6.4 g). Column chromatography (50 mL of silica, CH_2Cl_2) gave 2.60 g (10 mmol, 100%) of pure hydrocarbon **7**. ^{1}H NMR (200 MHz, $CDCl_3$) δ 6.81 (dd, 2H, J_1 = 10.9, J_2 = 17.4 Hz), 6.60–6.40 (m, 6H), 5.36 (dd, 2H, J_1 = 1.5, J_2 = 17.4 Hz), 5.08 (dd, 2H, J_1 = 1.5 , J_2 = 10.9 Hz), 3.60–3.40 (m, 2H), 3.05–2.86 (m, 6H) ppm; ^{13}C NMR (50.3 MHz, $CDCl_3$) δ 139.3, 138.0, 137.2, 135.5 (+), 134.6 (+), 132.4 (+), 129.8 (+), 114.6 (−), 35.0 (−), 32.5 (−) ppm; MS (EI, 70 eV) *m*/*z* (%): 261 (8), 260 (34), 131 (36), 130 (39), 129 (100), 128 (24), 115 (34).

4,15-bis(butadien-1-yl)[2.2]paracyclophane (**11**): A freshly prepared solution of potassium *tert*-butoxide (2.69 g, 24.0 mmol) in anhydrous THF (50 mL) was added dropwise over 30 min into the cooled (ice/water bath), vigorously stirred disper-

sion of methyltriphenylphosphonium bromide (8.57 g, 24.0 mmol) in 50 mL of anhydrous THF under a N_2 gas flow. The bath was removed and the mixture was stirred for 1 h at ambient temperature, then re-cooled to 0 °C, after which a solution of **10** (0.95 g, 3.0 mmol) in anhydrous THF (30 mL) was added dropwise over 1 h. The bath was removed and the mixture was stirred for an additional 2 h. The resulting mixture was poured into a vigorously stirred mixture of ice (200 g), water (100 mL) and conc. (37%) aq. HCl solution (100 mL), and the mixture stirred until the ice had completely melted. The precipitate was suction filtered on a glass frit, washed with dilute (1:3) aq. HCl (3 × 30 mL) and water (3 × 30 mL), and dissolved in CH_2Cl_2 (100 mL). The organic solution was dried over Na_2SO_4, filtered and concentrated under reduced pressure without warming to give a colorless solid residue (0.94 g, 3.0 mmol, 100%) of hydrocarbon **11**, pure by NMR analysis. ^{1}H NMR (200 MHz, $CDCl_3$) δ 6.60–6.24 (m, 12H), 5.28–4.89 (m, 4H), 3.57–3.28 (m, 2H), 3.11–2.74 (m, 6H) ppm; ^{13}C NMR (50.3 MHz, $CDCl_3$) δ 138.7, 137.1 (+), 136.9, 136.7, 134.1 (+), 131.5, 131.1 (+), 129.7 (+), 129.2 (+), 116.1 (–), 34.4 (–), 32.0 (–) ppm.

Irradiation of 4,15-dibutadien-1-yl[2.2]paracyclophane – [2.2.2]tricyclophanes **13**, **14** and **15**: The solution of **11** (230.0 mg, 736 μmol) was irradiated by UV-lamp for 20 h. When the starting material was completely consumed (TLC monitoring), the reaction mixture was separated by column chromatography (silica, pentane) to give 14.3 mg of *bis*-vinyl derivative **14** and 145.8 mg of the mixture of cyclooctadienyl derivatives **13** and **15**. Total yield 160.1 mg (70%).

Bis-vinyl derivative **14**: ^{1}H NMR (200 MHz, $CDCl_3$) δ 6.48 (dd, 2H, J_1 = 1.73, J_2 = 7.79 Hz), 6.35 (d, 2H, J = 1.73 Hz), 6.23 (d, 2H, J = 7.79 Hz), 6.33–6.15 (m, 2H), 5.21–5.05 (m, 4H), 4.28–4.17 (m, 2H), 3.70–3.33 (m, 2H), 3.93–3.22 (m, 6H), 2.64–2.49 (m, 2H) ppm; ^{13}C NMR (50.3 MHz, $CDCl_3$) δ 140.1, 139.8, 139.5, 139.3 (+), 134.1 (+), 133.2 (+), 128.6 (+), 115.0 (−), 49.1 (+), 40.1 (+), 36.4 (−), 32.5 (−) ppm; MS (EI, 70 eV) *m*/*z* (%): 312 (8), 157 (31), 156 (41), 155 (100), 142 (12), 141 (56), 129 (16), 128 (21), 115 (16).

Anti-cyclooctadiene derivative **15**: ^{1}H NMR (600 MHz, $CDCl_3$) δ 6.45 (dd, 2H, J_1 = 1.84, J_2 = 7.80 Hz), 6.41 (d, 2H, J = 1.84 Hz), 6.31 (d, 2H, J = 7.80 Hz), 6.05–6.00 (m, 2H), 5.94–5.88 (m, 2H), 4.89–4.82 (m, 2H), 3.39–3.29 (m, 2H), 3.19–3.09 (m, 2H), 3.06–2.96 (m, 2H), 2.92–2.83 (m, 2H), 2.78–2.68 (m, 2H), 2.34–2.26 (m, 2H) ppm; ^{13}C NMR (150.9 MHz, $CDCl_3$) δ 143.6, 140.2, 139.4, 136.6 (+), 132.9 (+), 131.4 (+), 130.7 (+), 128.8 (+), 48.5 (+), 36.3 (−), 33.3 (−), 27.2 (−) ppm; MS (EI, 70 eV) *m*/*z* (%): 312 (19), 157 (33), 156 (40), 155 (100), 142 (12), 141 (55), 129 (18), 128 (22), 115 (17).

Syn-cyclooctadiene derivative **13**: ^{1}H NMR (200 MHz, $CDCl_3$) δ 6.40 (dd, 2H, J_1= 1.68, J_2 = 7.92 Hz), 6.30 (d, 2H, J = 1.68 Hz), 6.19 (d, 2H, J = 7.92 Hz), 5.91–5.72 (m, 4H), 4.57–4.40 (m, 2H), 3.39–3.22 (m, 2H), 3.19–2.83 (m, 4H), 2.82–2.49 (m, 4H), 2.33–2.11 (m, 2H) ppm; ^{13}C NMR (50.3 MHz, $CDCl_3$) δ 144.6, 139.7, 139.6, 139.4 (+), 134.4 (+), 130.8 (+), 130.4 (+), 129.5 (+), 54.2 (+), 36.4 (−), 33.6 (−), 27.7 (−) ppm; MS (EI, 70 eV) *m*/*z* (%): 312 (20), 157 (31), 156 (42), 155 (100), 142 (11), 141 (58), 129 (16), 128 (25), 115 (14).

4,15-Bis[(*Z*)-2-cyclopropylvinyl][2.2]paracyclophane (**22**): A freshly prepared solution of potassium *tert*-butoxide (898 mg, 8.0 mmol) in anhydrous THF (30 mL) was added dropwise over 30 min to a cooled (ice/water bath), vigorously stirred dispersion of cyclopropylmethyltriphenylphosphonium bromide (3178 mg, 8.0 mmol) in 30 mL of anhydrous THF under a N_2 gas flow. The bath was removed and the mixture stirred for 1 h at ambient temperature, then re-cooled to 0 °C, after which a solution of **9** (264 mg, 1.0 mmol) in anhydrous THF (30 mL) was added dropwise over 1 h. The bath was removed and the mixture stirred for an additional 2 h. The resulting mixture was poured into a vigorously stirred mixture of ice (100 g), water (50 mL) and conc. (37%) aq. HCl solution (50 mL) and the mixture stirred until the ice had completely melted. The precipitate was suction filtered on a glass frit, washed with dilute (1:3) aq. HCl (3 × 30 mL) and water (3 × 30 mL), and dissolved in CH_2Cl_2 (50 mL): The organic solution was dried over Na_2SO_4, filtered and concentrated under reduced pressure without warming to give a colorless solid residue (333 mg, 98%) of hydrocarbon **22**, as a mixture of stereoisomers, pure by NMR. ^{1}H NMR (200 MHz, $CDCl_3$) δ 6.53–6.26 (m, 8H), 5.35 (dd, 0.04H, J_1 = 8.6, J_2 = 15.5 Hz), 5.24 (dd, 0.30H, J_1 = 8.7, J_2 = 15.6 Hz), 4.77 (dd, 1.36H, J_1 = 10.3, J_2 = 11.3 Hz), 4.75 (dd, 0.30H, J_1 = 10.3, J_2 = 11.5 Hz), 3.59–3.32 (m, 2H), 3.07–2.69 (m, 6H), 1.59–1.33 (m, 2H), 0.88–0.17 (m, 8H) ppm; ^{13}C NMR for main isomer (50.3 MHz, $CDCl_3$) δ 138.0, 137.4, 136.6, 135.0 (+), 133.6 (+), 132.9 (+), 130.9 (+), 126.5 (+), 34.4 (−), 32.7 (−), 10.4 (+), 6.8 (−), 6.5 (−) ppm; MS (EI, 70 eV) *m*/*z* (%): 340 (19), 171 (21), 170 (23), 169 (100), 155 (38), 142 (23), 141 (32), 129 (62), 128 (26), 115 (11).

Irradiation of 4,15-Bis[(*Z*)-2-cyclopropylvinyl][2.2]paracyclophane – [2.2.2]tricyclophanes **23** and **24**: A solution of **22** (51.0 mg, 150 μmol) was irradiated by a halogen torch lamp from a distance of 15 cm for 12 h. When the starting material had been completely consumed (TLC monitoring), the reaction mixture was separated by column chromatography (silica gel, pentane) to give 13.4 mg of *cis*-[2.2.2]tricyclophane **23** and 22.3 mg of *trans*-[2.2.2]tricyclophane **24**; total yield: 35.7 mg (70%).

Cis-[2.2.2]tricyclophane derivative (**23**): ^{1}H NMR (200 MHz, $CDCl_3$) δ 7.08 (d, 2H, J = 1.8 Hz), 6.46 (dd, 2H, J_1 = 1.8, J_2 = 7.8 Hz), 6.21 (d, 2H, J = 7.8 Hz), 4.53–4.41 (m, 2H), 3.21–2.89 (m, 6H), 2.69–2.29 (m, 2H), 1.66–1.48 (m, 2H), 0.79–0.64 (m, 2H), 0.59–0.46 (m, 2H), 0.24–0.09 (m, 4H) ppm; ^{13}C NMR (50.3 MHz, $CDCl_3$) δ 141.5, 140.0, 139.4, 136.4 (+), 133.1 (+), 127.9 (+), 48.4 (+), 46.8 (+), 36.5 (−), 33.3 (−), 9.8 (+), 7.8 (−), 4.7 (−) ppm; MS (EI, 70 eV) *m*/*z* (%): 340 (15), 171 (22), 170 (24), 169 (100), 155 (33), 142 (20), 141 (27), 129 (51), 128 (22), 115 (11).

Trans-[2.2.2]tricyclophane derivative (**24**): ^{1}H NMR (200 MHz, $CDCl_3$) δ 6.44 (dd, 2H, J_1 = 1.7, J_2 = 7.8 Hz), 6.19 (d, 2H, J = 7.8 Hz), 6.15 (d, 2H, J = 1.7 Hz), 4.16–4.00 (m, 2H), 3.26–2.89 (m, 4H), 2.60–2.45 (m, 2H), 2.26–2.10 (m, 2H), 1.48–1.31 (m, 2H), 0.74–0.41 (m, 4H), 0.30–0.07 (m, 4H) ppm; ^{13}C NMR (50.3 MHz, $CDCl_3$) δ 141.4, 140.5, 140.2, 136.4 (+), 133.6 (+), 129.0 (+), 50.3 (+), 41.7 (+), 37.0 (−), 33.2 (−), 13.5 (+), 5.2 (−), 4.1 (−) ppm; MS (EI, 70 eV) *m*/*z* (%): 340 (15), 171 (21), 170 (21), 169 (100), 155 (27), 142 (11), 141(19), 129 (44), 128 (20), 115 (10).

X-ray structure determination

Numerical details are presented in Table 1. Data collection and reduction: Crystals were mounted in inert oil on glass fibres and transferred to the cold gas stream of the appropriate Oxford diffractometer. Measurements were performed with monochromatic Mo-*K*α (λ = 0.71073 Å; **23**) or mirror-focussed Cu-*K*α radiation (λ = 1.54184 Å; all others). Absorption corrections were performed for the Cu data sets only, on the basis of multi-scans. Structure refinement: The structures were refined anisotropically against F^2 (program SHELXL-97 [25]). Hydrogen atoms were included with a riding model. *Exceptions and special features*: For **23**, hydrogen atoms of the three- and four-membered rings were refined freely but with C–H distance restraints. For (*Z*,*Z*)-**22** and **23**, which crystallize in non-

Table 1: Crystallographic data for compounds **13**, **15**, (*Z*,*Z*)-**22**, **23** and **24**.

Compound	**13**	**15**	(*Z*,*Z*)-**22**	**23**	**24**
Formula	$C_{24}H_{24}$	$C_{24}H_{24}$	$C_{26}H_{28}$	$C_{26}H_{28}$	$C_{26}H_{28}$
M_r	312.43	312.43	340.48	340.48	340.48
Habit	colourless prism	colourless plate	colourless tablet	colourless tablet	colourless lath
Cryst. size (mm)	0.2 × 0.1 × 0.08	0.08 × 0.06 × 0.015	0.25 × 0.2 × 0.1	0.4 × 0.35 × 0.2	0.25 × 0.04 × 0.01
Crystal system	monoclinic	monoclinic	orthorhombic	monoclinic	monoclinic
Space group	$P2_1/c$	$P2_1/c$	$P2_12_12_1$	$C2$	$P2_1/c$
Cell constants:					
a (Å)	11.4023(3)	17.4745(12)	7.75839(15)	20.1622(5)	12.4933(5)
b (Å)	7.5646(2)	8.4668(6)	15.1450(2)	8.1838(2)	7.5363(3)
c (Å)	19.2444(5)	11.3625(7)	32.3931(6)	12.4063(3)	19.7420(7)
α (°)	90	90	90	90	90
β (°)	92.696(3)	104.052(7)	90	117.394(4)	96.997(4)
γ (°)	90	90	90	90	90
V (Å^3)	1658.08	1630.8	3806.23	1817.54	1844.93
Z	4	4	8	4	4
D_x (Mg m^{-3})	1.252	1.273	1.188	1.244	1.226
μ (mm^{-1})	0.52	0.53	0.50	0.07	0.51
F(000)	672	672	1472	736	736
T (°C)	−173	−173	−173	−173	−173
Wavelength (Å)	1.54184	1.54184	1.54184	0.71073	1.54184
$2\theta_{max}$	152	146	152	61	152
Refl. measured	34233	25579	69531	60932	35396
Refl. indep.	3449	3218	4469	2945	3839
R_{int}	0.029	0.087	0.025	0.031	0.056
Parameters	217	217	469	291	252
Restraints	0	0	0	44	29
$wR(F^2$, all refl.)	0.105	0.109	0.088	0.090	0.126
$R(F$, >4σ(F))	0.041	0.043	0.033	0.032	0.045
S	1.07	0.97	1.04	1.05	1.07
max. Δ/ρ (e Å^{-3})	0.35	0.26	0.20	0.31	0.28

centrosymmetric space groups, anomalous scattering was negligible and Friedel opposite reflections were therefore merged. For **24**, the atoms C23–26 show a slight (9%) disorder. The disorder model was refined using a system of similarity restraints. Dimensions of the minor disorder component should be interpreted with great caution.

Crystallographic data have been deposited with the Cambridge Crystallographic Data Centre as supplementary publications no. CCDC-797335 (**13**), -797336 (**15**), -797337 (*Z*,*Z*-**22**), -797338 (**23**), -797339 (**24**). Copies of the data can be obtained free of charge from http://www.ccdc.cam.ac.uk/data_request/cif.

References

1. Hopf, H.; Beck, C.; Desvergne, J.-P.; Bouas-Laurent, H.; Jones, P. G.; Ernst, L. *Beilstein J. Org. Chem.* **2009,** *5,* No. 20. doi:10.3762/bjoc.5.20
2. Schmidt, G. M. J. *Pure Appl. Chem.* **1971,** *27,* 647–678. doi:10.1351/pac197127040647
3. Ito, Y. *Synthesis* **1998,** *1,* 1–32. doi:10.1055/s-1998-2005
4. Feldman, K. S.; Campbell, R. F.; Saunders, J. C.; Ahn, C.; Masters, K. M. *J. Org. Chem.* **1997,** *62,* 8814–8820. doi:10.1021/jo9714167
5. Kaupp, G. *Angew. Chem., Int. Ed.* **1992,** *31,* 595–598. doi:10.1002/ange.19921040514
6. Ramamurthy, V.; Schanze, K. S. *Photochemistry of Organic Molecules in Isotropic and Anisotropic Media;* Marcel Dekker, Inc.: New York, 2003.
7. Kaupp, G. In *Comprehensive Supramolecular Chemistry;* Davies, J. E.; Ripmeester, J. A., Eds.; Elsevier: Oxford, U.K., 1996; Vol. 6, p 381.
8. Kaupp, G. AFM and STM in Photochemistry Including Photon Tunneling. In *Advances in Photochemistry;* Neckers, D. C.; Volman, D. H.; von Bünau, G., Eds.; John Wiley & Sons Inc.: Hoboken, NJ, USA, 2007; Vol. 19. doi:10.1002/9780470133507.ch2
9. Toda, F. In *Comprehensive Supramolecular Chemistry;* Macnicol, D. D.; Toda, F.; Bishop, R., Eds.; Elsevier: Oxford, U.K., 1996; Vol. 6, p 465.
10. Gao, X.; Friscic, T.; MacGillivray, L. R. *Angew. Chem., Int. Ed.* **2003,** *116,* 234–238. doi:10.1002/anie.200352713
11. Toda, F.; Miyamoto, H. *J. Chem. Soc., Perkin Trans. 1* **1993,** 1129–1132. doi:10.1039/P19930001129
12. Ramamurthy, V.; Natarajan, A.; Kaanumalle, L. S.; Karthikeyan, S.; Sivaguru, J.; Shailaja, J.; Joy, A. In *Mol. Supramol. Photochem.;* Inoue, Y.; Ramamurthy, V., Eds.; CRC Press, 2004; Vol. 11, pp 563–632.
13. Sivaguru, J.; Natarajan, A.; Kaanumalle, L. S.; Shailaja, J.; Uppili, S.; Joy, A.; Ramamurthy, V. *Acc. Chem. Res.* **2003,** *36,* 509–521. doi:10.1021/ar020269i
14. Ramamurthy, V.; Garcia-Garibay, M. A. In *Comprehensive Supramolecular Chemistry;* Alberti, G.; Bein, T., Eds.; Elsevier: Oxford, U.K., 1996; Vol. 7, p 693.
15. Mandelkern, M.; Elias, J. G.; Eden, D.; Crothers, D. M. *J. Mol. Biol.* **1981,** *152,* 153–161. doi:10.1016/0022-2836(81)90099-1
16. Hopf, H.; Noble, K. L.; Ernst, L. *Chem. Ber.* **1984,** *117,* 474–488. doi:10.1002/cber.19841170206
17. Mulzer, J.; Schein, K.; Bats, J. W.; Buschmann, J.; Luger, P. *Angew. Chem., Int. Ed.* **1998,** *110,* 1625–1628. doi:10.1002/(SICI)1521-3773(19980619)37:11<1566::AID-ANIE1566>3.0.CO;2-U
18. Mulzer, J.; Schein, K.; Böhm, I.; Trauner, D. *Pure Appl. Chem.* **1998,** *70,* 1487–1493. doi:10.1351/pac199870081487
19. Zitt, H.; Dix, I.; Hopf, H.; Jones, P. G. *Eur. J. Org. Chem.* **2002,** 2298–2307. doi:10.1002/1099-0690(200207)2002:14<2298::AID-EJOC2298>3.0.CO;2-E
20. Greiving, H.; Hopf, H.; Jones, P. G.; Bubenitschek, P.; Desvergne, J.-P.; Bouas-Laurent, H. *Eur. J. Org. Chem.* **2005,** 558–566. doi:10.1002/ejoc.200400592
21. Hopf, H.; Greiving, H.; Beck, C.; Dix, I.; Jones, P. G.; Desvergne, J.-P.; Bouas-Laurent, H. *Eur. J. Org. Chem.* **2005,** 567–581. doi:10.1002/ejoc.200400596
22. Brogaard, R. Y.; Boguslavskiy, A. E.; Schalk, O.; Enright, G. D.; Hopf, H.; Raev, V. A.; Jones, P. G.; Thomsen, D. L.; Sølling, T. I.; Stolow, A. *Chem.–Eur. J.* **2011,** *17,* 3922–3931. doi:10.1002/chem.201002928
23. Hudlicky, T.; Reed, J. W. *Angew. Chem., Int. Ed.* **2010,** *122,* 4982–4994. doi:10.1002/anie.200906001
24. Cresp, T. M.; Sargent, M. V.; Vogel, P. *J. Chem. Soc., Perkin Trans. 1* **1974,** 37–41. doi:10.1039/P19740000037
25. Sheldrick, G. M. *Acta Crystallogr. Sect. A.* **2008,** *A64,* 112–122. doi:10.1107/S0108767307043930

License and Terms

Beilstein Journal of Organic Chemistry

Fine-tuning alkyne cycloadditions: Insights into photochemistry responsible for the double-strand DNA cleavage via structural perturbations in diaryl alkyne conjugates

Wang-Yong Yang, Samantha A. Marrone, Nalisha Minors, Diego A. R. Zorio and Igor V. Alabugin*

Full Research Paper

Open Access

Address:
Department of Chemistry and Biochemistry, Florida State University, Tallahassee, FL 32306-4390, USA

Email:
Wang-Yong Yang - yang@chem.fsu.edu; Diego A. R. Zorio - zorio@chem.fsu.edu; Igor V. Alabugin* - alabugin@chem.fsu.edu

* Corresponding author

Keywords:
cancer cell proliferation assay; DNA alkylation; lysine conjugate; photocycloaddition; photo-DNA cleavage; plasmid relaxation assay; triplet excitation

Beilstein J. Org. Chem. **2011,** *7,* 813–823.
doi:10.3762/bjoc.7.93

Received: 14 February 2011
Accepted: 26 May 2011
Published: 16 June 2011

This article is part of the Thematic Series "Photocycloadditions and photorearrangements".

Guest Editor: A. G. Griesbeck

Abstract

Hybrid molecules combining photoactivated aryl acetylenes and a dicationic lysine moiety cause the most efficient double-strand (ds) DNA cleavage known to date for a small molecule. In order to test the connection between the alkylating ability and the DNA-damaging properties of these compounds, we investigated the photoreactivity of three isomeric aryl–tetrafluoropyridinyl (TFP) alkynes with amide substituents in different positions (*o*-, *m*-, and *p*-) toward a model π-system. Reactions with 1,4-cyclohexadiene (1,4-CHD) were used to probe the alkylating properties of the triplet excited states in these three isomers whilst Stern–Volmer quenching experiments were used to investigate the kinetics of photoinduced electron transfer (PET). The three analogous isomeric lysine conjugates cleaved DNA with different efficiencies (34, 15, and 0% of ds DNA cleavage for *p*-, *m*-, and *o*-substituted lysine conjugates, respectively) consistent with the alkylating ability of the respective acetamides. The significant protecting effect of the hydroxyl radical and singlet oxygen scavengers to DNA cleavage was shown only with *m*-lysine conjugate. All three isomeric lysine conjugates inhibited human melanoma cell growth under photoactivation: The *p*-conjugate had the lowest CC_{50} (50% cell cytotoxicity) value of 1.49×10^{-7} M.

Introduction

Triggering chemical processes with light offers numerous practical advantages. Not only does photochemistry open an additional dimension for the control of chemical reactivity by enabling many, otherwise impossible, synthetic transformations, but this mode of activation also provides useful spatial and temporal control of chemical processes that are required to

occur in the right place and at the right time. Such selectivity is particularly useful in biological applications such as cancer therapy where it accounts for the increasing importance of photodynamic therapy and related methods [1-11]. Previously, we expanded our studies of alkyne reactivity [12-23] to the design of photoactivated DNA cleavers, which combine a DNA-damaging part derived from diaryl alkynes and benzannelated enediynes with a cationic DNA-binding moiety.

The hybrid molecules that combined photoactivated alkynes with a dicationic moiety derived from lysine (C-lysine conjugates in Figure 1) displayed a combination of unique properties such as the ability to cause true double-strand (ds) DNA cleavage [24], amplification of ds cleavage dramatically at the lower pH of cancer cells [25], as well as the ability to recognize terminal phosphate monoester groups at the site of initial single-strand (ss) DNA damage and convert it into the more therapeutically important ds DNA damage [26].

We have shown that these compounds also could break intercellular DNA [27] and induce >90% cancer cell death at concentrations as low as 10 nM [25]. In spite of these remarkable properties, the mechanism of DNA cleavage by photoactivated alkynes and enediynes is still not fully understood.

Some light has been shed on the mechanism by the sequence selectivity of DNA cleavage in internally labeled DNA oligomers [28]. All enediyne-, alkyne-, and fulvene-based lysine conjugates displayed G-selective cleavage, especially at GG and GGG sites adjacent to the AT-rich sequence (the AT-tract), the preferred binding location for protonated amines. The G-selectivity is typical for oxidative DNA damage via PET for the most easily oxidized base, guanine. However, a noticeable amount of cleavage at a single G site in the AT-rich region is not consistent with purely oxidative DNA damage in the presence of spatially close GG and GGG sites, both of which are better sinks for the transient hole in the DNA. This observation suggests the presence of competitive DNA-cleavage mechanisms, such as guanine alkylation [29-35], which combine with the oxidative DNA damage to account for the efficient ds cleavage of plasmid DNA.

In the case of enediyne conjugate **2**, the additional DNA-cleavage mechanism may be provided by either photo-Bergman cyclization [3,36-44] (akin to such well-known DNA cleavers as enediyne antibiotics) [45,46] or C1–C5 cyclization [47-52] (Figure 2). In the latter process, which transforms enediynes into indenes, four hydrogens are transferred from the environment (two as H-atoms and two as protons), and thus DNA can be damaged via H-atom abstraction in a particularly efficient manner.

Efficient DNA cleavage by the monoacetylene conjugate **1**, which is capable of neither Bergman nor C1–C5 cyclization, suggests that other scenarios are possible and a more detailed understanding of alkyne photochemistry is vital for unraveling the mechanistic scenarios that account for DNA cleavage by these compounds (Figure 3) [25].

As illustrated in Figure 3, multiple reaction pathways are potentially unlocked by the photoactivation of alkyne conjugates. In the past, we observed dramatic differences in reactivity as a result of structural perturbations in the aryl moiety of diaryl alkynes. For example, introduction of strongly acceptor TFP substituents at the alkyne terminus changed the cyclization direction from the photo-Bergman closure to the C1–C5 cyclization due to the change in the nature of the key photophysical step and the involvement of PET from 1,4-cyclohexadiene (1,4-CHD) to the enediyne excited singlet state. In contrast, substituents that accelerate the intersystem crossing (ISC) through a "phantom state" effect [53-55] direct reactivity along an alternative triplet cycloaddition pathway.

Our previous mechanistic studies suggested that neither singlet oxygen nor diffusing oxygen- and carbon-centered radical species play a significant role under the conditions where the most efficient ds cleavage by monoalkynes is observed (pH 6) [25]. From the narrowed list of mechanistic scenarios, base

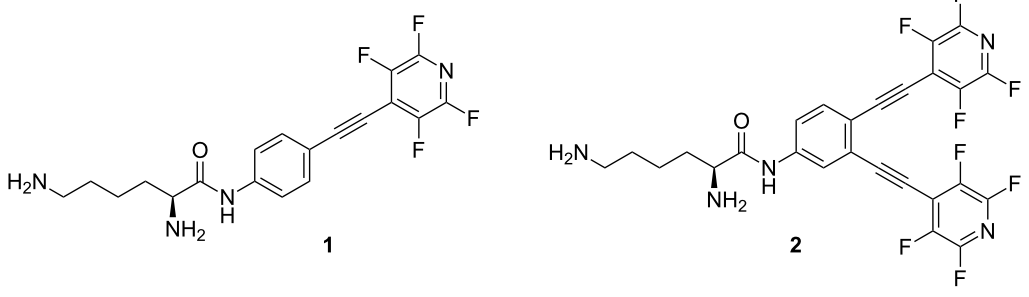

Figure 1: Structure of C-lysine conjugates.

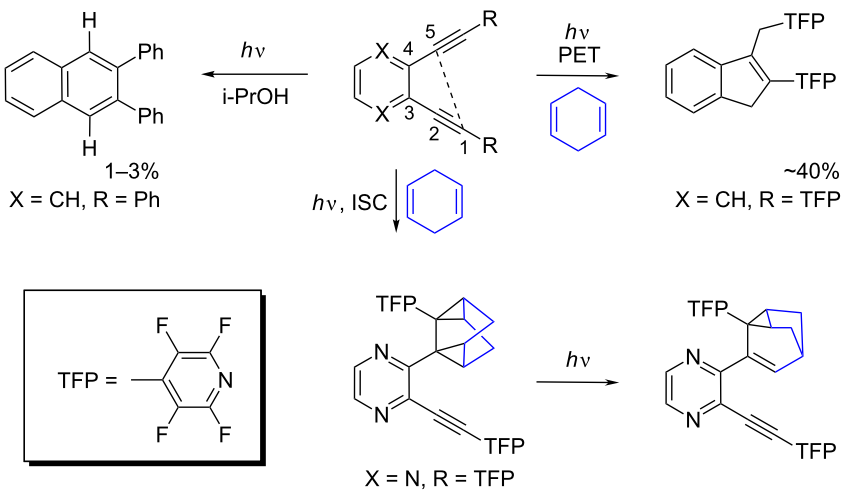

Figure 2: Alternative pathways of enediyne photoreactivity: photo-Bergman cyclization (left), C1–C5 cyclization (right), and triplet photocycloaddition (bottom). TFP = tetrafluoropyridinyl.

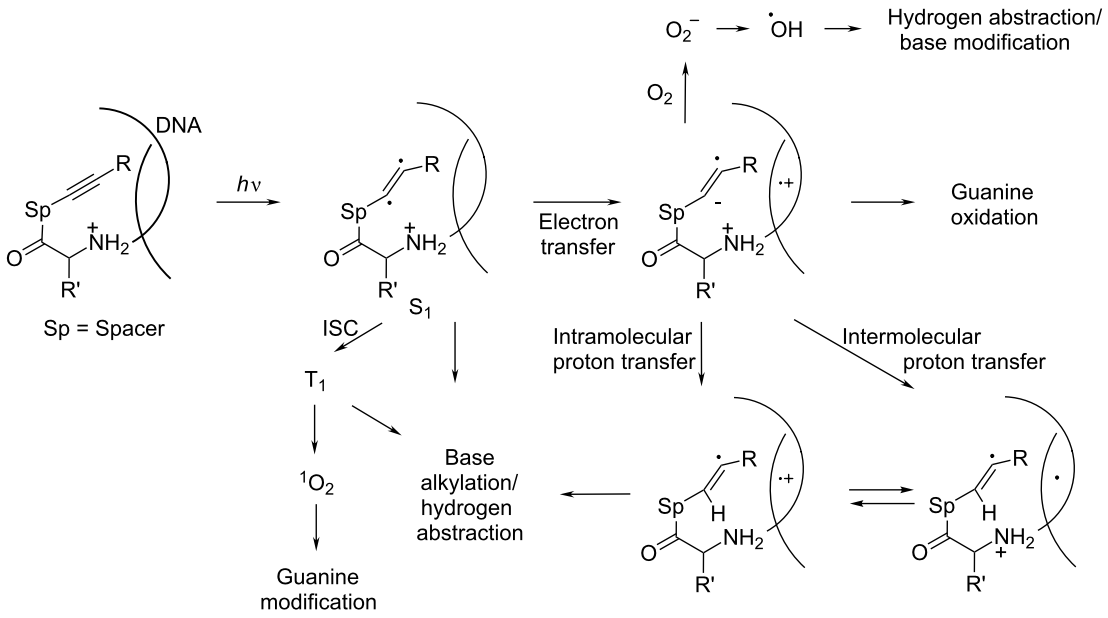

Figure 3: Summary of possible mechanistic alternatives for the observed DNA cleavage by monoacetylene conjugate **1**.

alkylation remains a likely origin of the photodamaging ability of such alkynes. Such reactivity is consistent with the above-mentioned ability of alkynes to act as electrophilic alkylating agents toward electron-rich π-systems observed in triplet photocycloaddition of TFP-substituted diaryl acetylenes [53].

The mechanism of triplet photocycloaddition involves a sequence of radical closures initiated by the formation of a triplet 1,4-diradical via the reaction of 1,4-CHD and the alkyne π,π*-triplet state. Although several plausible mechanistic pathways converge at the same homoquadricyclane product in Scheme 1, the maximum quantum yield of 0.50 along with the DFT activation barriers at the triplet hypersurface suggest that 5-exo-trig attack of electrophilic vinyl radical at the remaining 1,4-CHD double bond is the most likely subsequent step.

Because this photocycloaddition occurs from the triplet state, the competition between triplet and singlet-state reactivity is likely to be important for the specifics of DNA photodamage. In particular, this competition would control the relative impor-

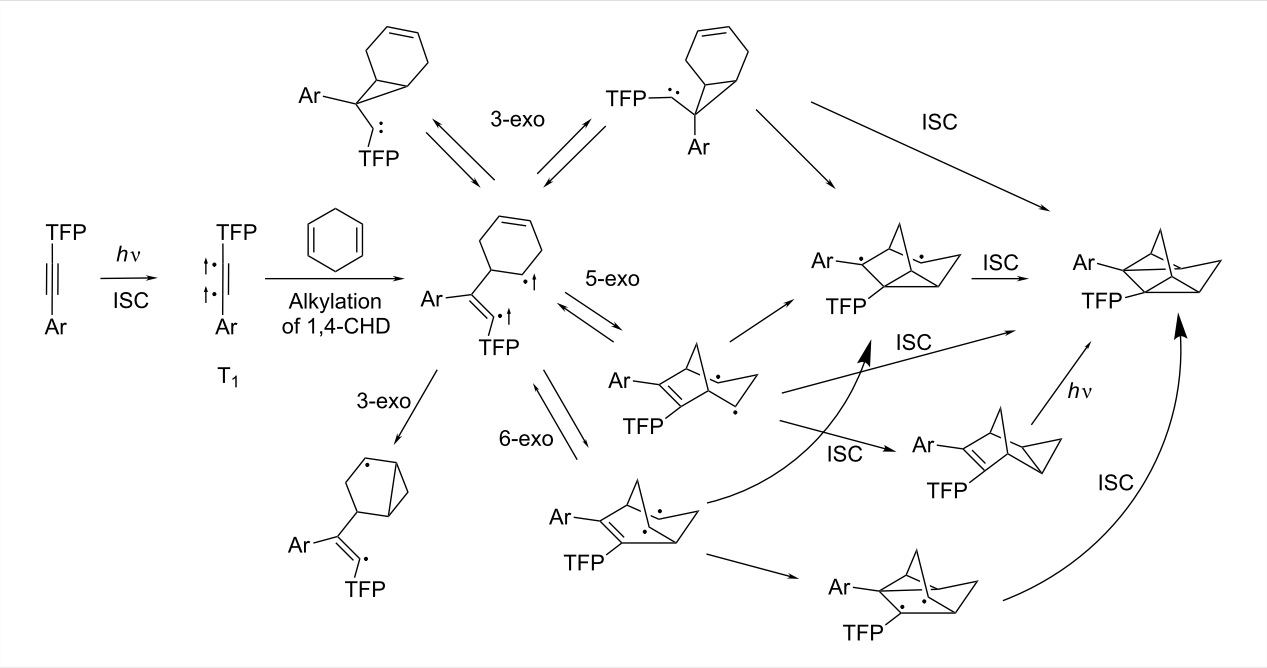

Scheme 1: Proposed mechanism of photocycloaddition of acetylene with 1,4-CHD.

tance of PET which, in the case of moderately efficient electron donors, is only energetically favorable from the singlet excited state. The relative contribution of these two pathways should be reflected in two different mechanisms of DNA damage, i.e., oxidative DNA cleavage versus DNA alkylation.

In the present paper, we investigate the reactivity of three isomeric aryl-TFP alkynes with the amide substituent in different positions (*o*-, *m*-, and *p*-) relative to the alkyne (acetamides in Figure 4). Such variations in the substitution pattern are known to impose significant effects on photochemical reactivity [56,57]. Reactions with cyclohexadiene were used to probe the properties of the triplet excited states in these three isomers, whilst Stern–Volmer quenching experiments were used to investigate the kinetics of PET in these three systems. In the final part of this paper, we examine whether the observed trends in photochemical and photophysical properties correlate with DNA-cleaving activities of the corresponding lysine conjugates shown in Figure 4.

Results and Discussion

Synthesis

The regioisomeric diaryl alkynes were synthesized following the synthetic strategy previously outlined by us for compound **1** [25]. The Sonogashira coupling of the corresponding iodonitrobenzene with trimethylsilyl (TMS) acetylene produced acetylenes **8a**–**c**. The TMS group of acetylene **8** was directly substituted with a tetrafluoropyridyl (TFP) group by a CsF-promoted reaction with pentafluoropyridine in DMF. Reduction of the nitrobenzenes **9a**–**c** with $SnCl_2$ produced anilines **10a**–**c**, which were reacted with acetyl chloride to form amides **3**, **4**, and **5** (Scheme 2).

Conjugates **1**, **6**, and **7** were prepared via coupling of the corresponding anilines **10a**–**c** with Boc-protected lysine in the presence of $POCl_3$ in pyridine. The Boc groups were removed by treatment with gaseous HCl in MeOH.

Photochemical reactions of TFP-alkynes with 1,4-cyclohexadiene

Previously, Zeidan and Alabugin have shown that TFP-substituted aryl alkynes are powerful photochemical alkylating agents and attack a variety of π-systems (Scheme 3) [58].

We chose 1,4-CHD to probe alkyne photoreactivity because, similar to excited alkynes, 1,4-CHD displays multichannel reactivity and can act as a source of H-atoms, as a source of electrons in PET, or as a reactive π-system. Photocycloaddition of the three acetylene molecules with 1,4-CHD was investigated via irradiation in acetonitrile with a Luzchem LED photoreactor and UVB (310 nm) irradiation (Scheme 4). The *m*-substituted acetylene **4** provided the homoquadricyclane product **12** in 42% yield after 2 h of UV irradiation in the presence of 100 equiv of 1,4-CHD. Under the same conditions, the *p*-substituted acetylene **3** reacts with 1,4-CHD sluggishly and gave <5% of product after 8.5 h of UV irradiation according to the ^{1}H NMR spectrum of the reaction mixture. This observation suggests that the ISC to the triplet state with *m*-acetamidyl

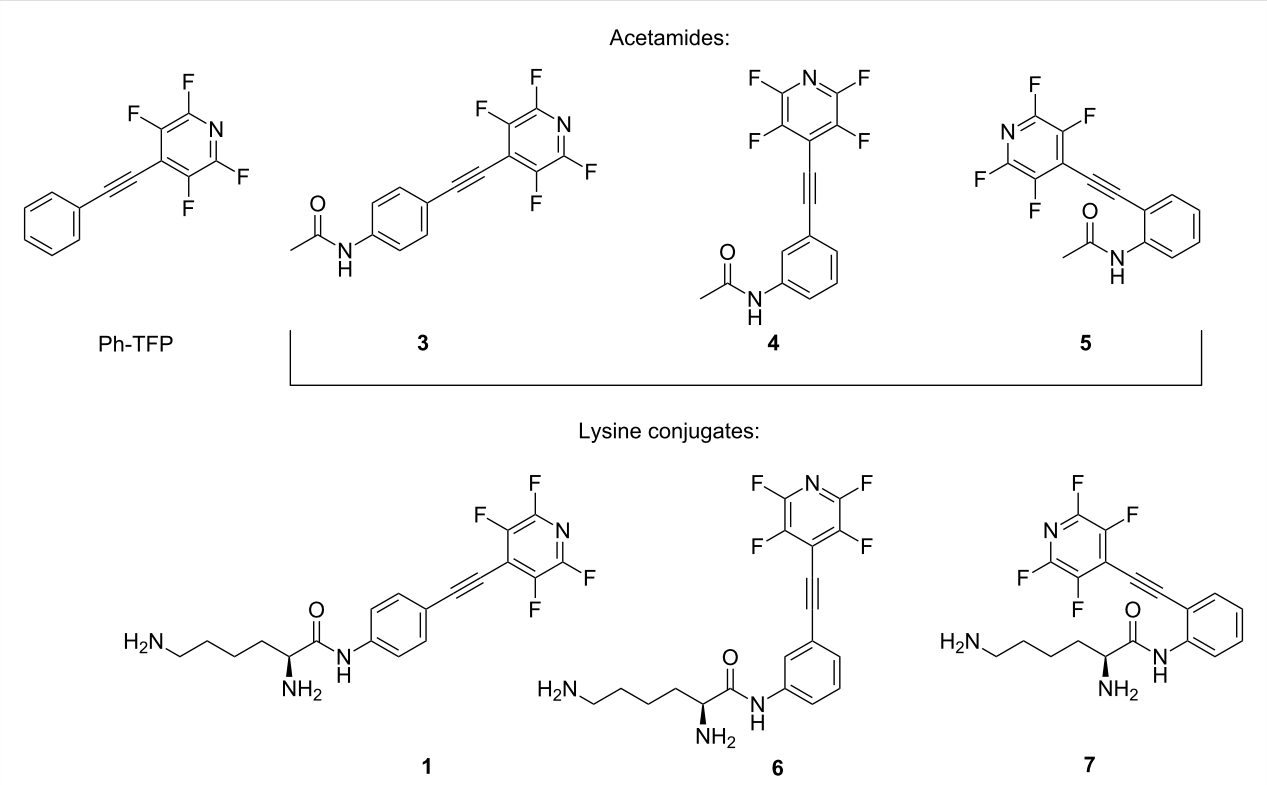

Figure 4: *p*-, *m*-, and *o*-amidyl acetylenes and respective lysine conjugates.

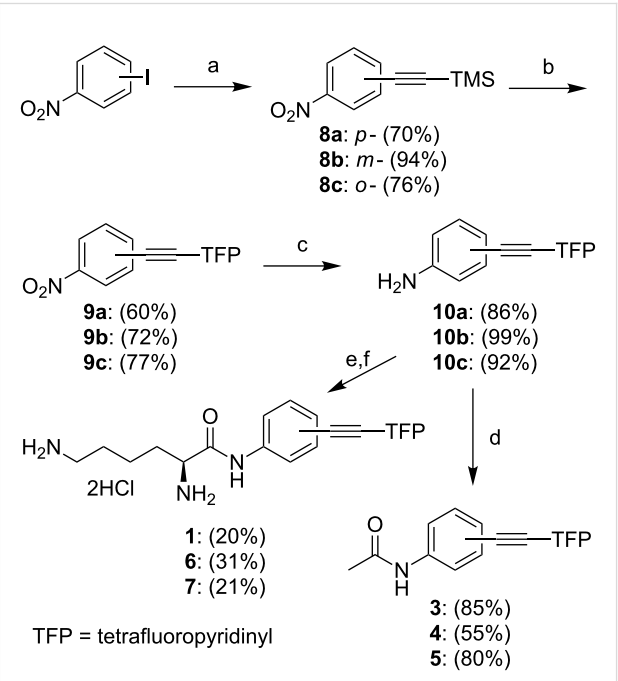

Scheme 2: Synthesis of amido-substituted monoacetylenes and lysine conjugates. Reagents and conditions: a. $PdCl_2(PPh_3)_2$, CuI, $HCCSiMe_3/Et_3N$, rt; b. CsF, pentfluoropyridine/DMF; c. $SnCl_2$, EtOH, reflux; d. $(CH_3CO)_2O$, Et_3N/CH_2Cl_2; e. $POCl_3$, Boc-Lys(Boc)-OH/pyridine; f. HCl(g)/MeOH.

acetylene **4** is more efficient than with *p*-acetamidyl acetylene **3**, the lifetime of the triplet of **4** is longer than that of **3**, or the triple state of **4** is more electrophilic than the triplet state of **3**. However, when the reaction was repeated in neat 1,4-CHD, the corresponding homoquadricyclane product **11** was isolated in 95% yield after only 1 h of UV irradiation. This result indicates that the photoaddition reaction of **3** can occur efficiently under more favorable conditions when there is a higher probability of intercepting the reactive excited state via reaction with a π-system.

The photochemical reactivity for the *o*-substituted acetylene **5** was drastically changed (Scheme 5). In this case, photoexcitation leads to the formation of an oxygen–carbon bond between the amide group and the triple bond. The cyclized product, benzoxazepine **13**, and the ketone product **14** were isolated. Whereas **13** was produced by a 7-endo cyclization (unprecedented in these systems), the ketone **14** can be formed either by direct hydration of the alkyne or by a known pathway that involves the corresponding six-membered product, a benzoxazine. The formation of benzoxazines has been previously reported by Roberts and coworkers, who suggested cyclization via triplet excitation following hydration [59-62]. The presence of vinyl peaks at 6.2 and 5.9 ppm in the reaction mixture and their quick disappearance upon the addition of a drop of water

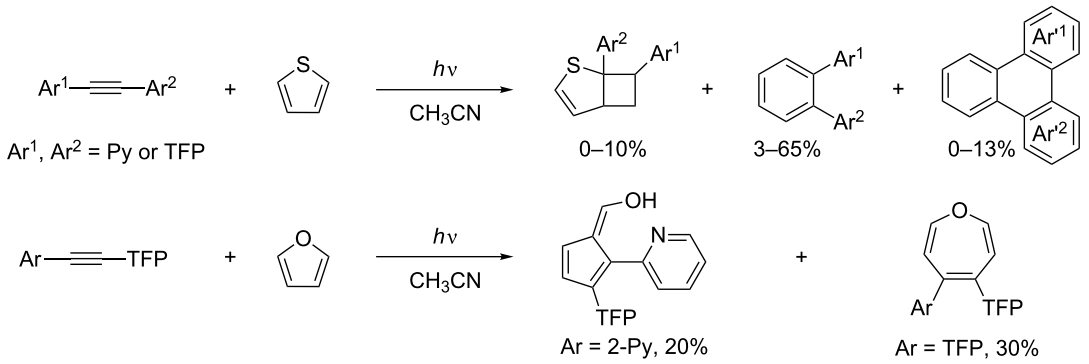

Scheme 3: Photochemical reactions of TFP-substituted aryl alkynes with selected π-systems. In short, the reaction proceeds through the photoinduced electron transfer from thiophene to the singlet excited state of the diaryl acetylene. The initially formed cyclobutene product undergoes further photorearrangement via a formal 1,3-shift.

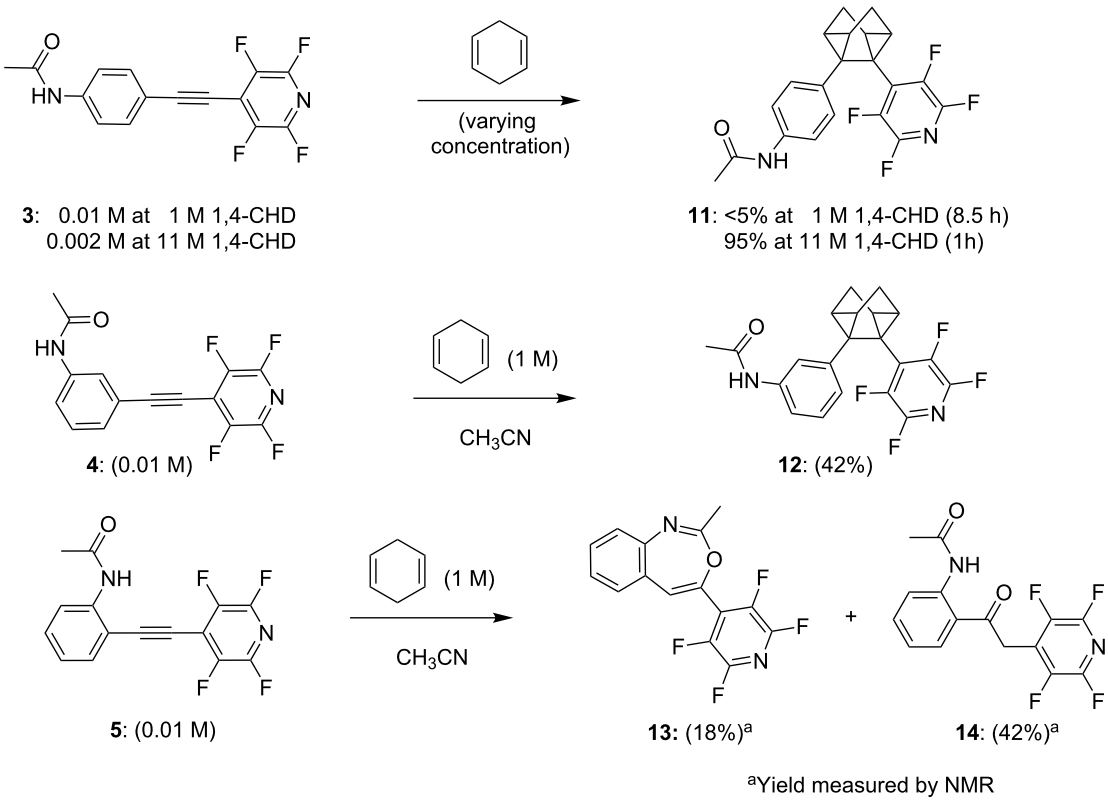

Scheme 4: Photocycloaddition of amido acetylenes with 1,4-CHD.

suggest that benzoxazines are also the intermediate products in our case but are rapidly hydrolyzed during work-up and purification. Although one can suggest the intermediacy of the triplet diradical in the photocyclization of *o*-amido acetylene **6**, this transformation does not require H-atom abstraction from an external H-atom source such as CHD and DNA, and thus the DNA-damaging ability of this chromophore is not expected to be significant.

Photophysics and kinetics of photoinduced electron transfer

The fluorescence quenching by triethylamine (Et_3N) was examined in order to gauge the relative efficiencies of these compounds as DNA photo-oxidizers (Figure 5).

In the quenching experiments, the *meta*-isomer **4** showed the largest Stern–Volmer constant (K_{sv} = 45.51) among the three

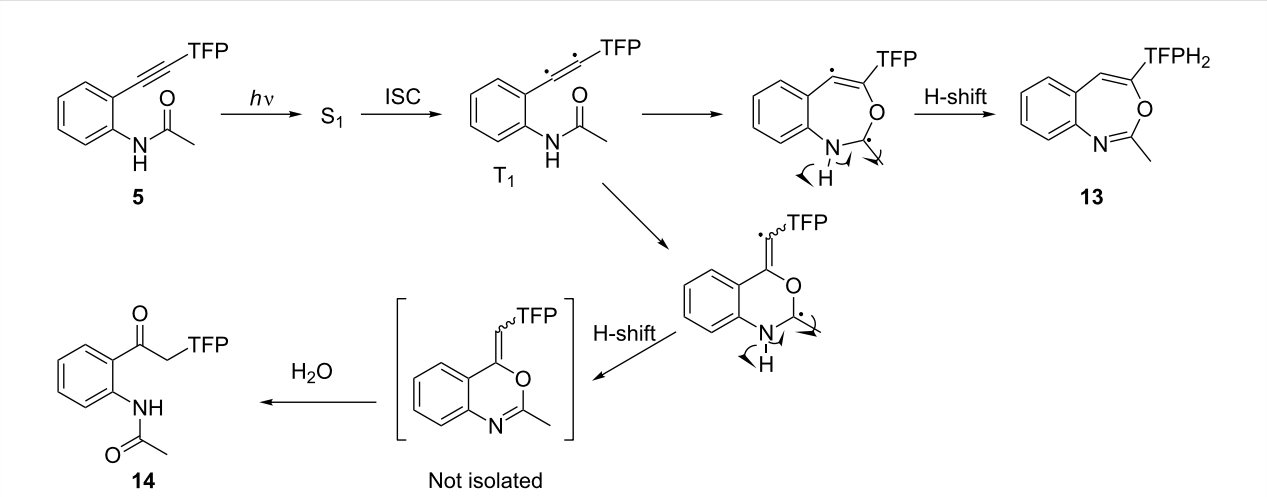

Scheme 5: Possible mechanism for photochemical hydration of diaryl acetylene moiety catalyzed by the *ortho*-amide substituent.

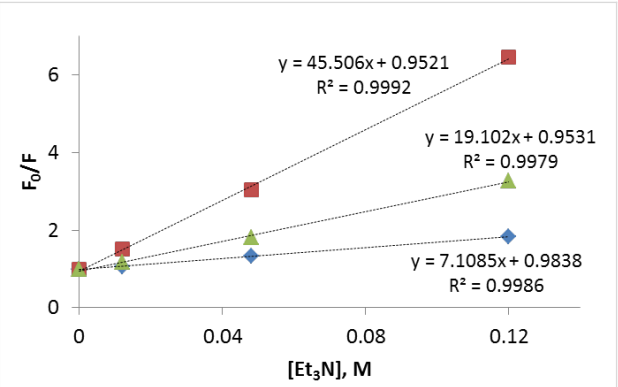

Figure 5: Stern–Volmer plots of three regioisomers, **3** (blue diamond), **4** (red square), and **5** (green triangle), in acetonitrile (10 μM). The solutions were excited at 310 nm.

isomers, whereas the *para*-isomer **3** displayed the lowest efficiency of quenching. The measured singlet lifetimes allowed us to determine the quenching rate constant, k_q, which, in this system, should be very close in magnitude to the rate of electron transfer, k_{ET} (Table 1).

Table 1: Stern–Volmer quenching constants (Et_3N as a quencher) and singlet lifetimes for the isomeric acetylenes 3–5.

Compound	K_{sv} (M^{-1})	τ (ns)	k_q ($M\ s^{-1}$)
3 (*para*)	7.11	$1.26 \pm 3.22 \times 10^{-3}$	5.64×10^{9}
4 (*meta*)	45.5	$3.35 \pm 9.30 \times 10^{-3}$	1.36×10^{10}
5 (*ortho*)	19.1	$1.34 \pm 3.52 \times 10^{-3}$	1.43×10^{10}

The two- to three-fold increase in the rate of electron transfer from Et_3N to the excited singlet state of the *meta*- and *ortho*-isomers in comparison to the *para*-isomer is consistent with the well-known photochemical *ortho*, *meta* effect of an acceptor substituent [56,57].

Although the fluorescence of all three isomers is quenched by the amine, the efficient quenching of singlet excitation in compound **4** can potentially lead to a stronger pH-dependency on the photochemistry of the respective lysine conjugate, which is controlled by the protonation-gated intramolecular electron transfer from the α-amino group [25]. Interestingly, the *meta*-isomer has a noticeably longer singlet lifetime than the other two isomers. A similar trend has been previously observed for the lifetimes of *m*-substituted enediynes [63].

The absorption spectra of all four acetylenes are shown in Figure 6. The core Ph-TFP-acetylene (**Ph-TFP**) chromophore without the amide group has no significant absorption at >320 nm.

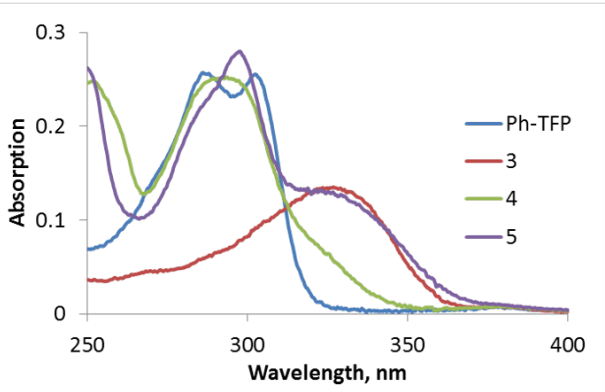

Figure 6: Absorption spectra of three isomers, **3**, **4**, **5**, and **Ph-TFP** in acetonitrile (10 μM).

The lowest absorptions of the *para*- and *ortho*-isomers **3**, **5** are red-shifted (λ_{max} ~ 330 nm) as a consequence of increased conjugation in the ground state. In contrast, the absorption of the *meta*-isomer **4** is closer to that of **Ph-TFP**, with the lower energy absorption band appearing as a lower-intensity shoulder.

Efficiency of DNA photocleavage

The results of plasmid relaxation assay with three lysine conjugates are summarized in Figure 7.

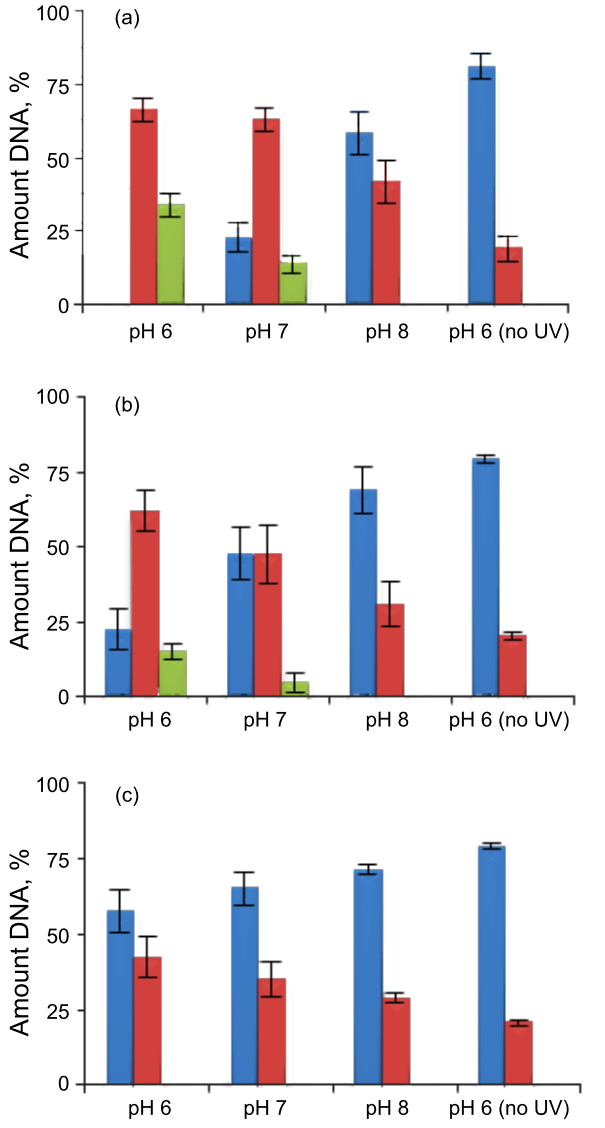

Figure 7: Quantified DNA cleavage data for **1** (a), **6** (b) and **7** (c). Blue: Form I (supercoiled) DNA; red: Form II (relaxed) DNA; green: Form III (linear) DNA. Reported values represent the average of four experiments.

These experiments were carried out on 15 μM of lysine conjugate with 30 μM/base pair of pBR322 plasmid DNA at pH 6, 7 and 8. The DNA-cleaving ability of conjugates does not directly follow the order of the photocycloaddition of their acetamides. Although the *m*-substituted acetylene was more photoreactive toward 1,4-CHD, the corresponding conjugate **6** produced less DNA cleavage than conjugate **1**. This suggests that either the difference in DNA binding overshadows the intrinsic differences in reactivity or the acetamide group is not a good surrogate for the lysine amides [64].

Nevertheless, both *p*- and *m*-lysine conjugates exhibit efficient ds DNA damage at pH 6 where the α-amino group of the lysine moiety is protonated and incapable of direct interference with the singlet photochemical process. On the other hand, compound **7**, which is unlikely to be a strong alkylating agent in the excited state, was the least-efficient DNA cleaver and did not produce any ds breaks. Interestingly, all three C-lysine conjugates broke DNA more efficiently at lower pH.

Effects of radical scavengers on DNA cleavage

In order to get further insight into the mechanism of the DNA cleavage by the three conjugates, we used the plasmid relaxation assays for the cleavage with conjugates **1**, **6**, and **7** in the presence of hydroxyl radicals (glycerol, DMSO) and singlet oxygen (NaN_3) scavengers [65]. The results are summarized in Figure 8.

For compound **1** (Figure 8a), the hydroxyl radical scavengers have no effect at pH 6 while the singlet oxygen scavenger slightly decreases the amount of ds DNA cleavage. At pH 8, >10% of the protecting effect was observed for all of the scavengers. The protecting effect of the scavengers on the reactivity of conjugate **1** is insignificant considering the very large excess (>1000-fold) of the scavengers. Conjugate **1** still leaves no undamaged DNA and produces significant amounts of linear DNA at pH 6. This observation suggests that the main DNA damage mechanism by conjugate **1** is not sensitive to the presence of hydroxyl radical/singlet oxygen scavengers, which can only block the alternative minor mechanisms.

In contrast, the photocleavage by the *meta*-substituted conjugate **6** (Figure 8b) is inhibited by both types of scavengers among the three conjugates at pH 6. The hydroxyl radical scavengers, glycerol and DMSO, protected DNA from the cleavage by 33 and 26%, respectively, whereas NaN_3 showed ~43% protection. The large protecting effect of NaN_3, the singlet oxygen scavenger, is consistent with the efficient photoaddition reaction of its chromophore via triplet excitation. This suggests that *m*-conjugate is not tightly bound to DNA and the most damage is propagated via two different oxygen-centered species, likely to be generated via the triplet manifold. The hydroxyl radical scavengers protected DNA from ss DNA

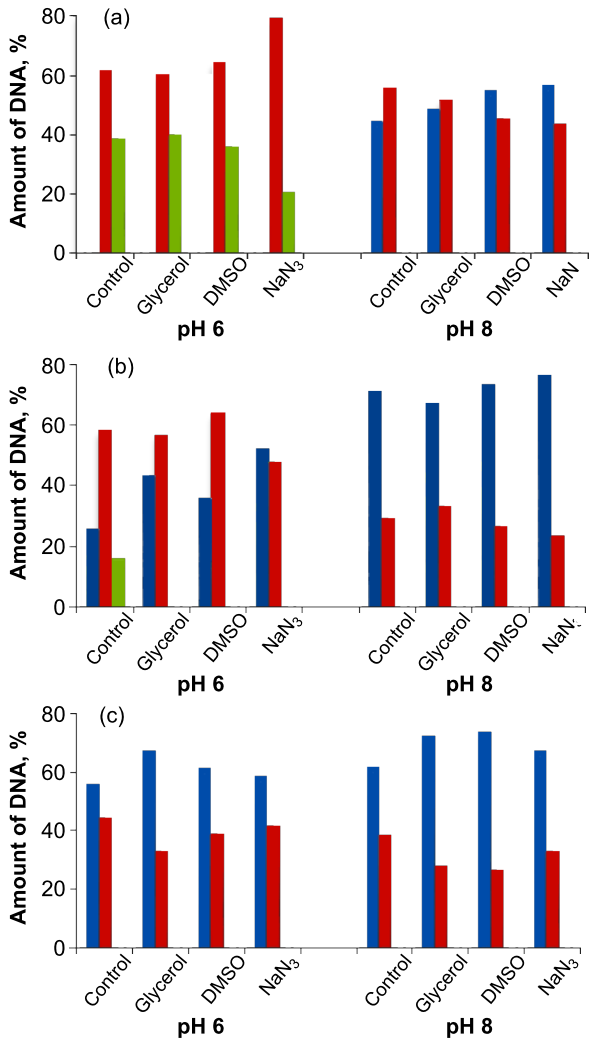

Figure 8: Effect of hydroxyl radical/singlet oxygen scavengers (20 mM) on the efficiency of DNA cleavage at pH 6 and 8 by 15 μM of conjugates **1** (a), **6** (b), and **7** (c) after 10 min of irradiation. Color coding: Blue: Form I (supercoiled) DNA; red: Form II (relaxed) DNA; green: Form III (linear) DNA.

cleavage by compound **7**, but the effect was small (Figure 8c). Only glycerol at pH 6 and glycerol and DMSO at pH 8 showed ~10% of protection. Little effect was observed for NaN_3, suggesting that the formation of singlet oxygen via triplet energy transfer is inefficient, possibly because of a short triplet lifetime and fast intramolecular photocyclization. The observed scavenger effects suggest different DNA damage mechanisms for the three lysine conjugates: Guanine oxidation and/or base alkylation for conjugate **1**, guanine oxidation and generation of reactive oxygen species for conjugate **6**, and guanine oxidation for conjugate **7**.

Cell proliferation assay

The ability of compounds **1**, **6**, and **7** to inhibit cell proliferation in human melanoma cell lines was tested in the dark and under photoactivation (Figure 9).

According to the control experiments with all three conjugates in the dark, these compounds do not inhibit cell proliferation at concentrations of <1 μM. On the other hand, conjugate **1** displayed strong phototoxicity toward the human melanoma A375 cell line in the nanomolar range ($CC_{50} = 1.49 \times 10^{-7}$ M) after 10 min of UV irradiation at 360 nm. Conjugates **6** and **7** also showed some phototoxicity. This result of cell proliferation inhibition by the conjugates is consistent with their respective DNA-cleaving abilities.

Conclusion

Three isomeric aryl-TFP alkynes with amide substituents in different positions (*o*-, *m*-, and *p*-) were synthesized, and the variations of their photochemical reactivity toward cyclohexadiene were investigated. Only *p*- and *m*-isomers were capable of alkylating 1,4-CHD. In contrast, the *o*-isomer only underwent an intramolecular reaction. The three analogous isomeric lysine conjugates cleaved DNA with different efficiencies: 15 μM of

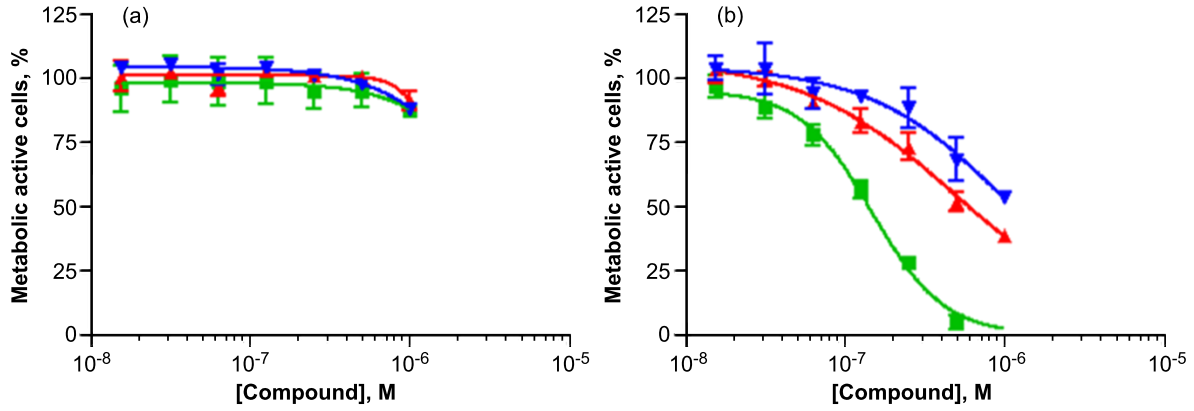

Figure 9: Cell proliferation assay using A375 cells (human melanoma) and compound **1** (green square), **6** (red up-pointing triangle), and **7** (blue down-pointing triangle) in dark (a) and after 10 min of UV (360 nm) irradiation.

the *p*-, *m*-, and *o*-conjugates **1**, **6**, and **7** produced 34, 15, and 0% of ds DNA cleavage, respectively. The large DNA-protecting effect on reactivity of the *meta*-conjugate **6**, imposed by hydroxyl radical/singlet oxygen scavengers, suggests triplet photoreactivity which leads to efficient sensitization of singlet oxygen. This observation is consistent with the efficient triplet reactivity of its chromophore. The inhibition of human melanoma cell growth by the three conjugates was also tested. The *para*-substituted conjugate **1** has the lowest CC_{50} value of 1.49×10^{-7} M.

Supporting Information

Supporting information features details for experimental procedures, emission titration spectra, fluorescence decay traces, picture of plasmid relaxation assay, characterization data, and NMR spectra (^{1}H, ^{13}C NMR, HSQC, and HMBC).

Supporting Information File 1

Experimental details, characterization data, emission titration spectra, fluorescence decay traces, plasmid relaxation assays and NMR spectra (^{1}H, ^{13}C NMR, HSQC, and HMBC).
[http://www.beilstein-journals.org/bjoc/content/supplementary/1860-5397-7-93-S1.pdf]

Acknowledgements

Partial support from the National Science Foundation (CHE-0848686) and James & Esther King Biomedical Research Program (09KC-03) is gratefully appreciated.

References

1. Armitage, B. *Chem. Rev.* **1998,** *98,* 1171–1200. doi:10.1021/cr960428+
2. Shiraki, T.; Sugiura, Y. *Biochemistry* **1990,** *29,* 9795–9798. doi:10.1021/bi00494a006
3. Jones, G. B.; Wright, J. M.; Plourde, G., II; Purohit, A. D.; Wyatt, J. K.; Hynd, G.; Fouad, F. *J. Am. Chem. Soc.* **2000,** *122,* 9872–9873. doi:10.1021/ja000766z
4. Kar, M.; Basak, A. *Chem. Rev.* **2007,** *107,* 2861–2890. doi:10.1021/cr068399i
5. Kagan, J.; Wang, X.; Chen, X.; Lau, K. Y.; Batac, I. V.; Tuveson, R. W.; Hudson, J. B. *J. Photochem. Photobiol., B: Biol.* **1993,** *21,* 135–142. doi:10.1016/1011-1344(93)80175-9
6. Benites, P. J.; Holmberg, R. C.; Rawat, D. S.; Kraft, B. J.; Klein, L. J.; Peters, D. G.; Thorp, H. H.; Zaleski, J. M. *J. Am. Chem. Soc.* **2003,** *125,* 6434–6446. doi:10.1021/ja020939f
7. Schmittel, M.; Viola, G.; Dall'Acqua, F.; Morbach, G. *Chem. Commun.* **2003,** 646–647. doi:10.1039/B211783E
8. Poloukhtine, A.; Popik, V. V. *J. Org. Chem.* **2003,** *68,* 7833–7840. doi:10.1021/jo034869m
9. Polukhtine, A.; Karpov, G.; Popik, V. V. *Curr. Top. Med. Chem.* **2008,** *8,* 460–469. doi:10.2174/156802608783955700
10. Alabugin, I. V.; Yang, W.-Y.; Pal, R. Enediyne photochemistry. In *CRC Handbook of Organic Photochemistry and Photobiology*, 3rd ed.; Taylor & Francis: Boca Raton, FL, in press.
11. Celli, J. P.; Spring, B. Q.; Rizvi, I.; Evans, C. L.; Samkoe, K. S.; Verma, S.; Pogue, B. W.; Hasan, T. *Chem. Rev.* **2010,** *110,* 2795–2838. doi:10.1021/cr900300p
12. Alabugin, I. V.; Timokhin, V. I.; Abrams, J. N.; Manoharan, M.; Abrams, R.; Ghiviriga, I. *J. Am. Chem. Soc.* **2008,** *130,* 10984–10995. doi:10.1021/ja801478n
13. Pal, R.; Clark, R. J.; Manoharan, M.; Alabugin, I. V. *J. Org. Chem.* **2010,** *75,* 8689–8692. doi:10.1021/jo101838a
14. Zeidan, T. A.; Kovalenko, S. V.; Manoharan, M.; Alabugin, I. V. *J. Org. Chem.* **2006,** *71,* 962–975. doi:10.1021/jo0520801
15. Pickard, F. C., IV; Shepherd, R. L.; Gillis, A. E.; Dunn, M. E.; Feldgus, F.; Kirschner, K. N.; Shields, G. C.; Manoharan, M.; Alabugin, I. V. *J. Phys. Chem. A* **2006,** *110,* 2517–2526. doi:10.1021/jp0562835
16. Vasilevsky, S. F.; Mikhailovskaya, T. F.; Mamatyuk, V. I.; Salnikov, G. E.; Bogdanchikov, G. A.; Manoharan, M.; Alabugin, I. V. *J. Org. Chem.* **2009,** *74,* 8106–8117. doi:10.1021/jo901551g
17. Alabugin, I. V.; Gilmore, K.; Patil, S.; Manoharan, M.; Kovalenko, S. V.; Clark, R. J.; Ghiviriga, I. *J. Am. Chem. Soc.* **2008,** *130,* 11535–11545. doi:10.1021/ja8038213
18. Vasilevsky, S. F.; Baranov, D. S.; Mamatyuk, V. I.; Gatilov, Y. V.; Alabugin, I. V. *J. Org. Chem.* **2009,** *74,* 6143–6150. doi:10.1021/jo9008904
19. Alabugin, I. V.; Manoharan, M. *J. Am. Chem. Soc.* **2005,** *127,* 12583–12594. doi:10.1021/ja052677y
20. Alabugin, I. V.; Manoharan, M. *J. Am. Chem. Soc.* **2005,** *127,* 9534–9545. doi:10.1021/ja050976h
21. Zeidan, T.; Manoharan, M.; Alabugin, I. V. *J. Org. Chem.* **2006,** *71,* 954–961. doi:10.1021/jo051857n
22. Baroudi, A.; Mauldin, J.; Alabugin, I. V. *J. Am. Chem. Soc.* **2010,** *132,* 967–979. doi:10.1021/ja905100u
23. Alabugin, I. V.; Manoharan, M. *J. Comput. Chem.* **2007,** *28,* 373–390. doi:10.1002/jcc.20524
24. Kovalenko, S. V.; Alabugin, I. V. *Chem. Commun.* **2005,** 1444–1446.
25. Yang, W.-Y.; Breiner, B.; Kovalenko, S. V.; Ben, C.; Singh, M.; LeGrand, S. N.; Sang, Q.-X.; Strouse, G. F.; Copland, J. A.; Alabugin, I. V. *J. Am. Chem. Soc.* **2009,** *131,* 11458–11470. doi:10.1021/ja902140m
26. Breiner, B.; Schlatterer, J. C.; Alabugin, I. V.; Kovalenko, S. V.; Greenbaum, N. L. *Proc. Natl. Acad. Sci. U. S. A.* **2007,** *104,* 13016–13021. doi:10.1073/pnas.0705701104
27. Yang, W.-Y.; Cao, Q.; Callahan, C.; Galvis, C.; Sang, Q.-X.; Alabugin, I. V. *J. Nucleic Acids* **2010,** 931394. doi:10.4061/2010/931394
28. Breiner, B.; Schlatterer, J. C.; Kovalenko, S. V.; Greenbaum, N. L.; Alabugin, I. V. *Angew. Chem., Int. Ed.* **2006,** *45,* 3666–3670. doi:10.1002/anie.200504479
29. Nielsen, P. E.; Jeepesen, C.; Egholm, M.; Buchardt, O. *Nucleic Acids Res.* **1988,** *16,* 3877–3888. doi:10.1093/nar/16.9.3877
30. Chatterjee, M.; Rokita, S. E. *J. Am. Chem. Soc.* **1990,** *112,* 6397–6399. doi:10.1021/ja00173a038
31. Henriksen, U.; Larsen, C.; Karup, G.; Jeepesen, C.; Nielsen, P. E.; Buchardt, O. *Photochem. Photobiol.* **1991,** *53,* 299–305. doi:10.1111/j.1751-1097.1991.tb03632.x
32. Chatterjee, M.; Rokita, S. E. *J. Am. Chem. Soc.* **1994,** *116,* 1690–1697. doi:10.1021/ja00084a009

33. Saito, I.; Takayama, M.; Sakurai, T. *J. Am. Chem. Soc.* **1994,** *116,* 2653–2654.
34. Nakatani, K.; Shirai, J.; Tamaki, R.; Saito, I. *Tetrahedron Lett.* **1995,** *36,* 5363–5366. doi:10.1016/0040-4039(95)01040-O
35. Hosford, M. E.; Muller, J. G.; Burrows, C. J. *J. Am. Chem. Soc.* **2004,** *126,* 9540–9541. doi:10.1021/ja047981q
36. Turro, N. J.; Evenzahav, A.; Nicolaou, K. C. *Tetrahedron Lett.* **1994,** *35,* 8089–8092. doi:10.1016/0040-4039(94)88250-9
37. Evenzahav, A.; Turro, N. J. *J. Am. Chem. Soc.* **1998,** *120,* 1835–1841. doi:10.1021/ja9722943
38. Kaneko, T.; Takanashi, M.; Hirama, M. *Angew. Chem., Int. Ed.* **1999,** *38,* 1267–1268. doi:10.1002/(SICI)1521-3773(19990503)38:9<1267::AID-ANIE1267>3.0.CO;2-F
39. Funk, R. L.; Young, E. R. R.; Williams, R. M.; Flanagan, M. F.; Cecil, T. L. *J. Am. Chem. Soc.* **1996,** *118,* 3291–3292. doi:10.1021/ja9521482
40. Choy, N.; Blanco, B.; Wen, J.; Krishan, A.; Russell, K. C. *Org. Lett.* **2000,** *2,* 3761–3764. doi:10.1021/ol006061j
41. Russell, K. C.; Jones, G. B. The Photo-Bergman Cycloaromatization of Enediynes. In *CRC Handbook of Organic Photochemistry and Photobiology;* Lenci, F.; Horspool, W., Eds.; CRC Press: Boca Raton, 2004; chapter 29.
42. Spence, J. D.; Hargrove, A. E.; Crampton, H. L.; Thomas, D. W. *Tetrahedron Lett.* **2007,** *48,* 725–728. doi:10.1016/j.tetlet.2006.10.164
43. Zhao, Z.; Peacock, J. G.; Gubler, D. A.; Peterson, M. A. *Tetrahedron Lett.* **2005,** *46,* 1373–1375. doi:10.1016/j.tetlet.2004.12.136
44. Wandel, H.; Wiest, O. *J. Org. Chem.* **2002,** *67,* 388–393. doi:10.1021/jo0106041
45. Nicolaou, K. C.; Smith, A. L.; Yue, E. W. *Proc. Natl. Acad. Sci. U. S. A.* **1993,** *90,* 5881–5888. doi:10.1073/pnas.90.13.5881
46. Galm, U.; Hager, M. H.; Van Lanen, S. G.; Ju, J.; Thorson, J. S.; Shen, B. *Chem. Rev.* **2005,** *105,* 739–758. doi:10.1021/cr030117g
47. Alabugin, I. V.; Kovalenko, S. V. *J. Am. Chem. Soc.* **2002,** *124,* 9052–9053. doi:10.1021/ja026630d
48. Alabugin, I. V.; Manoharan, M. *J. Am. Chem. Soc.* **2003,** *125,* 4495–4509. doi:10.1021/ja029664u
49. Alabugin, I. V.; Breiner, B.; Manoharan, M. *Adv. Phys. Org. Chem.* **2007,** *42,* 1–33. doi:10.1016/S0065-3160(07)42001-9
50. Prall, M.; Wittkopp, A.; Schreiner, P. R. *J. Phys. Chem. A* **2001,** *105,* 9265–9274.
51. Vavilala, C.; Byrne, N.; Kraml, C. M.; Ho, D. M.; Pascal, R. A., Jr. *J. Am. Chem. Soc.* **2008,** *130,* 13549–13551. doi:10.1021/ja803413f
52. Ramkumar, D.; Kalpana, M.; Varghese, B.; Sankararaman, S.; Jagadeesh, M. N.; Chandrasekhar, J. *J. Org. Chem.* **1996,** *61,* 2247–2250.
53. Zeidan, T. A.; Kovalenko, S. V.; Manoharan, M.; Clark, R. J.; Ghiviriga, I.; Alabugin, I. V. *J. Am. Chem. Soc.* **2005,** *127,* 4270–4285. doi:10.1021/ja043803l
54. Zeidan, T. A.; Clark, R. J.; Ghiviriga, I.; Kovalenko, S. V.; Alabugin, I. V. *Chem.–Eur. J.* **2005,** *11,* 4953–4960. doi:10.1002/chem.200500180
55. Zhou, Z.; Fahrni, C. J. *J. Am. Chem. Soc.* **2004,** *126,* 8862–8863.
56. Zimmerman, H. E. *J. Am. Chem. Soc.* **1995,** *117,* 8988–8991. doi:10.1021/ja00140a014
57. Zimmerman, H. E.; Alabugin, I. V. *J. Am. Chem. Soc.* **2001,** *123,* 2265–2270. doi:10.1021/ja002402c
58. Zeidan, T. A. Thermal and Photochemical Reactions of Acetylenes: I-*Ortho*-Effect in the Bergman Cyclization of Benzannelated Enediynes II-Photocycloaddition of Diaryl Acetylenes to Cyclic Dienes Mechanisms and Applications. Ph.D. Thesis, Florida State University, USA, 2005. http://etd.lib.fsu.edu/theses_1/available/etd-09302005-153610/unrestricted/Zeidan_TA.pdf
59. Roberts, T. D.; Ardemagni, L.; Shechter, H. *J. Am. Chem. Soc.* **1969,** *91,* 6185–6186. doi:10.1021/ja01050a046
60. Munchausen, L.; Ookuni, I.; Roberts, T. D. *Tetrahedron Lett.* **1971,** 1917–1920. doi:10.1016/S0040-4039(01)96742-5
61. Staudenmayer, R.; Roberts, T. D. *Tetrahedron Lett.* **1974,** 1141–1144. doi:10.1016/S0040-4039(01)82428-X
62. Roberts, T. D.; Munchausen, L.; Shechter, H. *J. Am. Chem. Soc.* **1975,** *97,* 3112–3117. doi:10.1021/ja00844a032
63. Kauffman, J. F.; Turner, J. M.; Alabugin, I. V.; Breiner, B.; Kovalenko, S. V.; Badaeva, E. A.; Masunov, A.; Tretiak, S. *J. Phys. Chem. A* **2006,** *110,* 241–251. doi:10.1021/jp056127y
64. We have shown before that the α-amino group (which is missing in the acetamides) has an effect on the reactivity. See Ref. [25].
65. Devasagayam, T. P. A.; Steenken, S.; Obendorf, M. S. W.; Schulz, W. A.; Sies, H. *Biochemistry* **1991,** *30,* 6283–6289. doi:10.1021/bi00239a029

License and Terms